

June 2018

Toward Verifiable Adaptive Control Systems: High-Performance and Robust Architectures

Benjamin Charles Gruenwald

University of South Florida, bcgruenwald@mail.usf.edu

Follow this and additional works at: <https://scholarcommons.usf.edu/etd>

 Part of the [Mechanical Engineering Commons](#)

Scholar Commons Citation

Gruenwald, Benjamin Charles, "Toward Verifiable Adaptive Control Systems: High-Performance and Robust Architectures" (2018).
Graduate Theses and Dissertations.
<https://scholarcommons.usf.edu/etd/7676>

This Dissertation is brought to you for free and open access by the Graduate School at Scholar Commons. It has been accepted for inclusion in Graduate Theses and Dissertations by an authorized administrator of Scholar Commons. For more information, please contact scholarcommons@usf.edu.

Toward Verifiable Adaptive Control Systems: High-Performance and Robust Architectures

by

Benjamin Charles Gruenwald

A dissertation submitted in partial fulfillment
of the requirements for the degree of
Doctor of Philosophy in Mechanical Engineering
Department of Mechanical Engineering
College of Engineering
University of South Florida

Major Professor: Tansel Yucelen, Ph.D.
Jonathan Muse, Ph.D.
Rajiv Dubey, Ph.D.
Kyle Reed, Ph.D.
Yasin Yilmaz, Ph.D.

Date of Approval:
June 7, 2018

Keywords: Uncertain dynamical systems, Model reference adaptive control, Transient performance,
Actuator dynamics, Interconnected systems

Copyright © 2018, Benjamin Charles Gruenwald

DEDICATION

To my parents, Mark and Margaret Gruenwald, and my brothers, David and Matthew Gruenwald.

ACKNOWLEDGMENTS

I would like to take this opportunity to express my deepest gratitude to the many people who have made the completion of this work possible. First and foremost, I would like to thank my advisor Dr. Tansel Yucelen for his continuous guidance and support. He has consistently encouraged and motivated me through the years I have worked with him. This along with his wisdom and insight has helped me to grow into the researcher and engineer I am today. I would also like to thank Dr. Jonathan Muse with the Air Force Research Laboratory, who has been like a co-advisor to me. Without his support and insightful suggestions, a large portion of this work would not have been possible. In addition, I would like to thank my remaining committee members Dr. Rajiv Dubey, Dr. Kyle Reed, and Dr. Yasin Yilmaz for their valuable suggestions and critiques which have improved the quality of this work. I would also like to thank Dr. Rasim Guldiken for all his assistance during my time at the University of South Florida.

I would also like to thank Dr. S. N. Balakrishnan from Missouri University of Science and Technology, Dr. Eric A. Butcher from the University of Arizona, Dr. Animesh Chakravarthy from Wichita State University, Dr. Gerardo De La Torre from Northrop Grumman, Dr. Mario L. Fravolini from the University of Perugia, Dr. Frank Fresconi from the Army Research Laboratory, Dr. Florian Holzapfel from the Technical University of Munich, Dr. Eric N. Johnson from Pennsylvania State University, Dr. Antonio Moschitta from the University of Perugia, Dr. Marcello R. Napolitano from West Virginia University, Dr. Nhan Nguyen from NASA, Dr. Jagannathan Sarangapani from Missouri University of Science and Technology, Dr. James Steck from Wichita State University, and Simon P. Schatz from the Technical University of Munich, for the opportunities to collaborate.

In addition, I would like to acknowledge the support from the Air Force Research Laboratory Aerospace Systems Directorate under the Universal Technology Corporation Grants 15-S2606-04-C27 and 17-S8401-02-C1 as well as the National Aeronautics and Space Administration under Grants NNX15AM51A and NNX15AN04A.

I am also thankful for the valuable experiences I have had interacting with my past and present co-workers both here at the University of South Florida and my previous institution the Missouri University of Science and Technology. I would like to thank Merve Dogan, Ali Albattat, Ehsan Arabi, Drew McNeely, Daniel Peterson, Benjamin Rigsby, Burak Sarsilmaz, Dzung Tran, Daniel Wagner, and Emre Yildirim. I have had the great opportunity to collaborate on work with them, learn from them, assist them, and enjoy non-work related times with them. In addition, I would like to especially thank Ehsan Arabi for his help in setting up the baseline control design for the experimental testbed used in Chapter 3.

Finally, I would like to thank my family; my parents, my brothers and sister-in-law, my extended family, and my church families. Without their constant love, support, and prayers, I would not have achieved this work like many other things in my life.

TABLE OF CONTENTS

LIST OF FIGURES	v
ABSTRACT.....	x
CHAPTER 1: INTRODUCTION	1
1.1 Transient Performance Improvement and Guarantees	3
1.2 Nonlinear Reference Models	4
1.3 Actuator Dynamics	4
1.4 Interconnected Systems	6
1.5 Organization.....	7
CHAPTER 2: ON TRANSIENT PERFORMANCE IMPROVEMENT OF ADAPTIVE CONTROL ARCHITECTURES.....	9
2.1 Introduction.....	9
2.2 Mathematical Preliminaries	11
2.3 Artificial Basis Functions for Transient Performance Improvement.....	15
2.4 Practical Considerations.....	19
2.5 Illustrative Example.....	23
2.6 Conclusion	27
CHAPTER 3: DIRECT UNCERTAINTY MINIMIZATION FRAMEWORK FOR SYSTEM PERFORMANCE IMPROVEMENT IN MODEL REFERENCE ADAPTIVE CONTROL	28
3.1 Introduction.....	28
3.2 Notation and Mathematical Preliminaries.....	29
3.3 Direct Uncertainty Minimization for Adaptive System Performance Improvement: Linear Reference Model Case.....	34
3.4 Generalization to a Class of Nonlinear Reference Models	39
3.5 Illustrative Numerical Examples.....	42
3.5.1 Example 1: Application to a Hypersonic Vehicle Model	42
3.5.1.1 Longitudinal Control Design	44
3.5.1.2 Lateral Control Design.....	45
3.5.1.3 Nominal System without Uncertainty.....	46
3.5.1.4 Uncertainty in Control Effectiveness and Stability Derivatives	47
3.5.2 Example 2: Wing Rock Dynamics with Nonlinear Reference Model	50
3.6 Experimental Results on Dual-Rotor Helicopter Testbed.....	53
3.6.1 Nominal Control Results without Uncertainty.....	55

3.6.2 Adaptive Control Results with Uncertainty in Control Effectiveness	56
3.7 Conclusion	60
CHAPTER 4: COMPUTING STABILITY LIMITS OF ADAPTIVE CONTROL LAWS WITH HIGH-ORDER ACTUATOR DYNAMICS	62
4.1 Introduction.....	62
4.2 Mathematical Preliminaries	64
4.3 Model Reference Adaptive Control with High-Order Actuator Dynamics	67
4.4 Convergence Analysis	73
4.5 Illustrative Example	79
4.6 Conclusion	82
CHAPTER 5: GENERALIZATIONS AND APPLICATIONS OF THE LMI-BASED HEDGING APPROACH FOR HIGH-ORDER ACTUATOR DYNAMICS	83
5.1 Adaptive Control for a Class of Uncertain Nonlinear Dynamical Systems in the Presence of High-Order Actuator Dynamics	83
5.1.1 Introduction.....	84
5.1.2 Preliminaries	85
5.1.3 Closed-Loop Adaptive Control System Stability with Actuator Dynamics	89
5.1.4 Illustrative Numerical Example	95
5.1.5 Conclusion	98
5.2 A Model Reference Adaptive Control Framework for Uncertain Dynamical Systems with High-Order Actuator Dynamics and Unknown Actuator Outputs	99
5.2.1 Introduction.....	99
5.2.2 Mathematical Preliminaries	101
5.2.3 Adaptive Control with Unknown Actuator Output.....	104
5.2.4 Illustrative Numerical Example	107
5.2.5 Conclusion	110
5.3 Model Reference Adaptive Control in the Presence of Actuator Dynamics with Applications to the Input Time-Delay Problem.....	110
5.3.1 Introduction.....	110
5.3.2 Mathematical Preliminaries	111
5.3.3 Adaptive Control in the Presence of High-Order Linear Time-Invariant Actuator Dynamics with Throughput Term.....	114
5.3.4 Illustrative Numerical Examples.....	117
5.3.5 Conclusion	121
5.4 Computing the Stability Limits of Pole-Zero Actuator Dynamics on Adaptive Control Laws for Aerospace Applications.....	121
5.4.1 Introduction.....	121
5.4.2 The LMI-Based Hedging Approach for Adaptive Control: A Concise Overview.....	122
5.4.2.1 Uncertain Dynamical System with Actuator Dynamics	122
5.4.2.2 Adaptive Control for Command Following.....	123
5.4.2.3 Utilizing LMIs for Safe Adaptive Control.....	125

5.4.3 Evaluation of LMI-Based Hedging Approach for Adaptive Control of a Hypersonic Vehicle Model with Pole-Zero Actuator Dynamics	129
5.4.3.1 Computing Limits for Second Order Actuator Dynamics	130
5.4.3.2 Computing Limits for Second Order Actuator Dynamics with One Zero	132
5.4.3.3 Computing Limits for Third Order Actuator Dynamics with One Zero and Three Poles	134
5.4.4 Conclusion	140
CHAPTER 6: EXPANDED REFERENCE MODELS FOR UNCERTAIN DYNAMICAL SYSTEMS WITH ACTUATOR DYNAMICS: STABILITY, PERFORMANCE, AND ROBUSTNESS	141
6.1 Introduction.....	141
6.1.1 Motivation and Background	141
6.1.2 Contribution and Notation	142
6.2 Problem Formulation	143
6.2.1 Actuators with Sufficiently Fast Dynamics	144
6.2.2 Actuators without Sufficiently Fast Dynamics	146
6.2.3 Objectives of the Paper	147
6.3 Expanded Reference Models for Uncertain Dynamical Systems with Actuator Dynamics	148
6.4 A Command Governor Architecture for Performance Guarantees.....	154
6.5 Robustness of Expanded Reference Model Architecture to Unknown Actuator Bandwidths	160
6.6 Illustrative Example	167
6.7 Conclusion	171
CHAPTER 7: DECENTRALIZED ADAPTIVE ARCHITECTURES FOR CONTROL OF LARGE-SCALE ACTIVE-PASSIVE MODULAR SYSTEMS WITH STABILITY AND PERFORMANCE GUARANTEES.....	172
7.1 Introduction.....	172
7.2 Problem Formulation	175
7.3 Decentralized Adaptive Control for Active-Passive Modular Systems	180
7.4 Stability and Performance Guarantees	183
7.5 Illustrative Numerical Example	190
7.6 Conclusion	197
CHAPTER 8: ON ADAPTIVE CONTROL OF UNACTUATED DYNAMICAL SYSTEMS THROUGH INTERCONNECTIONS WITH STABILITY AND PERFORMANCE GUARANTEES.....	198
8.1 Introduction.....	198
8.2 Problem Formulation	201
8.3 Adaptive Control for Unactuated Dynamics Through Interconnections	203
8.3.1 Control Design for Actuated Dynamics.....	204

8.3.2 Control Design to Account for Unactuated Dynamics	205
8.4 Stability and Performance Guarantees	206
8.5 Illustrative Numerical Example	212
8.6 Conclusion	214
CHAPTER 9: CONCLUDING REMARKS AND FUTURE RESEARCH.....	216
9.1 Concluding Remarks.....	216
9.2 Future Research	217
REFERENCES	219
APPENDIX A: PROJECTION OPERATOR.....	236
APPENDIX B: COPYRIGHT PERMISSIONS	237

LIST OF FIGURES

Figure 1.1	Model reference adaptive control framework and verification challenges.....	2
Figure 2.1	Standard adaptive control performance with (2.5), (2.6), (2.8), (2.9), and (2.10) for a given square-wave tracking command ($\gamma_\sigma = 0.5$ and $\gamma_{u_n} = 0.5$).....	24
Figure 2.2	Standard adaptive control performance with (2.5), (2.6), (2.8), (2.9), and (2.10) for a given square-wave tracking command ($\gamma_\sigma = 10$ and $\gamma_{u_n} = 10$).....	24
Figure 2.3	Standard adaptive control performance with (2.5), (2.6), (2.8), (2.9), and (2.10) for a given square-wave tracking command ($\gamma_\sigma = 50$ and $\gamma_{u_n} = 50$).....	25
Figure 2.4	Proposed adaptive control performance with (2.5), (2.6), (2.23), (2.31), (2.32), (2.33), and (2.44) for a given square-wave tracking command ($\widehat{W}_{a0} = 0.1$, $\sigma_{a0} = 0.1$, $\gamma_\sigma = 0.5$, $\gamma_{u_n} = 1$, $\gamma_a = 1$, $k = 5$, and $\mu = 1$).....	25
Figure 2.5	Proposed adaptive control performance with (2.5), (2.6), (2.23), (2.31), (2.32), (2.33), and (2.44) for a given square-wave tracking command ($\widehat{W}_{a0} = 0.1$, $\sigma_{a0} = 0.1$, $\gamma_\sigma = 0.5$, $\gamma_{u_n} = 1$, $\gamma_a = 1$, $k = 25$, and $\mu = 1$).....	26
Figure 2.6	Proposed adaptive control performance with (2.5), (2.6), (2.23), (2.31), (2.32), (2.33), and (2.44) for a given square-wave tracking command ($\widehat{W}_{a0} = 0.1$, $\sigma_{a0} = 0.1$, $\gamma_\sigma = 0.5$, $\gamma_{u_n} = 1$, $\gamma_a = 1$, $k = 100$, and $\mu = 1$).....	26
Figure 3.1	A candidate $f(e)$ for (3.44).	38
Figure 3.2	Block diagram of separated longitudinal control design.	44
Figure 3.3	Block diagram of separated lateral control design.....	46
Figure 3.4	Nominal controller performance without uncertainty.....	46
Figure 3.5	Nominal controller performance with uncertainty in Λ , C_{m_α} , and C_{n_β}	47
Figure 3.6	Standard adaptive controller performance with uncertainty in Λ , C_{m_α} , and C_{n_β} ($\Gamma_{l_0} = I_{2 \times 2}$ and $\Gamma_{l_a} = I_{3 \times 3}$).	48
Figure 3.7	Standard adaptive controller performance with uncertainty in Λ , C_{m_α} , and C_{n_β} ($\Gamma_{l_0} = 100I_{2 \times 2}$ and $\Gamma_{l_a} = 100I_{3 \times 3}$).	48

Figure 3.8	Proposed gain varying adaptive control performance with uncertainty in Λ , $C_{m\alpha}$, and $C_{n\beta}$ ($\Gamma_{l0} = I_{2 \times 2}$ and $\Gamma_{la} = \text{diag}[0.1, 1, 1]$, $\xi_0 = 10$, and $a = 2$).	49
Figure 3.9	System error bounds and adaptation gain for Figure 3.8.	49
Figure 3.10	Standard adaptive controller performance ($\gamma = 1$).	51
Figure 3.11	Proposed gain varying adaptive control performance ($\gamma = 1$ and $\gamma_\xi = 1$, $\xi_0 = 1$, and $a = 2$).	52
Figure 3.12	System error bounds and adaptation gain for Figure 3.11.	52
Figure 3.13	Nominal controller performance without uncertainty in the control effectiveness.	55
Figure 3.14	Nominal system error without uncertainty in the control effectiveness.	55
Figure 3.15	Nominal controller performance with uncertainty in the control effectiveness.	57
Figure 3.16	Nominal system error with uncertainty in the control effectiveness.	57
Figure 3.17	Standard adaptive control performance with low learning gain.	58
Figure 3.18	System error, adaptive control signal, and weight estimate for low learning gain.	58
Figure 3.19	Standard adaptive control performance with increased learning gain.	59
Figure 3.20	System error, adaptive control signal, and weight estimate for increased learning gain.	59
Figure 3.21	Proposed control tracking performance.	60
Figure 3.22	System error and adaptation gain for proposed adaptive control.	60
Figure 3.23	Adaptive control signal and weight estimates for proposed adaptive control.	61
Figure 4.1	LMI calculated feasible region for actuator dynamics.	80
Figure 4.2	Proposed controller performance with actuator dynamics ($(\zeta, \omega_n) = (0.55, 2.98)$, $\gamma_1 = 25$).	81
Figure 4.3	Proposed controller performance with actuator dynamics ($(\zeta, \omega_n) = (0.55, 2.19)$, $\gamma_1 = 25$).	81
Figure 5.1	LMI calculated feasible region for actuator dynamics.	97
Figure 5.2	Proposed controller performance with actuator dynamics ($(\zeta, \omega_n) = (0.525, 5.28)$, $\gamma = 25$).	97

Figure 5.3	Proposed controller performance with actuator dynamics ($(\zeta, \omega_n) = (0.525, 3.46)$, $\gamma = 25$).....	98
Figure 5.4	LMI calculated feasible region for actuator dynamics.	108
Figure 5.5	Proposed controller performance with actuator dynamics ($(\zeta, \omega_n) = (0.55, 4.46)$, $\gamma_1 = 100, \mu = 1000$).....	109
Figure 5.6	Proposed controller performance with actuator dynamics ($(\zeta, \omega_n) = (0.55, 3.45)$, $\gamma_1 = 100, \mu = 1000$).....	109
Figure 5.7	Comparison of the maximum allowable input time-delay between proposed approach of this paper and the results in [115].	118
Figure 5.8	Linear matrix inequality calculated maximum allowable input time-delay.	119
Figure 5.9	Proposed controller performance with input time-delay ($\tau^* = 0.3(s)$, $\gamma = 10$).....	120
Figure 5.10	Proposed controller performance with input time-delay ($\tau^* = 0.4(s)$, $\gamma = 10$).....	120
Figure 5.11	LMI calculated feasible region for second order actuator dynamics with $K_a \in [0.65, 3.0]$	132
Figure 5.12	LMI calculated feasible region for second order actuator dynamics with additional zero.	133
Figure 5.13	LMI calculated feasible region for third order actuator dynamics with one zero ($\lambda_1 = 1.0$) and three poles.	135
Figure 5.14	LMI calculated feasible region for third order actuator dynamics with one zero ($\lambda_1 = 0.5$) and three poles.	136
Figure 5.15	LMI calculated feasible region for third order actuator dynamics with one zero ($\lambda_1 = 0.1$) and three poles.	136
Figure 5.16	LMI feasible region with additional simulation points for third order actuator model from Figure 5.13 with $\lambda_1 = 1.0$ and $\lambda_2 = 0.5$	137
Figure 5.17	Reference model performance for data points 1-5 of Figure 5.16.	138
Figure 5.18	State tracking and controller performance for data point 1 (i.e., $(\zeta, \omega_n) = (0.53, 60)$) of Figure 5.16.....	138
Figure 5.19	State tracking and controller performance for data point 2 (i.e., $(\zeta, \omega_n) = (0.53, 18.7)$) of Figure 5.16.	139

Figure 5.20	State tracking and controller performance for data point 6 (i.e., $(\zeta, \omega_n) = (0.53, 16.7)$) of Figure 5.16.	139
Figure 6.1	Convergence of expanded reference model trajectories to the ideal reference model trajectories for different rates of convergence.	169
Figure 6.2	Expanded reference model trajectories exactly capturing the ideal reference model trajectories for zero initial conditions.	170
Figure 6.3	Comparison of the proposed expanded reference model control performance and a hedging based control performance.	170
Figure 6.4	Control inputs and actuator outputs for Figure 6.3.	171
Figure 7.1	A large-scale modular system representation of wing shaping aircraft in Remark 7.2.1, where thick lines represent unknown physical interconnections between the modules.	177
Figure 7.2	A large-scale modular system in Remark 7.2.2 with active modules (blue boxes) and passive modules (yellow boxes), where thick lines represent unknown physical interconnections between the modules.	177
Figure 7.3	An interconnected large-scale system consisting of five carts.	190
Figure 7.4	Position tracking and pendulum stabilization of the proposed adaptive decentralized controller with the performance bound $\varepsilon_i = 1.0$	192
Figure 7.5	Proposed adaptive decentralized control performance, error dependent learning gain, and weighted norm of the active module system with the performance bound $\varepsilon_i = 1.0$	193
Figure 7.6	Position tracking and pendulum stabilization of the proposed adaptive decentralized controller with the performance bound $\varepsilon_i = 0.5$	193
Figure 7.7	Proposed adaptive decentralized control performance, error dependent learning gain, and weighted norm of the active module system with the performance bound $\varepsilon_i = 0.5$	194
Figure 7.8	Position tracking and pendulum stabilization of the proposed adaptive decentralized controller with the mass of the passive module decreased to $M = 0.1$ (kg).	195
Figure 7.9	Proposed adaptive decentralized control performance, error dependent learning gain, and weighted norm of the active module system with the mass of the passive module decreased to $M = 0.1$ (kg).	195

Figure 7.10	Position tracking and pendulum stabilization of the proposed adaptive decentralized controller with the mass of the passive module increased to $M = 25$ (kg).....	196
Figure 7.11	Proposed adaptive decentralized control performance, error dependent learning gain, and weighted norm of the active module system with the mass of the passive module increased to $M = 25$ (kg).....	196
Figure 8.1	Block diagram representation of the open-loop interconnected uncertain dynamical system setup considered in this paper with $u(t)$, $z(t)$, and $x(t)$ respectively denoting the control signal applied to G_1 , the state vector of G_1 , and the state vector of G_2	199
Figure 8.2	An interconnected system with an actuated cart physically connected to an unactuated cart with inverted pendulum.....	213
Figure 8.3	Proposed set-theoretic adaptive control performance for interconnected actuated and unactuated carts.....	215
Figure 8.4	Control signals, error dependent learning gains, and enforced performance bounds.	215

ABSTRACT

In this dissertation, new model reference adaptive control architectures are presented with stability, performance, and robustness considerations, to address challenges related to the verification of adaptive control systems.

The challenges associated with the transient performance of adaptive control systems is first addressed using two new approaches that improve the transient performance. Specifically, the first approach is predicated on a novel controller architecture, which involves added terms in the update law entitled artificial basis functions. These terms are constructed through a gradient optimization procedure to minimize the system error between an uncertain dynamical system and a given reference model during the learning phase of an adaptive controller. The second approach is an extension of the first one and minimizes the effect of the system uncertainties more directly in the transient phase. In addition, this approach uses a varying gain to enforce performance bounds on the system error and is further generalized to adaptive control laws with nonlinear reference models.

Another challenge in adaptive control systems is to achieve system stability and a prescribed level performance in the presence of actuator dynamics. It is well-known that if the actuator dynamics do not have sufficiently high bandwidth, their presence cannot be practically neglected in the design since they limit the achievable stability of adaptive control laws. Another major contribution of this dissertation is to address this challenge. In particular, first a linear matrix inequalities-based hedging approach is proposed, where this approach modifies the ideal reference model dynamics to allow for correct adaptation that is not affected by the presence of actuator dynamics. The stability limits of this approach are computed using linear matrix inequalities revealing the fundamental stability interplay between the parameters of the actuator dynamics and the allowable system uncertainties. In addition, these computations are used to provide a depiction of the feasible region of the actuator parameters such that the robustness to variation in the parameters is addressed. Furthermore, the convergence properties of the modified reference model to the ideal reference model are analyzed. Generalizations and applications of the proposed approach are then provided. Finally,

to improve upon this linear matrix inequalities-based hedging approach a new adaptive control architecture using expanded reference models is proposed. It is shown that the expanded reference model trajectories more closely follow the trajectories of the ideal reference model as compared to the hedging approach and through the augmentation of a command governor architecture, asymptotic convergence to the ideal reference model can be guaranteed. To provide additional robustness against possible uncertainties in the actuator bandwidths an estimation of the actuator bandwidths is incorporated.

Lastly, the challenge presented by the unknown physical interconnection of large-scale modular systems is addressed. First a decentralized adaptive architecture is proposed in an active-passive modular framework. Specifically, this architecture is based on a set-theoretic model reference adaptive control approach that allows for command following of the active module in the presence of module-level system uncertainties and unknown physical interconnections between both active and passive modules. The key feature of this framework allows the system error trajectories of the active modules to be contained within a-priori, user-defined compact sets, thereby enforcing strict performance guarantees. This architecture is then extended such that performance guarantees are enforced on not only the actuated portion (active module) of the interconnected dynamics but also the unactuated portion (passive module).

For each proposed adaptive control architecture, a system theoretic approach is included to analyze the closed-loop stability properties using tools from Lyapunov stability, linear matrix inequalities, and matrix mathematics. Finally, illustrative numerical examples are included to elucidate the proposed approaches.

CHAPTER 1: INTRODUCTION

At a high level, control design consists of two parts; mathematically model the dynamical system (process or plant) to be controlled and design a control law based on this model to achieve some desired level of performance. In order to obtain a feasible control law, model simplifications of the dynamical system are typically made. This can include making idealized assumptions, linearizations of a highly nonlinear dynamical system, neglecting external disturbances, and neglecting different unmodeled dynamics. In addition, there can exist a wide array of unpredictable conditions that can create uncertainty in the actual physical system (e.g., structural damage in aircraft and spacecraft). As a result, there unavoidably exist system uncertainties between the control model and the actual physical system. There exist two common approaches that can account for these system uncertainties; robust control and adaptive control. While robust control techniques are well developed in literature (see, for example [1, 2] and references therein), they may not be able to guarantee certain levels of performance in the presence of large system uncertainties. In addition, since robust controllers are tuned to the worst-case possible uncertainty, they can be (overly) conservative effecting the achievable performance in order to ensure stability. In contrast, adaptive controllers are tuned to the physical system in real time, not a worst-case scenario (that may never happen in practice). Thus, adaptive controllers have the natural capability to estimate and suppress the effect of system uncertainties, without necessarily sacrificing performance.

While adaptive controllers have been used in numerous applications to provide stability and even achieve desired levels of performance without excessive reliance on mathematical models, widespread adoption of these adaptive control systems is limited due to their lack of a-priori, verifiable performance and robustness guarantees. For verifiable adaptive control systems, it is necessary to have system theoretic approaches that allow for one to check and satisfy different conditions such that the adaptive control system is guaranteed to perform as expected with a desired amount of robustness. A selection of different challenges for verifiable adaptive control systems are depicted in Figure 1.1 in the context of a model reference adaptive control framework which is considered throughout this dissertation. Briefly, the design of the

model reference adaptive control framework [3–7] has three major components — a reference model, an update law, and the adaptive feedback control law (typically augmented to an existing nominal control design). In this framework, a desired closed-loop system performance is captured by the reference model such as tracking an applied command $c(t)$ as in Figure 1.1. The system error given as $e(t)$ between the state of this reference model $x_r(t)$ and the state of the uncertain dynamical system $x(t)$ is used to drive the update law online. This then allows the control law to adapt its feedback gains using the information received from the update law for suppressing the system error.

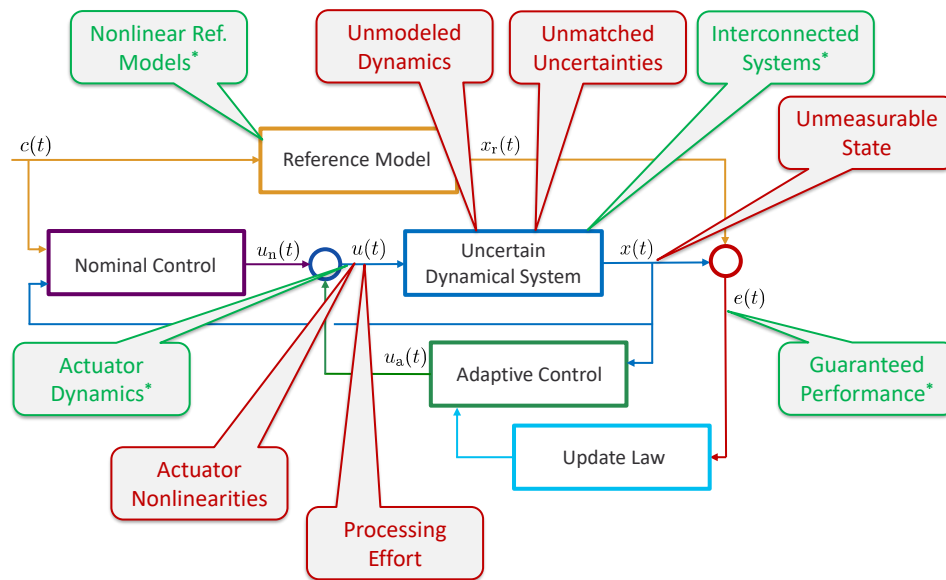


Figure 1.1: Model reference adaptive control framework and verification challenges.

This dissertation focuses on the challenges denoted with the asterisk in Figure 1.1. These will be discussed in the remaining sections, but first it should be noted that while not addressed in this dissertation, work has also been done, some by the author of this dissertation through collaborative efforts, to address the challenges from the presence of: unmodeled dynamics (see, for example, [8–12] and references therein), unmatched uncertainties (see, for example, [13–19] and references therein), unmeasurable states through output feedback control (see, for example, [15, 20, 21] and references therein), and the processing effort of control signals through event-triggering techniques (see, for example, [22] and references therein). In addition, there are several approaches addressing the presence of actuator nonlinearities (see, for example, [23–34] and references therein), where this is considered as a future research direction.

1.1 Transient Performance Improvement and Guarantees

A well-known result in adaptive control theory is that the system error can be guaranteed to asymptotically vanish in the presence of system uncertainties; however, there are limited (more conservative) guarantees in the transient portion that the system error does not violate physical constraints. Thus, the ability to obtain predictable transient performance is still an important problem to the adaptive control field – especially for applications to safety-critical systems and when there is no *a priori* knowledge on the upper bounds of the existing system uncertainties [35–38]. One way to address this problem is to use a high-gain learning rate in the update law which minimizes the worst-case system error such that the transient performance can be improved during the learning phase. Even though this can be justified theoretically [6], an update law subject to a high learning rate may not always be practically feasible [39, 40], since it can lead to control signals with high-frequency content which can result in system instability for practical applications. To avoid this, different approaches are proposed in [41–48] that introduce additional mechanisms to model reference adaptive control laws that capture a form of the system uncertainty in order to suppress its effect.

In this dissertation, two approaches are presented to address this problem. The first approach is predicated on a novel controller architecture which, unlike the work [41–48], includes modification terms in both the adaptive controller and the update law that are constructed through a gradient minimization procedure. In this way, the system error between an uncertain dynamical system and a given reference model can be minimized during the learning phase of the adaptive controller. A detailed stability analysis of the proposed approach is provided as well as a discussion of the practical aspects of its implementation. This approach is then illustrated through a numerical example.

Motivated by the first approach, the second one similarly uses a gradient minimization procedure to suppress more directly the effect of system uncertainty on the transient system response. To go beyond the first approach, the second approach is modified to be computationally less expensive and it can enforce the system error to approximately stay in an *a priori* given, user-defined error performance bound. In addition, this second approach is not only developed for adaptive control laws with linear reference models, but also generalized using tools and methods from [49], for adaptive control laws with nonlinear reference models. It is illustrated through two numerical examples; for the linear reference model the approach is applied to a linearized hypersonic vehicle model and for the nonlinear reference model a wing rock like example is

considered where the pilot authority has been limited. Finally, experimental results are included from an application to the Quanser AERO platform [50].

1.2 Nonlinear Reference Models

While it is of common practice to use linear reference models, this can limit the achievable closed-loop dynamical system performance — especially for applications involving highly-capable dynamical systems such as highly-maneuverable aircraft, missiles, and space launch vehicles. This is due to the fact that linear reference models can only approximate the desired closed-loop behavior of these nonlinear dynamical systems in narrow regions of the state-space. Notable contributions that utilize reference models with nonlinear dynamics are presented by the authors of [51–54]. However, these approaches either consider specific theoretical frameworks requiring restrictive assumptions or they consider specific applications which cannot be easily generalized.

Previous work by the author [49] proposes an adaptive control architecture using nonlinear reference models, where under minimal assumptions the system error is shown to asymptotically vanish. As mentioned in the previous section the second gradient minimization based approach is generalized using the adaptive control architecture in [49], but it goes beyond by enforcing performance bounds during the transient-time.

1.3 Actuator Dynamics

As already mentioned, while addressing system uncertainties, the presence of unmodeled dynamics are often neglected in the modeling process for model reference adaptive control designs. A practical form of unmodeled dynamics, which is present in every physical system, is the actuator dynamics. Typically, the effect of the actuators are neglected using the assumption that the actuator dynamics have sufficiently high bandwidth. Yet, if the bandwidths of each actuator channel are not sufficiently large, then the closed-loop system trajectories may not behave close to the reference model trajectories and, importantly, the stability of the closed-loop system can be lost. Thus, from a verification standpoint, additional steps are necessary to show the allowable bandwidth range of the actuator dynamics for safety-critical and human-in-the-loop applications such that the adaptive control algorithms correctly suppress the system uncertainties.

The authors of [55–57] propose approaches that allow the design of model reference adaptive controllers in the presence of actuator dynamics. These works include the actuator dynamics in the uncertain

dynamical system such that the resulting closed-loop dynamical systems is analyzed. However, this can result in imprecise estimation of the system uncertainties for the suppression of their effects. The authors of [58] investigate how slow the actuator dynamics need to become before the closed-loop stability is negatively effected for a scalar system. In addition, they then propose different modifications to the control law to provide additional robustness when the actuator dynamics are not sufficiently fast. The authors of [30–33] propose a well-respected practical approach in the aerospace engineering field known as (pseudo-control) hedging. In particular, based on a given reference model capturing a desired closed-loop dynamical system performance, the hedging approach alters the trajectories of this model enabling adaptive control laws to be designed such that their stability is not affected by the presence of actuator dynamics. However, it is not analyzed that this modification to the reference model dynamics does not yield to unbounded reference model responses.

In this dissertation, several results for the actuator dynamics problem are presented. First, an approach to compute stability limits for model reference adaptive control laws for uncertain dynamical systems in the presence of high-order actuator dynamics is proposed. This approach, termed an LMI-based hedging approach, modifies the ideal reference model dynamics to allow for correct adaptation in the presence of high-order actuator dynamics. To compute the stability limit of the modified reference model, LMIs are used such that this computation reveals the fundamental stability interplay between the parameters of the actuator dynamics and the allowable system uncertainties. In addition, the distance between the modified reference model trajectories and ideal reference model trajectories are analyzed, and a condition for which these trajectories converge to each other is provided. These results are illustrated through a numerical example.

Second, additional extensions of this LMI-based hedging approach are provided. Specifically, three generalizations are considered for a class of uncertain nonlinear dynamical systems, unmeasurable actuator outputs, and actuator dynamics with an additional throughput term. In addition, for the actuator dynamics with an additional throughput term, an application for the input time-delay problem is presented. Furthermore, the method of computing the actuator parameters is more thoroughly addressed and an application to a hypersonic vehicle model for different cases of pole-zero actuator dynamics is presented.

Third, an improved adaptive control architecture to the LMI-based hedging approach is presented. While computing the stability limits is an important result for the presence of actuator dynamics, the LMI-based hedging approach modifies the ideal reference model such that it is limited to achieving bounded

controlled system trajectories around a neighborhood of this model capturing a desired closed-loop system performance. This improved adaptive control architecture uses expanded reference models allows the trajectories of the uncertain dynamical system to follow the trajectories of the expanded reference model that are shown to remain predictably close to the trajectories of the ideal reference model, as compared to the LMI-based hedging (and pseudo-control hedging) approach. In addition, a command governor architecture is augmented with the proposed expanded reference model in order to achieve asymptotic convergence of the expanded reference model trajectories to those of the ideal reference model such that the desired closed-loop system performance can be captured. To provide (additional) robustness against possible uncertainties in the actuator bandwidths an estimation of the actuator bandwidths is incorporated. This approach is also illustrated with a numerical hypersonic vehicle example.

1.4 Interconnected Systems

The design and implementation of decentralized architectures for controlling complex large-scale systems is a nontrivial control engineering task involving the consideration of components interacting with the physical processes to be controlled. Specifically, large-scale systems are characterized by a large number of highly-coupled heterogeneous components exchanging matter, energy, or information. Examples of such systems include but are not limited to network systems, power systems, communication systems, process control systems, water systems, highway systems, and air traffic control systems (see, for example, [59, 60] and references therein). An important class of large-scale systems is modular systems in which there exists a physical interconnection between modules. A major challenge in the control of modular systems is associated with the unknown physical interconnections between modules and module-level system uncertainties.

To this end, the authors of [61–73] propose notable adaptive control approaches to suppress the effect of such uncertainties providing an effective control design methodology for large-scale modular systems. However, these approaches require all modules of a large-scale system to be controlled, which may not be possible especially for highly complex large-scale modular systems. For example, there may exist a specific subset of modules in practice that cannot be accessed or some of the modules can be subject to actuator failures in that it may not be possible to drive such modules through control signals. In this case, the set of modules that cannot be driven by control signals affect the others as unmodeled dynamics.

This dissertation presents a new decentralized adaptive control architecture for large-scale modular systems using an active-passive framework. Here, active modules refer to modules that receive a control

signal and passive modules are modules that do not receive a control signal. Specifically, extending a set-theoretic adaptive control approach developed in [74], an adaptive decentralized control law is designed for each active module such that they can each effectively perform their individual objective in the presence of module-level system uncertainties and unknown physical interconnections between other active modules and passive modules. This framework allows the system error trajectories of the active modules to be contained within a-priori, user-defined compact sets, thereby strict performance guarantees are enforced. This result is also significant from the transient improvement perspective noted in Section 1.1. The efficacy of the proposed decentralized adaptive control architecture is demonstrated with an illustrative numerical example.

An extension of this result is also presented in which the control and performance enforcement for a class of uncertain dynamical systems consisting of actuated (active) and unactuated (passive) portions that are physically interconnected to each other is considered. In this extension, performance guarantees are enforced on not only the actuated portion of the interconnected dynamics but also the unactuated portion by means of the physical interconnection with the actuated portion of the dynamics. Specifically, the proposed approach stabilizes the overall interconnected system in the presence of unknown physical interconnections as well as system uncertainties. For enforcing performance guarantees, the set-theoretic model reference adaptive control approach is also adopted to restrict the respective system error trajectories of the actuated and unactuated dynamics inside a-priori, user-defined compact sets. In addition, drawing upon the work done for the actuator dynamics problem discussed in Section 1.3, the proposed extension uses LMIs to verify stability of appropriate control parameters as well as the allowable system uncertainties and unknown physical interconnections. An illustrative numerical example is included to demonstrate the efficacy of the proposed approach.

1.5 Organization

The organization of this dissertation is as follows. Chapter 2 presents a model reference adaptive control approach predicated on a gradient optimization procedure to improve the transient response. This is generalized in Chapter 3 to enforce performance guarantees and allow for the use of nonlinear reference models. Chapter 4 presents the LMI-based hedging approach for high-order actuator dynamics and Chapter 5 provides generalizations and applications of this approach. In Chapter 6, an adaptive control architecture using expanded reference models is presented for the actuator dynamics problem. Chapter 7 introduces a set-

theoretic decentralized adaptive control architecture for large-scale active-passive modular systems, where performance guarantees are enforced on the active modules. In Chapter 8 an extension is made to enforce performance guarantees not only on the active module (actuated dynamics) but also on the passive module (unactuated dynamics). Finally, concluding remarks and possible future research directions are presented in Chapter 9.

CHAPTER 2: ON TRANSIENT PERFORMANCE IMPROVEMENT OF ADAPTIVE CONTROL ARCHITECTURES¹

While adaptive control theory has been used in numerous applications to achieve given system stabilization or command following criteria without excessive reliance on mathematical models, the ability to obtain a predictable transient performance is still an important problem – especially for applications to safety-critical systems and when there is no *a priori* knowledge on upper bounds of existing system uncertainties. To address this problem, we present a new approach to improve the transient performance of adaptive control architectures. In particular, our approach is predicated on a novel controller architecture, which involves added terms in the update law entitled *artificial basis functions*. These terms are constructed through a gradient optimization procedure to minimize the system error between an uncertain dynamical system and a given reference model during the learning phase of an adaptive controller. We provide a detailed stability analysis of the proposed approach, discuss the practical aspects of its implementation, and illustrate its efficacy on a numerical example.

2.1 Introduction

Progress in adaptive control has been made to obtain desirable tracking and stabilization specifications while relaxing dependency on model accuracy. One of the challenges in adaptive control is to obtain a predictable transient performance [35–38]. One way to address this problem is to use a high-gain learning rate in the update law which minimizes the worst-case system error between an uncertain dynamical system and a given reference model to guarantee transient performance improvement during the learning phase. Even though this can be justified theoretically (see, for example, [6]), an update law subject to a very high learning rate is not practically feasible [39, 40], since it can lead to control signals with high-frequency dynamical system content (i.e., oscillations and high-levels of measurement noise) that can violate actuator limits [31] and excite unmodeled dynamics [8] – resulting in system instability for practical applications.

¹This chapter is previously published in [75]. Permission is included in Appendix B.

The authors in [76] and [77] present high-gain adaptive controllers to subvert high-frequency dynamical system content in the control signals so that their approaches become practically feasible. Even though these approaches are promising, they require the knowledge of a (conservative) upper bound on the unknown constant gain appearing in their uncertainty parameterization. While this upper bound may be available for some applications, the actual upper bound may change and exceed its conservative estimate, for example, when an aircraft undergoes a sudden change in dynamics as a result of reconfiguration, deployment of a payload, docking, or structural damage [78]. In such circumstances, the performance of these adaptive controllers may be poor, because tuning them online with a new upper bound is not possible. Furthermore, the performance of these adaptive controllers in the face of high uncertainty levels may not be satisfactory as well, because both controllers converge to a standard adaptive controller as the upper bound on the unknown constant gain becomes arbitrarily large (see, for example, Section 2.1.2 of [76] and Section 4 of [77]). Therefore, it is important to achieve transient performance guarantees when there is no *a priori* knowledge on such uncertainty upper bounds.

In this paper, we present a new approach to improve the transient performance of adaptive control architectures. In particular, our approach is predicated on a novel controller architecture, which involves added terms in the update law entitled *artificial basis functions*. These terms are constructed through a gradient optimization procedure to minimize the system error between an uncertain dynamical system and a given reference model during the learning phase of an adaptive controller – without requiring *a priori* knowledge on upper bounds of existing system uncertainties. The proposed approach is a theoretical and practical generalization of the method presented in [79]. Theoretically, this paper provides a stability analysis that holds for a larger class of uncertain dynamical systems. Practically, it should be noted that the method in [79] requires the differentiation of the system error, however this paper provides further results to highlight how to implement the proposed approach without this requirement, which is important for real world applications. We provide a detailed stability analysis of the proposed approach, discuss the practical aspects of its implementation, and illustrate its efficacy on a numerical example. Although this paper considers a particular adaptive control formulation, namely model reference adaptive control, the presented approach can be used in a complimentary way with many other approaches to adaptive control.

The notation used in this paper is fairly standard. Specifically, \mathbb{R} denotes the set of real numbers, \mathbb{R}^n denotes the set of $n \times 1$ real column vectors, $\mathbb{R}^{n \times m}$ denotes the set of $n \times m$ real matrices, \mathbb{R}_+ (resp. $\overline{\mathbb{R}}_+$) denotes the set of positive (resp. non-negative-definite) real numbers, $\mathbb{R}_+^{n \times n}$ (resp. $\overline{\mathbb{R}}_+^{n \times n}$) denotes the set of

$n \times n$ positive-definite (resp. non-negative-definite) real matrices, $\mathbb{S}^{n \times n}$ denotes the set of $n \times n$ symmetric real matrices, $\mathbb{D}^{n \times n}$ denotes the set of $n \times n$ real matrices with diagonal scalar entries, $(\cdot)^T$ denotes transpose, $(\cdot)^{-1}$ denotes inverse, $\text{tr}(\cdot)$ denotes the trace operator, and ‘ \triangleq ’ denotes equality by definition. In addition we write $\lambda_{\min}(A)$ (respectively $\lambda_{\max}(A)$) for the minimum and respectively maximum eigenvalue of the Hermitian matrix A and $\det(A)$ for the determinant of the Hermitian matrix A . We also use $\|\cdot\|_2$ for the Euclidian norm, $\|\cdot\|_\infty$ for the infinity norm, and $\|\cdot\|_F$ for the Frobenius matrix norm. Furthermore, for the signal $x(t) = [x_1(t), x_2(t), \dots, x_n(t)]^T \in \mathbb{R}^n$ defined for all $t \geq 0$, the truncated \mathcal{L}_∞ norm and the \mathcal{L}_∞ norm are defined as $\|x_\tau(t)\|_{\mathcal{L}_\infty} \triangleq \max_{1 \leq i \leq n} (\sup_{0 \leq t \leq \tau} |x_i(t)|)$ and $\|x(t)\|_{\mathcal{L}_\infty} \triangleq \max_{1 \leq i \leq n} (\sup_{t \geq 0} |x_i(t)|)$, respectively.

The organization of this paper is as follows. Section 2.2 considers a particular adaptive control formulation, namely model reference adaptive control, and presents the preliminaries associated with this framework. Section 2.3 introduces the proposed artificial basis function approach to model reference adaptive control and then provides performance improvement and stability results in detail. We discuss the practical aspects of the proposed approach in Section 2.4 and present an illustrative example in Section 2.5. Conclusions are summarized in Section 2.6.

2.2 Mathematical Preliminaries

Consider the uncertain dynamical system given by

$$\dot{x}(t) = Ax(t) + Bu(t) + D\delta(x(t)), \quad x(0) = x_0, \quad (2.1)$$

where $x(t) \in \mathbb{R}^n$ is the state vector available for feedback, $u(t) \in \mathbb{R}^m$ is the control input, $\delta: \mathbb{R}^n \rightarrow \mathbb{R}^m$ is an uncertainty, $A \in \mathbb{R}^{n \times n}$ is a known system matrix, $B \in \mathbb{R}^{n \times m}$ is an unknown control input matrix, $D \in \mathbb{R}^{n \times m}$ is a known uncertainty input matrix, and the pair (A, B) is controllable. As standard, we assume that the uncertainty in (2.1) can be parameterized as

$$\delta(x) = W^T \sigma(x), \quad x \in \mathbb{R}^n, \quad (2.2)$$

where $W \in \mathbb{R}^{s \times m}$ is an unknown weight matrix and $\sigma: \mathbb{R}^n \rightarrow \mathbb{R}^s$ is a known basis function of the form $\sigma(x) = [\sigma_1(x), \sigma_2(x), \dots, \sigma_s(x)]^T$, and the unknown control input matrix satisfies

$$B = D\Lambda, \quad (2.3)$$

where $\det(D^T D) \neq 0$ and $\Lambda \in \mathbb{R}_+^{m \times m} \cap \mathbb{D}^{m \times m}$ is an unknown control effectiveness matrix.

Next, consider the reference system capturing a desired closed-loop dynamical system performance given by

$$\dot{x}_r(t) = A_r x_r(t) + B_r c(t), \quad x_r(0) = x_{r0}, \quad (2.4)$$

where $x_r(t) \in \mathbb{R}^n$ is the reference state vector, $c(t) \in \mathbb{R}^m$ is a given uniformly continuous bounded command, $A_r \in \mathbb{R}^{n \times n}$ is the Hurwitz reference system matrix, and $B_r \in \mathbb{R}^{n \times m}$ is the command input matrix. The objective of the model reference adaptive control problem is to construct a feedback control law $u(t)$ such that the state vector $x(t)$ asymptotically follows the reference state vector $x_r(t)$ subject to (2.2) and (2.3).

For the purpose of stating the preliminaries associated with the model reference adaptive control problem, consider the feedback control law given by

$$u(t) = u_n(t) + u_a(t), \quad (2.5)$$

where $u_n(t) \in \mathbb{R}^m$ is the nominal feedback control law and $u_a(t) \in \mathbb{R}^m$ is the adaptive feedback control law. Additionally, let the nominal feedback control law be given by

$$u_n(t) = K_1 x(t) + K_2 c(t), \quad (2.6)$$

where $K_1 \in \mathbb{R}^{m \times n}$ and $K_2 \in \mathbb{R}^{m \times m}$ are the nominal feedback and the nominal feedforward gains, respectively, such that $A_r = A + DK_1$, $B_r = DK_2$, and $\det(K_2) \neq 0$ holds. Now, using (2.5) and (2.6) in (2.1) yields

$$\dot{x}(t) = A_r x(t) + B_r c(t) + D\Lambda[u_a(t) + W_\sigma^T \sigma(x(t)) + W_{u_n}^T u_n(t)], \quad (2.7)$$

where $W_\sigma \triangleq W\Lambda^{-1} \in \mathbb{R}^{s \times m}$ and $W_{u_n} \triangleq [I - \Lambda^{-1}] \in \mathbb{D}^{m \times m}$ are unknown.

Motivating from the structure of the uncertain terms appearing in (2.7), let the adaptive feedback control law be given by

$$u_a(t) = -\hat{W}_\sigma^T(t) \sigma(x(t)) - \hat{W}_{u_n}^T(t) u_n(t), \quad (2.8)$$

where $\hat{W}_\sigma(t) \in \mathbb{R}^{s \times m}$ and $\hat{W}_{u_n}(t) \in \mathbb{R}^{m \times m}$ are the estimates of W_σ and W_{u_n} , respectively, satisfying the weight update laws

$$\dot{\hat{W}}_\sigma(t) = \gamma_\sigma \sigma(x(t)) e^T(t) P D, \quad \hat{W}_\sigma(0) = \hat{W}_{\sigma 0}, \quad (2.9)$$

$$\dot{\hat{W}}_{u_n}(t) = \gamma_{u_n} u_n(t) e^T(t) P D, \quad \hat{W}_{u_n}(0) = \hat{W}_{u_n 0}, \quad (2.10)$$

where $\gamma_\sigma \in \mathbb{R}_+^{s \times s} \cap \mathbb{S}^{s \times s}$ and $\gamma_{u_n} \in \mathbb{R}_+^{m \times m} \cap \mathbb{S}^{m \times m}$ are the learning rate matrices, $e(t) \triangleq x(t) - x_r(t)$ is the system error state vector, and $P \in \mathbb{R}_+^{n \times n} \cap \mathbb{S}^{n \times n}$ is a solution of the Lyapunov equation

$$0 = A_r^T P + P A_r + R, \quad (2.11)$$

with $R \in \mathbb{R}_+^{n \times n} \cap \mathbb{S}^{n \times n}$. Note that because A_r is Hurwitz, it follows from the converse Lyapunov theory [80] that there exists a unique P satisfying (2.11) for a given R .

Now, using (2.8) in (2.7) yields

$$\dot{x}(t) = A_r x(t) + B_r c(t) - D \Lambda [\tilde{W}_\sigma^T(t) \sigma(x(t)) + \tilde{W}_{u_n}^T(t) u_n(t)], \quad (2.12)$$

and the system error dynamics is given using (2.4) and (2.12) as

$$\dot{e}(t) = A_r e(t) - D \Lambda [\tilde{W}_\sigma^T(t) \sigma(x(t)) + \tilde{W}_{u_n}^T(t) u_n(t)], \quad e(0) = e_0, \quad (2.13)$$

where $\tilde{W}_\sigma(t) \triangleq \hat{W}_\sigma(t) - W_\sigma \in \mathbb{R}^{s \times m}$ and $\tilde{W}_{u_n}(t) \triangleq \hat{W}_{u_n}(t) - W_{u_n} \in \mathbb{R}^{m \times m}$.

Remark 2.2.1 *The weight update laws given by (2.9) and (2.10) can be derived using Lyapunov analysis by considering the Lyapunov function candidate (see, for example, [81])*

$$\mathcal{V}(e, \tilde{W}_\sigma, \tilde{W}_{u_n}) = e^T P e + \gamma_\sigma^{-1} \text{tr} (\tilde{W}_\sigma \Lambda^{1/2})^T (\tilde{W}_\sigma \Lambda^{1/2}) + \gamma_{u_n}^{-1} \text{tr} (\tilde{W}_{u_n} \Lambda^{1/2})^T (\tilde{W}_{u_n} \Lambda^{1/2}). \quad (2.14)$$

Note that $\mathcal{V}(0, 0, 0) = 0$ and $\mathcal{V}(e, \tilde{W}_\sigma, \tilde{W}_{u_n}) > 0$ for all $(e, \tilde{W}_\sigma, \tilde{W}_{u_n}) \neq (0, 0, 0)$. Now, differentiating (2.14) yields

$$\begin{aligned}\dot{\mathcal{V}}(e(t), \tilde{W}_\sigma(t), \tilde{W}_{u_n}(t)) &= -e^T(t)Re(t) - 2e^T(t)PD\Lambda\tilde{W}_\sigma^T(t)\sigma(x(t)) - 2e^T(t)PD\Lambda\tilde{W}_{u_n}^T(t)u_n(t) \\ &\quad + 2\text{tr} \tilde{W}_\sigma^T(t)\gamma_\sigma^{-1}\dot{\tilde{W}}_\sigma(t)\Lambda + 2\text{tr} \tilde{W}_{u_n}^T(t)\gamma_{u_n}^{-1}\dot{\tilde{W}}_{u_n}(t)\Lambda,\end{aligned}\quad (2.15)$$

where using (2.9) and (2.10) in (2.15) results in

$$\dot{\mathcal{V}}(e(t), \tilde{W}_\sigma(t), \tilde{W}_{u_n}(t)) = -e^T(t)Re(t) \leq 0. \quad (2.16)$$

Since (2.16) holds, it follows from (Theorem 3.1, [80]) that the solution $(e(t), \tilde{W}_\sigma(t), \tilde{W}_{u_n}(t))$ of the closed-loop dynamical system is Lyapunov stable for all initial conditions and $t \in \overline{\mathbb{R}}_+$. This implies that the terms $e(t)$, $\tilde{W}_\sigma(t)$, $\tilde{W}_{u_n}(t)$, $\sigma(x(t))$, and $u_n(t)$ are bounded in (2.13), and hence, $\dot{e}(t)$ is bounded for all $t \in \overline{\mathbb{R}}_+$. Furthermore, since $\ddot{\mathcal{V}}(e(t), \tilde{W}_\sigma(t), \tilde{W}_{u_n}(t)) = -2e^T(t)R\dot{e}(t)$, the boundedness of $\dot{e}(t)$ results in the boundedness of $\ddot{\mathcal{V}}(e(t), \tilde{W}_\sigma(t), \tilde{W}_{u_n}(t))$. It now follows from Barbalat's lemma (Lemma 4.1, [80]) that

$$\lim_{t \rightarrow \infty} \dot{\mathcal{V}}(e(t), \tilde{W}_\sigma(t), \tilde{W}_{u_n}(t)) = 0, \quad (2.17)$$

which consequently shows that $e(t) \rightarrow 0$ as $t \rightarrow \infty$.

Remark 2.2.2 For the case when the nonlinear uncertain dynamical system given by (2.1) includes bounded exogenous disturbances, measurement noise, and/or the uncertainty in (2.1) cannot be perfectly parameterized, then (2.2) can be relaxed by considering

$$\delta(t, x) = W(t)^T \sigma(x) + \varepsilon(t, x), \quad x \in \mathcal{D}_x, \quad (2.18)$$

where $W(t) \in \mathbb{R}^{s \times m}$ is an unknown time-varying weight matrix satisfying $\|W(t)\|_F \leq w$ and $\|\dot{W}(t)\|_F \leq \dot{w}$ with $w \in \mathbb{R}_+$ and $\dot{w} \in \mathbb{R}_+$ being unknown scalars, $\sigma : \mathcal{D}_x \rightarrow \mathbb{R}^s$ is a sufficiently approximated basis function on $x \in \mathcal{D}_x$ using universal approximation tools such as neural networks, $\varepsilon : \overline{\mathbb{R}}_+ \times \mathcal{D}_x \rightarrow \mathbb{R}^m$ is the system modeling error satisfying $\|\varepsilon(t, x)\|_2 \leq \varepsilon$ with $\varepsilon \in \mathbb{R}_+$ being an unknown scalar, and \mathcal{D}_x is a compact subset of \mathbb{R}^n . In this case, the weight update laws given by (2.9) and (2.10) can be replaced by

$$\dot{\hat{W}}_\sigma(t) = \gamma_\sigma \text{Proj}[\hat{W}_\sigma(t), \sigma(x(t))e^T(t)PD], \quad \hat{W}_\sigma(0) = \hat{W}_{\sigma 0}, \quad (2.19)$$

$$\dot{\hat{W}}_{u_n}(t) = \gamma_{u_n} \text{Proj}[\hat{W}_{u_n}(t), u_n(t)e^T(t)PD], \quad \hat{W}_{u_n}(0) = \hat{W}_{u_n 0}, \quad (2.20)$$

to guarantee the uniform boundedness of the system error state vector $e(t)$ and the weight errors $\tilde{W}_\sigma(t)$ and $\tilde{W}_{u_n}(t)$, where Proj denotes the projection operator [82].

Even though Remark 2.2.1 highlights that $x(t)$ asymptotically converges to $x_r(t)$, $x(t)$ can be *far different* from $x_r(t)$ during the transient time (i.e., the learning phase of the adaptive controller). To address this problem, we introduce the artificial basis function approach in the next section for transient performance improvement.

2.3 Artificial Basis Functions for Transient Performance Improvement

In this section, we develop a new approach entitled *artificial basis functions* to improve the transient performance of the model reference adaptive control framework introduced in Section 2. In order to introduce our approach, we first write

$$\dot{e}(t) = A_r e(t) + D\Lambda[u_a(t) + W_\sigma^T \sigma(x(t)) + W_{u_n}^T u_n(t)], \quad e(0) = e_0. \quad (2.21)$$

using (2.4) and (2.7). Next, we add a new term “ $W_a^T \sigma_a(t)$ ” to (2.21) as

$$\dot{e}(t) = A_r e(t) + D\Lambda[u_a(t) + W_\sigma^T \sigma(x(t)) + W_{u_n}^T u_n(t) + W_a^T \sigma_a(t)], \quad e(0) = e_0, \quad (2.22)$$

where we set $W_a \equiv 0$ in this term so that (2.21) and (2.22) are equivalent. Since the added term “ $W_a^T \sigma_a(t)$ ” is zero by definition and it does not change the error dynamics, we call $W_a \in \mathbb{R}^{m \times q}$ as the *artificial weighting* and $\sigma_a(t) \in \mathbb{R}^q$ as the *artificial basis function*. Considering (2.22), we now let the new adaptive feedback control law be

$$u_a(t) = -\hat{W}_\sigma^T(t) \sigma(x(t)) - \hat{W}_{u_n}^T(t) u_n(t) - \hat{W}_a^T(t) \sigma_a(t), \quad (2.23)$$

with $\hat{W}_a(t) \in \mathbb{R}^{m \times q}$, which yields

$$\dot{e}(t) = A_r e(t) - D\Lambda[\tilde{W}_\sigma^T(t) \sigma(x(t)) + \tilde{W}_{u_n}^T(t) u_n(t) + \tilde{W}_a^T(t) \sigma_a(t)], \quad e(0) = e_0, \quad (2.24)$$

where $\tilde{W}_\sigma(t) \triangleq \hat{W}_\sigma(t) - W_\sigma \in \mathbb{R}^{s \times m}$, $\tilde{W}_{u_n}(t) \triangleq \hat{W}_{u_n}(t) - W_{u_n} \in \mathbb{R}^{m \times m}$, and $\tilde{W}_a(t) \triangleq \hat{W}_a(t) - W_a \in \mathbb{R}^{m \times q}$ (note that $\tilde{W}_a(t) = \hat{W}_a(t)$ since $W_a \equiv 0$). In the rest of this section, we choose the update laws for the artificial

basis function $\sigma_a(t)$ and the artificial weight update law $\hat{W}_a(t)$ in the proposed adaptive feedback control law (2.23) in order to improve the transient performance without sacrificing the asymptotic stability of the closed-loop system error dynamics in (2.24). To this end, the following two theorems present the main results of this section.

Theorem 2.3.1 Consider the system error dynamics given by (2.24) and the artificial basis function update law given by

$$\dot{\sigma}_a(t) = k\hat{W}_a(t)(D^T D)^{-1}D^T[\dot{e}(t) - A_r e(t)], \quad \sigma_a(0) = \sigma_{a0} \neq 0. \quad (2.25)$$

where $k \in \mathbb{R}_+$. Then, (2.25) is constructed through the negative gradient of

$$\mathcal{J}(\cdot) = \frac{1}{2} \|\Lambda^{1/2}(\tilde{W}_\sigma^T(t)\sigma(x(t)) + \tilde{W}_{u_n}^T u_n(t) + \tilde{W}_a^T(t)\sigma_a(t))\|_2^2, \quad (2.26)$$

with respect to $\sigma_a(t)$.

Proof. Consider the cost function given by (2.26) and note that its gradient with respect to $\sigma_a(t)$ has the form

$$\begin{aligned} \frac{\partial[-\mathcal{J}(\cdot)]}{\partial\sigma_a(t)} &= -\tilde{W}_a(t)\Lambda[\tilde{W}_\sigma^T(t)\sigma(x(t)) + \tilde{W}_{u_n}^T u_n(t) + \tilde{W}_a^T(t)\sigma_a(t)] \\ &= -\hat{W}_a(t)\Lambda[\tilde{W}_\sigma^T(t)\sigma(x(t)) + \tilde{W}_{u_n}^T u_n(t) + \tilde{W}_a^T(t)\sigma_a(t)], \end{aligned} \quad (2.27)$$

since $W_a \equiv 0$. Using the idea presented in [46, 83, 84], we now construct the update law for the artificial basis function as

$$\begin{aligned} \dot{\sigma}_a(t) &= k \frac{\partial[-\mathcal{J}(\cdot)]}{\partial\sigma_a(t)} \\ &= -k\hat{W}_a(t)\Lambda[\tilde{W}_\sigma^T(t)\sigma(x(t)) + \tilde{W}_{u_n}^T u_n(t) + \tilde{W}_a^T(t)\sigma_a(t)], \quad \sigma_a(0) = \sigma_{a0}. \end{aligned} \quad (2.28)$$

Here, one can notice that (2.28) has unknown terms (i.e., Λ is unknown and the first two terms inside the brackets are unknown since $W_\sigma \in \mathbb{R}^{s \times m}$ and $W_{u_n} \in \mathbb{R}^{m \times m}$ are unknown in $\tilde{W}_\sigma(t) = \hat{W}_\sigma(t) - W_\sigma \in \mathbb{R}^{s \times m}$ and $\tilde{W}_{u_n}(t) = \hat{W}_{u_n}(t) - W_{u_n} \in \mathbb{R}^{m \times m}$, respectively), and hence, it can not be implemented. To address this

problem, (2.24) can be rewritten as

$$-\Lambda[\tilde{W}_\sigma^T(t)\sigma(x(t)) + \tilde{W}_{u_n}^T u_n(t) + \tilde{W}_a^T(t)\sigma_a(t)] = (D^T D)^{-1} D^T [\dot{e}(t) - A_r e(t)]. \quad (2.29)$$

Since (2.28) along with (2.29) leads to the artificial basis function update law given by (2.25), it follows that (2.25) is the negative gradient of (2.26). ■

Remark 2.3.1 *The unknown magnitude of the mismatch term*

$$\tilde{W}_\sigma^T(t)\sigma(x(t)) + \tilde{W}_{u_n}^T u_n(t) + \tilde{W}_a^T(t)\sigma_a(t), \quad (2.30)$$

in (2.24) can lead to a large deviation of the state from the reference state during the learning phase of the adaptive controller given by (2.23). From this standpoint, the proposed artificial basis function allows to shape the system error by suppressing the mismatch term (2.30) in (2.24) due to gradient optimization, since it is constructed to be the negative gradient of (2.26) with respect to $\sigma_a(t)$ (see, for example, [46, 83, 84] and references included therein on other applications of gradient optimization in the context of adaptive control). Therefore, by adjusting k in (2.25), the uncertain dynamical system response and the reference system response can be made close to each other for all time including the transient phase.

Remark 2.3.2 *Even though the artificial basis function update law given by (2.25) has the time derivative of the system error on its right hand side, we will see in Corollary 2.4.1 of the next section that we can use an equivalent form of this update law without requiring this time derivative for real-world applications.*

In Theorem 2.3.1, we developed an update law for the artificial basis function in order to improve the transient performance of the system error dynamics. In the next theorem, we choose an appropriate artificial weight update law $\hat{W}_a(t)$ (and also update laws for $\hat{W}_\sigma(t)$ and $\hat{W}_{u_n}(t)$) to guarantee the asymptotic stability of the closed-loop system error dynamics in (2.24). We will also show the transient performance bounds satisfied by the system error dynamics.

Theorem 2.3.2 *Consider the nonlinear uncertain dynamical system given by (2.1), the reference system given by (2.4), the feedback control law given by (2.23) along with the update laws given by (2.25) and*

$$\dot{\hat{W}}_{\sigma}(t) = \gamma_{\sigma} \left[\sigma(x(t))e^T(t)PD + \mu\sigma(x(t))\sigma_a^T(t)\hat{W}_a(t) \right], \quad \hat{W}_{\sigma}(0) = \hat{W}_{\sigma 0}, \quad (2.31)$$

$$\dot{\hat{W}}_{u_n}(t) = \gamma_{u_n} \left[u_n(t)e^T(t)PD + \mu u_n(t)\sigma_a^T(t)\hat{W}_a(t) \right], \quad \hat{W}_{\sigma}(0) = \hat{W}_{\sigma 0}, \quad (2.32)$$

$$\dot{\hat{W}}_a(t) = \gamma_a \sigma_a(t)e^T(t)PD, \quad \hat{W}_a(0) = \hat{W}_{a0} \neq 0, \quad (2.33)$$

where $\gamma_{\sigma} \in \mathbb{R}_+$, $\gamma_{u_n} \in \mathbb{R}_+$, $\gamma_a \in \mathbb{R}_+$, and $\mu \in \mathbb{R}_+$. Then, the solution $(e(t), \tilde{W}_{\sigma}(t), \tilde{W}_{u_n}(t), \tilde{W}_a(t), \sigma_a(t))$ of the closed-loop dynamical system is Lyapunov stable for all initial conditions and $t \in \bar{\mathbb{R}}_+$, and $\lim_{t \rightarrow \infty} e(t) = 0$. In addition, the system error dynamics satisfy the transient performance bounds given by

$$\|e(t)\|_{\mathcal{L}_{\infty}} \leq \sqrt{\varepsilon/\lambda_{\min}(P)}, \quad (2.34)$$

where

$$\varepsilon \triangleq \lambda_{\max}(P)\|e(0)\|_2^2 + \gamma_{\sigma}^{-1}\|\tilde{W}_{\sigma 0}\Lambda^{1/2}\|_F^2 + \gamma_{u_n}^{-1}\|\tilde{W}_{u_n 0}\Lambda^{1/2}\|_F^2 + \gamma_a^{-1}\|\tilde{W}_{a0}\Lambda^{1/2}\|_F^2 + k^{-1}\|\sigma_a(0)\|_2^2. \quad (2.35)$$

Proof. Consider the Lyapunov function candidate given by

$$\begin{aligned} \mathcal{V}(e, \tilde{W}_{\sigma}, \tilde{W}_{u_n}, \tilde{W}_a, \sigma_a) &= e^T P e + \gamma_{\sigma}^{-1} \text{tr} \left(\tilde{W}_{\sigma} \Lambda^{1/2} \right)^T \left(\tilde{W}_{\sigma} \Lambda^{1/2} \right) + \gamma_{u_n}^{-1} \text{tr} \left(\tilde{W}_{u_n} \Lambda^{1/2} \right)^T \left(\tilde{W}_{u_n} \Lambda^{1/2} \right) \\ &\quad + \gamma_a^{-1} \text{tr} \left(\tilde{W}_a \Lambda^{1/2} \right)^T \left(\tilde{W}_a \Lambda^{1/2} \right) + \mu k^{-1} \sigma_a^T \sigma_a, \end{aligned} \quad (2.36)$$

where $\mathcal{V}(0, 0, 0, 0, 0) = 0$ and $\mathcal{V}(e, \tilde{W}_{\sigma}, \tilde{W}_{u_n}, \tilde{W}_a, \sigma_a) > 0$ for all $(e, \tilde{W}_{\sigma}, \tilde{W}_{u_n}, \tilde{W}_a, \sigma_a) \neq (0, 0, 0, 0, 0)$. It follows that

$$\begin{aligned} \dot{\mathcal{V}}(e(t), \tilde{W}_{\sigma}(t), \tilde{W}_{u_n}(t), \tilde{W}_a(t), \sigma_a(t)) &= 2e^T(t)P\dot{e}(t) + 2\gamma_{\sigma}^{-1} \text{tr} \tilde{W}_{\sigma}^T(t)\Lambda\dot{\tilde{W}}_{\sigma}(t) + 2\gamma_{u_n}^{-1} \text{tr} \tilde{W}_{u_n}(t)\Lambda\dot{\tilde{W}}_{u_n}(t) \\ &\quad + 2\gamma_a^{-1} \text{tr} \tilde{W}_a^T(t)\Lambda\dot{\tilde{W}}_a(t) + 2\mu k^{-1} \sigma_a^T(t)\dot{\sigma}_a(t) \\ &= -e^T(t)R e(t) - 2\mu \sigma_a^T(t)\tilde{W}_a(t)\Lambda\tilde{W}_a^T(t)\sigma_a(t) \\ &\leq -e^T(t)R e(t) \leq 0, \quad t \in \bar{\mathbb{R}}_+, \end{aligned} \quad (2.37)$$

which guarantees that $(e(t), \tilde{W}_{\sigma}(t), \tilde{W}_{u_n}(t), \tilde{W}_a(t), \sigma_a(t))$ is Lyapunov stable, and hence, is bounded for all $t \in \bar{\mathbb{R}}_+$. Since $\sigma(x(t))$, $u_n(t)$, and $\sigma_a(t)$ are bounded for all $t \in \bar{\mathbb{R}}_+$, it follows from (2.24) that $\dot{e}(t)$ is bounded,

and hence, $\dot{\mathcal{V}}(e(t), \tilde{W}_\sigma(t), \tilde{W}_{u_n}(t), \tilde{W}_a(t), \sigma_a(t))$ is bounded for all $t \in \overline{\mathbb{R}}_+$. Then according to Barbalat's lemma

$$\lim_{t \rightarrow \infty} \dot{\mathcal{V}}(e(t), \tilde{W}_\sigma(t), \tilde{W}_{u_n}(t), \tilde{W}_a(t), \sigma_a(t)) = 0, \quad (2.38)$$

which consequently shows that $e(t) \rightarrow 0$ as $t \rightarrow \infty$.

Additionally, because $\dot{\mathcal{V}}(e(t), \tilde{W}_\sigma(t), \tilde{W}_{u_n}(t), \tilde{W}_a(t), \sigma_a(t)) \leq 0$ for $t \in \overline{\mathbb{R}}_+$, this implies that

$$\mathcal{V}(e(t), \tilde{W}_\sigma(t), \tilde{W}_{u_n}(t), \tilde{W}_a(t), \sigma_a(t)) \leq \mathcal{V}(e(0), \tilde{W}_{\sigma 0}, \tilde{W}_{u_n 0}, \tilde{W}_{a 0}, \sigma_a(0)). \quad (2.39)$$

Then using the inequalities

$$\lambda_{\min}(P) \|e(t)\|_2^2 \leq \mathcal{V}(e(t), \tilde{W}_\sigma(t), \tilde{W}_{u_n}(t), \tilde{W}_a(t), \sigma_a(t)) \quad (2.40)$$

and

$$\begin{aligned} \mathcal{V}(e(0), \tilde{W}_{\sigma 0}, \tilde{W}_{u_n 0}, \tilde{W}_{a 0}, \sigma_a(0)) &\leq \lambda_{\max}(P) \|e(0)\|_2^2 + \gamma_\sigma^{-1} \|\tilde{W}_{\sigma 0} \Lambda^{1/2}\|_{\mathbb{F}}^2 + \gamma_{u_n}^{-1} \|\tilde{W}_{u_n 0} \Lambda^{1/2}\|_{\mathbb{F}}^2 \\ &\quad + \gamma_a^{-1} \|\tilde{W}_{a 0} \Lambda^{1/2}\|_{\mathbb{F}}^2 + k^{-1} \|\sigma_a(0)\|_2^2 \end{aligned} \quad (2.41)$$

in (2.39) results in

$$\|e(t)\|_2 \leq \sqrt{\varepsilon / \lambda_{\min}(P)}. \quad (2.42)$$

Since $\|\cdot\|_\infty \leq \|\cdot\|_2$, and this bound is uniform, then (2.42) yields

$$\|e_\tau(t)\|_{\mathcal{L}_\infty} \leq \sqrt{\varepsilon / \lambda_{\min}(P)} \quad (2.43)$$

therefore, (2.34) is a direct consequence of (2.43) because (2.43) holds uniformly in τ . ■

2.4 Practical Considerations

In Theorem 2.3.1 of the previous section, it is noted that (2.25) presents the update law for the artificial basis function that contains the time derivative of the system error in its right hand side. In practice,

it is desired to remove this term from the update law. Motivating from the methods used in [85], the next corollary presents an *equivalent* form of the update law in (2.25), but *without* the time derivative of the system error.

Corollary 2.4.1 *The update law for the artificial basis function given by (2.25) is identical to*

$$\begin{aligned} \sigma_a(t) = & \sigma_a(0) + k \left[\left(\hat{W}_a(t)(D^T D)^{-1} D^T e(t) - \hat{W}_a(0)(D^T D)^{-1} D^T e(0) \right) \right. \\ & \left. - \int_0^t \gamma_a \sigma_a(\tau) e^T(\tau) P D (D^T D)^{-1} D^T e(\tau) d\tau - \int_0^t \hat{W}_a(\tau)(D^T D)^{-1} D^T A_r e(\tau) d\tau \right]. \end{aligned} \quad (2.44)$$

Proof. To show that (2.25) is equivalent to (2.44), we first integrate both sides of (2.25) as

$$\int_0^t \frac{d\sigma_a}{d\tau} d\tau = k \left[\int_0^t \hat{W}_a(\tau)(D^T D)^{-1} D^T \frac{de(\tau)}{d\tau} d\tau - \int_0^t \hat{W}_a(\tau)(D^T D)^{-1} D^T A_r e(\tau) d\tau \right], \quad (2.45)$$

where k is constant. The first term on the right hand side of (2.45) can then be manipulated using integration by parts of the form

$$\int U dV = UV - \int dUV, \quad (2.46)$$

with $U = \hat{W}_a(\tau)(D^T D)^{-1} D^T$ and $V = e(\tau)$, and respectively $dU = \dot{\hat{W}}_a(\tau)(D^T D)^{-1} D^T d\tau$ and $dV = \frac{de(\tau)}{d\tau} d\tau$.

This produces an equivalent term of the form

$$\hat{W}_a(t)(D^T D)^{-1} D^T e(t) - \hat{W}_a(0)(D^T D)^{-1} D^T e(0) - \int_0^t \dot{\hat{W}}_a(\tau)(D^T D)^{-1} D^T e(\tau) d\tau, \quad (2.47)$$

that does not contain the time derivative of the system error. We can further expand this using (2.33) as

$$\hat{W}_a(t)(D^T D)^{-1} D^T e(t) - \hat{W}_a(0)(D^T D)^{-1} D^T e(0) - \int_0^t \gamma_a \sigma_a(\tau) e^T(\tau) P D (D^T D)^{-1} D^T e(\tau) d\tau. \quad (2.48)$$

Using (2.48) instead of the first term on the right hand side of (2.38) and integrating the left hand side yields

$$\begin{aligned}
\sigma_a(t) - \sigma_a(0) &= k \left[\left(\hat{W}_a(t)(D^T D)^{-1} D^T e(t) - \hat{W}_a(0)(D^T D)^{-1} D^T e(0) \right) \right. \\
&\quad - \int_0^t \gamma_a \sigma_a(\tau) e^T(\tau) P D (D^T D)^{-1} D^T e(\tau) d\tau \\
&\quad \left. - \int_0^t \hat{W}_a(\tau) (D^T D)^{-1} D^T A_r e(\tau) d\tau \right]. \tag{2.49}
\end{aligned}$$

Adding the initial condition $\sigma_a(0)$ to both sides concludes the proof. ■

Since the update law of the artificial basis function given by (2.25), or equivalently (2.44), is derived through a gradient optimization procedure, it may (or may not) induce oscillations to the system response as the value of k gets large. Even though we did *not* observe such a oscillative system response in the illustrative example of the next section (as well as in applications to various uncertain dynamical systems); if such a situation happens, then it is of practical importance to robustify the proposed approach against such oscillative (i.e., high-frequency) dynamical system content. To this end, one can adopt, for example, the *low-frequency learning* idea of [35] to achieve *both* improved transient performance and smooth system behavior. This is highlighted in the next corollary.

Corollary 2.4.2 *Consider the nonlinear uncertain dynamical system given by (2.1), the reference system given by (2.4), the feedback control law given by (2.23) along with the weight update laws given by (2.31), (2.32), (2.33),*

$$\dot{\sigma}_a(t) = k \hat{W}_a(t) (D^T D)^{-1} D^T [\dot{e}(t) - A_r e(t)] - c_1 (\sigma_a(t) - \sigma_{af}(t)), \tag{2.50}$$

and

$$\dot{\sigma}_{af}(t) = -c_2 (\sigma_{af}(t) - \sigma_a(t)), \tag{2.51}$$

where $c_1 \in \mathbb{R}_+$, and $c_2 \in \mathbb{R}_+$. Then the solution $(e(t), \tilde{W}_\sigma(t), \tilde{W}_{u_n}(t), \tilde{W}_a(t), \sigma_a(t), \sigma_{af}(t))$ of the closed-loop system given by (2.24), (2.31), (2.32), (2.33), (2.50), and (2.51) is Lyapunov stable for all initial conditions and $t \in \bar{\mathbb{R}}_+$, and $\lim_{t \rightarrow \infty} e(t) = 0$.

Proof. Considering the Lyapunov function candidate given by

$$\begin{aligned}
\mathcal{V}(e, \tilde{W}_\sigma, \tilde{W}_{u_n}, \tilde{W}_a, \sigma_a, \sigma_{af}) &= e^T P e + \gamma_\sigma^{-1} \text{tr} \left(\tilde{W}_\sigma \Lambda^{1/2} \right)^T \left(\tilde{W}_\sigma \Lambda^{1/2} \right) + \gamma_{u_n}^{-1} \text{tr} \left(\tilde{W}_{u_n} \Lambda^{1/2} \right)^T \left(\tilde{W}_{u_n} \Lambda^{1/2} \right) \\
&\quad + \gamma_a^{-1} \text{tr} \left(\tilde{W}_a \Lambda^{1/2} \right)^T \left(\tilde{W}_a \Lambda^{1/2} \right) + \mu k^{-1} \sigma_a^T \sigma_a + c_2^{-1} \mu k^{-1} c_1 \sigma_{af}^T \sigma_{af}, \tag{2.52}
\end{aligned}$$

where $\mathcal{V}(0,0,0,0,0,0) = 0$ and $\mathcal{V}(e, \tilde{W}_\sigma, \tilde{W}_{u_n}, \tilde{W}_a, \sigma_a, \sigma_{af}) > 0$ for all $(e, \tilde{W}_\sigma, \tilde{W}_{u_n}, \tilde{W}_a, \sigma_a, \sigma_{af}) \neq (0,0,0,0,0,0)$. Differentiating (2.52) along the closed-loop system trajectories of (2.24), (2.31), (2.32), (2.33), (2.50), and (2.51) yields

$$\begin{aligned} \dot{\mathcal{V}}(e(t), \tilde{W}_\sigma(t), \tilde{W}_{u_n}(t), \tilde{W}_a(t), \sigma_a(t), \sigma_{af}(t)) &= -e^T(t)Re(t) - 2\mu\sigma_a^T(t)\tilde{W}_a(t)\Lambda\tilde{W}_a^T(t)\sigma_a(t) \\ &\quad - 2\mu k^{-1}c_1(\sigma_a(t) - \sigma_{af}(t))^T(\sigma_a(t) - \sigma_{af}(t)) \\ &\leq -e^T(t)Re(t) \leq 0, \quad t \in \bar{\mathbb{R}}_+. \end{aligned} \quad (2.53)$$

Hence it is guaranteed that the closed-loop dynamical system given by (2.24), (2.31), (2.32), (2.33), (2.50), and (2.51) is Lyapunov stable, and therefore bounded for all $t \in \bar{\mathbb{R}}_+$. Since $\sigma(x(t))$, $u_n(t)$, and $\sigma_a(t)$ are bounded for all $t \in \bar{\mathbb{R}}_+$, it follows from (2.24) that $\dot{e}(t)$ is bounded, and hence, $\dot{\mathcal{V}}(e(t), \tilde{W}_\sigma(t), \tilde{W}_{u_n}(t), \tilde{W}_a(t), \sigma_a(t), \sigma_{af}(t))$ is bounded for all $t \in \bar{\mathbb{R}}_+$. It then follows from Barbalat's lemma that

$$\lim_{t \rightarrow \infty} \dot{\mathcal{V}}(e(t), \tilde{W}_\sigma(t), \tilde{W}_{u_n}(t), \tilde{W}_a(t), \sigma_a(t), \sigma_{af}(t)) = 0, \quad (2.54)$$

which consequently shows that $e(t) \rightarrow 0$ as $t \rightarrow \infty$. ■

It should be noted that using similar steps highlighted in Corollary 2.4.1, (2.50) can be equivalently written as

$$\begin{aligned} \sigma_a(t) &= \sigma_a(0) + k \left[\left(\hat{W}_a(t)(D^T D)^{-1} D^T e(t) - \hat{W}_a(0)(D^T D)^{-1} D^T e(0) \right) \right. \\ &\quad \left. - \int_0^t \gamma_a \sigma_a(\tau) e^T(\tau) P D (D^T D)^{-1} D^T e(\tau) d\tau - \int_0^t \hat{W}_a(\tau) (D^T D)^{-1} D^T A_r e(\tau) d\tau \right] \\ &\quad - \int_0^t c_1 (\sigma_a(\tau) - \sigma_{af}(\tau)) d\tau, \end{aligned} \quad (2.55)$$

without the time derivative of the system error.

Remark 2.4.1 *Following the discussion stated before Corollary 2.4.2, the added term to the right hand side of (2.50) (or equivalently (2.55)) filters out possible high-frequency dynamical system content in $\sigma_a(t)$ (while preserving asymptotic stability of the system error dynamics) as one increases the design parameter c_1 for driving the trajectories of $\sigma_a(t)$ closer to the trajectories of $\sigma_{af}(t)$. Note that the frequency content of such possible high-frequency oscillations that one desires to suppress is defined through the design parameter c_2 in (2.51), which denotes the bandwidth of $\sigma_{af}(t)$ (we refer to [35] for additional technical details and discussions).*

2.5 Illustrative Example

In order to illustrate the proposed adaptive control architecture based on artificial basis functions, consider the nonlinear dynamical system representing a controlled wing rock dynamics model given by

$$\dot{x}_1(t) = x_2(t), \quad x_1(0) = 0, \quad (2.56)$$

$$\dot{x}_2(t) = \Lambda u(t) + \delta(x(t)), \quad x_2(0) = 0, \quad (2.57)$$

where x_1 represents the roll angle in radians and x_2 represents the roll rate in radians per second. In (2.57), $\delta(x)$ represents an uncertainty of the form $\delta(x) = \alpha_1 x_1 + \alpha_2 x_2 + \alpha_3 |x_1| x_2 + \alpha_4 |x_2| x_2 + \alpha_5 x_1^3$, where α_i , $i = 1, \dots, 5$, are unknown parameters that are derived from the aircraft aerodynamic coefficients. For our numerical example, we set $\alpha_1 = 0.1414$, $\alpha_2 = 0.5504$, $\alpha_3 = -0.0624$, $\alpha_4 = 0.0095$, $\alpha_5 = 0.0215$, and $\Lambda = 0.5$. We choose $K_1 = [-0.16, -0.57]$ and $K_2 = 0.16$ for the nominal controller design that yields to a reference system with a natural frequency of $\omega_n = 0.40$ rad/s and a damping ratio $\zeta = 0.707$. For the standard adaptive controller design given by (2.5), (2.6), (2.8), (2.9), and (2.10)), $\sigma(x) = [x_1, x_2, |x_1| x_2, |x_2| x_2, x_1^3]^T$ is used for the basis function and we set $R = I_2$. For the proposed adaptive controller design given by (2.5), (2.6), (2.23), (2.31), (2.32), (2.33), and (2.44), we use the same basis function and R as well as $q = 1$ is chosen implying the artificial basis function is one-dimensional.

Figures 2.1–2.6 compare the standard control design with the proposed design for a given square-wave tracking command. In particular, Figures 2.1–2.3 show the standard model reference adaptive control design with adaptation gains of $\gamma_\sigma = \gamma_{u_n} = 0.5, 10, \text{ and } 50$, respectively. The higher adaptation gain used in Figure 2.3 yields to a better system performance pertaining to the roll angle, but it is not acceptable due to the oscillative content in the roll rate response and the control response. Figures 2.4–2.6 show the proposed design with the smallest adaptation gain used for the standard design, i.e., $\gamma_\sigma = 0.5$. As we increase k from 5 to 25, and then 25 to 100, these figures clearly highlight the improvement on the transient performance due to the nature of gradient optimization. In other words, the results with the proposed adaptive controller design, especially the ones in Figures 2.5 and 2.6, are superior as compared with the standard ones.

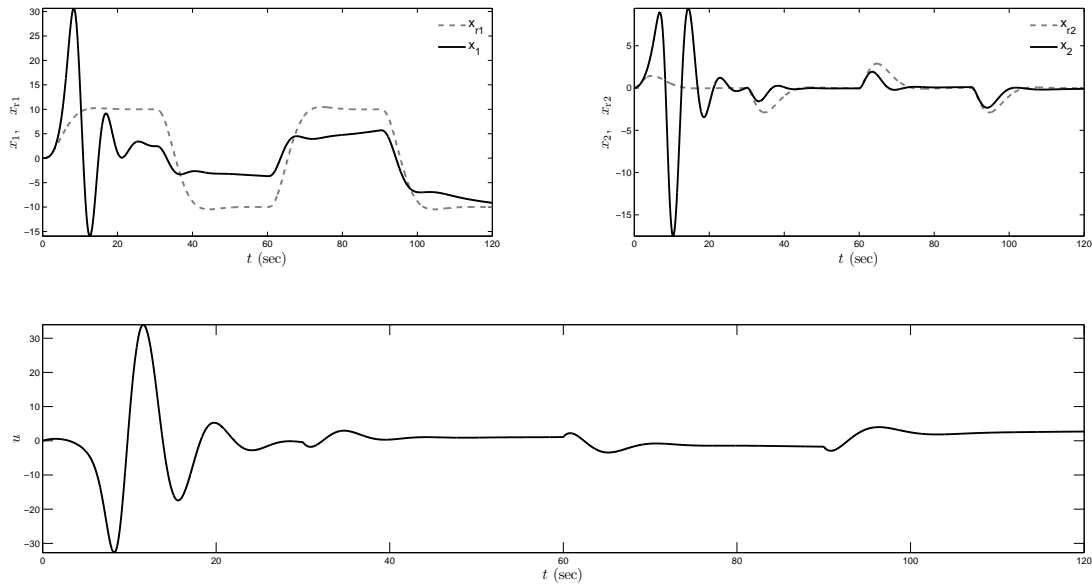


Figure 2.1: Standard adaptive control performance with (2.5), (2.6), (2.8), (2.9), and (2.10) for a given square-wave tracking command ($\gamma_\sigma = 0.5$ and $\gamma_{u_n} = 0.5$).

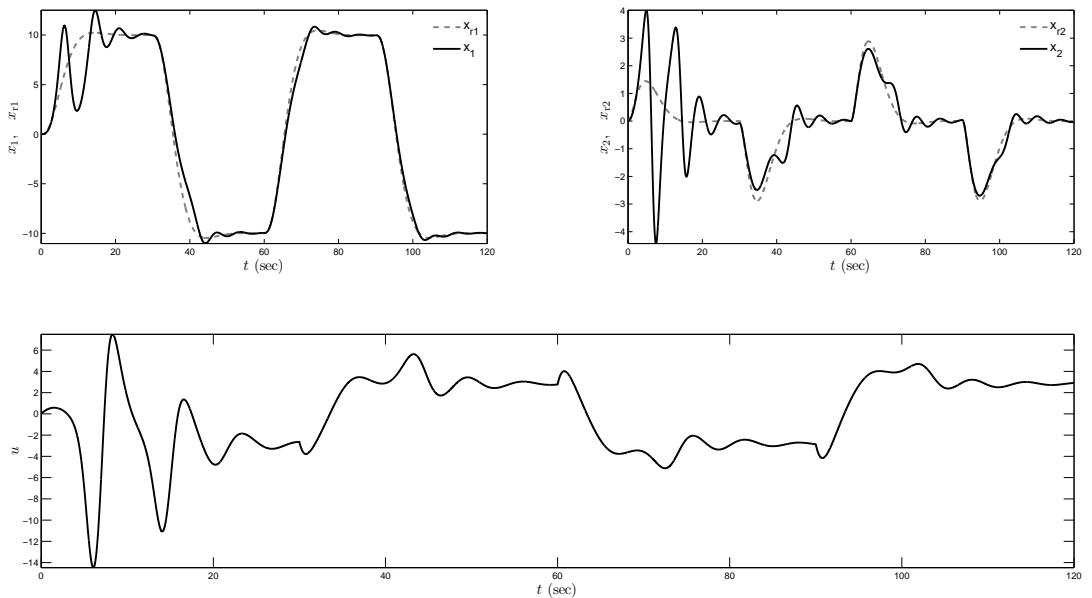


Figure 2.2: Standard adaptive control performance with (2.5), (2.6), (2.8), (2.9), and (2.10) for a given square-wave tracking command ($\gamma_\sigma = 10$ and $\gamma_{u_n} = 10$).

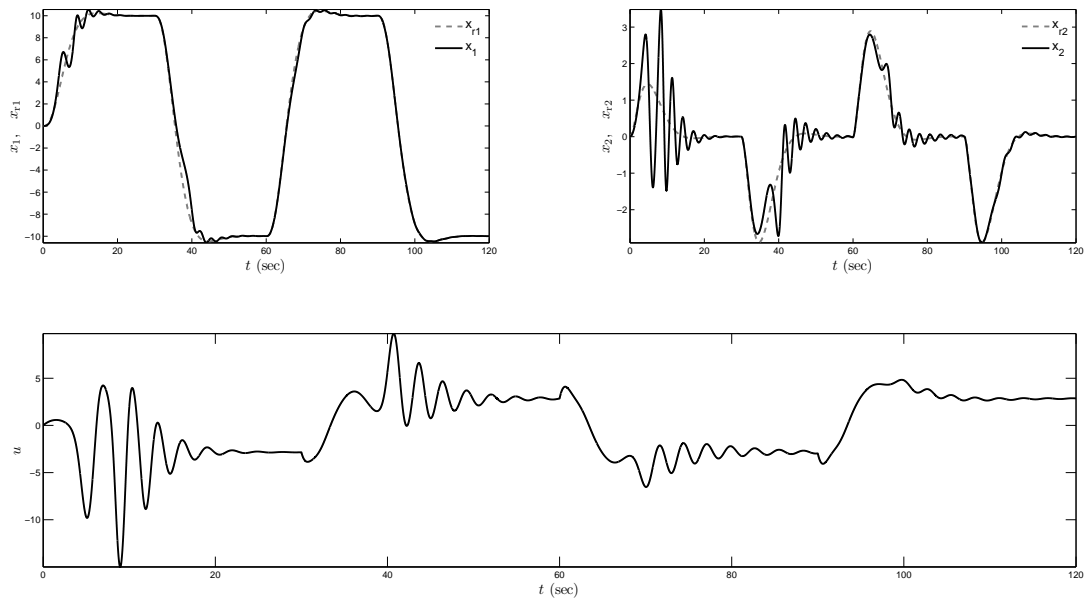


Figure 2.3: Standard adaptive control performance with (2.5), (2.6), (2.8), (2.9), and (2.10) for a given square-wave tracking command ($\gamma_\sigma = 50$ and $\gamma_{u_n} = 50$).

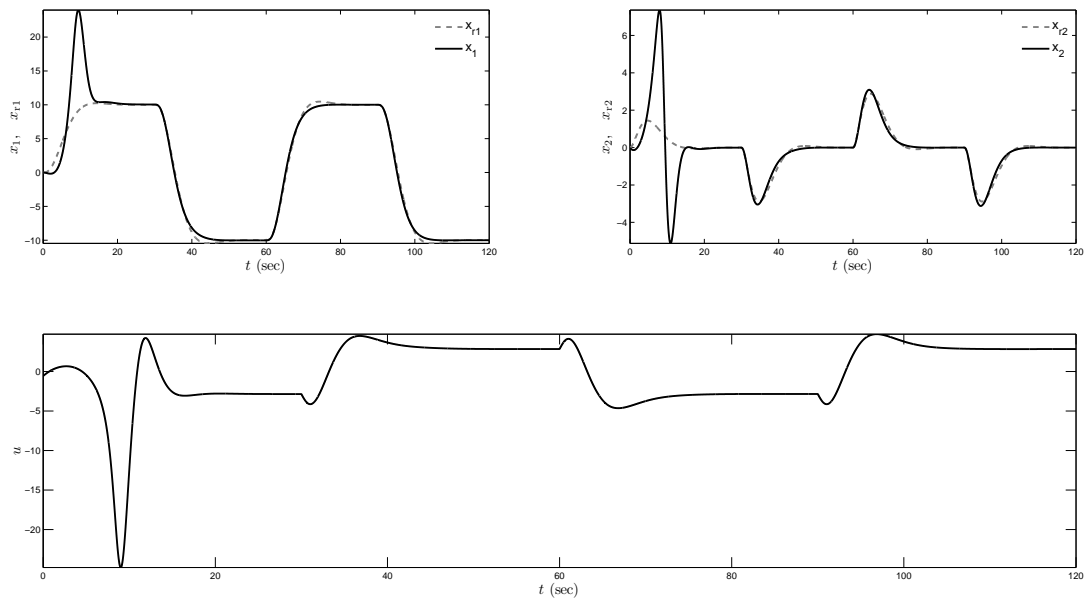


Figure 2.4: Proposed adaptive control performance with (2.5), (2.6), (2.23), (2.31), (2.32), (2.33), and (2.44) for a given square-wave tracking command ($\hat{W}_{a0} = 0.1$, $\sigma_{a0} = 0.1$, $\gamma_\sigma = 0.5$, $\gamma_{u_n} = 1$, $\gamma_a = 1$, $k = 5$, and $\mu = 1$).

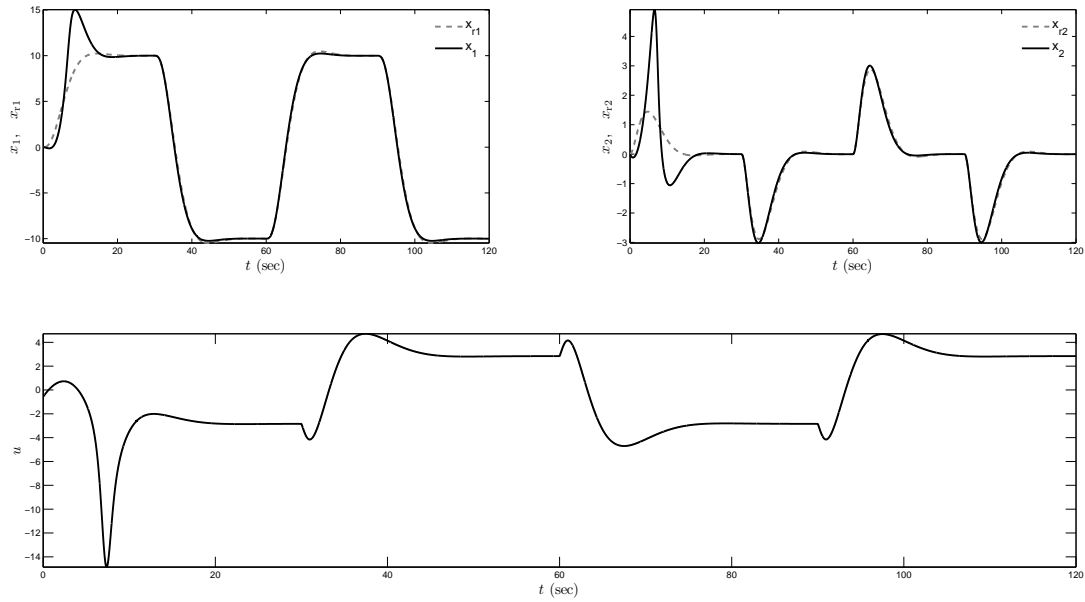


Figure 2.5: Proposed adaptive control performance with (2.5), (2.6), (2.23), (2.31), (2.32), (2.33), and (2.44) for a given square-wave tracking command ($\hat{W}_{a0} = 0.1$, $\sigma_{a0} = 0.1$, $\gamma_{\sigma} = 0.5$, $\gamma_{u_n} = 1$, $\gamma_a = 1$, $k = 25$, and $\mu = 1$).

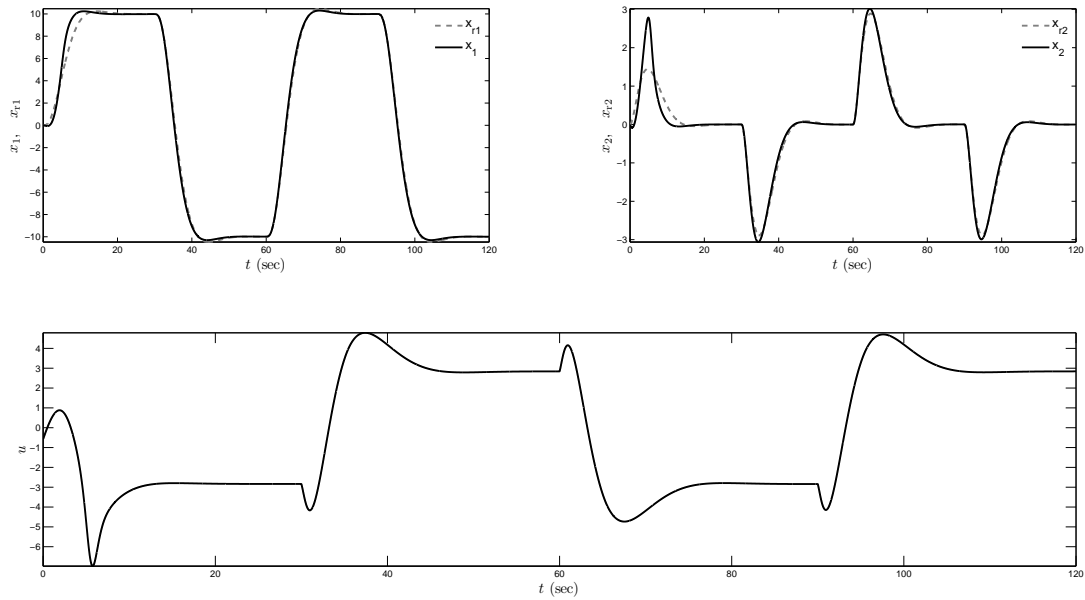


Figure 2.6: Proposed adaptive control performance with (2.5), (2.6), (2.23), (2.31), (2.32), (2.33), and (2.44) for a given square-wave tracking command ($\hat{W}_{a0} = 0.1$, $\sigma_{a0} = 0.1$, $\gamma_{\sigma} = 0.5$, $\gamma_{u_n} = 1$, $\gamma_a = 1$, $k = 100$, and $\mu = 1$).

2.6 Conclusion

To contribute to the previous studies in adaptive control theory, we investigated a new approach based on artificial basis functions. Specifically, we showed that these functions, which are constructed based on gradient optimization, can improve the transient response of an adaptively controlled system, and hence, can be used to achieve predictable closed-loop system performance. We further discussed in detail regarding the practical aspects of the proposed design and included a detailed illustrative example. Future research will include extensions to uncertain dynamical systems with limited state information (i.e., output feedback adaptive control), state constraints, and control constraints.

CHAPTER 3: DIRECT UNCERTAINTY MINIMIZATION FRAMEWORK FOR SYSTEM PERFORMANCE IMPROVEMENT IN MODEL REFERENCE ADAPTIVE CONTROL¹

In this paper, a direct uncertainty minimization framework is developed and demonstrated for model reference adaptive control laws. The proposed framework consists of a novel architecture involving modification terms in the adaptive control law and the update law. In particular, these terms are constructed through a gradient minimization procedure in order to achieve improved closed-loop system performance with adaptive control laws. The proposed framework is first developed for adaptive control laws with linear reference models and then generalized to adaptive control laws with nonlinear reference models. Two illustrative numerical examples and experimental results are included to demonstrate the efficacy of the proposed framework.

3.1 Introduction

Research in adaptive control algorithms is primarily motivated by the fact that these algorithms have the capability to estimate and suppress the effect of system uncertainties resulting from imperfect system modeling, degraded modes of operation, abrupt changes in dynamics, damaged control surfaces, and sensor failures; to name but a few examples. Although government and industry agree on the potential of these algorithms in providing safety and reducing system development costs, a major issue is their poor transient performance.

To address this problem, authors of [41–48] present modifications to adaptive update laws. In particular, the work in [41–43] uses filtered versions of the control input and state, [44–46] uses a moving time window of the system uncertainty, and [47, 48] uses recorded and instantaneous data concurrently. In contrast to these approaches, the authors of [75, 79, 87] present an approach called *artificial basis functions* that adds modification terms not only to the update law but also to the adaptive controller and show that

¹Portions of this chapter are previously published in [86]. It is an open access article distributed under the terms and conditions of the Creative Commons Attribution (CC BY) license (<http://creativecommons.org/licenses/by/4.0/>). The license is included in Appendix B.

the system error can be suppressed during the transient system response. The common denominator of the approaches in [41–48, 75, 79, 87] is that they introduce additional mechanisms to model reference adaptive control laws that capture a form of the system uncertainty in order to suppress its effect.

In this paper, we introduce a novel framework called *direct uncertainty minimization* for model reference adaptive control laws. Unlike the approaches in [41–48], the proposed framework consists of an architecture involving modification terms in both the adaptive controller and the update law such that these terms are activated when the system error is nonzero and vanishes as the system reaches its steady state. In addition, this new framework directly allows to suppress the effect of system uncertainty on the transient system response through a gradient minimization procedure, and hence, leads to improved system performance. Furthermore, unlike the approaches in [75, 79, 87], the proposed framework is computationally less expensive and it can enforce the system error to approximately stay in an a priori given, user-defined error performance bound. The proposed framework is first developed for adaptive control laws with linear reference models and then generalized to adaptive control laws with nonlinear reference models. This generalization adopts tools and methods from [49].

The organization of this paper is as follows. Section 3.2 highlights the notation used in this paper and states necessary mathematical preliminaries. Section 3.3 introduces the proposed direct uncertainty minimization framework, while Section 3.4 generalizes the results of Section 3.3 to a class of nonlinear reference models. Two illustrative numerical examples and experimental results are provided in Sections 3.5 and 3.6 to demonstrate the efficacy of the proposed approach to model reference adaptive control and conclusions are finally summarized in Section 3.7.

3.2 Notation and Mathematical Preliminaries

We use a fairly standard notation, where \mathbb{R} denotes the set of real numbers, \mathbb{R}^n denotes the set of $n \times 1$ real column vectors, $\mathbb{R}^{n \times m}$ denotes the set of $n \times m$ real matrices, \mathbb{R}_+ (resp. $\overline{\mathbb{R}}_+$) denotes the set of positive (resp. non-negative-definite) real numbers, $\mathbb{R}_+^{n \times n}$ (resp. $\overline{\mathbb{R}}_+^{n \times n}$) denotes the set of $n \times n$ positive-definite (resp. non-negative-definite) real matrices, $\mathbb{D}^{n \times n}$ denotes the set of $n \times n$ real matrices with diagonal scalar entries, $(\cdot)^T$ denotes transpose, $(\cdot)^{-1}$ denotes inverse, $\text{tr}(\cdot)$ denotes the trace operator, $\|\cdot\|_2$ denotes the Euclidian norm, $\|\cdot\|_F$ denotes the Frobenius matrix norm, and “ \triangleq ” denotes equality by definition. Furthermore, we write $\lambda_{\min}(A)$ (resp., $\lambda_{\max}(A)$) for the minimum (resp. maximum) eigenvalue of the Hermitian matrix A .

We next state necessary preliminaries on the model reference adaptive control problem. For this purpose, consider the uncertain dynamical system given by

$$\dot{x}_p(t) = A_p x_p(t) + B_p \Lambda u(t) + B_p \delta_p(x_p(t)), \quad x_p(0) = x_{p0}, \quad (3.1)$$

where $x_p(t) \in \mathbb{R}^{n_p}$ is the state vector available for feedback, $u(t) \in \mathbb{R}^m$ is the control input restricted to the class of admissible controls consisting of measurable functions, $\delta_p : \mathbb{R}^{n_p} \rightarrow \mathbb{R}^m$ is an uncertainty, $A_p \in \mathbb{R}^{n_p \times n_p}$ is a known system matrix, $B_p \in \mathbb{R}^{n_p \times m}$ is a known control input matrix with $B_p^T B_p$ being nonsingular, $\Lambda \in \mathbb{R}_+^{m \times m} \cap \mathbb{D}^{m \times m}$ is an unknown control effectiveness matrix, and the pair (A_p, B_p) is controllable. The next assumption is standard in adaptive control literature [5–7].

Assumption 3.2.1 *The uncertainty in (3.1) is parameterized as*

$$\delta_p(x_p(t)) = W_p^T \sigma_p(x_p(t)), \quad x_p(t) \in \mathbb{R}^{n_p}, \quad (3.2)$$

where $W_p \in \mathbb{R}^{s \times m}$ is an unknown weight matrix and $\sigma_p : \mathbb{R}^{n_p} \rightarrow \mathbb{R}^s$ is a known basis function of the form $\sigma_p(x_p(t)) = [\sigma_{p1}(x_p(t)), \sigma_{p2}(x_p(t)), \dots, \sigma_{ps}(x_p(t))]^T$.

For addressing command following, let $c(t) \in \mathbb{R}^{n_c}$ be a given piecewise continuous command and $x_c(t) \in \mathbb{R}^{n_c}$ be the integrator state given by the dynamics

$$\dot{x}_c(t) = E_p x_p(t) - c(t), \quad x_c(0) = x_{c0}, \quad (3.3)$$

where $E_p \in \mathbb{R}^{n_c \times n_p}$ selects a subset of $x_p(t)$ to follow $c(t)$. Based on the above construction, (3.1) and (3.3) are now augmented as

$$\dot{x}(t) = Ax(t) + B\Lambda u(t) + BW_p^T \sigma_p(x_p(t)) + B_r c(t), \quad x(0) = x_0, \quad (3.4)$$

where $x(t) \triangleq [x_p^T(t), x_c^T(t)]^T \in \mathbb{R}^n$, $n = n_p + n_c$, is the augmented state vector, $x_0 = [x_{p0}^T, x_{c0}^T]^T \in \mathbb{R}^n$, and

$$A \triangleq \begin{bmatrix} A_p & 0_{n_p \times n_c} \\ E_p & 0_{n_c \times n_c} \end{bmatrix} \in \mathbb{R}^{n \times n}, \quad (3.5)$$

$$B \triangleq [B_p^T, 0_{n_c \times m}^T]^T \in \mathbb{R}^{n \times m}, \quad (3.6)$$

$$B_r \triangleq [0_{n_p \times n_c}^T, -I_{n_c \times n_c}]^T \in \mathbb{R}^{n \times n_c}. \quad (3.7)$$

Consider now the feedback control law given by

$$u(t) = u_n(t) + u_a(t), \quad (3.8)$$

where $u_n(t)$ and $u_a(t)$ are the nominal feedback control law and the adaptive feedback control law, respectively. Let the nominal feedback control law be further given by

$$u_n(t) = -Kx(t), \quad K \in \mathbb{R}^{m \times n}, \quad (3.9)$$

such that $A_r \triangleq A - BK$ is Hurwitz. Using (3.8) and (3.9) in (3.4) yields

$$\dot{x}(t) = A_r x(t) + B_r c(t) + B \Lambda [u_a(t) + W^T \sigma(x(t))], \quad (3.10)$$

where

$$W \triangleq [\Lambda^{-1} W_p^T, (\Lambda^{-1} - I)]^T \in \mathbb{R}^{(s+m) \times m} \quad (3.11)$$

is an unknown aggregated weight matrix and

$$\sigma(x(t)) \triangleq [\sigma_p^T(x_p(t)), x^T(t) K^T]^T \in \mathbb{R}^{(s+m)} \quad (3.12)$$

is a known aggregated basis function. Considering (3.10), the adaptive control law is given by

$$u_a(t) = -\hat{W}^T(t) \sigma(x(t)), \quad (3.13)$$

where $\hat{W}(t) \in \mathbb{R}^{(s+m) \times m}$ is the estimate of W satisfying the weight update law

$$\dot{\hat{W}}(t) = \gamma \sigma(x(t)) e^T(t) P B, \quad \hat{W}(0) = \hat{W}_0. \quad (3.14)$$

In (3.14), $\gamma \in \mathbb{R}_+$ is the learning rate, $e(t) \triangleq x(t) - x_r(t)$ is the system error state vector with $x_r(t) \in \mathbb{R}^n$ being the reference state vector satisfying the reference model dynamics

$$\dot{x}_r(t) = A_r x_r(t) + B_r c(t), \quad x_r(0) = x_{r0}, \quad (3.15)$$

and $P \in \mathbb{R}_+^{n \times n}$ is a symmetric solution of the Lyapunov equation

$$0 = A_r^T P + P A_r + R, \quad R \in \mathbb{R}_+^{n \times n}. \quad (3.16)$$

Now, using (3.13) in (3.10) yields

$$\dot{x}(t) = A_r x(t) + B_r c(t) - B \Lambda \tilde{W}^T(t) \sigma(x(t)), \quad (3.17)$$

and the system error dynamics are given using (3.15) and (3.17) as

$$\dot{e}(t) = A_r e(t) - B \Lambda \tilde{W}^T(t) \sigma(x(t)), \quad e(0) = e_0, \quad (3.18)$$

where $\tilde{W}(t) \triangleq \hat{W}(t) - W \in \mathbb{R}^{(s+m) \times m}$ and $e_0 \triangleq x_0 - x_{r0}$.

Remark 3.2.1 *The update law given by (3.14) can be derived using Lyapunov analysis by considering the Lyapunov function candidate (see, for example, [5–7])*

$$\mathcal{V}(e, \tilde{W}) = e^T P e + \gamma^{-1} \text{tr}(\tilde{W} \Lambda^{1/2})^T (\tilde{W} \Lambda^{1/2}). \quad (3.19)$$

Note that $\mathcal{V}(0, 0) = 0$ and $\mathcal{V}(e, \tilde{W}) > 0$ for all $(e, \tilde{W}) \neq (0, 0)$. Now, differentiating (3.19) yields

$$\dot{\mathcal{V}}(e(t), \tilde{W}(t)) = -e^T(t) R e(t) - 2e^T(t) P B \Lambda \tilde{W}^T(t) \sigma(x(t)) + 2\gamma^{-1} \text{tr} \tilde{W}^T(t) \dot{\hat{W}}(t) \Lambda, \quad (3.20)$$

where using (3.14) in (3.20) results in

$$\dot{\mathcal{V}}(e(t), \tilde{W}(t)) = -e^T(t) R e(t) \leq 0, \quad t \in \bar{\mathbb{R}}_+, \quad (3.21)$$

which guarantees that the system error state vector $e(t)$ and the weight error $\tilde{W}(t)$ are Lyapunov stable, and hence, are bounded for all $t \in \bar{\mathbb{R}}_+$. Since $\sigma(x(t))$ is bounded for all $t \in \bar{\mathbb{R}}_+$, it follows from (3.17) that $\dot{e}(t)$ is bounded, and hence, $\dot{V}(e(t), \tilde{W}(t))$ is bounded for all $t \in \bar{\mathbb{R}}_+$. Now, it follows from Barbalat's lemma [88] that

$$\lim_{t \rightarrow \infty} \dot{V}(e(t), \tilde{W}(t)) = 0, \quad (3.22)$$

which consequently shows that $e(t) \rightarrow 0$ as $t \rightarrow \infty$.

Remark 3.2.2 In this paper, we assume that the uncertainty can be perfectly parameterized as in (3.2), which implies that the structure of the uncertainty is known. To elucidate this point, consider an example with the uncertainty $\delta_p(x_p(t)) = \alpha_1 x_{p1}(t) + \alpha_2 x_{p1}^2(t) + \alpha_3 x_{p3}(t)$, where $x_p^T = [x_{p1}(t), x_{p2}(t)]$ is the state vector and α_1, α_2 , and α_3 are some unknown parameters. In this case, it follows from the parameterization in (3.2) that $W_p^T = [\alpha_1, \alpha_2, \alpha_3]$ and $\sigma_p^T(x_p(t)) = [x_{p1}(t), x_{p1}^2(t), x_{p3}(t)]$. That is, provided that one knows the structure of the uncertainty as in this representative example, the basis function can be easily formed. For situations when one does not know the structure of the uncertainty and the uncertainty in (3.1) cannot be perfectly parameterized, then Assumption 3.2.1 can be relaxed by considering [89, 90]

$$\delta_p(t, x_p(t)) = W_p^T(t) \sigma_p(x_p(t)) + \varepsilon_p(t, x_p(t)), \quad x_p(t) \in \mathcal{D}_{x_p}, \quad (3.23)$$

where $W_p(t) \in \mathbb{R}^{s \times m}$ is an unknown time-varying weight matrix satisfying $\|W_p(t)\|_F \leq w$ and $\|\dot{W}_p(t)\|_F \leq \dot{w}$ with $w \in \mathbb{R}_+$ and $\dot{w} \in \mathbb{R}_+$ being unknown scalars, $\sigma_p : \mathcal{D}_{x_p} \rightarrow \mathbb{R}^s$ is a known basis function of the form $\sigma_p(x_p(t)) = [1, \sigma_{p1}(x_p(t)), \sigma_{p2}(x_p(t)), \dots, \sigma_{ps-1}(x_p(t))]^T$, $\varepsilon_p : \bar{\mathbb{R}}_+ \times \mathcal{D}_{x_p} \rightarrow \mathbb{R}^m$ is the system modeling error satisfying $\|\varepsilon_p(t, x_p(t))\|_2 \leq \varepsilon$ with $\varepsilon \in \mathbb{R}_+$ being an unknown scalar, and \mathcal{D}_{x_p} is a compact subset of \mathbb{R}^{n_p} . In this case, the update law given by (3.14) can be replaced by, for example,

$$\dot{\hat{W}}(t) = \gamma \text{Proj}[\hat{W}(t), \sigma(x(t))e^T(t)PB], \quad \hat{W}(0) = \hat{W}_0, \quad (3.24)$$

to guarantee the uniform boundedness of the system error state vector $e(t)$ and the weight error $\tilde{W}(t)$, where Proj denotes the projection operator [82].

3.3 Direct Uncertainty Minimization for Adaptive System Performance Improvement: Linear Reference Model Case

For the model reference adaptive control framework introduced in Section 3.2, we now develop the direct uncertainty minimization mechanism to improve transient system response. In particular, we first modify the adaptive feedback control law given by (3.13) as

$$u_a(t) = -\hat{W}^T(t)\sigma(x(t)) - \phi(t), \quad (3.25)$$

where $\phi(t) \in \mathbb{R}^m$ is the *system performance improvement term* that satisfies

$$\phi(t) = \phi(0) + k(B^T B)^{-1} B^T \left[(e(t) - e(0)) - \int_0^t A_r e(\tau) d\tau \right], \quad (3.26)$$

with $k \in \mathbb{R}_+$ being a design parameter. Using (3.25), the system error dynamics in (3.18) become

$$\dot{e}(t) = A_r e(t) - B\Lambda \left[\tilde{W}^T(t)\sigma(x(t)) + \phi(t) \right], \quad e(0) = e_0. \quad (3.27)$$

Notice that the ideal system error dynamics have the form

$$\dot{e}(t) = A_r e(t), \quad e(0) = e_0, \quad (3.28)$$

under nominal conditions with $\phi(t) \equiv 0$ when there is no system uncertainty or control uncertainty. Motivating from this standpoint, the mismatch term $\tilde{W}^T(t)\sigma(x(t)) + \phi(t)$ in (3.27) has to be minimized during the transient system response to improve system performance. In the next theorem, we show that the proposed system performance improvement term given by (3.26) achieves this objective through a gradient minimization procedure.

Theorem 3.3.1 *The modification term of the adaptive feedback control law in (3.26) is the negative gradient of the cost function given by*

$$\mathcal{J}(\cdot) = \frac{k}{2} \|\Lambda^{1/2} (\tilde{W}^T(t)\sigma(x(t)) + \phi(t))\|_2^2. \quad (3.29)$$

Proof. The negative gradient of the cost function given by (3.29) with respect to $\phi(t)$ has the form given by

$$-\frac{\partial \mathcal{J}(\cdot)}{\partial \phi(t)} = -k \left[\Lambda(\tilde{W}^T(t)\sigma(x(t)) + \phi(t)) \right], \quad (3.30)$$

which can be rewritten using (3.27) as

$$-\frac{\partial \mathcal{J}(\cdot)}{\partial \phi(t)} = k(B^T B)^{-1} B^T \left[\dot{e}(t) - A_r e(t) \right]. \quad (3.31)$$

In (3.31), note that $B^T B = B_p^T B_p$ is nonsingular by its definition in Section 3.2. To construct the modification term of the adaptive feedback control law in (3.26), let

$$\begin{aligned} \dot{\phi}(t) &= -\frac{\partial \mathcal{J}(\cdot)}{\partial \phi(t)} \\ &= k(B^T B)^{-1} B^T \left[\dot{e}(t) - A_r e(t) \right], \end{aligned} \quad (3.32)$$

where (3.26) is a direct consequence of (3.32) using integration by parts. ■

Remark 3.3.1 *The proposed modification term of the adaptive feedback control law in (3.26) allows for the system error to be shaped by suppressing the mismatch term $\tilde{W}^T(t)\sigma(x(t)) + \phi(t)$ in (3.27) due to gradient minimization, since it is constructed to be the negative gradient of (3.29) with respect to $\phi(t)$. Therefore, by adjusting k in (3.26), the uncertain dynamical system response and the reference model response can be made close to each other for all time including the transient phase. See Section 3.5 for illustrative numerical examples.*

Next, to maintain closed-loop system stability under the modified adaptive control signal given by (3.25), we now modify the update law given by (3.14) as

$$\dot{W}(t) = \gamma \sigma(x(t)) \left[e^T(t) P B + \xi \phi^T(t) \right], \quad \hat{W}(0) = \hat{W}_0, \quad (3.33)$$

with $\xi = k/a$ and $a \in \mathbb{R}_+$ being a design parameter.

Remark 3.3.2 *Note that the structure of (3.26) is much simpler than the structure of (44) in [75], in that the former does not involve $\hat{W}(t)$ dependence and additional integration terms. Furthermore, the same*

conclusion is also true when (3.33) is compared with (31)-(33) of [75], where the later has an extra differential equation in addition to the modification terms. Thus, the approach proposed here is much less computationally expensive than [75, 79, 87].

Now, we are ready to state the following theorem, which shows the asymptotic stability of the pair $(e(t), \phi(t))$ as well as the Lyapunov stability of $\tilde{W}(t)$.

Theorem 3.3.2 Consider the uncertain dynamical system given by (3.1) subject to Assumption 3.2.1, the reference model given by (3.15), the feedback control law given by (3.25) with (3.26) and (3.33). In addition, let ξ be chosen such that

$$\lambda_{\min}(R) - \frac{1}{\xi} \|PB\|_F^2 \Lambda^* > 0 \quad (3.34)$$

holds, where $\|\Lambda\|_F \leq \Lambda^*$ (here $\Lambda^* \in \mathbb{R}_+$ is a known, possibly conservative bound on the control effectiveness). Then, the solution $(e(t), \phi(t), \tilde{W}(t))$ of the closed-loop dynamical system is Lyapunov stable for all initial conditions and $t \in \bar{\mathbb{R}}_+$, $\lim_{t \rightarrow \infty} e(t) = 0$, and $\lim_{t \rightarrow \infty} \phi(t) = 0$.

Proof. To show Lyapunov stability of the solution $(e(t), \phi(t), \tilde{W}(t))$, consider the Lyapunov function candidate given by

$$\mathcal{V}(e, \phi, \tilde{W}) = e^T P e + a^{-1} \phi^T \phi + \gamma^{-1} \text{tr}(\tilde{W} \Lambda^{1/2})^T (\tilde{W} \Lambda^{1/2}). \quad (3.35)$$

Note that $\mathcal{V}(0, 0, 0) = 0$ and $\mathcal{V}(e, \phi, \tilde{W}) > 0$ for all $(e, \phi, \tilde{W}) \neq (0, 0, 0)$. Differentiating (3.35) along the closed-loop dynamical system trajectories yields

$$\dot{\mathcal{V}}(e(t), \phi(t), \tilde{W}(t)) = -e^T(t) R e(t) - 2\xi \phi^T(t) \Lambda \phi(t) - 2e^T(t) P B \Lambda^{1/2} \Lambda^{1/2} \phi(t). \quad (3.36)$$

Using Young's inequality [14] for the last term in (3.36) gives

$$\begin{aligned} -2e^T(t) P B \Lambda^{1/2} \Lambda^{1/2} \phi(t) &\leq |-2e^T(t) P B \Lambda^{1/2} \Lambda^{1/2} \phi(t)| \\ &\leq \frac{1}{\mu} e^T(t) P B \Lambda B^T P e(t) + \mu \phi^T(t) \Lambda \phi(t). \end{aligned} \quad (3.37)$$

Now, setting $\mu = \xi$ and using (3.37) in (3.36) yields

$$\begin{aligned}
\dot{V}(e(t), \phi(t), \tilde{W}(t)) &\leq -e^T(t)Re(t) + \frac{1}{\xi}e^T(t)PB\Lambda B^TPe(t) - \xi\phi^T(t)\Lambda\phi(t) \\
&\leq -\lambda_{\min}(R)\|e(t)\|_2^2 + \frac{1}{\xi}\|e(t)\|_2^2\|PB\|_F^2\Lambda^* - \xi\lambda_{\min}(\Lambda)\|\phi(t)\|_2^2 \\
&= -\|e(t)\|_2^2\left[\lambda_{\min}(R) - \frac{1}{\xi}\|PB\|_F^2\Lambda^*\right] - \xi\lambda_{\min}(\Lambda)\|\phi(t)\|_2^2. \tag{3.38}
\end{aligned}$$

Using the condition (3.34) in (3.38), it follows that $\dot{V}(e(t), \phi(t), \tilde{W}(t)) \leq 0$, which guarantees the Lyapunov stability of the solution $(e(t), \phi(t), \tilde{W}(t))$. Since this implies the boundedness of $e(t)$, $\phi(t)$, and $\tilde{W}(t)$ for all $t \in \bar{\mathbb{R}}_+$, it follows from (3.27) and (3.32) that $\dot{e}(t)$ and $\dot{\phi}(t)$ are bounded for all $t \in \bar{\mathbb{R}}_+$, and hence, $\ddot{V}(e(t), \phi(t), \tilde{W}(t))$ is bounded for all $t \in \bar{\mathbb{R}}_+$. It now follow from Barbalat's lemma [88]

$$\lim_{t \rightarrow \infty} \dot{V}(e(t), \phi(t), \tilde{W}(t)) = 0, \tag{3.39}$$

which shows that $\lim_{t \rightarrow \infty} e(t) = 0$ and $\lim_{t \rightarrow \infty} \phi(t) = 0$. ■

From a practical standpoint, if $e(t)$ is sufficiently small, then the design parameter ξ , which affects both modification terms in (3.25) and (3.33) can be chosen to be small such that (3.34) holds. However, as $e(t)$ becomes large, then ξ may need to be increased accordingly to put more weight on minimizing the cost function given by (3.29), and hence, to enforce system error to approximately stay in a priori given, user-defined performance bounds. To achieve this practical objective, we can let $\xi(t) = k(t)/a$, where $\xi(t) \in [\xi_{\min}, \xi_{\max}]$, $\xi_{\min} \in \mathbb{R}_+$, $\xi_{\max} \in \mathbb{R}_+$, and consider the cost function given by

$$\mathcal{J}(\cdot) = \frac{k(t)}{2} \|\Lambda^{1/2}(\tilde{W}^T(t)\sigma(x(t)) + \phi(t))\|_2^2. \tag{3.40}$$

Choosing the modification term in (3.25) as the negative gradient of (3.40), i.e., $\dot{\phi}(t) = -\frac{\partial \mathcal{J}(\cdot)}{\partial \phi(t)}$, and following similar steps as highlighted in the proof of Theorem 3.3.1, it follows by integration by parts that

$$\begin{aligned}
\phi(t) &= \phi(0) + a \left[\xi(t)(B^TB)^{-1}B^Te(t) - \xi(0)(B^TB)^{-1}B^Te(0) - \int_0^t \dot{\xi}(\tau)(B^TB)^{-1}B^Te(\tau)d\tau \right. \\
&\quad \left. - \int_0^t \xi(\tau)(B^TB)^{-1}B^TA_r e(\tau)d\tau \right]. \tag{3.41}
\end{aligned}$$

Notice that in this case the modified update law becomes

$$\dot{\hat{W}}(t) = \gamma \sigma(x(t)) \left[e^T(t) P B + \xi(t) \phi^T(t) \right], \quad \hat{W}(0) = \hat{W}_0, \quad (3.42)$$

and the condition (3.34) needs to be replaced with

$$\lambda_{\min}(R) - \frac{1}{\xi_{\min}} \|PB\|_F^2 \Lambda^* > 0, \quad (3.43)$$

where $\|\Lambda\|_F \leq \Lambda^*$ (here $\Lambda^* \in \mathbb{R}_+$ is a known bound on the control effectiveness). In addition, we choose

$$\dot{\xi}(t) = -\gamma_{\xi} \left[f(e) (\xi(t) - \xi_{\min}) + (1 - f(e)) (\xi(t) - \xi_{\max}) \right], \quad \xi(0) = \xi_0 \in [\xi_{\min}, \xi_{\max}], \quad (3.44)$$

where $\gamma_{\xi} \in \mathbb{R}_+$ and $f(e) \in [0, 1]$ is a continuously differentiable function such that it is close to 1 when $e(t)$ is sufficiently small and otherwise close to 0. It follows from (3.44) that $\xi(t) \in [\xi_{\min}, \xi_{\max}]$ and $\xi(t)$ approaches to ξ_{\min} (resp., ξ_{\max}) when $f(e) = 1$ (resp., $f(e) = 0$). A candidate $f(e)$ has the form $f(e) = 1 - [1 - \text{sech}(c_1 \|e(t)\|_P)]^{c_2}$, $\|e(t)\|_P \triangleq \sqrt{e^T(t) P e(t)}$, where it is depicted in Figure 3.1 for $c_1 = 5$ (this is chosen to drive $\xi(t)$ to ξ_{\max} if $\|e(t)\|_P$ is larger than 0.5) and $c_2 = 10$.

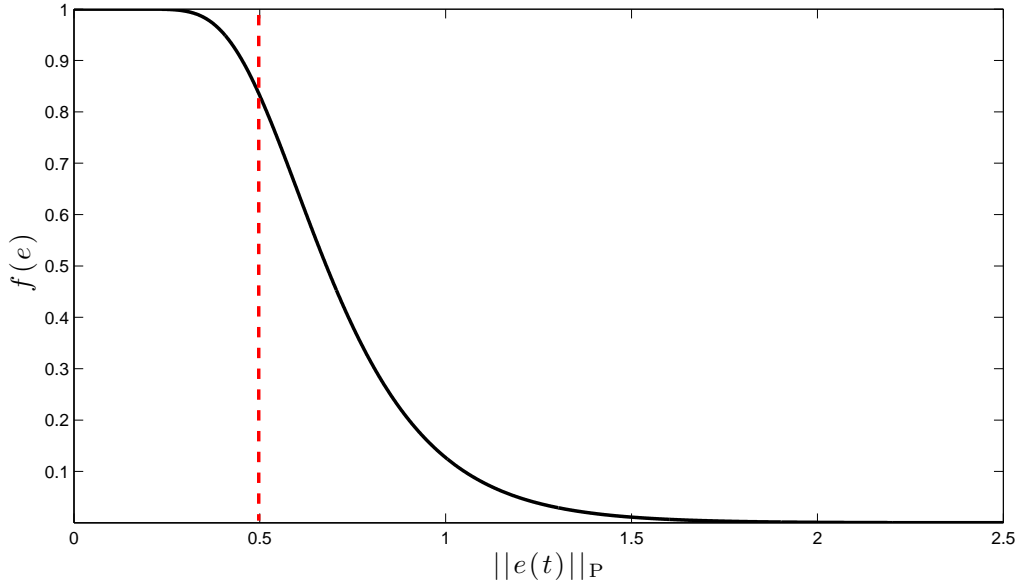


Figure 3.1: A candidate $f(e)$ for (3.44).

3.4 Generalization to a Class of Nonlinear Reference Models

In most of the model reference adaptive control literature, it is common to design a reference model with linear dynamics as given by (3.15). While this is practical for several applications, the control designer may prefer to use a nonlinear reference model to better capture the desired closed-loop system performance for many robotics and flight control applications. By adopting the tools and methods from [49, 74], we now generalize the results in Section 3.3 such that the proposed direct uncertainty minimization adaptive control architecture can be used to suppress the effect of the system uncertainty on the transient system response and drive the states of a nonlinear uncertain dynamical system to the states of a class of nonlinear reference models.

For this purpose, we recast the uncertain dynamical system given by (3.1) with a more general class of affine-in-control nonlinear system dynamics given by

$$\dot{x}_p(t) = f_p(x_p(t)) + B_p \Lambda u(t) + B_p \delta_p(x_p(t)), \quad x_p(0) = x_{p0}, \quad (3.45)$$

where $x_p(t) \in \mathbb{R}^{n_p}$ is the state vector, $u(t) \in \mathbb{R}^m$ is the control input restricted to the class of admissible controls consisting of measurable functions such that , $f_p : \mathbb{R}^{n_p} \rightarrow \mathbb{R}^{n_p}$ is a known system function that satisfies $f_p(0) = 0$, $B_p \in \mathbb{R}^{n_p \times m}$ is a known control input matrix, $\Lambda \in \mathbb{R}_+^{m \times m} \cap \mathbb{D}^{m \times m}$ is an unknown control effectiveness matrix, $\delta_p : \mathbb{R}^{n_p} \rightarrow \mathbb{R}^m$ is the system uncertainty, and it is implicitly assumed that the required properties for the existence and uniqueness of solutions are satisfied for the controllable uncertain dynamical system such that (3.45) has a unique solution forward in time [80, 88].

Once again, to address command following, (3.45) can be augmented with the integrator state dynamics given by (3.3) in the following form subject to Assumption 3.2.1

$$\dot{x}(t) = f(x(t), c(t)) + B \Lambda u(t) + B W_p^T \sigma_p(x_p(t)), \quad x(0) = x_0, \quad (3.46)$$

where $x(t) \triangleq [x_p^T(t), x_c^T(t)]^T \in \mathbb{R}^n$, $n = n_p + n_c$, is the augmented state vector, $x_0 = [x_{p0}^T, x_{c0}^T]^T \in \mathbb{R}^n$, $c(t) \in \mathbb{R}^{n_c}$ is a given bounded command, B is given by (3.6), and $f : \mathbb{R}^n \times \mathbb{R}^{n_c} \rightarrow \mathbb{R}^n$ is the aggregated system function with the integrator state dynamics that satisfies $f(0, 0) = 0$ and

$$f(x(t), c(t)) = \begin{bmatrix} f_p(x_p(t)) \\ E_p x_p(t) - c(t) \end{bmatrix}. \quad (3.47)$$

Next, consider the nonlinear reference model given by

$$\dot{x}_r(t) = f_r(x_r(t), c(t)), \quad x_r(0) = x_{r0}, \quad (3.48)$$

where $x_r(t) \in \mathbb{R}^n$ is the reference state vector and $f_r : \mathbb{R}^n \times \mathbb{R}^{n_c} \rightarrow \mathbb{R}^n$ is the reference model function that satisfies $f_r(0, 0) = 0$ and

$$f_r(x_r(t), c(t)) \triangleq f(x_r(t), c(t)) - Bk(x_r(t)), \quad (3.49)$$

with $k : \mathbb{R}^n \rightarrow \mathbb{R}^m$ being a feedback law such that $x_r(t)$ is bounded for all $t \in \bar{\mathbb{R}}_+$. In addition, it is implicitly assumed that (3.48) has a unique solution forward in time.

Let the nominal control law be given by

$$u_n(t) = -k(x(t)), \quad (3.50)$$

such that with (3.8), (3.46) can be rewritten as

$$\begin{aligned} \dot{x}(t) &= f(x(t), c(t)) - Bk(x(t)) + B\Lambda[u_a(t) + \Lambda^{-1}W_p^T\sigma_p(x_p(t)) + (\Lambda^{-1} - I)k(x(t))] \\ &= f_r(x(t), c(t)) + B\Lambda[u_a(t) + W_o^T\sigma_o(x(t))], \end{aligned} \quad (3.51)$$

where $W_o \triangleq [\Lambda^{-1}W_p^T, (\Lambda^{-1} - I)]^T \in \mathbb{R}^{(s+m) \times m}$ and $\sigma_o(x(t)) \triangleq [\sigma_p^T(x_p(t)), k^T(x(t))]^T \in \mathbb{R}^{(s+m)}$. The system error dynamics then follow from (3.48) and (3.51) as

$$\dot{e}(t) = f_r(x(t), c(t)) - f_r(x_r(t), c(t)) + B\Lambda[u_a(t) + W_o^T\sigma_o(x(t))], \quad e(0) = e_0. \quad (3.52)$$

Note that there exists a known signal $v(x(t), x_r(t), c(t)) \in \mathbb{R}^m$ which can be used as a feedback linearization term such that

$$A_r e(t) = f_r(x(t), c(t)) - f_r(x_r(t), c(t)) + Bv(\cdot) \quad (3.53)$$

holds, and hence, (3.52) can be written as

$$\begin{aligned} \dot{e}(t) &= A_r e(t) + B\Lambda[u_a(t) + W_o^T\sigma_o(x(t)) - \Lambda^{-1}v(\cdot)] \\ &= A_r e(t) + B\Lambda[u_a(t) + W^T\sigma(\cdot)], \end{aligned} \quad (3.54)$$

with $W \triangleq [W_0^T, -\Lambda^{-1}]^T \in \mathbb{R}^{(s+2m) \times m}$ being the unknown aggregated weight matrix and $\sigma(\cdot) \triangleq [\sigma_0^T(x(t)), v^T(\cdot)]^T \in \mathbb{R}^{(s+2m)}$ being the known aggregated basis function.

Now, consider the adaptive feedback control law given by

$$u_a(t) = -\hat{W}^T(t)\sigma(\cdot) - \phi(t), \quad (3.55)$$

where $\phi(t) \in \mathbb{R}^m$ satisfies (3.41) with (3.44) and $\hat{W}(t) \in \mathbb{R}^{(s+2m) \times m}$ satisfies

$$\dot{\hat{W}}(t) = \gamma\sigma(\cdot) \left[e^T(t)PB + \xi(t)\phi^T(t) \right], \quad \hat{W}(0) = \hat{W}_0. \quad (3.56)$$

Using (3.55) in (3.54), it follows that the system error dynamics can be written as

$$\dot{e}(t) = A_r e(t) - B\Lambda [\tilde{W}^T(t)\sigma(\cdot) + \phi(t)], \quad (3.57)$$

where $\tilde{W}(t) \triangleq \hat{W}(t) - W \in \mathbb{R}^{(s+2m) \times m}$.

Remark 3.4.1 *It should be noted that the term $v(\cdot)$ acts similar to a feedback linearization signal, which is an important feature in generalizing the direct uncertainty minimization framework for the considered class of nonlinear reference models. By appropriately selecting $v(\cdot)$, when possible, for the given application such that (3.53) holds and then embedding $v(\cdot)$ into the unknown weight matrix W and the known basis function $\sigma(\cdot)$, the resulting system error dynamics given by (3.57) have an identical structure to the system error dynamics given by (3.27) in Section 3.3 for the linear reference model. It then follows that the analysis and synthesis of the direct uncertainty minimization mechanism and stability analysis presented in Section 3.3 directly translates to the case in which nonlinear reference models are used.*

Theorem 3.4.1 *Consider the nonlinear uncertain dynamical system given by (3.45) subject to Assumption 3.2.1, the nonlinear reference model given by (3.48), the feedback control law given by (3.55) with (3.41), (3.44) and (3.56). In addition, let ξ_{\min} be chosen such that (3.43) holds. Then, the solution $(e(t), \phi(t), \tilde{W}(t))$ of the closed-loop dynamical system is Lyapunov stable for all initial conditions and $t \in \overline{\mathbb{R}}_+$, $\lim_{t \rightarrow \infty} e(t) = 0$, and $\lim_{t \rightarrow \infty} \phi(t) = 0$.*

Proof. As a consequence of the discussion highlighted in Remark 3.4.1, the proof is similar to the proof of Theorem 3.3.2, and hence, is omitted. ■

3.5 Illustrative Numerical Examples

To demonstrate the efficacy of the proposed direct uncertainty minimization framework, we now present two examples in the following two subsections. We first investigate the application to a hypersonic vehicle using a linear reference model. The second example considers a wing rock dynamics model for an aircraft with a nonlinear reference model, where the purpose of the nonlinear reference model is to limit the pilot authority for envelope protection.

3.5.1 Example 1: Application to a Hypersonic Vehicle Model

For this example, we first formulate a state space model of a generic hypersonic vehicle (GHV). Then, it is explained how the model is decoupled into longitudinal and lateral dynamics for which separate controllers are designed. The longitudinal and lateral controllers have both a nominal and adaptive portion where the simulation results illustrate both nominal control performance, a standard adaptive control performance, and the proposed adaptive control performance.

For the configuration with an altitude of 80,000 feet and a Mach number of 6, a linearized model under nominal conditions ($\delta_p(x_p(t)) = 0$ and $\Lambda = I$) is obtained in the form of (3.1) with

$$A_p = \begin{bmatrix} -3.70 \times 10^{-3} & -7.17 \times 10^{-1} & 0 & -3.18 \times 10^1 & -2.67 \times 10^{-4} \\ -5.35 \times 10^{-7} & -2.39 \times 10^{-1} & 1 & -2.95 \times 10^{-12} & 2.23 \times 10^{-7} \\ -2.79 \times 10^{-5} & 4.26 & -1.19 \times 10^{-1} & 0 & 3.94 \times 10^{-5} \\ -4.76 \times 10^{-8} & 1.31 \times 10^{-13} & 1 & -4.45 \times 10^{-14} & -1.33 \times 10^{-11} \\ -5.53 \times 10^{-10} & -5.87 \times 10^3 & 0 & 5.87 \times 10^3 & 0 & \dots \\ 5.99 \times 10^{-16} & -3.14 \times 10^{-11} & 0 & -3.04 \times 10^{-19} & -9.74 \times 10^{-16} \\ 1.47 \times 10^{-10} & -4.45 \times 10^{-6} & 0 & 0 & -1.00 \times 10^{-11} \\ -5.29 \times 10^{-12} & 3.98 \times 10^{-8} & 0 & 0 & 1.28 \times 10^{-12} \\ 8.08 \times 10^{-28} & 2.04 \times 10^{-22} & 1.01 \times 10^{-20} & 1.17 \times 10^{-16} & -1.73 \times 10^{-31} \end{bmatrix}$$

$$\begin{array}{cccc}
-8.81 \times 10^{-1} & 0 & 0 & -1.77 \times 10^{-15} \\
-1.06 \times 10^{-3} & 0 & 0 & -3.18 \times 10^{-21} \\
-1.47 & 0 & 0 & 0 \\
-1.08 \times 10^{-19} & 4.44 \times 10^{-16} & -9.58 \times 10^{-16} & -2.58 \times 10^{-18} \\
\dots & 0 & 0 & -3.26 \times 10^{-13} \\
-6.97 \times 10^{-2} & -1.04 \times 10^{-2} & -9.99 \times 10^{-1} & -5.35 \times 10^{-3} \\
-1.31 \times 10^3 & -2.03 & -7.54 \times 10^{-3} & 0 \\
2.07 & -1.55 \times 10^{-3} & -5.31 \times 10^{-2} & 0 \\
-2.38 \times 10^{-4} & 8.54 \times 10^{-1} & -8.84 \times 10^{-3} & -3.00 \times 10^{-6}
\end{array} \quad (3.58)$$

$$B_p = \begin{bmatrix}
-6.53 \times 10^{-3} & -1.24 \times 10^{-13} & -2.98 \times 10^{-3} \\
-1.33 \times 10^{-4} & -2.44 \times 10^{-13} & 1.17 \times 10^{-7} \\
-1.84 \times 10^{-1} & -1.60 \times 10^{-13} & 2.48 \times 10^{-4} \\
0 & 0 & 0 \\
0 & 0 & 0 \\
-1.40 \times 10^{-16} & -2.47 \times 10^{-5} & -2.18 \times 10^{-4} \\
-5.90 \times 10^{-11} & -8.04 & 10.3 \\
8.56 \times 10^{-14} & 3.17 \times 10^{-2} & 2.85 \times 10^{-1} \\
0 & 0 & 0
\end{bmatrix} \quad (3.59)$$

with the state vector being defined as $x_p(t) = [V(t), \alpha(t), q(t), \theta(t), h(t), \beta(t), p(t), r(t), \phi(t)]^T$, where $V(t)$ denotes the total velocity, $\alpha(t)$ denotes the angle of attack, $q(t)$ denotes the pitch rate, $\theta(t)$ denotes the pitch angle, $h(t)$ denotes the altitude, $\beta(t)$ denotes the sideslip angle, $p(t)$ denotes the roll rate, $r(t)$ denotes the yaw rate, and $\phi(t)$ denotes the roll angle. The control input vector is defined as $u(t) = [\delta_e(t), \delta_a(t), \delta_r(t)]^T$, where $\delta_e(t)$ denotes the elevator deflection, $\delta_a(t)$ denotes the aileron deflection, and $\delta_r(t)$ denotes the rudder deflection. To control the model described above, we decouple the system into its longitudinal and lateral dynamics, design nominal and adaptive controllers for the decoupled system, and then combine the separate controllers to control the overall coupled GHV model (see Figures 3.2 and 3.3).

3.5.1.1 Longitudinal Control Design

For the decoupled longitudinal dynamics, we consider the state vector defined as $x_{p_{10}}(t) = [\alpha(t), q(t)]^T$, with the respective system matrices

$$A_{p_{10}} = \begin{bmatrix} -2.39 \times 10^{-1} & 1 \\ 4.26 & -1.19 \times 10^{-1} \end{bmatrix}, \quad (3.60)$$

$$B_{p_{10}} = \begin{bmatrix} -1.33 \times 10^{-4} \\ -1.84 \times 10^{-1} \end{bmatrix}. \quad (3.61)$$

LQR theory is used to design the nominal controller with $E_{p_{10}} = [1, 0]$ such that a desired angle of attack command is followed. The controller gain matrix K_{10} is obtained using the highlighted augmented formulation ((3.5) and (3.6)), along with the weighting matrices $Q_{10} = \text{diag}[20000, 25000, 400000]$ to penalize $x_{10}(t)$ and $R_{10} = 12.5$ to penalize $u_{10}(t)$, resulting in the following gain matrix

$$K_{10} = \begin{bmatrix} -1.65 \times 10^2 & -6.09 \times 10^1 & -1.79 \times 10^2 \end{bmatrix}. \quad (3.62)$$

The solution to $A_{r_{10}}^T P_{10} + P_{10} A_{r_{10}} + R_{10} = 0$, where $A_{r_{10}} \triangleq A_{10} - B_{10} K_{10}$, is calculated using $R_{10} = \text{diag}[1, 1, 100]$ for both the standard adaptive control design and the proposed controller. For the proposed design, we use (3.25), (3.41), and (3.42), and resort to (3.44) for enforcing $\|e_{10}(t)\|_{p_{10}} \leq 0.5$. Additionally, note that $\xi_{\min} = 10$ is selected to satisfy (3.43) and we choose $a = 2$. To visualize the overall longitudinal control design, a block diagram is provided in Figure 3.2.

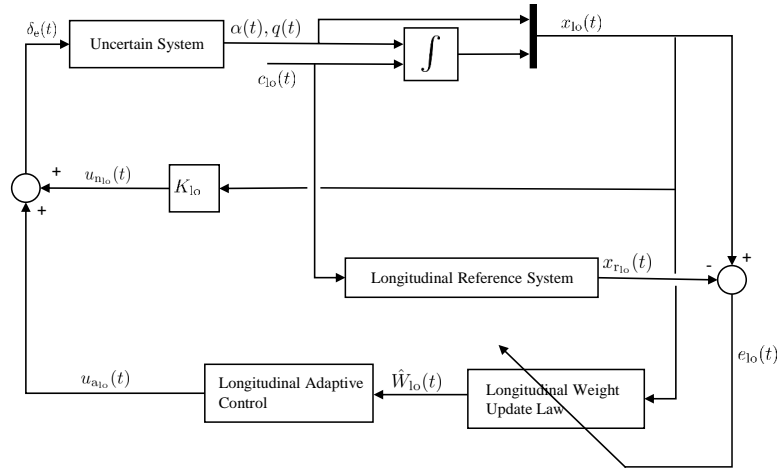


Figure 3.2: Block diagram of separated longitudinal control design.

3.5.1.2 Lateral Control Design

The decoupled lateral dynamics follow similarly. Specifically, we consider the state vector defined as $x_{pla}(t) = [\beta(t), p(t), r(t), \phi(t)]^T$, with the respective system matrices

$$A_{pla} = \begin{bmatrix} -6.97 \times 10^{-2} & -1.04 \times 10^{-2} & -9.99 \times 10^{-1} & -5.35 \times 10^{-3} \\ -1.31 \times 10^3 & -2.03 & -7.54 \times 10^{-3} & 0 \\ 2.07 & -1.55 \times 10^{-3} & -5.31 \times 10^{-2} & 0 \\ -2.38 \times 10^{-4} & 8.54 \times 10^{-1} & -8.84 \times 10^{-3} & -3.00 \times 10^{-6} \end{bmatrix}, \quad (3.63)$$

$$B_{pla} = \begin{bmatrix} -2.47 \times 10^{-5} & -2.18 \times 10^{-4} \\ -8.04 & 10.3 \\ 3.17 \times 10^{-2} & 2.85 \times 10^{-1} \\ 0 & 0 \end{bmatrix}. \quad (3.64)$$

LQR theory is used to design the nominal controller with

$$E_{pla} = \begin{bmatrix} 1 & 0 & 0 & 0 \\ 0 & 0 & 0 & 1 \end{bmatrix} \quad (3.65)$$

such that a desired sideslip angle command and roll angle command are followed. The controller gain matrix K_{la} is obtained using the highlighted augmented formulation along with the weighting matrices $Q_{la} = \text{diag}[100, 100, 100, 100, 400000, 2500]$ to penalize $x_{la}(t)$ and $R_{la} = \text{diag}[1.25, 50]$ to penalize $u_{la}(t)$, resulting in the following gain matrix

$$K_{la} = \begin{bmatrix} 2.78 \times 10^2 & -9.08 & -3.62 \times 10^1 & -3.15 \times 10^1 & 1.21 \times 10^2 & -4.37 \times 10^1 \\ 8.70 \times 10^1 & 1.52 \times 10^{-1} & -2.72 \times 10^1 & 1.30 & 8.74 \times 10^1 & 1.51 \end{bmatrix}. \quad (3.66)$$

The solution to $A_{r_{la}}^T P_{la} + P_{la} A_{r_{la}} + R_{1_{la}} = 0$, where $A_{r_{la}} \triangleq A_{la} - B_{la} K_{la}$ is calculated using $R_{1_{la}} = \text{diag}[1, 1, 1, 1, 100, 100]$ for both the standard adaptive control design and the proposed controller. For the proposed design, we use (3.25), (3.41), and (3.42), and resort to (3.44) for enforcing $\|e_{la}(t)\|_{P_{la}} \leq 0.5$. Additionally, note that $\xi_{\min} = 10$ is selected to satisfy (3.43) and we choose $a = 2$. Similar to the previous section, a block diagram is provided in Figure 3.3 to visualize the control design using the decoupled lateral dynamics to control the overall uncertain system.

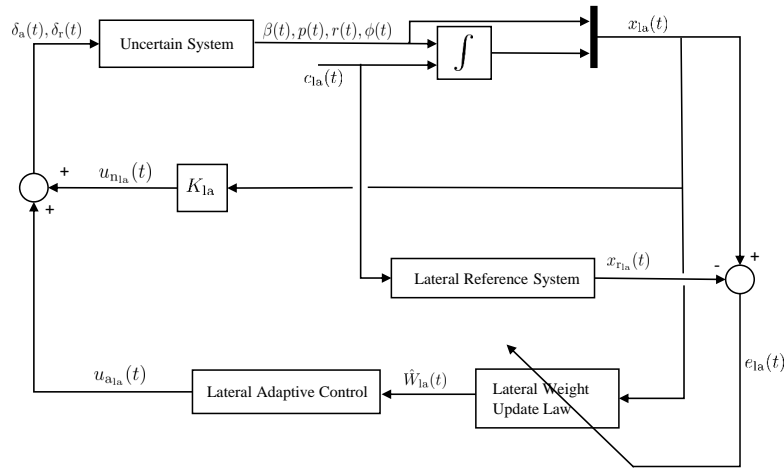


Figure 3.3: Block diagram of separated lateral control design.

3.5.1.3 Nominal System without Uncertainty

The longitudinal and lateral controllers are augmented and applied to the overall coupled system. We first consider the case when there is no uncertainty in the system to show the nominal performance of the control designs. Figure 3.4 shows the response of the nominal control performance. It can also be seen from this figure that the error signals are not equal to zero which is expected due to the coupling effects.

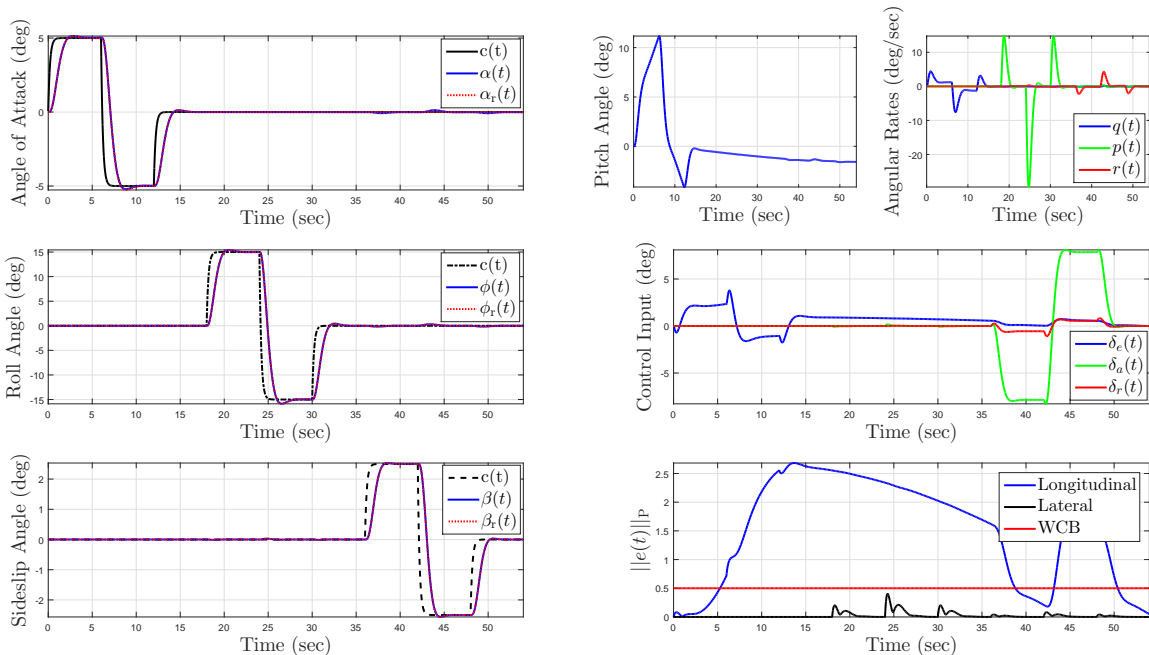


Figure 3.4: Nominal controller performance without uncertainty.

3.5.1.4 Uncertainty in Control Effectiveness and Stability Derivatives

We now consider the case when the control effectiveness matrix is unknown as well as the stability derivatives $C_{m\alpha}$ and $C_{n\beta}$. For this purpose, we let $\Lambda = 0.5I$ and we increase $C_{m\alpha}$ and decrease $C_{n\beta}$. Figure 3.5 shows the response with the nominal control, which goes unstable.

A standard adaptive control design is first implemented. For the standard adaptive controllers, we select the basis functions $\sigma_{10}(x_{10}(t)) = [x_{10}^T(t)K_{10}^T, \alpha(t)]^T$ and $\sigma_{1a}(x_{1a}(t)) = [x_{1a}^T(t)K_{1a}^T, \beta(t)]^T$ respectively for the longitudinal and lateral controllers. Figures 3.6 and 3.7 show the standard adaptive control response. Specifically, Figure 3.6 shows that for a low learning gain the system transient performance in the sideslip angle and angle of attack is poor. In addition, the control surface deflection angles exceed practical working limits. To improve the performance, the learning gain is increased as shown in Figure 3.7. Both the tracking performance and the control response improve; however, as seen in the bottom part of the figure, the standard adaptive controller is unable to enforce a pre-defined bound on the error.

To improve performance further and enforce a user-defined bound on the error, the proposed adaptive controller is then implemented using the same basis functions as the standard adaptive control design. Figures 3.8 and 3.9 show the proposed controller performance using the gain varying control. Specifically, Figure 3.8 illustrates the superior tracking performance and Figure 3.9 shows the guaranteed bound $\|e(t)\|_p \leq 0.5$ for both the longitudinal and lateral dynamics.

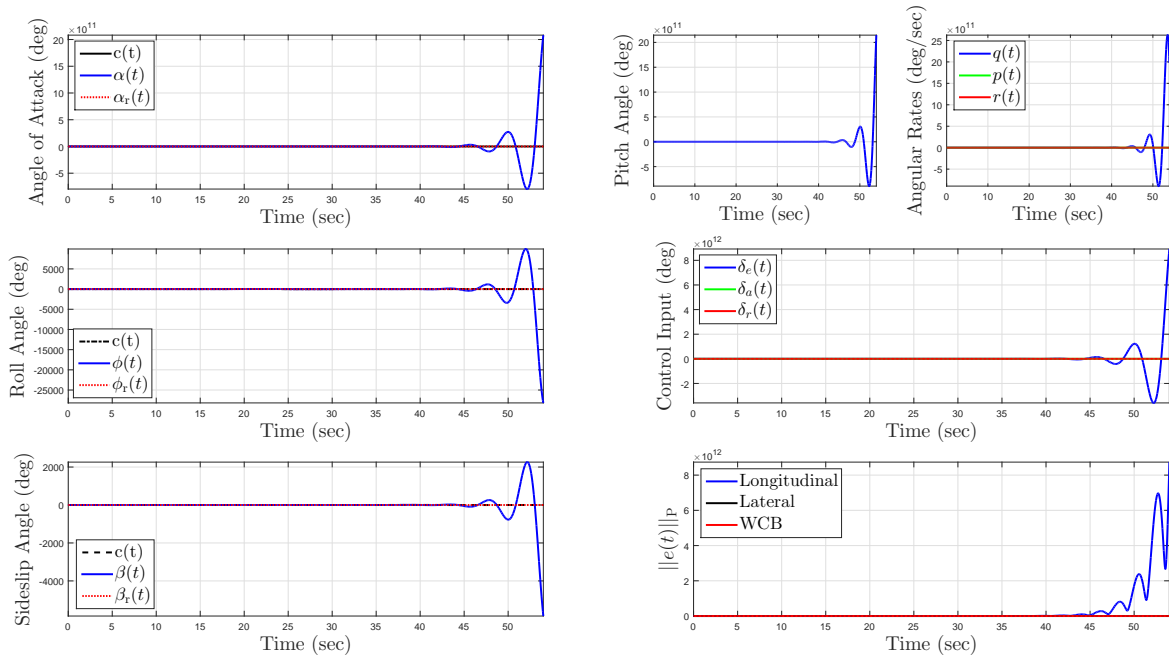


Figure 3.5: Nominal controller performance with uncertainty in Λ , $C_{m\alpha}$, and $C_{n\beta}$.

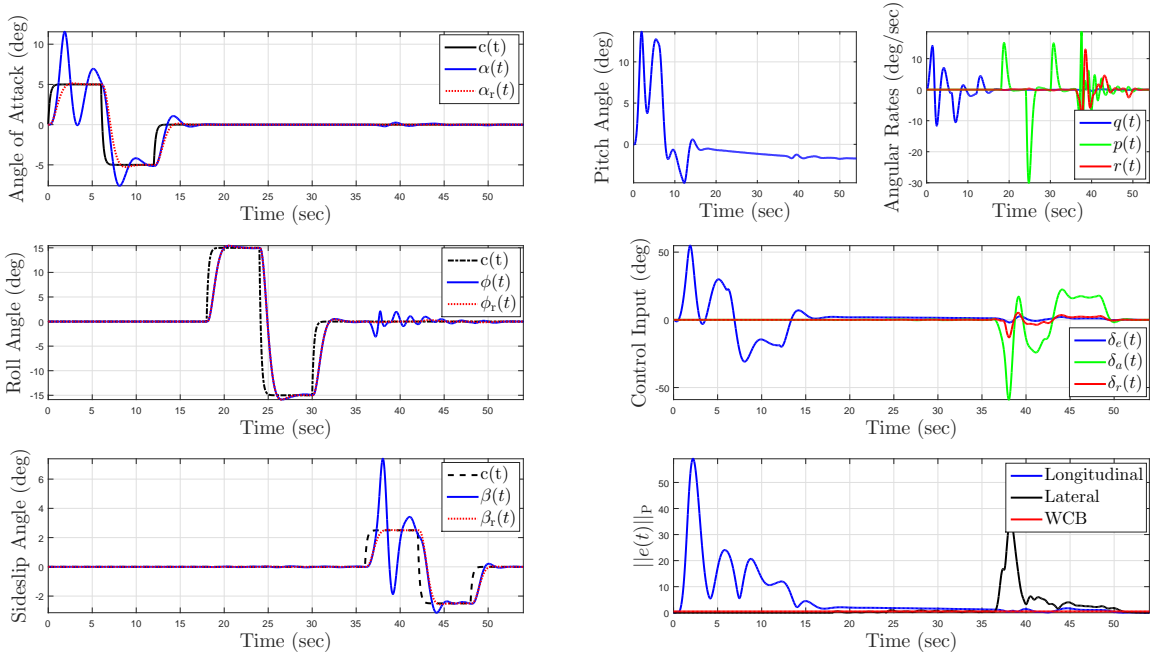


Figure 3.6: Standard adaptive controller performance with uncertainty in Λ , $C_{m\alpha}$, and $C_{n\beta}$ ($\Gamma_{l_0} = I_{2 \times 2}$ and $\Gamma_{l_a} = I_{3 \times 3}$).

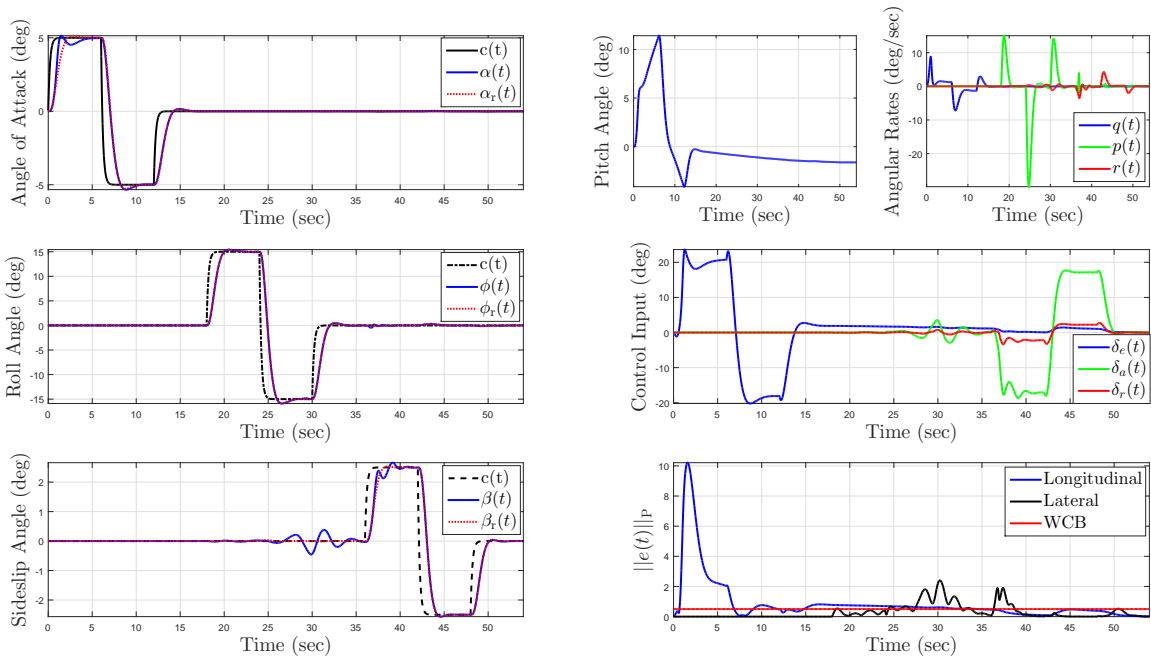


Figure 3.7: Standard adaptive controller performance with uncertainty in Λ , $C_{m\alpha}$, and $C_{n\beta}$ ($\Gamma_{l_0} = 100I_{2 \times 2}$ and $\Gamma_{l_a} = 100I_{3 \times 3}$).

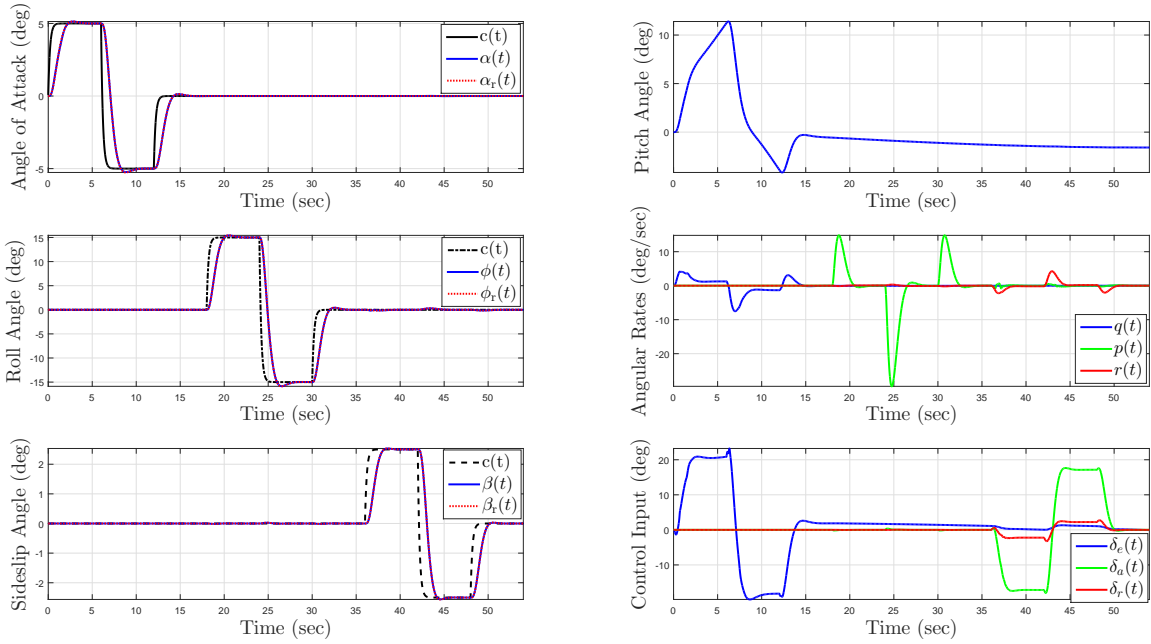


Figure 3.8: Proposed gain varying adaptive control performance with uncertainty in Λ , $C_{m\alpha}$, and $C_{n\beta}$ ($\Gamma_{l0} = I_{2 \times 2}$ and $\Gamma_{la} = \text{diag}[0.1, 1, 1]$, $\xi_0 = 10$, and $a = 2$).

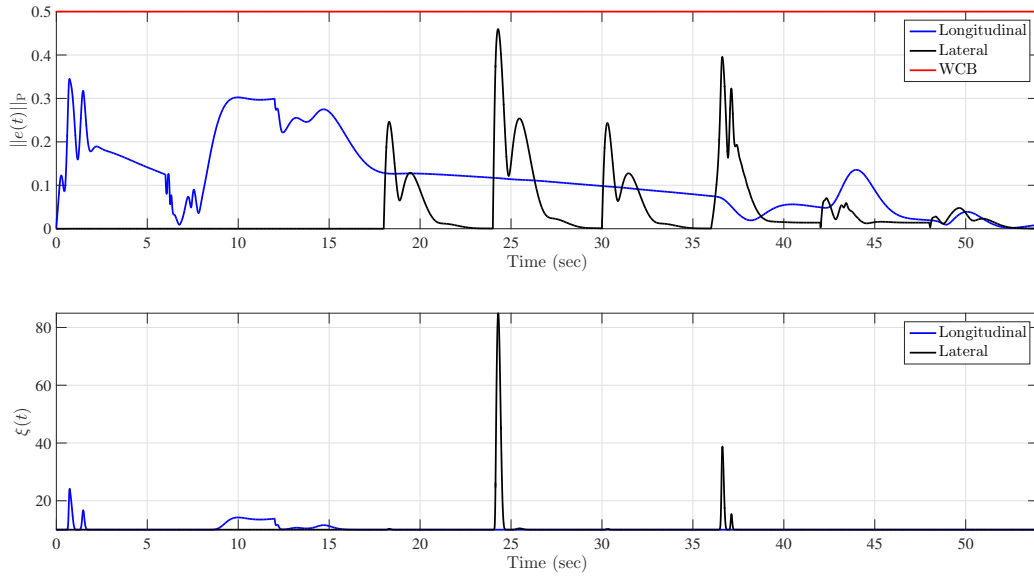


Figure 3.9: System error bounds and adaptation gain for Figure 3.8.

3.5.2 Example 2: Wing Rock Dynamics with Nonlinear Reference Model

We now consider the nonlinear dynamical system representing a controlled wing rock dynamics model given by

$$\begin{bmatrix} \dot{x}_{p1}(t) \\ \dot{x}_{p2}(t) \end{bmatrix} = \begin{bmatrix} 0 & 1 \\ 0 & 0 \end{bmatrix} \begin{bmatrix} x_{p1}(t) \\ x_{p2}(t) \end{bmatrix} + \begin{bmatrix} 0 \\ 1 \end{bmatrix} \left(\Lambda u(t) + \delta_p(x_p(t)) \right), \quad \begin{bmatrix} x_{p1}(0) \\ x_{p2}(0) \end{bmatrix} = \begin{bmatrix} 0 \\ 0 \end{bmatrix}, \quad (3.67)$$

where x_{p1} represents the roll angle in radians and x_{p2} represents the roll rate in radians per second. In (3.67), $\delta_p(x_p)$ represents an uncertainty of the form $\delta_p(x_p) = \alpha_1 x_{p1} + \alpha_2 x_{p2} + \alpha_3 |x_{p1}| x_{p2} + \alpha_4 |x_{p2}| x_{p2} + \alpha_5 x_{p1}^3$, where $\alpha_i, i = 1, \dots, 5$, are unknown parameters that are derived from the aircraft aerodynamic coefficients. For this numerical example, we set $\alpha_1 = 0.5$, $\alpha_2 = 1.0$, $\alpha_3 = -1.0$, $\alpha_4 = 1.0$, $\alpha_5 = 0.5$, and $\Lambda = 0.5$.

Note that for this example, the wing rock dynamics are linear such that $f_p(x_p(t))$ in (3.45) is written as $A_p x_p(t)$. As a result, we let $E_p = [1, 0]$ such that the roll angle command is followed and use LQR theory with the augmented formulation ((3.5) and (3.6)), along with the weighting matrices $Q = \text{diag}[50, 1, 100]$ and $R = 1$ to obtain the gain matrix $K = [12.30, 5.06, 10.0]$. In addition, we adopt the same nominal control structure to limit pilot authority as in [74] to design the nonlinear reference model as

$$\dot{x}_r(t) = \begin{bmatrix} 0 & 1 & 0 \\ 0 & 0 & 0 \\ 1 & 0 & 0 \end{bmatrix} x_r(t) - \begin{bmatrix} 0 \\ 1 \\ 0 \end{bmatrix} k(x_r(t)) + \begin{bmatrix} 0 \\ 0 \\ -1 \end{bmatrix} c(t), \quad x_r(t) = 0, \quad (3.68)$$

with $k(x_r(t)) = K[x_{r1}(t), x_{r2}(t), \Phi(x_r(t))x_{r3}(t)]^T$, $c(t) = c_d(t)\Phi(x_r(t))$, and

$$\Phi(x_r(t)) = \tanh\left(5\left||x_{r1}(t)| - 2\right|\right). \quad (3.69)$$

Note that $c_d(t)$ is a desired command applied by the pilot and $\Phi(x_r(t))$ is a nonlinear function which limits the pilot authority by constraining the absolute value of the roll angle to remain less than or equal to 2. Motivated by the structure of the nonlinear reference model, the feedback linearization term is designed as

$$v(\cdot) = -Ke(t) + K[x_1(t), x_2(t), \Phi(x(t))x_3(t)]^T - K[x_{r1}(t), x_{r2}(t), \Phi(x_r(t))x_{r3}(t)]^T, \quad (3.70)$$

such that (3.53) holds. Using this, we select the basis function as

$$\sigma(\cdot) = [x_{p1}, x_{p2}, |x_{p1}|x_{p2}, |x_{p2}|x_{p1}, x_{p1}^3, x^T(t)K^T, v^T(\cdot)]^T, \quad (3.71)$$

and we set $R = I_{3 \times 3}$ for both the standard adaptive controller and the proposed adaptive controller. Furthermore, for the proposed design, we use (3.55), (3.41), and (3.56), and resort to (3.44) for enforcing $\|e(t)\|_p \leq 0.5$. Additionally, note that $\xi_{\min} = 1$ is selected to satisfy (3.43) and we choose $a = 2$.

Figure 3.10 shows the standard adaptive control response. It can be seen from the figure that even though the roll angle command is reasonably followed, the roll rate and the control response have undesirable high-frequency content which can cause instability. In addition, as seen in the bottom part of the figure, the standard adaptive controller is unable to enforce a pre-defined bound on the error.

To improve performance and enforce a user-defined bound on the error, the proposed adaptive controller is then implemented. Figures 3.11 and 3.12 show the proposed controller performance using the gain varying control. It is clear from Figure 3.11 that the proposed adaptive controller obtains superior command following performance and Figure 3.12 shows that the system error stays in the a priori given, user-defined performance bound.

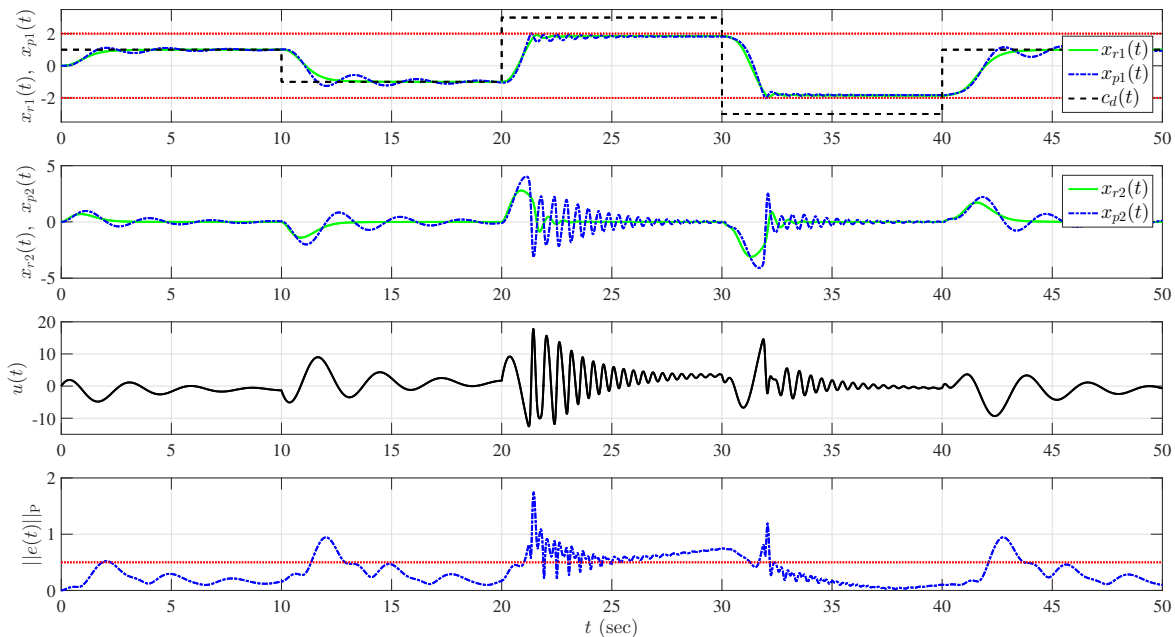


Figure 3.10: Standard adaptive controller performance ($\gamma = 1$).

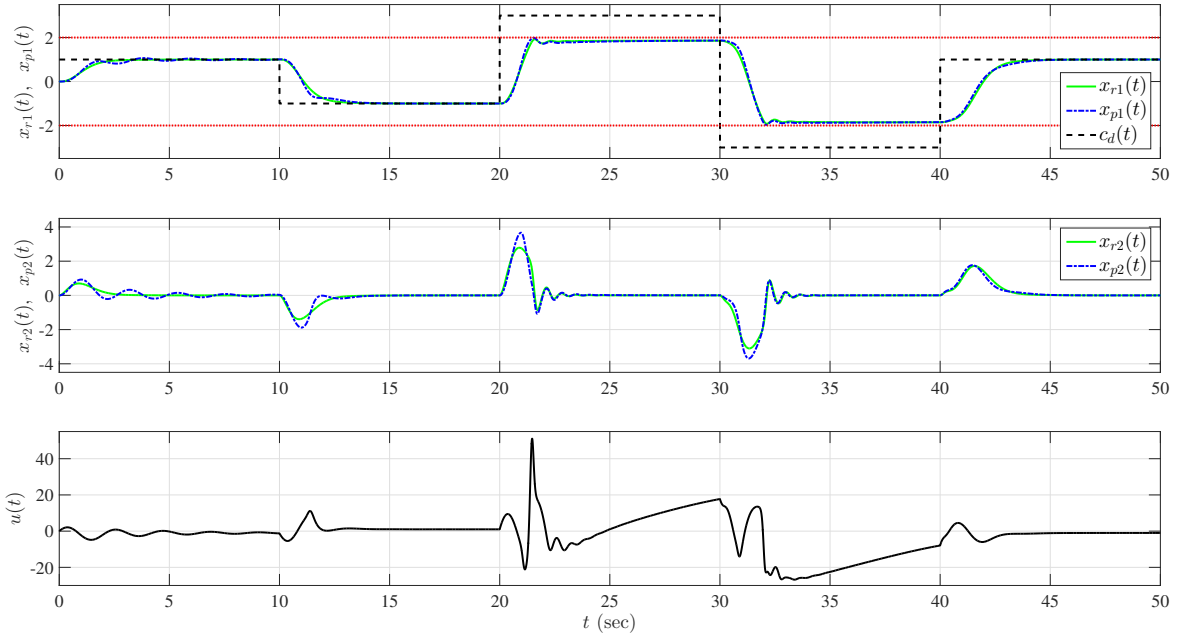


Figure 3.11: Proposed gain varying adaptive control performance ($\gamma = 1$ and $\gamma_\xi = 1$, $\xi_0 = 1$, and $a = 2$).

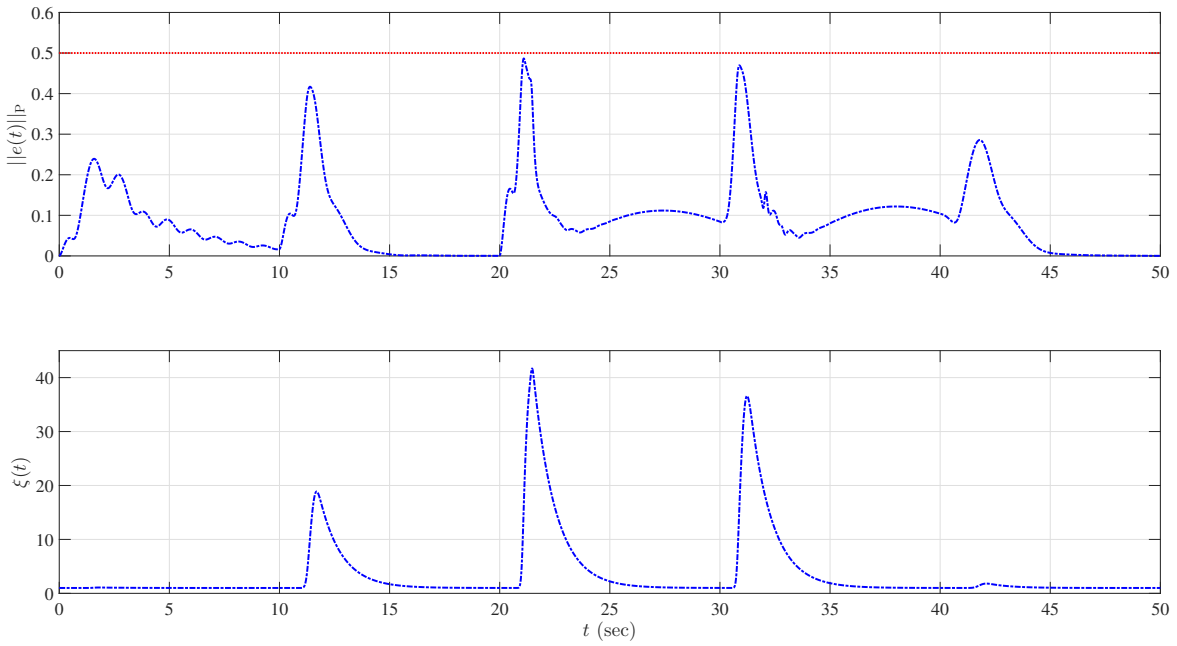


Figure 3.12: System error bounds and adaptation gain for Figure 3.11.

3.6 Experimental Results on Dual-Rotor Helicopter Testbed

In this section, the proposed adaptive control architecture is implemented on the Quanser AERO testbed [50] in dual-rotor helicopter configuration. In order to proceed with the control design, we focus the linearized model of the Quanser AERO testbed given by

$$J_\theta \ddot{\theta}(t) + D_\theta \dot{\theta}(t) + K_{s\theta} \theta(t) = \tau_\theta(t), \quad \theta(0) = \theta_0, \quad (3.72)$$

$$J_\psi \ddot{\psi}(t) + D_\psi \dot{\psi}(t) = \tau_\psi(t), \quad \psi(0) = \psi_0. \quad (3.73)$$

Here, $\theta(t)$ denotes the pitch angle in radians and $\psi(t)$ denotes the yaw angle in radians. Moreover, J_θ stands for the total moment of inertia about the pitch axis, J_ψ stands for the total moment of inertia about the yaw axis, D_θ stands for the damping about the pitch axis, D_ψ stands for the damping about the yaw axis, and $K_{s\theta}$ is the stiffness about the pitch axis. The control torques, which act on the pitch and yaw axes, satisfy

$$\tau_\theta(t) = K_{\theta\theta} u_\theta(t) + K_{\theta\psi} u_\psi(t), \quad (3.74)$$

$$\tau_\psi(t) = K_{\psi\theta} u_\theta(t) + K_{\psi\psi} u_\psi(t). \quad (3.75)$$

with $u_\theta(t)$ and $u_\psi(t)$ being the feedback control signals applied as motor voltages to the pitch and yaw rotors, respectively. Here, $K_{\theta\theta}$ is the torque thrust gain from the pitch rotor, $K_{\psi\psi}$ is the torque thrust gain from the yaw rotor, $K_{\theta\psi}$ is the cross-torque thrust gain acting on the pitch from the yaw rotor, and $K_{\psi\theta}$ is the cross-torque thrust gain acting on the yaw pitch rotor. Finally, we also note that $J_\theta = 0.0219$ [kg m^2], $J_\psi = 0.0220$ [kg m^2], $D_\theta = 0.0071$ [$\text{kg m}^2 \text{s}^{-1}$], $D_\psi = 0.0220$ [$\text{kg m}^2 \text{s}^{-1}$], $K_{\theta\theta} = 0.0011$ [$\text{kg m}^2 \text{s}^{-2} \text{V}^{-1}$], $K_{s\theta} = 0.0375$ [$\text{kg m}^2 \text{s}^{-2}$], $K_{\psi\psi} = 0.0022$ [$\text{kg m}^2 \text{s}^{-2} \text{V}^{-1}$], $K_{\psi\theta} = -0.0027$ [$\text{kg m}^2 \text{s}^{-2} \text{V}^{-1}$], $K_{\theta\psi} = 0.0021$ [$\text{kg m}^2 \text{s}^{-2} \cdot \text{V}^{-1}$] are used from the Quanser AERO user manual [50].

Next, let $x_p(t) = [\theta(t), \psi(t), \dot{\theta}(t), \dot{\psi}(t)]^T \in \mathbb{R}^4$ and $u(t) = [u_\theta(t), u_\psi(t)]^T \in \mathbb{R}^2$. Then, one can equivalently rewrite (3.72)–(3.75) as

$$\dot{x}_p(t) = A_p x_p(t) + B_p \Lambda u(t), \quad x_p(0) = x_{p0}, \quad (3.76)$$

where the controllable matrices A_p and B_p satisfy

$$A_p = \begin{bmatrix} 0 & 0 & 1 & 0 \\ 0 & 0 & 0 & 1 \\ -K_{s\theta}/J_\theta & 0 & -D_\theta/J_\theta & 0 \\ 0 & 0 & 0 & -D_\psi/J_\psi \end{bmatrix}, \quad B_p = \begin{bmatrix} 0 & 0 \\ 0 & 0 \\ K_{\theta\theta}/J_\theta & K_{\theta\psi}/J_\theta \\ K_{\psi\theta}/J_\psi & K_{\psi\psi}/J_\psi \end{bmatrix}. \quad (3.77)$$

Notice that we introduce Λ to (3.76), which is ideally equal to I . That is, we introduce uncertainty to Λ in the experimental results presented below and we do not consider other system uncertainty in the form “ $W_p^T \sigma_p(x_p(t))$ ”.

In the selection of the gain matrix K for the nominal control design, we resort to linear quadratic regulator theory (e.g., see [91]). Specifically, we select E_p as

$$E_p = \begin{bmatrix} 1 & 0 & 0 & 0 \\ 0 & 1 & 0 & 0 \end{bmatrix} \quad (3.78)$$

such that a desired pitch command and yaw angle command can be ideally followed. The controller gain matrix K is obtained using the highlighted augmented formulation along with the weighting matrices $Q = \text{diag}([2, 2, 0, 0, 50, 50])$ to penalize $x(t)$ and $R = 0.001I_2$ to penalize $u(t)$ as in [92], resulting in the following gain matrix

$$K = \begin{bmatrix} 82.85 & -124.21 & 29.70 & -32.29 & 125.18 & -185.28 \\ 117.26 & 78.55 & 38.95 & 19.04 & 185.28 & 125.18 \end{bmatrix}, \quad (3.79)$$

which has desirable phase margins of 61.9° and 62° and crossover frequencies of 5.95 rad/sec and 5.73 rad/sec for the pitch and yaw control channels respectively.

For the considered experimental set-up, a 30° yaw maneuver is considered as desired command following objective, while the pitch command remains as 0° . The yaw command is applied practically as a filtered 30° square signal. From the experimental viewpoint, it should be noted that the pitch and yaw motor voltages saturate at $\pm 24V$.

3.6.1 Nominal Control Results without Uncertainty

We first consider the case when there is no added uncertainty in the control effectiveness matrix to show the nominal performance of the experimental setup. In particular, Figures 3.13 and 3.14 respectively show the nominal control performance and the system error. It can be seen from these figures that the nominal control performs in a desirable manner and that the error signals are not equal to zero that is expected due to possible modeling inaccuracies of the experimental setup.

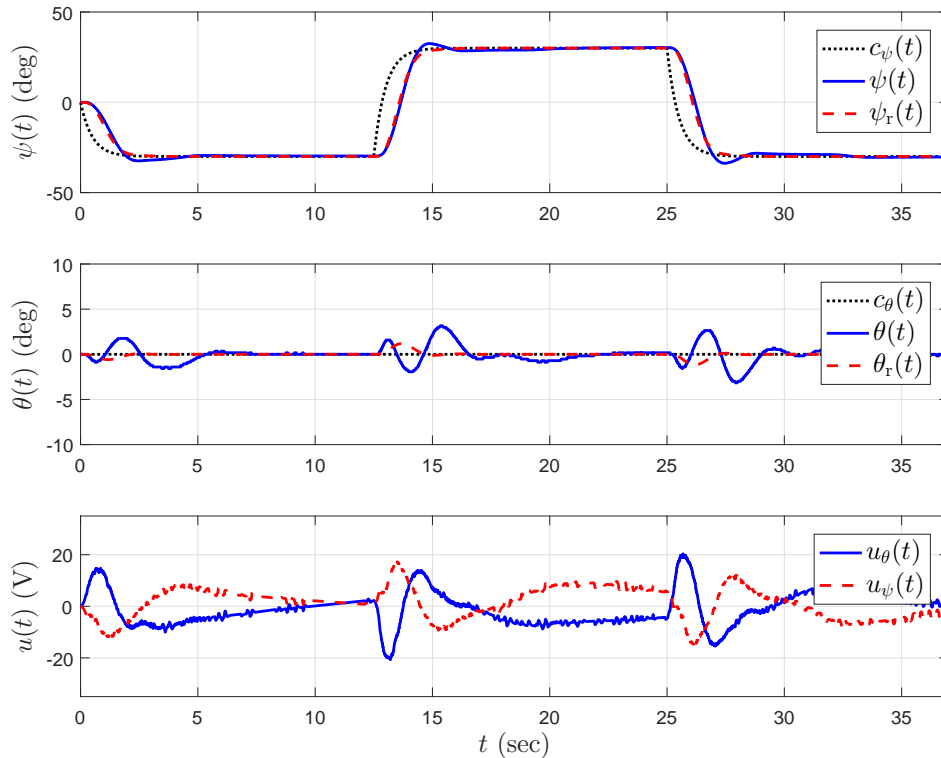


Figure 3.13: Nominal controller performance without uncertainty in the control effectiveness.

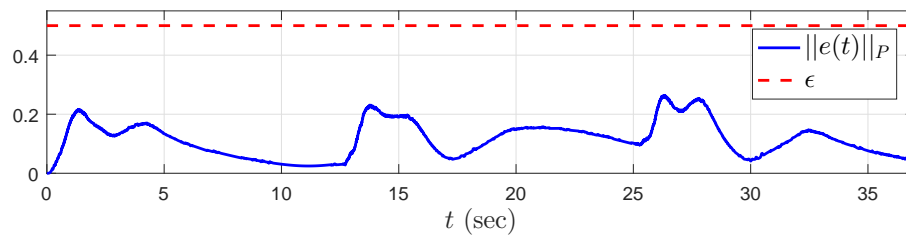


Figure 3.14: Nominal system error without uncertainty in the control effectiveness.

3.6.2 Adaptive Control Results with Uncertainty in Control Effectiveness

We next consider the case when the control effectiveness matrix is uncertain. For this purpose, we let $\Lambda = 0.1I_2$. Figures 3.15 and 3.16 show the response with the nominal control and the system error, which goes unstable. A standard adaptive control design is now implemented to stabilize the the unstable nominal control response. Since we only consider the uncertainty in the control effectiveness, we select the basis function as $\sigma(x(t)) = [x^T(t)K^T]^T$ for the control design. In addition, it should be noted that without loss of generality, a projection based weight update law is used which adds additional robustness owing to the modeling inaccuracies of the Quanser AERO testbed. The projection bounds are set elementally for the considered uncertainty, $W = \Lambda^{-1} - I_2$, as $4.5 \leq [\hat{W}(t)]_{i,i} \leq 13.5, i = 1, 2$ (see Appendix A for details on the projection operator). Moreover, we use $R = 1.5I_{6 \times 6}$ to calculate P from (3.16) for the considered A_f matrix. Figures 3.17 and 3.18 show the standard adaptive control response with a low learning gain of $\gamma = 0.1$. It can be seen from Figure 3.17, the system, while stable in the presence of the considered uncertainty, has poor transient performance in the yaw and pitch response. In addition, as shown in Figure 3.18, the system error exceeds the performance bound of $\varepsilon = 0.5$. To improve the performance, the learning gain is increased to $\gamma = 10$ as shown in Figures 3.19 and 3.20. As seen in Figure 3.19, the tracking performance improves and Figure 3.20 shows the system error is now contained within the performance bound. In addition, comparison of Figures 3.18 and 3.20 shows improved adaptation in the adaptive control signal and the weight estimates for the increased learning gain. At this point, it should be noted that the performance obtained for the increased learning gain (shown in Figures 3.19 and 3.20) is only obtained by judiciously increasing the learning gain, and hence, is not guaranteed and is subject to change if the system uncertainties change.

To improve performance and enforce the user-defined bound on the error, the proposed adaptive controller is then implemented using the same basis function, projection bounds, and P solution as the standard adaptive control design. The learning gain is set to $\gamma = 0.1$ as in the low gain learning gain case of the standard adaptive control design previously discussed. This allows for better comparison to the standard adaptive control which was unable to enforce the user-defined performance bound shown in Figures 3.17 and 3.18. The additional parameters for the proposed control are selected as $\xi_{\min} = 0.1, \xi_{\max} = 100, a = 2$, and $\gamma_{\xi} = 100$ such that the condition given by (3.43) is satisfied. Figures 3.21–3.23 show the proposed controller performance using the gain varying control. Specifically, Figure 3.21 shows that the tracking performance is better as compared to the standard adaptive control cases, and Figure 3.22 shows the guaranteed bound

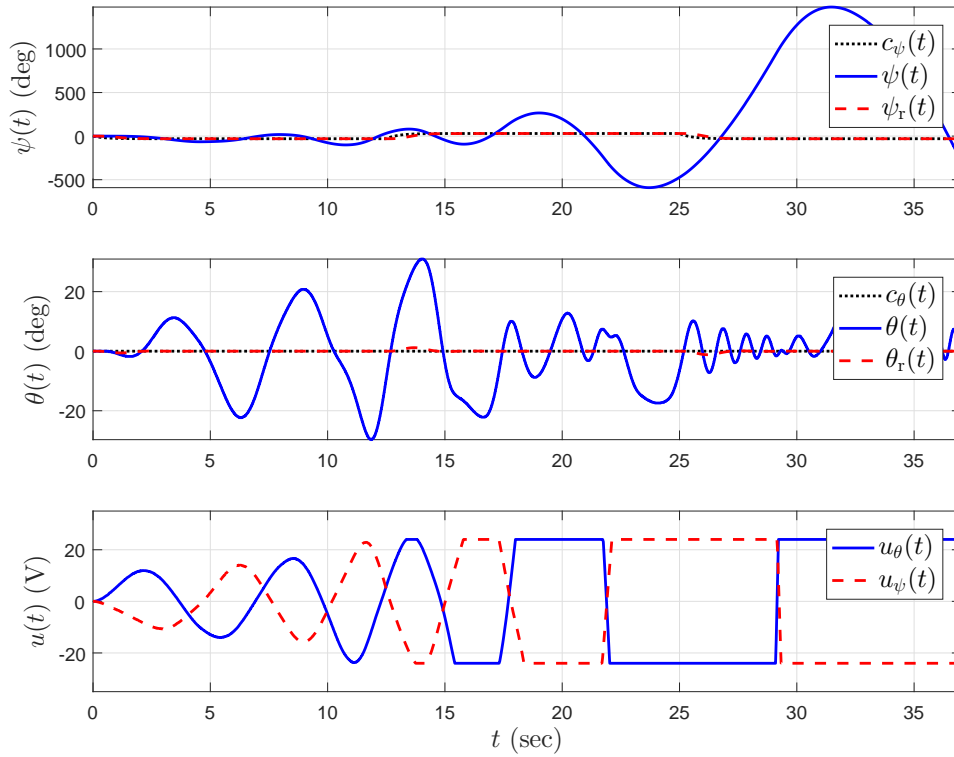


Figure 3.15: Nominal controller performance with uncertainty in the control effectiveness.

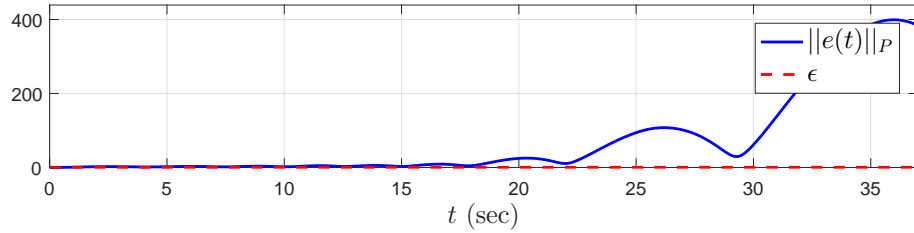


Figure 3.16: Nominal system error with uncertainty in the control effectiveness.

$\|e(t)\|_P \leq 0.5$ is enforced by the error dependent gain term $\xi(t)$. In addition, Figure 3.23 shows a steadier adaptive control response as compared to the responses in Figures 3.18 and 3.20 for the standard adaptive control cases.

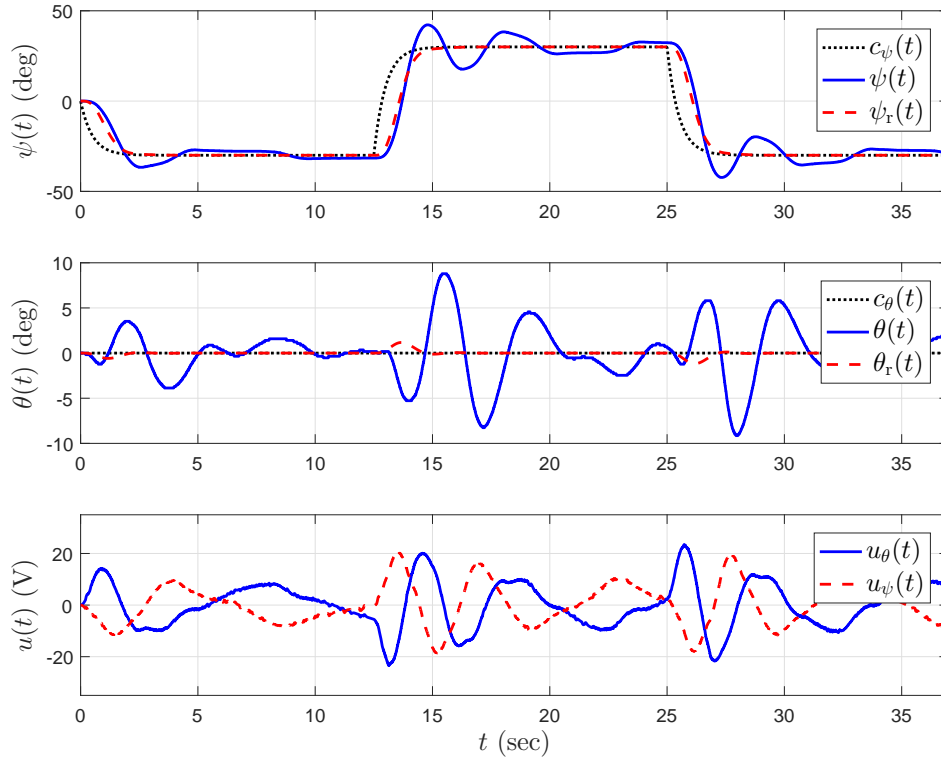


Figure 3.17: Standard adaptive control performance with low learning gain.

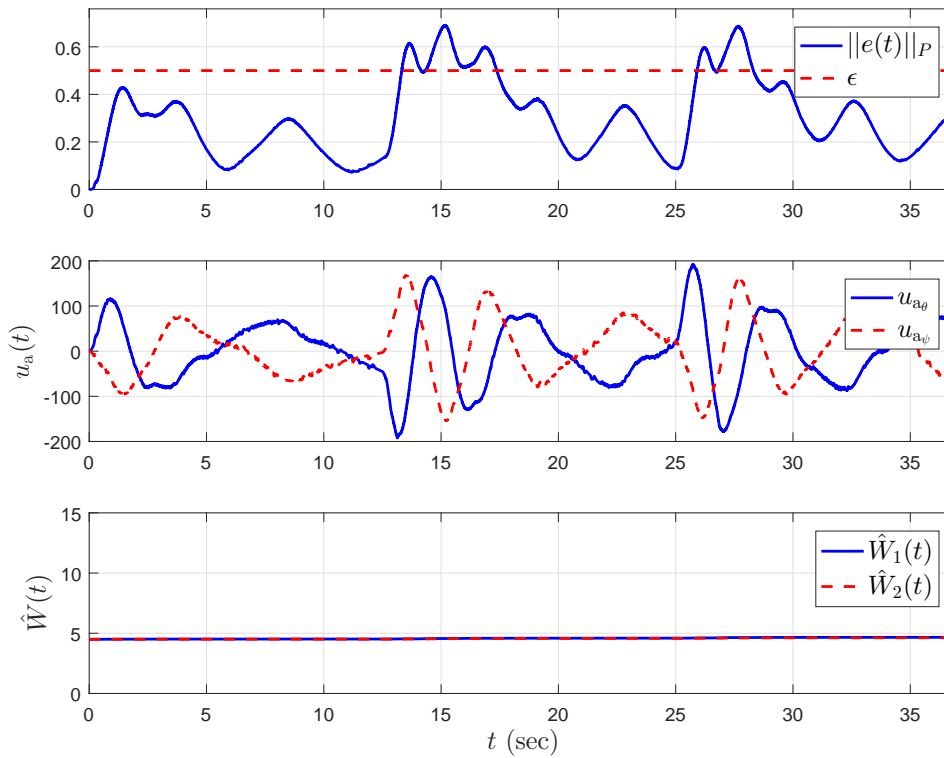


Figure 3.18: System error, adaptive control signal, and weight estimate for low learning gain.

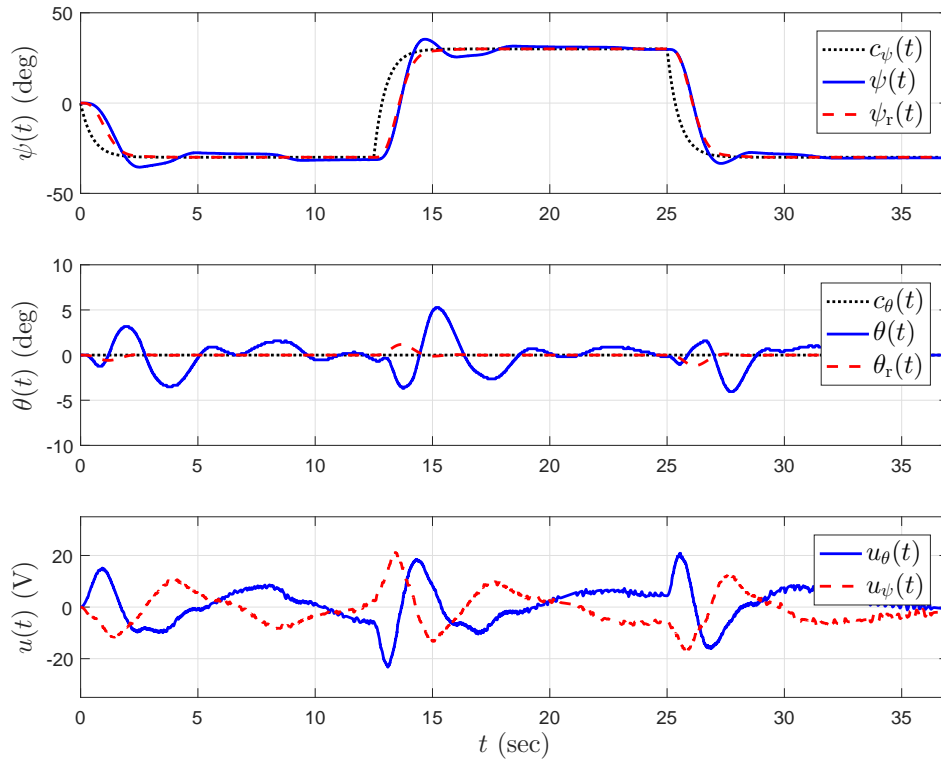


Figure 3.19: Standard adaptive control performance with increased learning gain.

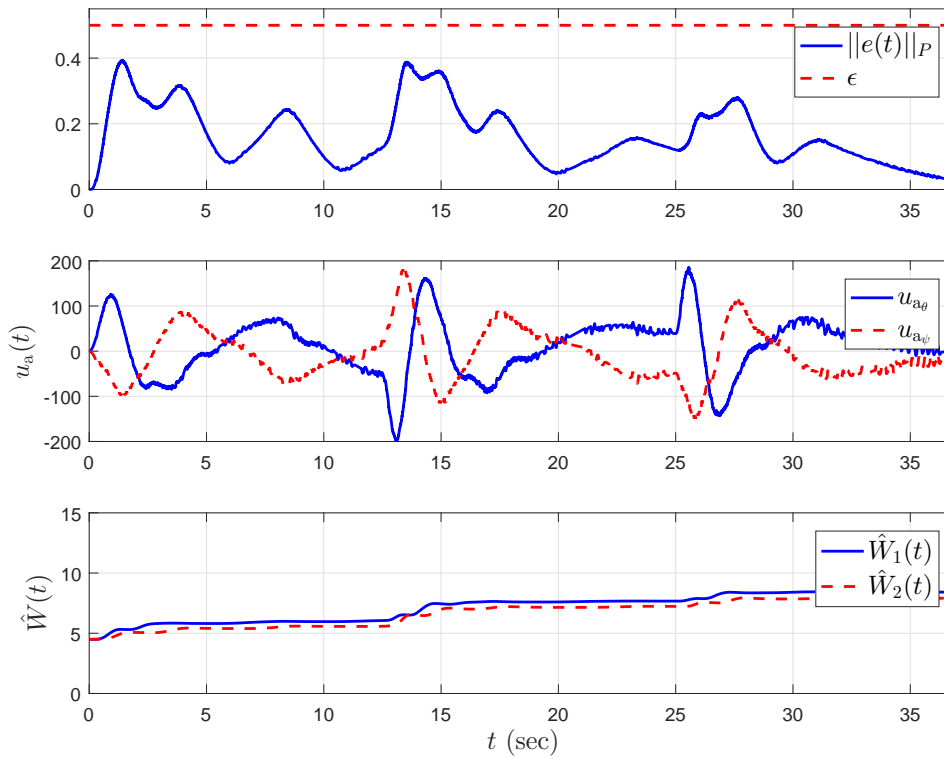


Figure 3.20: System error, adaptive control signal, and weight estimate for increased learning gain.

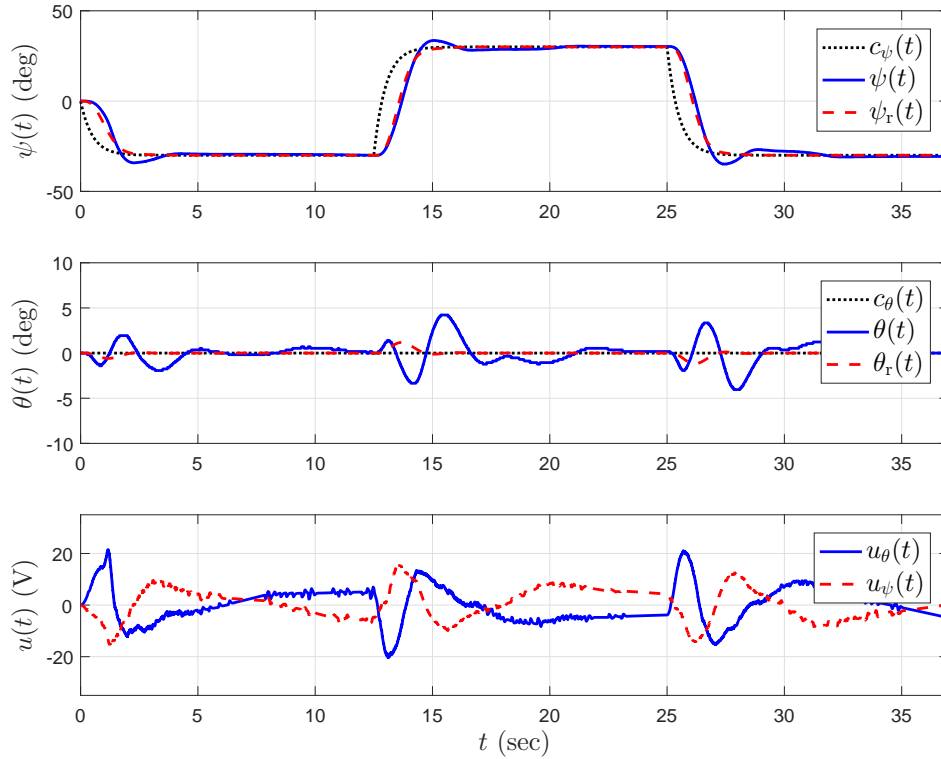


Figure 3.21: Proposed control tracking performance.

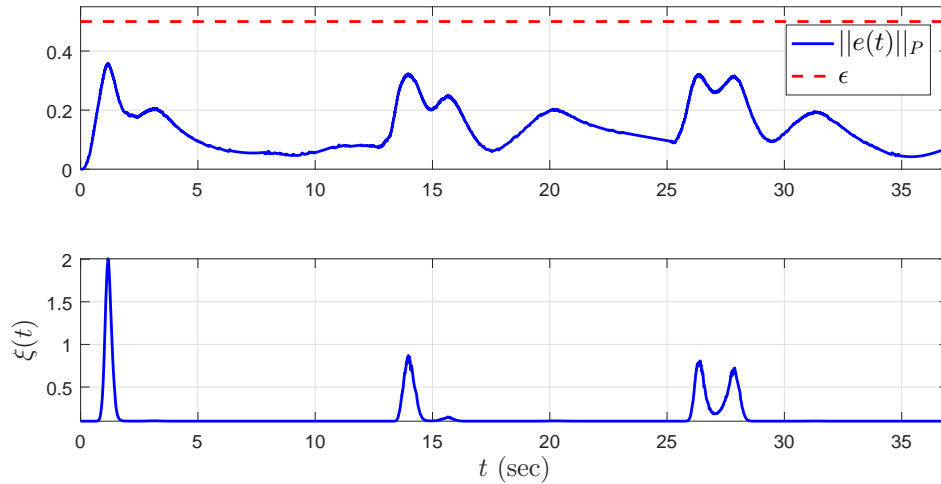


Figure 3.22: System error and adaptation gain for proposed adaptive control.

3.7 Conclusion

We proposed a direct uncertainty minimization approach that uses modification terms in the adaptive control law and the update law to suppress the effect of system uncertainty on the transient system response through a gradient minimization procedure for improved system performance. In addition, the use of a

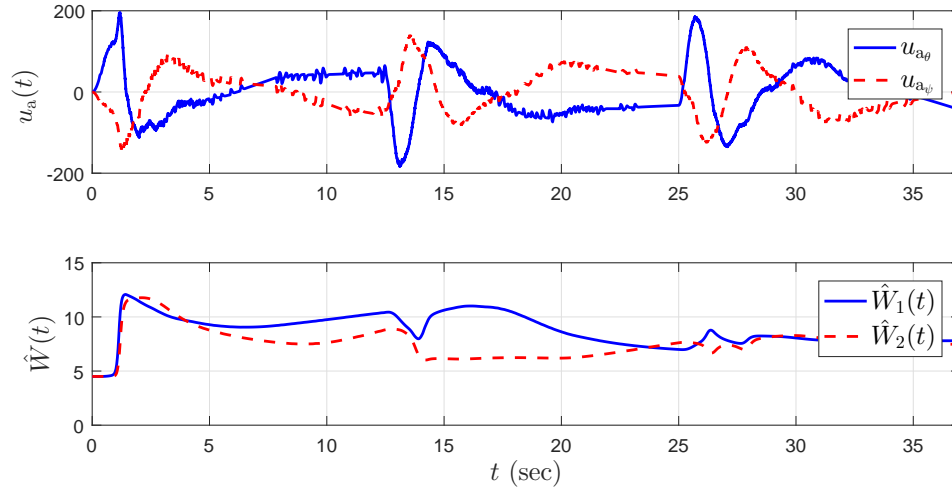


Figure 3.23: Adaptive control signal and weight estimates for proposed adaptive control.

varying gain on the modification term was shown to keep the system error approximately within *a priori* given, user-defined error performance bounds. The proposed approach was then generalized to incorporate a nonlinear reference model to better capture the desired closed-loop system performance for a class of nonlinear uncertain dynamical systems. Two illustrative numerical examples and experimental results were included to demonstrate the efficacy of the proposed adaptive control framework. Future research will include generalizations of the proposed framework to output feedback adaptive control as well as applications to large-scale dynamical systems.

CHAPTER 4: COMPUTING STABILITY LIMITS OF ADAPTIVE CONTROL LAWS WITH HIGH-ORDER ACTUATOR DYNAMICS¹

A challenge in the design of adaptive control laws for uncertain dynamical systems is to achieve system stability and a prescribed level of command following performance in the presence of actuator dynamics. It is well-known that if the actuator dynamics do not have sufficiently high bandwidth, their presence cannot be practically neglected in the design since they limit the achievable stability of adaptive control laws. In this paper, we consider the design of model reference adaptive control laws for uncertain dynamical systems in the presence of high-order actuator dynamics. Specifically, a linear matrix inequalities-based hedging approach is proposed, where this approach modifies the ideal reference model dynamics to allow for correct adaptation that is not affected by the presence of actuator dynamics. The stability of the modified reference model is then computed using linear matrix inequalities, which reveals the fundamental stability interplay between the parameters of the actuator dynamics and the allowable system uncertainties. In addition, we analyze the convergence properties of the modified reference model to the ideal reference model. The presented theoretical results are finally illustrated through a numerical example.

4.1 Introduction

Mathematical models used in feedback control design are often based on first principles of physics and are derived using fundamental physical laws. However, due to system complexity, idealized assumptions and simplifications, system uncertainty, and exogenous disturbances, first principle models are often not accurate to capture the exact physical phenomena that undergo spatial and temporal evolution. To this end, adaptive control laws have the capability to guarantee system stabilization and a prescribed level of command following performance for dynamical systems subject to inaccurate mathematical models and degraded modes of operation [5–7, 93]. Yet, one of the importance challenges in the design of adaptive control laws for uncertain dynamical systems is to achieve system stability and a prescribed level of command

¹This chapter has been submitted to the journal *Automatica* for possible publication.

following performance in the presence of actuator dynamics. It is well-known that if the actuator dynamics do not have sufficiently high bandwidth, their presence cannot be practically neglected in the design since they limit the achievable stability of adaptive control laws.

In the literature, while there exist a few approaches to the design of adaptive control laws in the presence of actuator dynamics (see, for example, [57, 94] and references therein), the constructive nature of these approaches couple the uncertain dynamical systems with their actuator dynamics, which can result in imprecise estimation of the system uncertainties for the suppression of their effects — with a notable exception called the hedging method [30, 31, 33]. In particular, the hedging method enables adaptive control laws to be designed such that their capability to estimate the system uncertainties are not affected by the presence of actuator dynamics. This is accomplished by modifying the ideal reference model dynamics with a hedge signal such that standard closed-loop system dynamics are obtained to allow for correct adaptation even in the presence of actuator dynamics. Yet, until our recent work [95] focusing on the presence of first-order actuator dynamics, it has not been analyzed that this modification to the ideal reference model dynamics does not yield to unbounded reference model responses. Although this is an important result, it is known that many actuator dynamics utilized in real-world application do not necessarily follow a first-order model.

In this paper, we consider the design of model reference adaptive control laws with projection operator for uncertain dynamical systems in the presence of high-order actuator dynamics, unlike our previous results documented in [95]. To this end, a linear matrix inequalities-based hedging approach is proposed. Specifically, this approach modifies the ideal reference model dynamics to allow for correct projection operator-based adaptation that is not affected by the presence of high-order actuator dynamics. To compute the stability limit of the modified reference model, we utilize linear matrix inequalities, where this computation reveals the fundamental stability interplay between the parameters of the actuator dynamics and the allowable system uncertainties through the selection of the projection operator bounds. Moreover, we analyze, for the first time, the distance between the modified reference model trajectories and ideal reference model trajectories, and determine a condition for which these trajectories converge to each other. This is another significant departure from the results documented in not only [95] but also [30, 31, 33]. Finally, our results do not adopt small-gain type arguments as in [57, 94] in the stability analysis, where it is known that these small-gain type approaches tend to be more conservative than linear matrix inequalities-based

approaches (see, for example, [96]). The presented theoretical results of our paper are further illustrated through a numerical example.

The notation used throughout this paper is fairly standard. Specifically, \mathbb{R} denotes the set of real numbers, \mathbb{R}^n denotes the set of $n \times 1$ real column vectors, $\mathbb{R}^{n \times m}$ denotes the set of $n \times m$ real matrices, \mathbb{R}_+ (resp. $\overline{\mathbb{R}}_+$) denotes the set of positive (resp., nonnegative) real numbers, $\mathbb{R}_+^{n \times n}$ (resp., $\overline{\mathbb{R}}_+^{n \times n}$) denotes the set of $n \times n$ positive-definite (resp. nonnegative-definite) real matrices, $(\cdot)^T$ denotes the transpose operator, $(\cdot)^{-1}$ denotes the inverse operator, $\text{tr}(\cdot)$ denotes the trace operator, $\text{diag}(a)$ denotes the diagonal matrix with the vector a on its diagonal, $\|\cdot\|_2$ denotes the Euclidian norm, $\|\cdot\|_F$ denotes the Frobenius matrix norm, $[A]_{ij}$ denotes the ij -th entry of the real matrix $A \in \mathbb{R}^{n \times m}$, $\lambda_{\min}(A)$ (resp., $\lambda_{\max}(A)$) denotes the minimum (resp., maximum) eigenvalue of the real matrix $A \in \mathbb{R}^{n \times n}$, and “ \triangleq ” denotes the equality by definition.

4.2 Mathematical Preliminaries

In this section, we introduce some fundamental results needed to develop the main results of this paper. We begin with the definition of the projection operator [6].

Definition 4.2.1 Consider a convex hypercube in the form $\Omega_0 = \{\theta_0 \in \mathbb{R}^n : (\theta_{0i}^{\min} \leq \theta_{0i} \leq \theta_{0i}^{\max})_{i=1,2,\dots,n}\}$, where $\Omega_0 \in \mathbb{R}^n$, and θ_{0i}^{\min} and θ_{0i}^{\max} respectively represent the minimum and maximum bounds for the i^{th} component of the n -dimensional parameter vector θ_0 (we set $\theta_{0i}^{\min} = -\theta_{0i}^{\max}$ for the results of this paper without loss of generality). Furthermore, for a sufficiently small positive constant ε_0 , consider another hypercube in the form $\Omega_\varepsilon = \{\theta_0 \in \mathbb{R}^n : (\theta_{0i}^{\min} + \varepsilon_0 \leq \theta_{0i} \leq \theta_{0i}^{\max} - \varepsilon_0)_{i=1,2,\dots,n}\}$, where $\Omega_\varepsilon \subset \Omega$. The projection operator $\text{Proj} : \mathbb{R}^n \times \mathbb{R}^n \rightarrow \mathbb{R}^n$ is then defined component-wise by

$$\text{Proj}(\theta, y) \triangleq \begin{cases} \left(\frac{\theta_{0i}^{\max} - \theta_{0i}}{\varepsilon_0} \right) y_i, & \text{if } \theta_{0i} > \theta_{0i}^{\max} - \varepsilon_0 \text{ and } y_i > 0, \\ \left(\frac{\theta_{0i} - \theta_{0i}^{\min}}{\varepsilon_0} \right) y_i, & \text{if } \theta_{0i} < \theta_{0i}^{\min} + \varepsilon_0 \text{ and } y_i < 0, \\ y_i, & \text{otherwise,} \end{cases}$$

where $y \in \mathbb{R}^n$.

Remark 4.2.1 Based on Definition 4.2.1 and $\theta_0^* \in \Omega_\varepsilon$, one can show the inequality $(\theta_0 - \theta_0^*)^T (\text{Proj}(\theta_0, y) - y) \leq 0$, holds for $\theta_0 \in \Omega_0$ and $y \in \mathbb{R}^n$ [6]. We use a generalization of this definition to matrices as $\text{Proj}_m(\Theta, Y) = (\text{Proj}(\text{col}_1(\Theta), \text{col}_1(Y)), \dots, \text{Proj}(\text{col}_m(\Theta), \text{col}_m(Y)))$, where $\Theta \in \mathbb{R}^{n \times m}$, $Y \in \mathbb{R}^{n \times m}$, and $\text{col}_i(\cdot)$

denotes the i -th column operator. In this case, for a given matrix Θ^* , it follows that $\text{tr} \left[(\Theta - \Theta^*)^T (\text{Proj}_m(\Theta, Y) - Y) \right] = \sum_{i=1}^m \left[\text{col}_i(\Theta - \Theta^*)^T (\text{Proj}(\text{col}_i(\Theta), \text{col}_i(Y)) - \text{col}_i(Y)) \right] \leq 0$, holds.

We now briefly overview the standard model reference control problem in the absence of actuator dynamics. Consider the uncertain dynamical system given by

$$\dot{x}(t) = Ax(t) + Bu(t), \quad x(0) = x_0, \quad (4.1)$$

where $x(t) \in \mathbb{R}^n$ is the state vector available for feedback, $u(t) \in \mathbb{R}^m$ is the control input restricted to the class of admissible controls consisting of measurable functions, $A \in \mathbb{R}^{n \times n}$ is an unknown system matrix, $B \in \mathbb{R}^{n \times m}$ is a known input matrix, and the pair (A, B) is controllable. In addition, consider the reference model capturing a desired, ideal closed-loop dynamical system performance

$$\dot{x}_r(t) = A_r x_r(t) + B_r c(t), \quad x_r(0) = x_{r0}, \quad (4.2)$$

where $x_r(t) \in \mathbb{R}^n$ is the reference state vector, $c(t) \in \mathbb{R}^m$ is a given uniformly continuous bounded command, $A_r \in \mathbb{R}^{n \times n}$ is the Hurwitz reference model matrix, and $B_r \in \mathbb{R}^{n \times m}$ is the command input matrix. The objective of the model reference adaptive control problem is to construct an adaptive feedback control law $u(t)$ such that the state vector $x(t)$ asymptotically follows the reference state vector $x_r(t)$. We now make the following assumption, which is standard in the model reference adaptive control literature and is known as the matching condition.

Assumption 4.2.1 *There exists an unknown matrix $K_1 \in \mathbb{R}^{m \times n}$ and a known matrix $K_2 \in \mathbb{R}^{m \times m}$ such that $A_r = A - BK_1$ and $B_r = BK_2$ hold.*

Remark 4.2.2 *While Assumption 4.2.1 is a widely-adopted standard assumption in the model reference adaptive control literature [5–7], several works have considered the case in which the uncertainties are unmatched, see for example, [13–19] and references therein. The results of this paper can be applied to those results.*

It follows from Assumption 4.2.1 that (4.1) can be written as

$$\dot{x}(t) = A_r x(t) + B_r c(t) + B[u(t) + W_1^T x(t) - K_2 c(t)], \quad (4.3)$$

where $W_1 \triangleq K_1^T \in \mathbb{R}^{n \times m}$ is unknown. Now, let the adaptive feedback control law be given by

$$u(t) = -\hat{W}_1^T(t)x(t) + K_2c(t), \quad (4.4)$$

where $\hat{W}_1(t) \in \mathbb{R}^{n \times m}$ is the estimate of W_1 satisfying the weight update law

$$\dot{\hat{W}}_1(t) = \gamma_1 \text{Proj}_m[\hat{W}_1(t), x(t)e^T(t)PB], \quad \hat{W}_1(0) = \hat{W}_{10}, \quad (4.5)$$

with $\gamma_1 \in \mathbb{R}_+$ being the learning rate, $e(t) \triangleq x(t) - x_r(t)$ being the system error state vector, and $P \in \mathbb{R}_+^{n \times n}$ being the solution of the Lyapunov equation given by

$$0 = A_r^T P + P A_r + R, \quad (4.6)$$

$R \in \mathbb{R}_+^{n \times n}$. Note that since A_r is Hurwitz, it follows from the converse Lyapunov theory [80] that there exists a unique P satisfying (4.6) for a given R . In addition, the projection bounds are defined such that $|\hat{W}_1(t)_{ij}| \leq \hat{W}_{1, \max, i+(j-1)n}$, for $i = 1, \dots, n$ and $j = 1, \dots, m$, where $\hat{W}_{1, \max, i+(j-1)n} \in \mathbb{R}_+$ denotes (symmetric) element-wise projection bounds. Note that the results of this paper can be trivially applied to the case when asymmetric projection bounds are considered.

Now, using (4.4) in (4.3) along with (4.2), the system error dynamics can be written as

$$\dot{e}(t) = A_r e(t) - B \tilde{W}_1^T(t)x(t), \quad e(0) = e_0, \quad (4.7)$$

where $\tilde{W}_1(t) \triangleq \hat{W}_1(t) - W_1 \in \mathbb{R}^{n \times m}$.

Remark 4.2.3 *The weight update law given by (4.5) can be derived using Lyapunov analysis by considering the Lyapunov function candidate given by (see, for example, [5–7])*

$$\mathcal{V}(e, \tilde{W}_1) = e^T P e + \gamma_1^{-1} \text{tr} \tilde{W}_1^T \tilde{W}_1. \quad (4.8)$$

Note that $\mathcal{V}(0,0) = 0$ and $\mathcal{V}(e, \tilde{W}_1) > 0$ for all $(e, \tilde{W}_1) \neq (0,0)$. Now, differentiating (4.8) yields $\dot{\mathcal{V}}(e(t), \tilde{W}_1(t)) \leq -e^T(t) R e(t) \leq 0$, which guarantees that the system error state vector $e(t)$ and the weight error $\tilde{W}_1(t)$ are Lyapunov stable, and hence, are bounded for all $t \in \overline{\mathbb{R}}_+$. Since $x(t)$ is bounded for all $t \in \overline{\mathbb{R}}_+$, it follows from (4.7) that $\dot{e}(t)$ is bounded, and hence, $\ddot{\mathcal{V}}(e(t), \tilde{W}_1(t))$ is bounded for all $t \in \overline{\mathbb{R}}_+$. It then follows from Barbalat's lemma that $\lim_{t \rightarrow \infty} \dot{\mathcal{V}}(e(t), \tilde{W}_1(t)) = 0$, which consequently shows that $e(t) \rightarrow 0$ as $t \rightarrow \infty$. It

should also be noted that owing to the use of the projection operator in the weight update law given by (4.5), the above discussion can be readily extended to the case of time-varying uncertainties (i.e., $W_1(t) \in \mathbb{R}^{n \times m}$ with $\|W_1(t)\|_F \leq w$ and $\|\dot{W}_1(t)\|_F \leq \dot{w}$, $w \in \mathbb{R}_+$, $\dot{w} \in \mathbb{R}_+$) are considered. In this case, the boundedness of the pair $(e(t), \tilde{W}_1(t))$ follows using (4.8), where the bound on $e(t)$ can be adjusted by the user to achieve a desired level of performance [6].

4.3 Model Reference Adaptive Control with High-Order Actuator Dynamics

The standard model reference adaptive control formulation overviewed in the previous section has the capability to suppress the effect of any system uncertainties to achieve desirable tracking performance specifications, when the actuator dynamics are not present in the closed-loop dynamical system. Building on the results of the previous section, we now present a new model reference adaptive control design procedure to ensure guaranteed stability and performance in the presence of high-order actuator dynamics. Specifically, consider the uncertain dynamical system subject to actuator dynamics given by

$$\dot{x}(t) = Ax(t) + Bv(t), \quad x(0) = x_0, \quad (4.9)$$

where $v(t) \in \mathbb{R}^m$ is the actuator output of the actuator dynamics \mathcal{G}_A given by

$$\begin{aligned} \dot{x}_c(t) &= Fx_c(t) + Gu(t), \quad x_c(0) = x_{c0}, \\ v(t) &= Hx_c(t), \end{aligned} \quad (4.10)$$

with $x_c(t) \in \mathbb{R}^p$ being the actuator state vector, $G \in \mathbb{R}^{p \times m}$ being the actuator input matrix, $H \in \mathbb{R}^{m \times p}$ being the actuator output matrix, and $F \in \mathbb{R}^{p \times p}$ being Hurwitz such that there exists $S \in \mathbb{R}_+^{p \times p}$ that satisfies $0 = F^T S + SF + I$.

By adding and subtracting $Bu(t)$ and using Assumption 4.2.1, (4.9) can be rewritten as

$$\dot{x}(t) = A_r x(t) + B_r c(t) + B[u(t) + W_1^T x(t) - K_2 c(t)] + B[v(t) - u(t)]. \quad (4.11)$$

Based on the hedging approach², we now consider the modified reference model dynamics given by

²It is known that in the presence of actuator dynamics, not all reference model trajectories can be tracked. Motivated from this, the hedging method introduces the deficit term “ $B[v(t) - u(t)]$ ” to the ideal reference model trajectories such that the resulting reference model can be tracked by the uncertain dynamical system. For more details, we refer to [30, 31, 33].

$$\dot{x}_r(t) = A_r x_r(t) + B_r c(t) + B[v(t) - u(t)], \quad x_r(0) = x_{r0}. \quad (4.12)$$

Now, by considering the uncertain dynamical system subject to actuator dynamics given by (4.11), with the adaptive feedback control law given by (4.4) and (4.5), and the modified reference model given by (4.12), the system error dynamics between (4.11) and (4.12) is given in the form of (4.7). This is the result of introducing the hedging signal $B[v(t) - u(t)]$ to the ideal reference model dynamics.

Assumption 4.3.1 *The matrix*

$$\mathcal{A}(\hat{W}_1(t), \mathcal{G}_A) = \begin{bmatrix} A_r + B\hat{W}_1^T(t) & BH \\ -G\hat{W}_1^T(t) & F \end{bmatrix}, \quad (4.13)$$

is quadratically stable.

Remark 4.3.1 *By definition, (4.13) is quadratically stable if and only if there exists a $\mathcal{P} > 0$ such that $\mathcal{A}^T(\hat{W}_1(t), \mathcal{G}_A)\mathcal{P} + \mathcal{P}\mathcal{A}(\hat{W}_1(t), \mathcal{G}_A) < 0$ holds [97, 98]. We can use linear matrix inequalities (LMIs) to satisfy the quadratic stability of (4.13) by following a similar procedure documented in our recent works [95]. For this purpose, let $\bar{W}_{1_{i_1, \dots, i_r}} \in \mathbb{R}^{n \times m}$ be defined as*

$$\bar{W}_{1_{i_1, \dots, i_r}} = \begin{bmatrix} (-1)^{i_1} \hat{W}_{1, \max, 1} & (-1)^{i_1+n} \hat{W}_{1, \max, 1+n} & \dots & (-1)^{i_1+(m-1)n} \hat{W}_{1, \max, 1+(m-1)n} \\ (-1)^{i_2} \hat{W}_{1, \max, 2} & (-1)^{i_2+n} \hat{W}_{1, \max, 2+n} & \dots & (-1)^{i_2+(m-1)n} \hat{W}_{1, \max, 2+(m-1)n} \\ \vdots & \vdots & \ddots & \vdots \\ (-1)^{i_n} \hat{W}_{1, \max, n} & (-1)^{i_n} \hat{W}_{1, \max, 2n} & \dots & (-1)^{i_n m} \hat{W}_{1, \max, mn} \end{bmatrix}, \quad (4.14)$$

where $i_r \in \{1, 2\}$, $r \in \{1, \dots, 2^{mn}\}$, such that $\bar{W}_{1_{i_1, \dots, i_r}}$ represents the corners of the hypercube defining the maximum variation of $\hat{W}_1(t)$. Utilizing the results in [96, 99], if

$$\mathcal{A}_{i_1, \dots, i_r} = \begin{bmatrix} A_r + B\bar{W}_{1_{i_1, \dots, i_r}}^T & BH \\ -G\bar{W}_{1_{i_1, \dots, i_r}}^T & F \end{bmatrix}, \quad (4.15)$$

which depends affinely on the parameters $\bar{W}_{1_{i_1, \dots, i_r}}$, satisfies the matrix inequality

$$\mathcal{A}_{i_1, \dots, i_r}^T \mathcal{P} + \mathcal{P} \mathcal{A}_{i_1, \dots, i_r} < 0, \quad \mathcal{P} = \mathcal{P}^T > 0, \quad (4.16)$$

for all permutations of $\bar{W}_{1_{i_1, \dots, i_r}}$, and hence, is quadratically stable at all corners of the hypercube, then (4.13) is quadratically stable. From a practical standpoint, there exist actuator dynamics fast enough such that (4.16) is satisfied, and hence, we can cast it as a convex optimization problem and solve it using LMIs. A sufficient condition is provided in Lemma 4.3.1 to support this point.

Now that the quadratic stability of (4.13) in Assumption 4.3.1 can be determined through the use of LMIs, we present the following proposition.

Proposition 4.3.1 Consider the uncertain dynamical system given by (4.9) subject to Assumption 4.2.1, the reference model given by (4.12), the actuator dynamics given by (4.10), and the adaptive feedback control law given by (4.4) along with the update law (4.5). Under Assumption 4.3.1, the solution $(e(t), \tilde{W}_1(t), x_r(t), v(t))$ of the closed-loop dynamical system are bounded and $\lim_{t \rightarrow \infty} e(t) = 0$. In addition, the system error dynamics satisfy the transient performance bound given by

$$\|e(t)\|_{\mathcal{L}_\infty} \leq \left(\frac{1}{\lambda_{\min}(P)} \left(\lambda_{\max}(P) \|e(0)\|_2^2 + \gamma_1^{-1} \|\tilde{W}_1(0)\|_{\mathbb{F}}^2 \right) \right)^{\frac{1}{2}}. \quad (4.17)$$

Proof. To show Lyapunov stability and guarantee boundedness of the system error and the weight error, consider the Lyapunov function candidate given by (4.8). Differentiation of (4.8) yields $\dot{V}(e(t), \tilde{W}_1(t)) \leq -e^T(t)Re(t) \leq 0$, which guarantees the Lyapunov stability, and hence, the boundedness of the solution $(e(t), \tilde{W}_1(t))$.

To show the boundedness of $x_r(t)$ and $x_c(t)$, consider the reference model (4.12) and the actuator dynamics (4.10) subject to (4.4) as

$$\dot{x}_r(t) = A_r x_r(t) + B [H x_c(t) + \hat{W}_1^T(t) e(t) + \hat{W}_1^T(t) x_r(t)], \quad (4.18)$$

$$\dot{x}_c(t) = F x_c(t) - G \hat{W}_1^T(t) x_r(t) - G \hat{W}_1^T(t) e(t) + G K_2 c(t), \quad (4.19)$$

where (4.18) and (4.19) can be rewritten in compact form as

$$\dot{\xi}(t) = \mathcal{A}(\hat{W}_1(t), \mathcal{G}_A) \xi(t) + \omega(\cdot), \quad (4.20)$$

with $\xi(t) = [x_r^T(t), x_c^T(t)]^T$ and

$$\omega(\cdot) = \begin{bmatrix} B\hat{W}_1^T(t)e(t) \\ -G\hat{W}_1^T(t)e(t) + GK_2c(t) \end{bmatrix}. \quad (4.21)$$

Note that $\omega(\cdot)$ in (4.20) is a bounded perturbation as a result of Lyapunov stability of the pair $(e(t), \tilde{W}_1(t))$. Now, it follows that since $\omega(\cdot)$ is bounded and $\mathcal{A}(\hat{W}_1(t), \mathcal{G}_A)$ is quadratically stable by Assumption 4.3.1 (satisfied by LMIs in Remark 4.3.1), then $x_r(t)$ and $x_c(t)$ are also bounded [88]. This further implies that the actuator output $v(t)$ is bounded.

To show $\lim_{t \rightarrow \infty} e(t) = 0$, note that $x(t)$ is bounded as a consequence of the boundedness of $e(t)$ and $x_r(t)$. It now follows from (4.7) that $\dot{e}(t)$ is bounded, and hence, $\dot{\mathcal{V}}(e(t), \tilde{W}_1(t))$ is bounded. As a consequence of the boundedness of $\dot{\mathcal{V}}(e(t), \tilde{W}_1(t))$ and Barbalat's lemma [88], $\lim_{t \rightarrow \infty} \dot{\mathcal{V}}(e(t), \tilde{W}_1(t)) = 0$, and hence, $\lim_{t \rightarrow \infty} e(t) = 0$.

Finally, because $\dot{\mathcal{V}}(e(t), \tilde{W}_1(t)) \leq 0$ for $t \in \overline{\mathbb{R}}_+$, this implies that $\mathcal{V}(e(t), \tilde{W}_1(t)) \leq \mathcal{V}(e(0), \tilde{W}_1(0))$. Using the inequalities $\lambda_{\min}(P)\|e(t)\|_2^2 \leq \mathcal{V}(e(t), \tilde{W}_1(t))$ and $\mathcal{V}(e(0), \tilde{W}_1(0)) \leq \lambda_{\max}(P)\|e_0\|_2^2 + \gamma_1^{-1}\|\tilde{W}_{10}\|_F^2$ results in

$$\|e(t)\|_2 \leq \left(\frac{1}{\lambda_{\min}(P)} \left(\lambda_{\max}(P)\|e(0)\|_2^2 + \gamma_1^{-1}\|\tilde{W}_1(0)\|_F^2 \right) \right)^{\frac{1}{2}}. \quad (4.22)$$

Moreover, since $\|\cdot\|_{\infty} \leq \|\cdot\|_2$, and this bound is uniform, then (4.22) yields

$$\|e_{\tau}(t)\|_{\mathcal{L}_{\infty}} \leq \left(\frac{1}{\lambda_{\min}(P)} \left(\lambda_{\max}(P)\|e(0)\|_2^2 + \gamma_1^{-1}\|\tilde{W}_1(0)\|_F^2 \right) \right)^{\frac{1}{2}}, \quad (4.23)$$

such that (4.17) is a direct consequence of (4.23) since it holds uniformly in τ . ■

Once again, we note that through the use of the LMI analysis highlighted in Remark 4.3.1, the quadratic stability condition in Assumption 4.3.1 can be achieved for given actuator dynamics, \mathcal{G}_A , and projection enforced bounds on system uncertainties, $\hat{W}_{1, \max, i+(j-1)n}$, such that Proposition 4.3.1 holds. From a practical understanding, it is expected that there is a fundamental tradeoff between the allowable system uncertainties and the actuator dynamics. This being that if the system uncertainties are large, the actuator dynamics need to be fast enough such that close suppression of the system uncertainties through the control channel is possible, whereas if the the system uncertainties are small, the actuator dynamics can be slower

and still satisfy the quadratic stability condition in Assumption 4.3.1. To rigorously demonstrate this practical intuition, in what follows we provide a lemma which uses the following assumption on the form of the actuator dynamics which holds for a broad set of realistic actuators.

Assumption 4.3.2 *The static gain of the actuator dynamics given by (4.10) is unity (i.e., $-HF^{-1}G = I$) and F is in Jordan form with the algebraic multiplicity and geometric multiplicity being equal (i.e., F is diagonal).*

With the eigenvalues of F along the diagonal, scaling up all the eigenvalues is the mathematical equivalent of making the actuator faster, and hence, we let $F \triangleq kF_0$, where k scales the eigenvalues of an initial actuator state matrix $F_0 \triangleq \text{diag}([F_{011}, F_{022}, \dots, F_{0pp}])$, with $-F_{0ii} \in \mathbb{R}_+$ for $i = 1, \dots, p$. In addition, we let $H = kH_0$ and $G = G_0$ such that the unity static gain of Assumption 4.3.2 is satisfied, where H_0 and G_0 are the initial actuator output and input matrices. Furthermore, since F is in Jordan form, it follows from Assumption 4.3.2 and $0 = F^T S + SF + I$, that $S = k^{-1} \text{diag} \left(\left[-F_{011}^{-1}, -F_{022}^{-1}, \dots, -F_{0pp}^{-1} \right] \right) / 2 \triangleq k^{-1} S_0$, where $0 = F_0^T S_0 + S_0 F_0 + I$ and $S_0 \in \mathbb{R}_+^{p \times p}$.

Now, the following lemma provides a sufficient condition to ensure the quadratic stability of Assumption 4.3.1. For this purpose, let $\bar{\omega} \in \mathbb{R}_+$ be such that $\|\hat{W}_1(t)\|_F \leq \bar{\omega}$ and let $\underline{k} \in \mathbb{R}_+$ be such that $\underline{k} \leq k$.

Lemma 4.3.1 *Consider the actuator dynamics given by (4.10) subject to Assumption 4.3.2 and the parameter dependent matrix $\mathcal{A}^T(\hat{W}_1(t), \mathcal{G}_A)$ given by (4.13). For the positive definite matrix \mathcal{P} given by*

$$\mathcal{P} = \begin{bmatrix} P & -PBHF^{-1} \\ -F^{-T}H^TB^TP & \alpha S + F^{-T}H^TB^TPBHF^{-1} \end{bmatrix}, \quad (4.24)$$

with $\alpha \in \mathbb{R}_+$ being a free parameter, there exists a set $\kappa_1 \triangleq \{k : \underline{k} \leq k\} \cup \{\hat{W}_1(t) : \|\hat{W}_1(t)\|_F \leq \bar{\omega}\}$, such that for any arbitrary element in the set κ_1 , $\mathcal{A}^T(\hat{W}_1(t), \mathcal{G}_A)\mathcal{P} + \mathcal{P}\mathcal{A}(\hat{W}_1(t), \mathcal{G}_A) < 0$ is satisfied, such that (4.13) is quadratically stable in the set κ_1 .

Proof. We first note that the positive-definiteness of \mathcal{P} follows from the positive-definiteness of P , which is a solution of the Lyapunov equation given by (4.6) with $R = I$, and the positive-definiteness of the Schur complement of (4.24) given by

$$\begin{aligned}
S_1 &= \alpha S + F^{-T} H^T B^T P B H F^{-1} - F^{-T} H^T B^T P (P)^{-1} P B H F^{-1} \\
&= \alpha S > 0.
\end{aligned} \tag{4.25}$$

Now, for the positive definite matrix \mathcal{P} , quadratic stability of $\mathcal{A}(\hat{W}_1(t), \mathcal{G}_A)$ follows if the matrix given by

$$\begin{aligned}
\mathcal{Q} &= \mathcal{A}^T(\hat{W}_1(t), \mathcal{G}_A) \mathcal{P} + \mathcal{P} \mathcal{A}(\hat{W}_1(t), \mathcal{G}_A) \\
&= \begin{bmatrix} -I & -A_r^T P B H F^{-1} - \alpha \hat{W}_1(t) G^T S \\ * & -\alpha I \end{bmatrix},
\end{aligned} \tag{4.26}$$

is negative definite. First, note that $-I$ is clearly a negative-definite matrix. Second, it follows that if the Schur complement of (4.26) is negative definite, quadratic stability of $\mathcal{A}(\hat{W}_1(t), \mathcal{G}_A)$ holds. That is, we consider the Schur complement of (4.26) as

$$\begin{aligned}
S_2 &= -\alpha I + F^{-T} H^T B^T P A_r A_r^T P B H F^{-1} + \alpha^2 S G \hat{W}_1^T(t) \hat{W}_1(t) G^T S \\
&\quad + \alpha F^{-T} H^T B^T P A_r \hat{W}_1(t) G^T S + \alpha S G \hat{W}_1^T(t) A_r^T P B H F^{-1}.
\end{aligned} \tag{4.27}$$

Note that $S_2 < 0$ if and only if $x^T S_2 x < 0$ for any vector $x \neq 0$. Thus, we can write

$$\begin{aligned}
x^T S_2 x &\leq -\alpha \|x\|_2^2 + \|A_r^T P B H F^{-1} x\|_2^2 + \alpha^2 \|\hat{W}_1(t) G^T S x\|_2^2 \\
&\quad + 2\alpha \|A_r^T P B H F^{-1} x\|_2 \|\hat{W}_1(t) G^T S x\|_2.
\end{aligned} \tag{4.28}$$

Now, using Young's inequality [14] on the last term yields

$$x^T S_2 x \leq -\alpha \|x\|_2^2 + 2 \|A_r^T P B H F^{-1} x\|_2^2 + 2\alpha^2 \|\hat{W}_1(t) G^T S x\|_2^2. \tag{4.29}$$

Letting $m_1 \triangleq 2 \|A_r^T P B\|_F^2$, it follows from (4.29) that

$$\begin{aligned}
x^T S_2 x &\leq -\alpha \|x\|_2^2 + m_1 \|H\|_F^2 \|F^{-1}\|_F^2 \|x\|_2^2 + \alpha^2 \|\hat{W}_1(t)\|_F^2 \|S\|_F^2 \|G\|_F^2 \|x\|_2^2 \\
&= -\|x\|_2^2 \left[\alpha - m_1 \|H_0\|_F^2 \|F_0^{-1}\|_F^2 - \alpha^2 \|\hat{W}_1(t)\|_F^2 k^{-2} \|S_0\|_F^2 \|G_0\|_F^2 \right].
\end{aligned} \tag{4.30}$$

Letting $\alpha > m_1 \|H_0\|_F^2 \|F_0^{-1}\|_F^2$ in (4.30), it follows that $x^T S_2 x < 0$ when the term $\alpha^2 \|\hat{W}_1(t)\|_F^2 k^{-2} \|S_0\|_F^2 \|G_0\|_F^2$ is sufficiently small. This is the case if k is sufficiently large or $\|\hat{W}_1(t)\|_F$ is sufficiently small, and hence, (4.27) is negative-definite when \underline{k} is sufficiently large or $\bar{\omega}$ is sufficiently small, which yields the quadratic stability of (4.13). Finally, since there exist a (sufficiently large) \underline{k} or a (sufficiently small) $\bar{\omega}$ such that (4.13) is quadratically stable, the existence of set κ_1 is immediate. ■

Remark 4.3.2 Several things should be noted about the results of Lemma 4.3.1. First of all, it demonstrates the fundamental tradeoff between the allowable system uncertainties and the actuator dynamics as alluded to earlier in this section. This being that as the allowable system uncertainties get larger, the speed of the actuator needs to increase to ensure quadratic stability of $\mathcal{A}(\hat{W}_1(t), \mathcal{G}_A)$. It also informs from a practical standpoint that there exists a feasible starting point at which an LMI search can begin to compute the minimum feasible boundary. Lastly, even though the assumption of unity static gain is used to find this feasible starting point, an extension of the LMI search can include the effect of non-unity static gain actuator dynamics as it searches for the feasible limit.

Remark 4.3.3 Similar to the comment in Remark , the results in this section can be readily extended to the case in which the system uncertainties are time-varying (i.e., $W_1(t) \in \mathbb{R}^{n \times m}$ with $\|W_1(t)\|_F \leq w$ and $\|\dot{W}_1(t)\|_F \leq \dot{w}$, $w \in \mathbb{R}_+$, $\dot{w} \in \mathbb{R}_+$). While the result in Proposition 4.3.1 changes to the boundedness of the pair $(e(t), \tilde{W}_1(t))$ in this case, the quadratic stability condition given by (4.13) and satisfied through LMIs remains exactly the same for time-varying uncertainties. In addition, the feasibility result of Lemma 4.3.1 does not change.

4.4 Convergence Analysis

Stability of the overall closed-loop dynamical system for the proposed model reference adaptive control architecture with the LMI-based hedging approach is analyzed in the previous section. However, it is only shown that the distance between the uncertain dynamical system given by (4.9) and the *modified* reference model given by (4.12) asymptotically vanishes, where the *modified* reference model no longer captures the *ideal* closed-loop dynamical system behavior due to the presence of the term “ $B[v(t) - u(t)]$ ” in (4.12). To this end, we now analyze the distance between the uncertain dynamical system and the *ideal* (i.e., unmodified reference model). Since the *ideal* reference model given by (4.2) is modified in the Section 4.3.3, such that $x_r(t)$ denotes the *modified* reference model state, we restate the *ideal* reference model dynamics with different notation as

$$\dot{x}_r(t) = A_r x_r(t) + B_r c(t), \quad x_r(0) = x_{r0}, \quad (4.31)$$

where $x_r(t) \in \mathbb{R}^n$ denotes the *ideal* reference state vector.

We begin by defining $e_{\text{ref}}(t) \triangleq x_r(t) - x_{r_i}(t)$ as the error between the *modified* reference model given by (4.12) and the *ideal* reference model now given by (4.31). Note that

$$\begin{aligned} \|x(t) - x_{r_i}(t)\|_{\mathcal{L}_\infty} &= \|e(t) + e_{\text{ref}}(t)\|_{\mathcal{L}_\infty} \\ &\leq \|e(t)\|_{\mathcal{L}_\infty} + \|e_{\text{ref}}(t)\|_{\mathcal{L}_\infty}, \end{aligned} \quad (4.32)$$

which implies that by making the bounds on both of the error signals (i.e., $\|e(t)\|_{\mathcal{L}_\infty}$ and $\|e_{\text{ref}}(t)\|_{\mathcal{L}_\infty}$) small, the distance between the uncertain dynamical system and the *ideal* reference model becomes small for all time.

Remark 4.4.1 Under a realistic assumption that $e(0)$ can be chosen sufficiently small and/or zero, Proposition 4.3.1 shows that $\|e(t)\|_{\mathcal{L}_\infty}$ can be made small by judiciously increasing the learning gain γ_1 .

The next proposition shows that $\|e_{\text{ref}}(t)\|_{\mathcal{L}_\infty}$ can be made small if the actuator dynamics are fast, which is also expected by intuition.

Proposition 4.4.1 Consider the modified reference model given by (4.12), the ideal reference model given by (4.31), the actuator dynamics given by (4.10) subject to Assumption 3, and the adaptive feedback control law given by (4.4). If $(\underline{k}, \bar{\omega}) \in \kappa_1$, then an upper bound for $\|e_{\text{ref}}(t)\|_{\mathcal{L}_\infty}$ is given by

$$\|e_{\text{ref}}(t)\|_{\mathcal{L}_\infty} \leq \sqrt{\rho \left(\frac{5\psi^2}{4\eta^2 k^2} \right)}, \quad (4.33)$$

where $\eta \in \mathbb{R}_+$, $\rho \triangleq \frac{\lambda_{\max}(\mathcal{P})}{\lambda_{\min}(\mathcal{P})}$, and $\psi \triangleq 2\alpha \|S_0 G_0\|_{\text{F}} \omega_1^*$.

Proof. Making use of the arguments presented in [100], we begin by considering the reference model error dynamics that follow from the modified reference model (4.12) and the ideal reference model (4.31) subject to the actuator dynamics (4.10) and the feedback control law (4.4) as

$$\begin{aligned} \dot{e}_{\text{ref}}(t) &= A_r e_{\text{ref}}(t) + B[v(t) - u(t)] \\ &= A_r e_{\text{ref}}(t) + B[Hx_c(t) + \hat{W}_1^T(t)e(t) + \hat{W}_1^T(t)e_{\text{ref}}(t) + \hat{W}_1^T(t)x_{r_i}(t) - K_2 c(t)]. \end{aligned} \quad (4.34)$$

In addition, the actuator dynamics (4.10) subject to (4.4) can be written as

$$\dot{x}_c(t) = Fx_c(t) - G\hat{W}_1^T(t)e(t) - G\hat{W}_1^T(t)e_{\text{ref}}(t) - G\hat{W}_1^T(t)x_{r_i}(t) + GK_2c(t). \quad (4.35)$$

It follows that (4.34) and (4.35) can be written in compact form as

$$\dot{\bar{e}}(t) = \mathcal{A}(\hat{W}_1(t), \mathcal{G}_A)\bar{e}(t) + \mathcal{B}\omega_1(\cdot), \quad (4.36)$$

with $\bar{e}(t) = [e_{\text{ref}}^T(t), x_c^T(t)]^T$, $\mathcal{B} = [B^T, -G^T]^T$, and $\omega_1(\cdot) = \hat{W}_1^T(t)e(t) + \hat{W}_1^T(t)x_{r_i}(t) - K_2c(t)$.

Note that $\omega_1(\cdot)$ in (4.36) is bounded as a result of Proposition 4.3.1 and the boundedness of the ideal reference model (4.31). Furthermore, it follows that $\mathcal{A}(\hat{W}_1(t), \mathcal{G}_A)$ is quadratically stable for $(k, \hat{W}_1(t)) \in \kappa_1$ by Lemma 4.3.1 such that $\mathcal{A}^T(\hat{W}_1(t), \mathcal{G}_A)\mathcal{P} + \mathcal{P}\mathcal{A}(\hat{W}_1(t), \mathcal{G}_A) < 0$ holds, where \mathcal{P} is given by (4.24). This further implies by compactness that there exists an $\eta \in \mathbb{R}_+$ such that

$$\mathcal{A}^T(\hat{W}_1(t), \mathcal{G}_A)\mathcal{P} + \mathcal{P}\mathcal{A}(\hat{W}_1(t), \mathcal{G}_A) + \eta I_{n+p} \leq 0. \quad (4.37)$$

Now, consider the positive-definite energy function

$$\mathcal{V}(\bar{e}) = \bar{e}^T \mathcal{P} \bar{e}. \quad (4.38)$$

Differentiating (4.38) and using (4.36) yields

$$\begin{aligned} \dot{\mathcal{V}}(\bar{e}(t)) &= 2\bar{e}^T(t)\mathcal{P}\dot{\bar{e}}(t) \\ &= \bar{e}^T(t)[\mathcal{A}^T(\hat{W}_1(t), \mathcal{G}_A)\mathcal{P} + \mathcal{P}\mathcal{A}(\hat{W}_1(t), \mathcal{G}_A)]\bar{e}(t) + 2\bar{e}^T(t)\mathcal{P}\mathcal{B}\omega_1(\cdot). \end{aligned} \quad (4.39)$$

Using (4.24) and (4.37), one can write (4.39) as

$$\dot{\mathcal{V}}(\bar{e}(t)) \leq -\eta \|\bar{e}(t)\|_2^2 + 2\alpha \|SG\|_F \|x_c(t)\|_2 \|\omega_1(\cdot)\|_2. \quad (4.40)$$

Since $\omega_1(\cdot)$ consists of bounded terms, it follows that $\|\omega_1(\cdot)\|_2 \leq \omega_1^*$, where $\omega_1^* \in \mathbb{R}_+$, and (4.40) can then be written as

$$\begin{aligned}
\dot{\mathcal{V}}(\bar{e}(t)) &\leq -\eta \|\bar{e}(t)\|_2^2 + 2\alpha \|SG\|_F \|x_c(t)\|_2 \omega_1^* \\
&= -\eta \|e_{\text{ref}}(t)\|_2^2 - \eta \|x_c(t)\|_2^2 + 2\alpha k^{-1} \|S_0 G_0\|_F \|x_c(t)\|_2 \omega_1^* \\
&= -\eta \|e_{\text{ref}}(t)\|_2^2 - \|x_c(t)\|_2 \left(\eta \|x_c(t)\|_2 - k^{-1} \psi \right),
\end{aligned} \tag{4.41}$$

where $\psi = 2\alpha \|S_0 G_0\|_F \omega_1^*$. It then follows, similar to [100], that $\dot{\mathcal{V}}(\bar{e}(t)) < 0$ when $\|x_c(t)\|_2$ satisfies

$$\|x_c(t)\|_2 > \frac{\psi}{\eta k}. \tag{4.42}$$

To analyze $\|e_{\text{ref}}(t)\|_2$, first note that the right hand side of (4.41) is concave with a maximum at $\|x_c(t)\|_2 = \frac{\psi}{2\eta k}$, such that using this maximum in (4.41) gives the upper bound

$$\dot{\mathcal{V}}(\bar{e}(t)) \leq -\eta \|e_{\text{ref}}(t)\|_2^2 + \frac{\psi^2}{4\eta k^2}. \tag{4.43}$$

Hence, when $\|e_{\text{ref}}(t)\|_2$ satisfies

$$\|e_{\text{ref}}(t)\|_2 > \frac{\psi}{2\eta k}, \tag{4.44}$$

then $\dot{\mathcal{V}}(\bar{e}(t)) < 0$. Using (4.42) and (4.44), it follows that $\mathcal{V}(\bar{e})$ decreases outside the compact set $\Omega = \{e_{\text{ref}} \in \mathbb{R}^n, x_c \in \mathbb{R}^m : \|x_c(t)\|_2 \leq \frac{\psi}{\eta k} \text{ and } \|e_{\text{ref}}(t)\|_2 \leq \frac{\psi}{2\eta k}\}$. Next, it follows that $\mathcal{V}(\bar{e})$ is upper and lower bounded as $\lambda_{\min}(\mathcal{P}) \|\bar{e}(t)\|_2^2 \leq \mathcal{V}(\bar{e}) \leq \lambda_{\max}(\mathcal{P}) \|\bar{e}(t)\|_2^2$, and noting $\|e_{\text{ref}}(t)\|_2 \leq \|\bar{e}(t)\|_2$ it follows that

$$\begin{aligned}
\lambda_{\min}(\mathcal{P}) \|e_{\text{ref}}(t)\|_2^2 &\leq \lambda_{\max}(\mathcal{P}) \left(\|e_{\text{ref}}(t)\|_2^2 + \|x_c(t)\|_2^2 \right) \\
&\leq \lambda_{\max}(\mathcal{P}) \left(\left(\frac{\psi}{\eta k} \right)^2 + \left(\frac{\psi}{2\eta k} \right)^2 \right) \\
&= \lambda_{\max}(\mathcal{P}) \left(\frac{5\psi^2}{4\eta^2 k^2} \right).
\end{aligned} \tag{4.45}$$

From (4.45), we compute the bound for $\|e_{\text{ref}}(t)\|_2$ as

$$\|e_{\text{ref}}(t)\|_2 \leq \sqrt{\rho \left(\frac{5\psi^2}{4\eta^2 k^2} \right)}, \tag{4.46}$$

where $\rho = \frac{\lambda_{\max}(\mathcal{P})}{\lambda_{\min}(\mathcal{P})}$. Since $\|\cdot\|_{\infty} \leq \|\cdot\|_2$, and this bound is uniform, then (4.46) yields

$$\|e_{\text{ref}_\tau}(t)\|_{\mathcal{L}_\infty} \leq \sqrt{\rho \left(\frac{5\psi^2}{4\eta^2 k^2} \right)}, \quad (4.47)$$

such that (4.33) is a direct consequence of (4.47) because it holds uniformly in τ . ■

Similar to the discussion in Remark 4.3.3, the system uncertainty is not present in the above analysis, and hence, the above result also identically holds for time-varying system uncertainties

Remark 4.4.2 *Proposition 4.4.1 shows that $\|e_{\text{ref}}(t)\|_{\mathcal{L}_\infty}$ becomes small as the actuator dynamics become fast (i.e., when k is large). Hence, it follows from the results in Propositions 4.3.1 and 4.4.1 as well as the discussion in Remark 4.3.3 that the upper bound (4.32) on the distance between the uncertain dynamical system and the ideal reference model can be made small by judiciously increasing the learning gain γ_1 and utilizing an actuator with fast dynamics.*

The next proposition shows that the distance between the uncertain dynamical system given by (4.9) and the *ideal* reference model given by (4.31) asymptotically vanishes for constant reference commands (i.e., $c(t) = c$).

Proposition 4.4.2 *Consider the ideal reference model (4.31), the modified reference model (4.12), the actuator dynamics (4.10) subject to Assumption 4.3.2, and the feedback control law (4.4). If $(\underline{k}, \bar{\omega}) \in \kappa_1$ and the reference command is constant, the modified reference model (4.12) will asymptotically converge to the ideal reference model (4.31). In addition, using the results from Proposition 4.3.1, it follows that $x(t) - x_{r_i}(t) \rightarrow 0$ as $t \rightarrow \infty$.*

Proof. Let $\omega_2(\cdot) \triangleq B\hat{W}_1^T(t)e(t)$. It follows from (4.18) that

$$\dot{x}_r(t) = (A_r + B\hat{W}_1^T(t))x_r(t) + BHx_c(t) + \omega_2(\cdot). \quad (4.48)$$

In addition, let $\omega_3(\cdot) \triangleq -G\hat{W}_1^T(t)e(t) + GK_2c(t)$. Then, it follows from (4.19) that

$$\dot{x}_c(t) = Fx_c(t) - G\hat{W}_1^T(t)x_r(t) + \omega_3(\cdot). \quad (4.49)$$

Note that (4.49) can be rewritten as

$$x_c(t) = F^{-1} [\dot{x}_c(t) + G\hat{W}_1^T(t)x_r(t) - \omega_3(\cdot)], \quad (4.50)$$

where it follows from (4.48), (4.50), and Assumption 4.3.2 that

$$\dot{x}_r(t) = A_r x_r(t) + B_r c(t) + BHF^{-1} \dot{x}_c(t). \quad (4.51)$$

Using (4.31) and (4.51), one can write the reference model error dynamics as

$$\dot{e}_{\text{ref}}(t) = A_r e_{\text{ref}}(t) + BHF^{-1} \dot{x}_c(t), \quad (4.52)$$

which implies that if $\dot{x}_c(t) \rightarrow 0$ as $t \rightarrow \infty$, then $x_r(t)$ converges to $x_{r_i}(t)$.

Next, (4.49) can be rewritten as

$$\dot{x}_c(t) = Fx_c(t) + F\omega_4(\cdot), \quad (4.53)$$

where $\omega_4(\cdot) \triangleq z(\cdot) + F^{-1}q(\cdot)$, $z(\cdot) \triangleq F^{-1}[-G\hat{W}_1^T(t)x_{r_i}(t) - G\hat{W}_1^T(t)e(t) + GK_2c(t)]$, and $q(\cdot) \triangleq -G\hat{W}_1^T(t) \cdot e_{\text{ref}}(t)$. Note that (4.53) can be equivalently represented as

$$\dot{x}_c(t) = z_1(t) + Fz_2(t) + q(\cdot), \quad (4.54)$$

$$\dot{z}_1(t) = Fz_1(t) + F\dot{z}(t), \quad (4.55)$$

$$\dot{z}_2(t) = Fz_2(t) + q(\cdot). \quad (4.56)$$

Letting $x_0(t) = [e_{\text{ref}}^T(t), z_2^T(t), z_1^T(t)]$, we have

$$\dot{x}_0(t) = \underbrace{\begin{bmatrix} A_r + B\hat{W}_1^T(t) & BH & BHF^{-1} \\ -G\hat{W}_1^T(t) & F & 0 \\ 0 & 0 & F \end{bmatrix}}_{\mathcal{A}_0(\cdot)} x_0(t) + \underbrace{\begin{bmatrix} 0 \\ 0 \\ F \end{bmatrix}}_{\mathcal{B}_0} \dot{z}(t). \quad (4.57)$$

Note that since the upper left block of $\mathcal{A}_0(\cdot)$ is quadratically stable for $(\underline{k}, \bar{\omega}) \in \kappa_1$ by Lemma 4.3.1, F is Hurwitz, and $\mathcal{A}_0(\cdot)$ is in an upper triangular form, then it follows that $x_0(t) \rightarrow 0$ as $t \rightarrow \infty$ if $\dot{z}(t) \rightarrow 0$ as $t \rightarrow \infty$.

Finally, $\dot{z}(t)$ can be written for constant command case as

$$\dot{z}(t) = -F^{-1}G[\hat{W}_1^T(t)x_{r_i}(t) + \hat{W}_1^T(t)\dot{x}_{r_i}(t) + \hat{W}_1^T(t)e(t) + \hat{W}_1^T(t)\dot{e}(t)]. \quad (4.58)$$

From Proposition 4.3.1, it follows that $\dot{W}_1(t) \rightarrow 0$ as $t \rightarrow \infty$. In addition, since $c(t)$ is constant, then it follows from (4.31) that $\dot{x}_{r_i}(t) \rightarrow 0$ as $t \rightarrow \infty$. Moreover, since $\ddot{e}(t)$ is bounded and $\dot{e}(t)$ is uniformly continuous as a direct consequence of Proposition 4.3.1, then $\dot{e}(t) \rightarrow 0$ as $t \rightarrow \infty$. This argument shows that $\dot{z}(t) \rightarrow 0$ as $t \rightarrow \infty$, and hence, $x_0(t) \rightarrow 0$ as $t \rightarrow \infty$, which shows that the error between the ideal reference model (4.31) and the modified reference model (4.12) vanishes as $t \rightarrow \infty$. Finally, from Proposition 4.3.1, we know $e(t) \rightarrow 0$ as $t \rightarrow \infty$, and hence, $x(t) - x_{r_i}(t) = e(t) + e_{\text{ref}}(t) \rightarrow 0$ as $t \rightarrow \infty$. ■

4.5 Illustrative Example

To illustrate the proposed adaptive control architecture in the presence of high-order actuator dynamics, we consider the second-order system given by

$$\begin{bmatrix} \dot{x}_1(t) \\ \dot{x}_2(t) \end{bmatrix} = \begin{bmatrix} 0 & 1 \\ 0.5 & 0.5 \end{bmatrix} \begin{bmatrix} x_1(t) \\ x_2(t) \end{bmatrix} + \begin{bmatrix} 0 \\ 1 \end{bmatrix} v(t), \quad (4.59)$$

with zero initial conditions and let $x_1(t)$ represent the angle in radians and $x_2(t)$ represent the angular rate of change in radians per second. For the actuator dynamics, we consider

$$F = \begin{bmatrix} 0 & 1 \\ -\omega_n^2 & -2\zeta\omega_n \end{bmatrix}, \quad G = \begin{bmatrix} 0 \\ 1 \end{bmatrix}, \quad H = \begin{bmatrix} \omega_n^2 & 0 \end{bmatrix}. \quad (4.60)$$

where it is noted that F can be transformed into Jordan form such that Assumption 4.3.1 is satisfied. In addition, we use a filtered tracking command $c(t)$ and select a reference model with zero initial conditions, a natural frequency of $\omega_n = 0.7$ rad/s, and a damping ratio $\zeta = 0.707$. For the proposed adaptive control law, we set $R = I_2$, $|\hat{W}_1(t)_{1,1}| \leq 1.1$, and $|\hat{W}_1(t)_{2,1}| \leq 1.6$.

Figure 4.1 shows the feasible region of allowable actuator dynamics which is given by the ω_n and ζ values for the actuator dynamics. Note that Figure 4.1 provides both the LMI calculated feasible limit as well as the feasible limit provided by the simulation results, which correspond to the command profile, initial

conditions, and other parameters for the provided example. Due to space restrictions, we select two points to simulate the proposed controller performance as seen in Figures 4.2 and 4.3. Since the feasible boundary corresponds to calculated minimum feasible ω_n and ζ values for the actuator dynamics, it is expected that the system performances are guaranteed to be bounded for actuator dynamics at points greater than and equal to the calculated feasible boundary. This can be seen in Figure 4.2 when the actuator dynamics are at the minimum point $(\zeta, \omega_n) = (0.55, 2.98)$, which is located on the feasible boundary. In Figure 4.3, we let the actuator dynamics be outside the calculated feasible region to show that the closed-loop system remains bounded until the actuator dynamics reach a value of $(\zeta, \omega_n) = (0.55, 2.19)$. This is consistent with the presented theory, as we provide an upper bound on the allowable actuator dynamics such that the closed-loop system remains bounded.

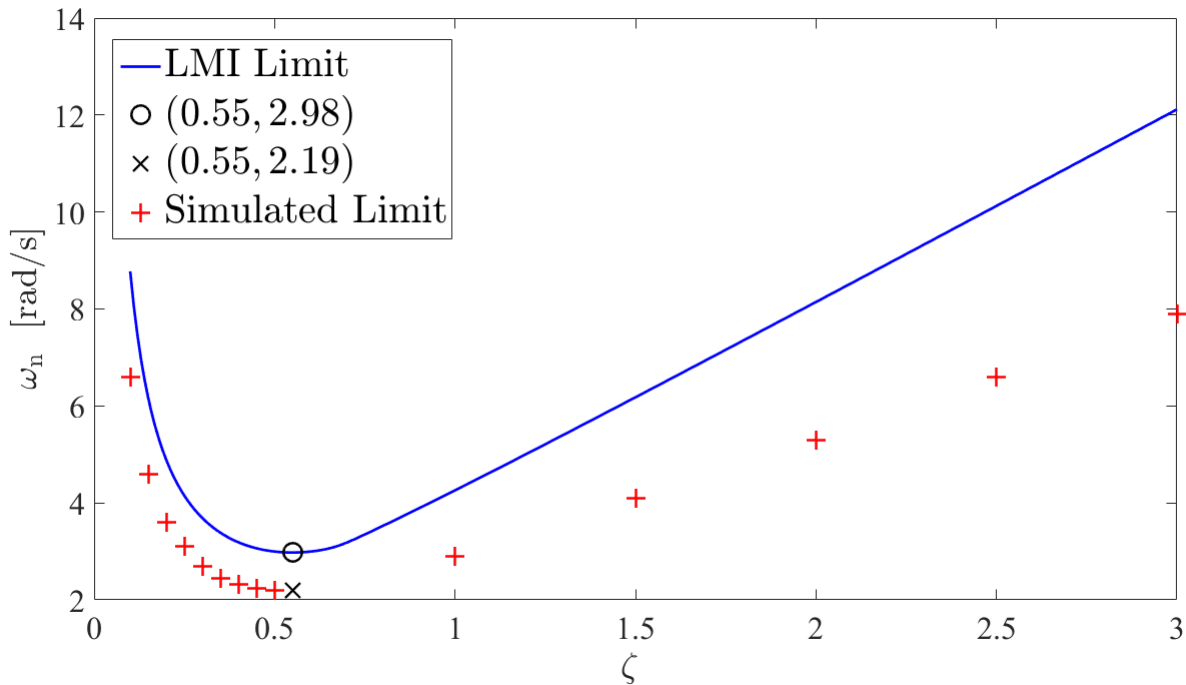


Figure 4.1: LMI calculated feasible region for actuator dynamics.

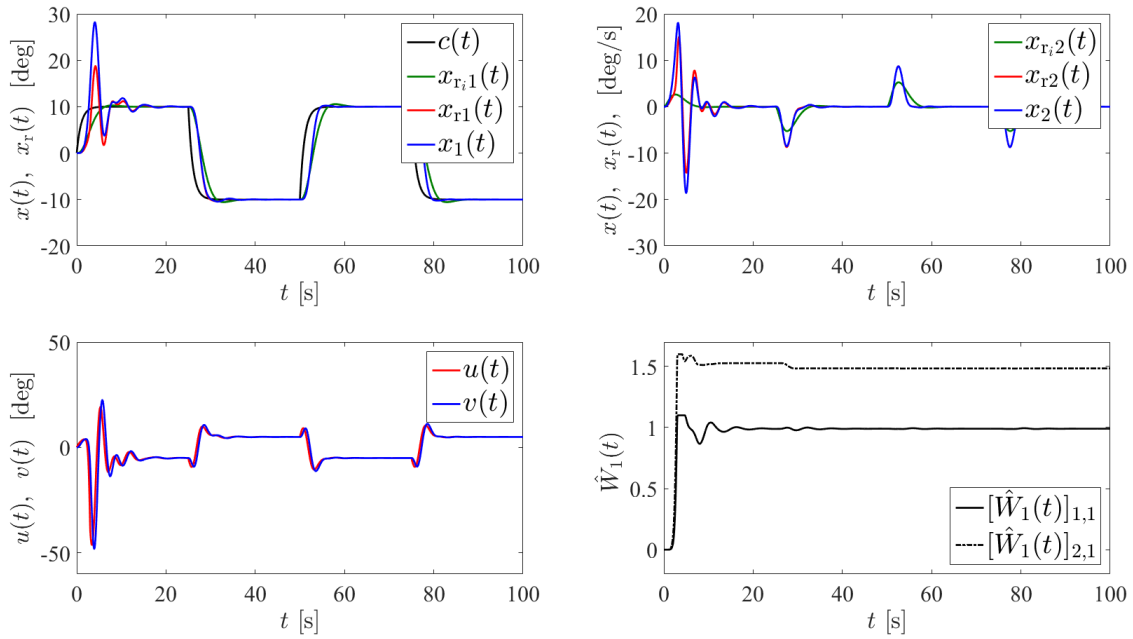


Figure 4.2: Proposed controller performance with actuator dynamics $((\zeta, \omega_n) = (0.55, 2.98), \gamma_1 = 25)$.

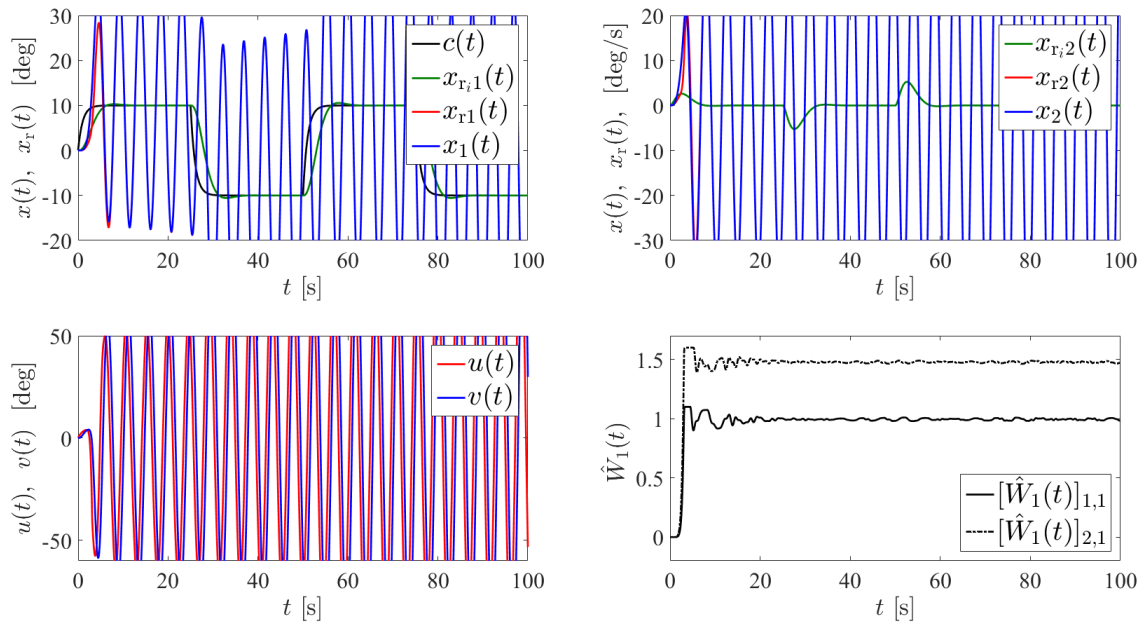


Figure 4.3: Proposed controller performance with actuator dynamics $((\zeta, \omega_n) = (0.55, 2.19), \gamma_1 = 25)$.

4.6 Conclusion

For contributing to the previous studies in adaptive control of uncertain dynamical systems in the presence of high-order actuator dynamics, we presented an LMI-based hedging approach for computing the fundamental stability interplay between the bandwidth of actuator dynamics and the allowable system uncertainties. Specifically, the proposed approach modifies the ideal reference model dynamics using the hedging method to allow correct adaptation, which is not affected by the presence of actuator dynamics. We analyzed the stability of this modified reference model coupled with the actuator dynamics using tools and methods from Lyapunov stability, matrix mathematics, and LMIs. In addition, the distance between the uncertain dynamical system and the ideal (i.e., unmodified) reference model dynamics were also analyzed and it was remarked that this distance either can be made small by increasing the learning gain and the bandwidth of the actuator dynamics or asymptotically vanishes when the uncertain dynamical system is driven by constant reference commands. An illustrative numerical example demonstrated the efficacy of the proposed approach in computing stability limits of adaptive controllers in the presence of high-order actuator dynamics. In future research, we will make extensions to the cases in which the control input is unknown and/or with the actuator output is unknown.

CHAPTER 5: GENERALIZATIONS AND APPLICATIONS OF THE LMI-BASED HEDGING APPROACH FOR HIGH-ORDER ACTUATOR DYNAMICS

This chapter provides additional extensions of the work presented in Chapter 4. Specifically, three generalizations of the proposed LMI-based hedging approach are considered for *i*) a class of uncertain nonlinear dynamical systems, *ii*) unmeasurable actuator outputs, and *iii*) actuator dynamics with an additional throughput term with an application for the input time-delay problem. In addition, the method of computing the actuator parameters is more thoroughly addressed and an application to a hypersonic vehicle model for different cases of pole-zero actuator dynamics is presented.

5.1 Adaptive Control for a Class of Uncertain Nonlinear Dynamical Systems in the Presence of High-Order Actuator Dynamics¹

Adaptive control is a powerful design methodology to achieve closed-loop system stability in the face of uncertainties resulting from modeling inaccuracies, degraded modes of operation, and changes in system dynamics. Yet, it is well known that the presence of actuator dynamics can seriously limit closed-loop system stability of any adaptive control framework. To address the problem of adaptive control design in the presence of actuator dynamics, we recently introduced a linear matrix inequalities-based adaptive control framework. The key feature of this approach is to reveal the fundamental stability interplay between the parameters of a given actuator dynamics model and the allowable uncertainties in the feedback loop. The contribution of this paper is to generalize our recent work for a class of uncertain *nonlinear* dynamical systems. Specifically, for a given high-order, linear time-invariant actuator dynamics model, we utilize tools and methods from Lyapunov stability and linear matrix inequalities for the computation of closed-loop system stability limits of adaptive control laws. An illustrative numerical example is also provided to demonstrate the efficacy and the practicality of the proposed design architecture.

¹This section is previously published in [101]. Permission is included in Appendix B. The omitted proofs follow readily from Chapter 4.

5.1.1 Introduction

Adaptive control is a powerful design methodology to achieve closed-loop system stability in the face of uncertainties resulting from modeling inaccuracies, degraded modes of operation, and changes in system dynamics. Yet, it is well known that the presence of actuator dynamics can seriously limit closed-loop system stability of any adaptive control framework. In particular, if the actuator dynamics do not have a sufficiently high bandwidth and/or for safety-critical applications of adaptive control laws, closed-loop system stability verification steps must be considered for precisely showing the safe actuator bandwidth limits such that adaptive control laws perform theoretically correct.

To address the problem of adaptive control design in the presence of actuator dynamics, we recently introduced a linear matrix inequalities-based adaptive control framework [95, 102–104]. Our framework is predicated on a hedging method originally proposed by the authors of [30, 31, 33], where this method modifies the ideal reference model dynamics to allow for theoretically correct adaptation that is not affected by the presence of actuator dynamics. Specifically, our results documented in [95, 102–104] show that this modification to the ideal reference model dynamics does not yield to unbounded reference model responses. The key common feature of these results is to reveal the fundamental stability interplay between the parameters of a given actuator dynamics model and the allowable uncertainties in the feedback loop.

The contribution of this paper is to generalize our recent work documented in [95, 102–104] for a class of uncertain *nonlinear* dynamical systems. Specifically, we first use Lyapunov stability to show closed-loop system stability predicated on a quadratic stability condition. We then utilize linear matrix inequalities to perform a computation to assess when this stability condition holds for a given high-order, linear time-invariant actuator dynamics model and bounds of parameters resulting from uncertainty parameterization. An illustrative numerical example is also provided to demonstrate the efficacy and the practicality of the proposed design architecture.

The contents of the paper are as follows. Section 5.1.2 presents the mathematical preliminaries necessary for the main results of this paper. In Section 5.1.3, we present the proposed linear matrix inequalities-based adaptive control approach predicated on the hedging method for a class of uncertain nonlinear dynamical systems in the presence of high-order, linear time-invariant actuator dynamics. The illustrative numerical example is provided in Section 5.1.4 and conclusions are summarized in Section 5.1.5. Finally, we use a fairly standard notation throughout this paper. Specifically, \mathbb{R} denotes the set of

real numbers, \mathbb{R}^n denotes the set of $n \times 1$ real column vectors, $\mathbb{R}^{n \times m}$ denotes the set of $n \times m$ real matrices, \mathbb{R}_+ (resp. $\overline{\mathbb{R}}_+$) denotes the set of positive (resp., nonnegative) real numbers, $\mathbb{R}_+^{n \times n}$ (resp., $\overline{\mathbb{R}}_+^{n \times n}$) denotes the set of $n \times n$ positive-definite (resp., nonnegative-definite) real matrices, $\mathbb{D}^{n \times n}$ denotes the set of $n \times n$ real matrices with diagonal scalar entries, $(\cdot)^T$ denotes the transpose operator, $\text{tr}(\cdot)$ denotes the trace operator, and “ \triangleq ” denotes the equality by definition.

5.1.2 Preliminaries

Some necessary mathematical preliminaries are introduced in this section briefly that are needed to develop the main results of this paper.

Definition 5.1.1 *Let*

$$\Omega = \{ \theta \in \mathbb{R}^n : (\theta_i^{\min} \leq \theta_i \leq \theta_i^{\max})_{i=1,2,\dots,n} \} \quad (5.1)$$

be a convex hypercube in \mathbb{R}^n , where $(\theta_i^{\min}, \theta_i^{\max})$ represent the minimum and maximum bounds for the i^{th} component of the n -dimensional parameter vector θ . In addition, let

$$\Omega_\varepsilon = \{ \theta \in \mathbb{R}^n : (\theta_i^{\min} + \varepsilon \leq \theta_i \leq \theta_i^{\max} - \varepsilon)_{i=1,2,\dots,n} \} \quad (5.2)$$

be a second hypercube for a sufficiently small positive constant ε , where $\Omega_\varepsilon \subset \Omega$. Then, the projection operator $\text{Proj} : \mathbb{R}^n \times \mathbb{R}^n \rightarrow \mathbb{R}^n$ is defined component-wise by

$$\text{Proj}(\theta, y) \triangleq \begin{cases} \left(\frac{\theta_i^{\max} - \theta_i}{\varepsilon} \right) y_i, & \text{if } \theta_i > \theta_i^{\max} - \varepsilon \text{ and } y_i > 0 \\ \left(\frac{\theta_i - \theta_i^{\min}}{\varepsilon} \right) y_i, & \text{if } \theta_i < \theta_i^{\min} + \varepsilon \text{ and } y_i < 0 \\ y_i, & \text{otherwise} \end{cases} \quad (5.3)$$

where $y \in \mathbb{R}^n$ [6].

As a consequence of the above definition, note that

$$(\theta - \theta^*)^T (\text{Proj}(\theta, y) - y) \leq 0, \quad \theta^* \in \Omega_\varepsilon, \quad (5.4)$$

holds [6, 82]. Note that we use the generalization of this definition to matrices throughout this paper as

$$\text{Proj}_m(\Theta, Y) = (\text{Proj}(\text{col}_1(\Theta), \text{col}_1(Y)), \dots, \text{Proj}(\text{col}_m(\Theta), \text{col}_m(Y))), \quad (5.5)$$

where $\Theta \in \mathbb{R}^{n \times m}$, $Y \in \mathbb{R}^{n \times m}$, and $\text{col}_i(\cdot)$ denotes the i -th column operator. In this case, for a given Θ^* , it follows from (5.4) that

$$\text{tr} \left[(\Theta - \Theta^*)^T (\text{Proj}_m(\Theta, Y) - Y) \right] = \sum_{i=1}^m \left[\text{col}_i(\Theta - \Theta^*)^T (\text{Proj}(\text{col}_i(\Theta), \text{col}_i(Y)) - \text{col}_i(Y)) \right] \leq 0, \quad (5.6)$$

holds.

For a concise overview of the standard model reference adaptive control problem, consider a class of uncertain *nonlinear* dynamical systems \mathcal{G} given by

$$\dot{x}(t) = Ax(t) + B[u(t) + \delta(x(t))], \quad x(0) = x_0, \quad (5.7)$$

where $x(t) \in \mathbb{R}^n$ is the state vector available for feedback, $u(t) \in \mathbb{R}^m$ is the control input restricted to the class of admissible controls consisting of measurable functions, $\delta: \mathbb{R}^n \rightarrow \mathbb{R}^m$ is an uncertainty, $A \in \mathbb{R}^{n \times n}$ is a known system matrix, $B \in \mathbb{R}^{n \times m}$ is a known input matrix, and the pair (A, B) is controllable.

Assumption 5.1.1 *The uncertainty in (5.7) is parameterized as*

$$\delta(x(t)) = W^T \sigma(x(t)), \quad x(t) \in \mathbb{R}^n, \quad (5.8)$$

where $W \in \mathbb{R}^{s \times m}$ is an unknown weight matrix and $\sigma: \mathbb{R}^n \rightarrow \mathbb{R}^s$ is a known basis function of the form $\sigma(x(t)) = [\sigma_1(x(t)), \sigma_2(x(t)), \dots, \sigma_s(x(t))]^T$, which satisfies

$$\sigma(x(t)) = K(x(t))x(t) + b(x(t)), \quad K: \mathbb{R}^n \rightarrow \mathbb{R}^{s \times n}, \quad b: \mathbb{R}^n \rightarrow \mathbb{R}^s, \quad (5.9)$$

with $b(x(t))$ being a bounded term. In addition, (5.9) satisfies the inequality given by

$$\|\sigma(x(t)) - \sigma_0\| \leq \alpha \|x(t)\|, \quad x(t) \in \mathbb{R}^n, \quad (5.10)$$

with $\sigma_0 \in \mathbb{R}_+$ and $\alpha \in \mathbb{R}_+$.

Next, consider the reference model capturing a desired, ideal closed-loop dynamical system performance given by

$$\dot{x}_r(t) = A_r x_r(t) + B_r c(t), \quad x_r(0) = x_{r0}, \quad (5.11)$$

where $x_r(t) \in \mathbb{R}^n$ is the reference state vector, $c(t) \in \mathbb{R}^m$ is a given uniformly continuous bounded command, $A_r \in \mathbb{R}^{n \times n}$ is the Hurwitz reference model matrix, and $B_r \in \mathbb{R}^{n \times m}$ is the command input matrix. The objective of the model reference adaptive control problem is to construct a feedback control law architecture $u(t)$ such that the state vector $x(t)$ asymptotically (or approximately) follows the reference state vector $x_r(t)$.

For the purpose of solving this problem, consider the feedback control law given by

$$u(t) = u_n(t) + u_a(t), \quad (5.12)$$

where $u_n(t)$ and $u_a(t)$ are the nominal feedback control law and the adaptive feedback control law, respectively. Let the nominal feedback control law be given by

$$u_n(t) = -K_1 x(t) + K_2 c(t), \quad (5.13)$$

where $K_1 \in \mathbb{R}^{m \times n}$ and $K_2 \in \mathbb{R}^{m \times m}$ are the nominal feedback and the nominal feedforward gains, respectively, such that $A_r = A - BK_1$ and $B_r = BK_2$ hold. Using (5.12) and (5.13) in (5.7) with Assumption 5.1.1 yields

$$\dot{x}(t) = A_r x(t) + B_r c(t) + B[u_a(t) + W^T \sigma(x(t))]. \quad (5.14)$$

Now, let the adaptive feedback control law be given by

$$u_a(t) = -\hat{W}^T(t) \sigma(x(t)), \quad (5.15)$$

where $\hat{W}(t) \in \mathbb{R}^{s \times m}$ is the estimate of W satisfying the weight update law

$$\dot{\hat{W}}(t) = \gamma \text{Proj}_m[\hat{W}(t), \sigma(x(t))e^T(t)PB], \quad \hat{W}(0) = \hat{W}_0, \quad (5.16)$$

where $\gamma \in \mathbb{R}_+$ is the learning rate gain, $e(t) \triangleq x(t) - x_r(t)$ is the system error state vector, and $P \in \mathbb{R}_+^{n \times n}$ is a solution of the Lyapunov equation

$$0 = A_r^T P + P A_r + R, \quad (5.17)$$

with $R \in \mathbb{R}_+^{n \times n}$. Note that since A_r is Hurwitz, it follows from the converse Lyapunov theory that there exists a unique P satisfying (5.17) for a given R . In addition, the projection bounds are defined such that

$$|[\hat{W}(t)]_{ij}| \leq \hat{W}_{\max, i+(j-1)s}, \quad (5.18)$$

for $i = 1, \dots, s$ and $j = 1, \dots, m$, where $\hat{W}_{\max, i+(j-1)s} \in \mathbb{R}_+$ denotes (symmetric) element-wise projection bounds. Note that the results of this paper can be readily applied to the case when asymmetric projection bounds are considered.

Now, using (5.15) in (5.14) along with (5.11), the system error dynamics can be written as

$$\dot{e}(t) = A_r e(t) - B \tilde{W}^T(t) \sigma(x(t)), \quad e(0) = e_0, \quad (5.19)$$

where $\tilde{W}(t) \triangleq \hat{W}(t) - W \in \mathbb{R}^{s \times m}$. Note that the weight update law given by (5.16) can be derived using Lyapunov analysis by considering the Lyapunov function candidate given by (see, for example, [6])

$$\mathcal{V}(e, \tilde{W}) = e^T P e + \gamma^{-1} \text{tr } \tilde{W}^T \tilde{W}. \quad (5.20)$$

Note that $\mathcal{V}(0, 0) = 0$ and $\mathcal{V}(e, \tilde{W}) > 0$ for all $(e, \tilde{W}) \neq (0, 0)$. Now, differentiating (5.20) yields $\dot{\mathcal{V}}(e(t), \tilde{W}(t)) \leq -e^T(t) R e(t) \leq 0$, which guarantees that the system error state vector $e(t)$ and the weight error $\tilde{W}(t)$ are Lyapunov stable, and hence, are bounded for all $t \in \overline{\mathbb{R}}_+$. Since $\sigma(x(t)) = \sigma(e(t) + x_r(t))$ is bounded for all $t \in \overline{\mathbb{R}}_+$ as a consequence of the fact that $e(t)$ and $x_r(t)$ are bounded for all $t \in \overline{\mathbb{R}}_+$, it follows from (5.19) that $\dot{e}(t)$ is bounded, and hence, $\dot{\mathcal{V}}(e(t), \tilde{W}(t))$ is bounded for all $t \in \overline{\mathbb{R}}_+$. It then follows from Barbalat's lemma that $\lim_{t \rightarrow \infty} \dot{\mathcal{V}}(e(t), \tilde{W}(t)) = 0$, which consequently shows that $e(t) \rightarrow 0$ as $t \rightarrow \infty$.

The above discussion highlights that the adaptive control formulation introduced in this section has the capability to suppress the effect of any nonlinear system uncertainty satisfying (5.8) to achieve desirable

command following performance specifications. Yet, it provides no guarantees in the presence actuator dynamics that appear in any practical application of feedback control laws.

In order to reach to the conclusion highlighted above, it should be noted that one does not necessarily need (5.9) and (5.10) given for the uncertainty parameterization in (5.8). However, they are necessary to utilize linear matrix inequalities (LMIs) in the next section with the proposed hedging-based adaptive control framework for ensuring closed-loop system stability in the presence of high-order, linear time-invariant actuator dynamics.

5.1.3 Closed-Loop Adaptive Control System Stability with Actuator Dynamics

Building on the mathematical preliminaries overviewed in Section 5.1.2, we now introduce the actuator dynamics problem and the LMIs-based adaptive control approach predicated on the hedging method. Specifically, consider the uncertain nonlinear dynamical system \mathcal{G} given by

$$\dot{x}(t) = Ax(t) + B[v(t) + \delta(x(t))], \quad x(0) = x_0, \quad (5.21)$$

where $v(t) \in \mathbb{R}^m$ is the actuator output of the actuator dynamics \mathcal{G}_A satisfying a high-order, linear time-invariant model

$$\begin{aligned} \dot{x}_c(t) &= Fx_c(t) + Gu(t), \quad x_c(0) = x_{c0}, \\ v(t) &= Hx_c(t), \end{aligned} \quad (5.22)$$

with $x_c(t) \in \mathbb{R}^p$ being the actuator state vector, $G \in \mathbb{R}^{p \times m}$ being the actuator input matrix, $H \in \mathbb{R}^{m \times p}$ being the actuator output matrix, and $F \in \mathbb{R}^{p \times p}$ being a Hurwitz matrix in Jordan form such that there exists $S \in \mathbb{R}_+^{p \times p}$ that satisfies $0 = F^T S + SF + I$. Note that we say F in Jordan form without loss of generality since state-space representations of differential equations are not unique. Throughout this paper, we inherently assume that the algebraic multiplicity of F is equal to its geometric multiplicity and $-HF^{-1}G = I$.

It follows from Assumption 5.1.1 that (5.21) can be equivalently rewritten as

$$\dot{x}(t) = Ax(t) + B[u(t) + W^T(t)\sigma(x(t))] + B[v(t) - u(t)]. \quad (5.23)$$

Using the feedback control given by (5.12), (5.13), and (5.15) in (5.23) yields

$$\dot{x}(t) = A_r x(t) + B_r c(t) - B\tilde{W}^T(t)\sigma(x(t)) + B[v(t) - u(t)]. \quad (5.24)$$

Utilizing the hedging approach originally proposed in [30, 31, 33], let the modified reference model dynamics be given by

$$\dot{x}_r(t) = A_r x_r(t) + B_r c(t) + B[v(t) - u(t)], \quad x_r(0) = x_{r0}, \quad (5.25)$$

such that the system error dynamics follow from (5.24) and (5.25) as

$$\dot{e}(t) = A_r e(t) - B\tilde{W}^T(t)\sigma(x(t)), \quad e(0) = e_0. \quad (5.26)$$

Notice that (5.26) is identical to the system error dynamics given by (5.19) due to the fact that the hedging signal $B[v(t) - u(t)]$ is introduced to the ideal reference model dynamics, and hence, the system error dynamics are not affected due to the presence of high-order, linear time-invariant actuator dynamics.

The following two lemmas are needed for the results in this section. For this purpose, let $\hat{\theta}(t, x(t)) \triangleq \hat{W}^T(t)K(x(t))$, let $\bar{\omega} \in \mathbb{R}_+$ be such that $\hat{W}_{\max, i+(j-1)s} \leq \bar{\omega}$ for all $i = 1, \dots, s$ and $j = 1, \dots, m$, and let $\underline{k}_0 \in \mathbb{R}_+$, $\underline{k}_1 \in \mathbb{R}_+$, and $\underline{k} \in \mathbb{R}_+$ be such that $\underline{k}_0 \leq k$, $\underline{k}_1 \leq k$, and $\underline{k} \leq k$, where k scales the eigenvalues of \mathcal{G}_A (this implies that we let $F \triangleq kF_0$, $H \triangleq kH_0$, $G \triangleq G_0$).

Lemma 5.1.1 *There exists a set $\kappa \triangleq \{\underline{k} : \underline{k} \leq k\} \cup \{\bar{\omega}, \underline{k}_0 : \hat{W}_{\max, i+(j-1)s} \leq \bar{\omega}, i = 1, \dots, s, j = 1, \dots, m \text{ and } \underline{k}_0 \leq k\}$ such that if $(\underline{k}, \bar{\omega}, \underline{k}_0) \in \kappa$ and $K(x(t))$ is bounded, then*

$$\mathcal{A}(\hat{\theta}(t, x(t)), \mathcal{G}_A) = \begin{bmatrix} A + B\hat{\theta}(t, x(t)) & BH \\ -GK_1 - G\hat{\theta}(t, x(t)) & F \end{bmatrix} \quad (5.27)$$

is quadratically stable.

Proof. Due to page restrictions, the proof is omitted. ■

Consistent with our prior work [95, 102–104], Lemma 5.1.1 reveals the fundamental stability interplay between the allowable system uncertainties (through the selection of the projection operator bounds) and the bandwidth of the high-order actuator dynamics.

Lemma 5.1.2 *There exists a set $\kappa_1 \triangleq \{\underline{k}_1 : \underline{k}_1 \leq k\}$, such that if $\underline{k}_1 \in \kappa_1$, then*

$$\mathcal{A}(\mathcal{G}_A) = \begin{bmatrix} A & BH \\ -GK_1 & F \end{bmatrix}, \quad (5.28)$$

is quadratically stable.

Proof. Due to page restrictions, the proof is omitted. ■

The results given in Lemma 5.1.1 are predicated on the boundedness of $K(x(t))$, where this automatically holds in our case as shown as a part of the proof of the next theorem presenting the main contribution of this paper.

Theorem 5.1.1 *Consider the uncertain nonlinear dynamical system given by (5.21) subject to Assumption 5.1.1, the reference model given by (5.25), the actuator dynamics given by (5.22), and the feedback control law given by (5.12), (5.13), and (5.15) along with the update law (5.16). If*

$$(\underline{k}, \bar{\omega}, \underline{k}_0) \in \kappa, \quad \underline{k}_1 \in \kappa_1, \quad (5.29)$$

then the solution $(e(t), \tilde{W}(t), x_r(t), v(t))$ of the closed-loop dynamical system are bounded and

$$\lim_{t \rightarrow \infty} e(t) = 0. \quad (5.30)$$

Proof. To show Lyapunov stability and guarantee boundedness of the system error state $e(t)$ and the weight error $\tilde{W}(t)$, consider the Lyapunov function candidate given by (5.20). Differentiating (5.20) yields $\dot{V}(e(t), \tilde{W}(t)) \leq -e^T(t)Re(t) \leq 0$, which guarantees the Lyapunov stability, and hence, the boundedness of the solution $(e(t), \tilde{W}(t))$.

To show the boundedness of $x_r(t)$ and $x_c(t)$ (and therefore $v(t)$), consider the reference model (5.25) and the actuator dynamics (5.22) subject to (5.12), (5.13), and (5.15) as $\dot{x}_r(t) = Ax_r(t) + B[Hx_c(t) + K_1e(t) + \hat{W}^T(t)\sigma(x(t))]$, and $\dot{x}_c(t) = Fx_c(t) - GK_1x_r(t) - GK_1(t)e(t) + GK_2c(t) - G\hat{W}^T(t)\sigma(x(t))$, these dynamics can be rewritten in compact form as

$$\dot{\xi}(t) = \mathcal{A}(\mathcal{G}_A)\xi(t) + \zeta(\cdot) + \omega(\cdot), \quad (5.31)$$

with

$$\xi(t) = [x_r^T(t), x_c^T(t)]^T, \quad (5.32)$$

and

$$\zeta(\cdot) = \begin{bmatrix} B\hat{W}^T(t)\sigma(x(t)) \\ -G\hat{W}^T(t)\sigma(x(t)) \end{bmatrix}, \quad (5.33)$$

$$\omega(\cdot) = \begin{bmatrix} BK_1e(t) \\ -GK_1e(t) + GK_2c(t) \end{bmatrix}. \quad (5.34)$$

Note that $\omega(\cdot)$ in (5.31) is a bounded perturbation for all $t \in \bar{\mathbb{R}}_+$ as a result of the boundedness of the signals $e(t)$ and $\tilde{W}(t)$ for all $t \in \bar{\mathbb{R}}_+$. In the remainder of the proof, we consider two cases.

In Case 1, for $\|x(t)\| < \varepsilon$, we use Assumption 5.1.1 and let $K(x(t)) = 0$ such that $\sigma(x(t)) = b(x(t))$ and is therefore bounded for all $t \in \bar{\mathbb{R}}_+$. It then follows that (5.31) can be rewritten as

$$\dot{\xi}(t) = \mathcal{A}(\mathcal{G}_A)\xi(t) + \omega(\cdot), \quad (5.35)$$

with

$$\omega(\cdot) = \begin{bmatrix} B\hat{W}^T(t)b(x(t)) + BK_1e(t) \\ -G\hat{W}^T(t)b(x(t)) - GK_1e(t) + GK_2c(t) \end{bmatrix}. \quad (5.36)$$

Now, it follows that since $\omega(\cdot)$ is bounded for all $t \in \bar{\mathbb{R}}_+$ and $\mathcal{A}(\mathcal{G}_A)$ is quadratically stable for $\underline{k}_1 \in \kappa_1$ by Lemma 5.1.2, then $x_r(t)$ and $x_c(t)$ are also bounded [88]. This further implies that the actuator output $v(t)$ is bounded.

In Case 2, we now consider $\|x(t)\| \geq \varepsilon$. For this purpose, once again, we use Assumption 5.1.1 and let $b(x(t)) = 0$ such that

$$\sigma(x(t)) = K(x(t))x(t). \quad (5.37)$$

We first show that $K(x(t))$ is bounded for all $t \in \bar{\mathbb{R}}_+$. Specifically, it follows from (5.37) that

$$\begin{aligned}
\frac{\|K(x(t))x(t)\|}{\|x(t)\|} &= \frac{\|\sigma(x(t))\|}{\|x(t)\|} \\
&= \frac{\|\sigma(x(t)) - \sigma_0 + \sigma_0\|}{\|x(t)\|} \\
&\leq \frac{\|\sigma(x(t)) - \sigma_0\|}{\|x(t)\|} + \frac{\|\sigma_0\|}{\|x(t)\|} \\
&\leq \frac{\alpha \|x(t)\|}{\|x(t)\|} + \frac{\|\sigma_0\|}{\|x(t)\|}.
\end{aligned} \tag{5.38}$$

Taking the supremum of both sides yields

$$\sup_{\|x(t)\| \neq 0} \frac{\|K(x(t))x(t)\|}{\|x(t)\|} \leq \sup_{\|x(t)\| \neq 0} \left(\alpha + \frac{\|\sigma_0\|}{\|x(t)\|} \right), \tag{5.39}$$

which further implies

$$\|K(x(t))\| \leq \alpha + \frac{\|\sigma_0\|}{\varepsilon}, \tag{5.40}$$

for $\|x(t)\| \geq \varepsilon$, and hence, $K(x(t))$ is bounded for all $t \in \bar{\mathbb{R}}_+$.

Next, the matrix $\zeta(\cdot)$ in (5.31) can be rewritten as

$$\zeta(\cdot) = \begin{bmatrix} B\hat{W}^T(t)K(x(t))(x_r(t) + e(t)) \\ -G\hat{W}^T(t)K(x(t))(x_r(t) + e(t)) \end{bmatrix}. \tag{5.41}$$

Note that since $\hat{W}(t)$ is bounded for all $t \in \bar{\mathbb{R}}_+$ as a result of the projection based weight update law and the boundedness of $K(x(t))$ for all $t \in \bar{\mathbb{R}}_+$,

$$\hat{\theta}(t, x(t)) = \hat{W}^T(t)K(x(t)), \tag{5.42}$$

is bounded for all $t \in \bar{\mathbb{R}}_+$ and it follows from (5.41)

$$\zeta(\cdot) = \begin{bmatrix} B\hat{\theta}(t, x(t))(x_r(t) + e(t)) \\ -G\hat{\theta}(t, x(t))(x_r(t) + e(t)) \end{bmatrix}. \tag{5.43}$$

Then, using (5.43), (5.31) can be rewritten as

$$\dot{\xi}(t) = \mathcal{A}(\hat{\theta}(t, x(t)), \mathcal{G}_A)\xi(t) + \omega(\cdot), \quad (5.44)$$

with

$$\omega(\cdot) = \begin{bmatrix} B\hat{\theta}(t, x(t))e(t) + BK_1e(t) \\ -G\hat{\theta}(t, x(t))e(t) - GK_1e(t) + GK_2c(t) \end{bmatrix}. \quad (5.45)$$

Now, as in Case 1, it follows that since $\omega(\cdot)$ is bounded for all $t \in \overline{\mathbb{R}}_+$ and $\mathcal{A}(\hat{\theta}(t, x(t)), \mathcal{G}_A)$ is quadratically stable for $(\underline{k}, \overline{\omega}, \underline{k}_0) \in \kappa$ by Lemma 5.1.1, then $x_r(t)$ and $x_c(t)$ are also bounded for all $t \in \overline{\mathbb{R}}_+$, which further implies that the actuator output $v(t)$ is bounded for all $t \in \overline{\mathbb{R}}_+$.

To show $\lim_{t \rightarrow \infty} e(t) = 0$, note that $x(t)$ is bounded for all $t \in \overline{\mathbb{R}}_+$ as a consequence of the boundedness of $e(t)$ and $x_r(t)$ for all $t \in \overline{\mathbb{R}}_+$ for both cases. It now follows from (5.26) that $\dot{e}(t)$ is bounded for all $t \in \overline{\mathbb{R}}_+$, and hence, $\ddot{v}(e(t), \tilde{W}(t))$ is bounded for all $t \in \overline{\mathbb{R}}_+$. As a consequence of the boundedness of $\dot{v}(e(t), \tilde{W}(t))$ and Barbalat's lemma [88], $\lim_{t \rightarrow \infty} \dot{v}(e(t), \tilde{W}(t)) = 0$, and hence, $\lim_{t \rightarrow \infty} e(t) = 0$. ■

To satisfy the quadratic stability of (5.27), we can utilize LMIs by following a similar procedure documented in our recent works [95, 102–104]. For this purpose, let $\overline{W}_{i_1, \dots, i_l} \in \mathbb{R}^{s \times m}$ be defined as

$$\overline{W}_{i_1, \dots, i_l} = \begin{bmatrix} (-1)^{i_1} \hat{W}_{\max, 1} & (-1)^{i_1+s} \hat{W}_{\max, 1+s} & \dots & (-1)^{i_1+(m-1)s} \hat{W}_{\max, 1+(m-1)s} \\ (-1)^{i_2} \hat{W}_{\max, 2} & (-1)^{i_2+s} \hat{W}_{\max, 2+s} & \dots & (-1)^{i_2+(m-1)s} \hat{W}_{\max, 2+(m-1)s} \\ \vdots & \vdots & \ddots & \vdots \\ (-1)^{i_s} \hat{W}_{\max, n} & (-1)^{i_s} \hat{W}_{\max, 2s} & \dots & (-1)^{i_{ms}} \hat{W}_{\max, ms} \end{bmatrix}, \quad (5.46)$$

where $i_l \in \{1, 2\}$, $l \in \{1, \dots, 2^{ms}\}$, such that $\overline{W}_{i_1, \dots, i_l}$ represents the corners of the hypercube defining the maximum variation of $\hat{W}(t)$. Furthermore, since we define $\hat{\theta}(t, x(t)) \triangleq \hat{W}^T(t)K(x(t))$, let $\overline{\theta}_{i_1, \dots, i_r} \in \mathbb{R}^{m \times n}$ be

defined as

$$\bar{\theta}_{i_1, \dots, i_r} = \begin{bmatrix} (-1)^{i_1} \hat{\theta}_{\max, 1} & (-1)^{i_1+m} \hat{\theta}_{\max, 1+m} & \dots & (-1)^{i_1+(n-1)m} \hat{\theta}_{\max, 1+(n-1)m} \\ (-1)^{i_2} \hat{\theta}_{\max, 2} & (-1)^{i_2+m} \hat{\theta}_{\max, 2+m} & \dots & (-1)^{i_2+(n-1)m} \hat{\theta}_{\max, 2+(n-1)m} \\ \vdots & \vdots & \ddots & \vdots \\ (-1)^{i_m} \hat{\theta}_{\max, n} & (-1)^{i_m} \hat{\theta}_{\max, 2m} & \dots & (-1)^{i_m} \hat{\theta}_{\max, nm} \end{bmatrix}, \quad (5.47)$$

where $i_r \in \{1, 2\}$, $r \in \{1, \dots, 2^{ms+1}\}$, such that $\bar{\theta}_{i_1, \dots, i_r}$ represent the corners of the hypercube defining the maximum variation of the product of $\hat{W}^T(t)K(x(t))$. Utilizing the results in [96, 97], if

$$\mathcal{A}_{i_1, \dots, i_r} = \begin{bmatrix} A + B\bar{\theta}_{i_1, \dots, i_r} & BH \\ -G\bar{\theta}_{i_1, \dots, i_r} & F \end{bmatrix}, \quad (5.48)$$

satisfies the matrix inequality

$$\mathcal{A}_{i_1, \dots, i_r}^T \mathcal{P} + \mathcal{P} \mathcal{A}_{i_1, \dots, i_r} < 0, \quad \mathcal{P} = \mathcal{P}^T > 0, \quad (5.49)$$

for all permutations of $\bar{\theta}_{i_1, \dots, i_r}$, then (5.27) is quadratically stable. Since it can be readily shown that (5.27) is quadratically stable for large values of k , we can cast (5.49) as a convex optimization problem and solve it using LMIs.

5.1.4 Illustrative Numerical Example

In order to illustrate the proposed LMIs-based adaptive control architecture predicated on the hedging method, we consider the second-order uncertain nonlinear dynamical system given by

$$\begin{bmatrix} \dot{x}_1(t) \\ \dot{x}_2(t) \end{bmatrix} = \begin{bmatrix} 0 & 1 \\ 1 & 1 \end{bmatrix} \begin{bmatrix} x_1(t) \\ x_2(t) \end{bmatrix} + \begin{bmatrix} 0 \\ 1 \end{bmatrix} (v(t) + \delta(x(t))), \quad (5.50)$$

with zero initial conditions, where $x_1(t)$ represents the angle in radians and $x_2(t)$ represents the angular rate of change in radians per second. Here, in addition, $\delta(x(t))$ represents an uncertainty of the form $\delta(x) = \beta_1 x_2(t) \sin(x_1(t)) + \beta_2 x_1(t) \cos(x_2(t))$, where β_i , $i = 1, 2$, are unknown.

For the actuator dynamics, we consider the second-order model given by

$$F = \begin{bmatrix} 0 & 1 \\ -\omega_n^2 & -2\zeta\omega_n \end{bmatrix}, \quad G = \begin{bmatrix} 0 \\ 1 \end{bmatrix}, \quad H = \begin{bmatrix} \omega_n^2 & 0 \end{bmatrix}, \quad (5.51)$$

where it is noted that F can be trivially transformed into Jordan form.

For our numerical example, we set $\beta_1 = \beta_2 = 1$ and choose $K_1 = [2, 2.4]$ and $K_2 = 1$ for the nominal controller design that yields to a reference model with a natural frequency of $\omega_{nr} = 1.0$ rad/s and a damping ratio $\zeta_r = 0.7$, which yields

$$A_r = \begin{bmatrix} 0 & 1 \\ -1 & -1.4 \end{bmatrix}, \quad B_r = \begin{bmatrix} 0 \\ 1 \end{bmatrix}. \quad (5.52)$$

In addition, we use a filtered tracking command $c(t)$ and we set $R = I_2$ from (5.17) for the proposed adaptive controller design. Using the rectangular projection operator, the bounds on the uncertainty are set element-wise such that $|\hat{W}(t)_{i,1}| \leq 1.1$ with $i = 1, 2$. We set all initial conditions to zero such that Assumption 5.1.1 is satisfied with $\alpha = 1$. Using this along with the bounds on $\hat{W}(t)$ in the LMI analysis highlighted in Section III, the feasible region of allowable actuator dynamics is calculated.

Figure 5.1 shows the feasible region of allowable actuator dynamics that is given by the ω_n and ζ values for the actuator dynamics. Note that Figure 5.1 provides both the LMI calculated feasible limit as well as the feasible limit provided by the simulation results. Due to space restrictions, we select two points to simulate the proposed controller performance as seen in Figures 5.2 and 5.3. Since the feasible boundary corresponds to calculated minimum feasible ω_n and ζ values for the actuator dynamics, it is expected that the system performances are guaranteed to be bounded for actuator dynamics at points greater than and equal to the calculated feasible boundary. This can be seen in Figure 5.2 when the actuator dynamics are at the minimum point $(\zeta, \omega_n) = (0.525, 5.28)$, which is located on the feasible boundary. In Figure 5.3, we let the actuator dynamics be outside the calculated feasible region to show that the closed-loop system remains bounded until the actuator dynamics reach a value of $(\zeta, \omega_n) = (0.525, 3.46)$. This is consistent with the presented theory, as we provide a (conservative) upper bound on the allowable actuator dynamics such that the closed-loop system remains bounded.

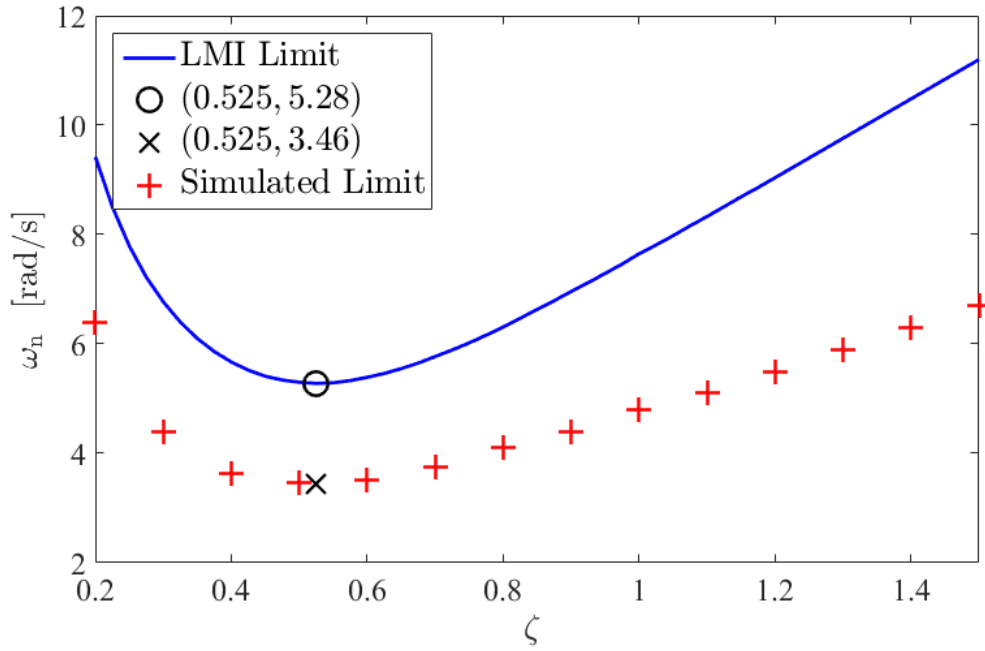


Figure 5.1: LMI calculated feasible region for actuator dynamics.

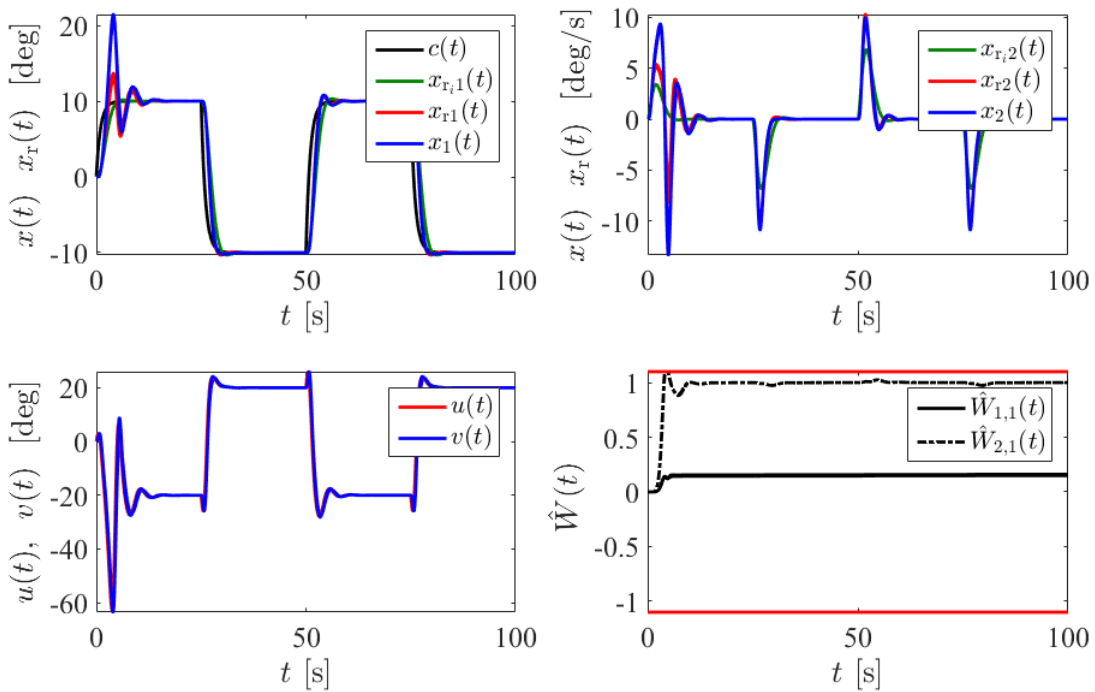


Figure 5.2: Proposed controller performance with actuator dynamics ($((\zeta, \omega_n) = (0.525, 5.28), \gamma = 25)$).

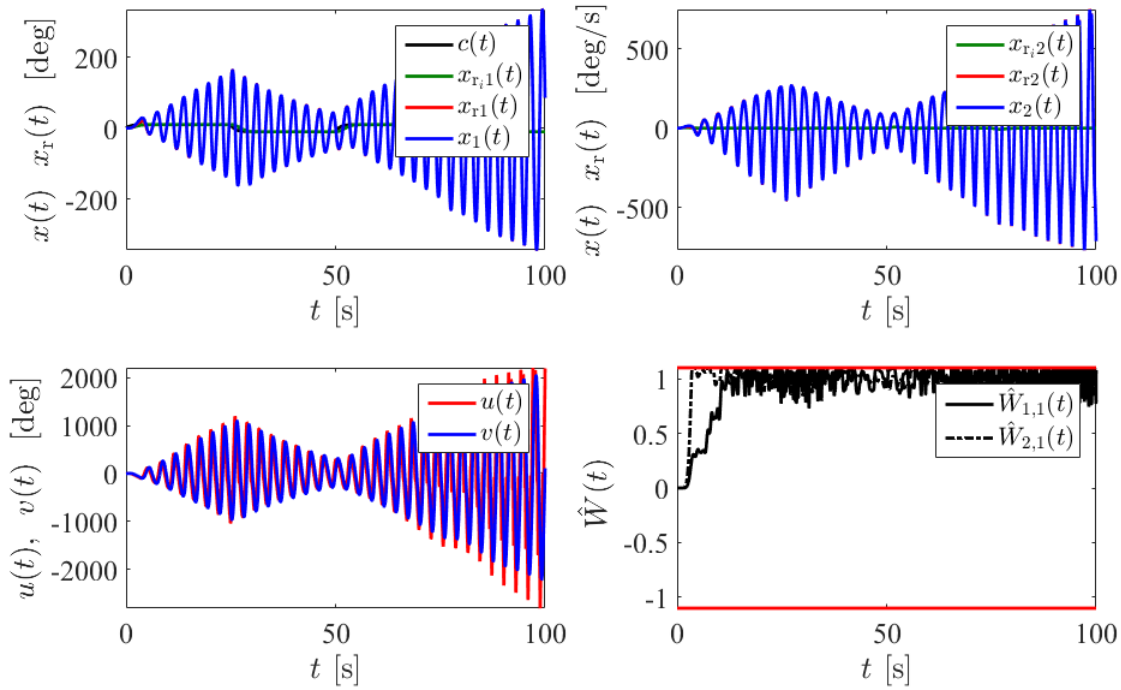


Figure 5.3: Proposed controller performance with actuator dynamics $((\zeta, \omega_n) = (0.525, 3.46), \gamma = 25)$.

5.1.5 Conclusion

Although adaptive control is a powerful design methodology to cope with a broad spectrum of uncertainties, the presence of actuator dynamics can seriously limit achievable closed-loop adaptive control system stability in any practical application. For addressing this problem, we considered a class of uncertain nonlinear dynamical systems in this paper and presented a LMI-based adaptive control framework predicated on the hedging method to ensure closed-loop system stability in the presence of high-order, linear time-invariant actuator dynamics. In addition to rigorously analyzing the overall stability of the proposed framework, which revealed the fundamental stability interplay between the parameters of a given actuator dynamics model and the allowable uncertainties in the feedback loop, we also provided an illustrative numerical example to demonstrate its efficacy and practicality. Finally, although this paper considered a particular adaptive control formulation, namely model reference adaptive control architecture, the presented design methodology can be used in a complimentary way with many other approaches to adaptive control.

5.2 A Model Reference Adaptive Control Framework for Uncertain Dynamical Systems with High-Order Actuator Dynamics and Unknown Actuator Outputs²

As it is well-known, the stability properties of model reference adaptive controllers can be seriously affected by the presence of actuator dynamics. To this end, the authors recently proposed linear matrix inequalities-based hedging approaches to compute the stability limits of model reference adaptive controllers in the presence of a) scalar actuator dynamics with known outputs, b) scalar actuator dynamics with unknown outputs, and c) high-order (linear time-invariant) actuator dynamics with known outputs. The common denominator of these approaches is that they have the capability to rigorously characterize the fundamental stability interplay between the system uncertainties and the necessary bandwidth of the actuator dynamics.

Building on these results, the purpose of this paper is to extend the recent work by the authors to the general case, where there exist high-order actuator dynamics with unknown outputs in the closed-loop model reference adaptive control systems. For this purpose, we propose an observer architecture to estimate the unknown output of the actuator dynamics and use the estimated actuator output to design the linear matrix inequalities-based hedging framework. Remarkably, with the proposed observer, the sufficient stability condition in this case of unknown actuator outputs is identical to the case with known actuator outputs that was established in the prior work by the authors. Therefore, a control designer can utilize the proposed framework for practical applications when the output of the actuator dynamics is not measurable, and hence, unknown (e.g., in hypersonic vehicle applications). An illustrative numerical example complements the proposed theoretical contribution.

5.2.1 Introduction

While model reference adaptive controllers have the capability to suppress the effect of wide classes of system uncertainties to achieve desired stabilization and command following system performances, it is well-known that their stability properties can be seriously affected by the presence of actuator dynamics (e.g., see [95] and references therein). To address this issue, the authors recently proposed linear matrix inequalities (LMI)-based hedging approaches, where the hedging technique [30, 31, 33] modifies the ideal reference model dynamics in order to allow correct adaptation that is not affected by the presence of actuator dynamics, and then LMIs are used to compute the stability limits of model reference adaptive controllers in

²This section is previously published in [105]. Permission is included in Appendix B.

the presence of *a*) scalar actuator dynamics with known outputs, *b*) scalar actuator dynamics with unknown outputs, and *c*) high-order (linear time-invariant) actuator dynamics with known outputs [95, 101–104]. These recent approaches have the capability to rigorously characterize the fundamental stability interplay between the system uncertainties and the necessary bandwidth of the actuator dynamics, and hence, allow safe implementation of model reference adaptive control systems for many real-world practical systems having actuator dynamics.

Building on our recent results documented in [95, 101–104], the main contribution of this paper is to extend the recent work by the authors to the general case, where there exist high-order actuator dynamics with unknown outputs in the closed-loop model reference adaptive control systems. For this purpose, we propose an observer architecture to estimate the unknown output of the actuator dynamics and use the estimated actuator output to design the LMI-based hedging framework. Remarkably (consistent with the results established for scalar actuator dynamics case [95, 102, 103]), the sufficient stability condition in this case of unknown high-order actuator outputs is identical to the case with known high-order actuator outputs that was established in the prior work by the authors [104]. Therefore, a control designer can utilize the proposed framework for practical applications when the output of the actuator dynamics is not measurable, and hence, unknown (e.g., in hypersonic vehicle applications). Although the proposed results in this paper focus on a particular model reference adaptive control framework, the results allowing for safe implementation of adaptive control systems can be readily applied to many other control designs such as [35, 75, 106–113] for improved performance.

In this paper, \mathbb{R} denotes the set of real numbers, \mathbb{R}^n denotes the set of $n \times 1$ real column vectors, $\mathbb{R}^{n \times m}$ denotes the set of $n \times m$ real matrices, \mathbb{R}_+ (resp. $\overline{\mathbb{R}}_+$) denotes the set of positive (resp., nonnegative) real numbers, $\mathbb{R}_+^{n \times n}$ (resp., $\overline{\mathbb{R}}_+^{n \times n}$) denotes the set of $n \times n$ positive-definite (resp. nonnegative-definite) real matrices, $\mathbb{S}^{n \times n}$ denotes the set of $n \times n$ symmetric real matrices, $\mathbb{D}^{n \times n}$ denotes the set of $n \times n$ real matrices with diagonal scalar entries, $(\cdot)^T$ denotes the transpose operator, $(\cdot)^{-1}$ denotes the inverse operator, $\text{tr}(\cdot)$ denotes the trace operator, $\|\cdot\|_2$ denotes the Euclidian norm, $\|\cdot\|_F$ denotes the Frobenius matrix norm, $[A]_{ij}$ denotes the ij -th entry of the real matrix $A \in \mathbb{R}^{n \times m}$, and $\lambda_{\min}(A)$ (resp., $\lambda_{\max}(A)$) denotes the minimum (resp., maximum) eigenvalue of the real matrix $A \in \mathbb{R}^{n \times n}$.

The organization of this paper is as follows. Section 5.2.2 covers the mathematical preliminaries necessary for the presented results in the paper. Section 5.2.3 introduces the proposed LMI-based hedging approach for uncertain dynamical systems subject to high-order actuator dynamics with unknown actuator

outputs. An illustrative numerical example is provided in Section 5.2.4 to demonstrate the efficacy of the proposed approach and conclusions are summarized in Section 5.2.5.

5.2.2 Mathematical Preliminaries

Consistent with our prior work [95, 101–104], we utilize projection operators in the design of model reference adaptive controllers throughout this paper (see below). As a consequence, we start with its following definition.

Definition 5.2.1 Let $\Omega = \{\theta \in \mathbb{R}^n : (\theta_i^{\min} \leq \theta_i \leq \theta_i^{\max})\}$, $i = 1, 2, \dots, n$ be a convex hypercube in \mathbb{R}^n , where $(\theta_i^{\min}, \theta_i^{\max})$ represent the minimum and maximum bounds for the i^{th} component of the n -dimensional parameter vector θ . In addition, let $\Omega_\varepsilon = \{\theta \in \mathbb{R}^n : (\theta_i^{\min} + \varepsilon \leq \theta_i \leq \theta_i^{\max} - \varepsilon)\}$, $i = 1, 2, \dots, n$ be a second hypercube for a sufficiently small positive constant ε , where $\Omega_\varepsilon \subset \Omega$. Then, the projection operator $\text{Proj} : \mathbb{R}^n \times \mathbb{R}^n \rightarrow \mathbb{R}^n$ is defined component-wise by

$$\text{Proj}(\theta, y) \triangleq \begin{cases} \left(\frac{\theta_i^{\max} - \theta_i}{\varepsilon}\right) y_i, & \text{if } \theta_i > \theta_i^{\max} - \varepsilon \text{ and } y_i > 0 \\ \left(\frac{\theta_i - \theta_i^{\min}}{\varepsilon}\right) y_i, & \text{if } \theta_i < \theta_i^{\min} + \varepsilon \text{ and } y_i < 0 \\ y_i, & \text{otherwise} \end{cases} \quad (5.53)$$

where $y \in \mathbb{R}^n$ [6].

Based on the above definition, we note that

$$(\theta - \theta^*)^T (\text{Proj}(\theta, y) - y) \leq 0, \quad \theta^* \in \Omega_\varepsilon, \quad (5.54)$$

holds [6, 82]. In this paper, we use the generalization of this definition to matrices as

$$\text{Proj}_m(\Theta, Y) = (\text{Proj}(\text{col}_1(\Theta), \text{col}_1(Y)), \dots, \text{Proj}(\text{col}_m(\Theta), \text{col}_m(Y))),$$

where $\Theta \in \mathbb{R}^{n \times m}$, $Y \in \mathbb{R}^{n \times m}$, and $\text{col}_i(\cdot)$ denotes the i -th column operator. For a given Θ^* , it now follows from (5.54) that

$$\text{tr} \left[(\Theta - \Theta^*)^T (\text{Proj}_m(\Theta, Y) - Y) \right] = \sum_{i=1}^m \left[\text{col}_i(\Theta - \Theta^*)^T (\text{Proj}(\text{col}_i(\Theta), \text{col}_i(Y)) - \text{col}_i(Y)) \right] \leq 0. \quad (5.55)$$

For completeness, we next present a concise overview of the standard model reference adaptive control problem. To this end, we consider the uncertain dynamical system given by

$$\dot{x}(t) = Ax(t) + Bu(t), \quad x(0) = x_0, \quad (5.56)$$

where $x(t) \in \mathbb{R}^n$ is the measurable state vector, $u(t) \in \mathbb{R}^m$ is the control input, $A \in \mathbb{R}^{n \times n}$ is an unknown system matrix, $B \in \mathbb{R}^{n \times m}$ is a known input matrix, and the pair (A, B) is controllable. In addition, we consider the (ideal) reference model given by

$$\dot{x}_r(t) = A_r x_r(t) + B_r c(t), \quad x_r(0) = x_{r0}, \quad (5.57)$$

where $x_r(t) \in \mathbb{R}^n$ is the reference state vector, $c(t) \in \mathbb{R}^m$ is a given uniformly continuous bounded command, $A_r \in \mathbb{R}^{n \times n}$ is the Hurwitz reference model matrix, and $B_r \in \mathbb{R}^{n \times m}$ is the command input matrix. The objective of the model reference adaptive control problem is to construct an adaptive feedback control law $u(t)$ such that the state vector $x(t)$ asymptotically follows the reference state vector $x_r(t)$.

We now make the following assumption, which is standard in the model reference adaptive control literature and is known as the matching condition [5–7].

Assumption 5.2.1 *There exists an unknown matrix $K_1 \in \mathbb{R}^{m \times n}$ and a known matrix $K_2 \in \mathbb{R}^{m \times m}$ such that $A_r = A - BK_1$ and $B_r = BK_2$ hold.*

Next, (5.56) can be rewritten based on Assumption 5.2.1 as

$$\dot{x}(t) = A_r x(t) + B_r c(t) + B[u(t) + W^T x(t) - K_2 c(t)], \quad (5.58)$$

where $W \triangleq K_1^T \in \mathbb{R}^{n \times m}$ is unknown. Now, we choose the adaptive feedback control law as

$$u(t) = -\hat{W}^T(t)x(t) + K_2 c(t), \quad (5.59)$$

where $\hat{W}(t) \in \mathbb{R}^{n \times m}$ is the estimate of W satisfying the weight update law

$$\dot{\hat{W}}(t) = \gamma \text{Proj}_m[\hat{W}(t), x(t)e^T(t)PB], \quad \hat{W}(0) = \hat{W}_{10}, \quad (5.60)$$

with $\gamma \in \mathbb{R}_+$ being the learning rate, $e(t) \triangleq x(t) - x_r(t)$ being the system error state vector, and $P \in \mathbb{R}_+^{n \times n}$ being the solution of the Lyapunov equation given by

$$0 = A_r^T P + P A_r + R, \quad (5.61)$$

$R \in \mathbb{R}_+^{n \times n}$. Note that since A_r is Hurwitz, it follows that there exists a unique P satisfying (5.61) for a given R [80]. For (5.60), the projection bounds are defined such that

$$|[\hat{W}(t)]_{ij}| \leq \hat{W}_{\max, i+(j-1)n}, \quad (5.62)$$

for $i = 1, \dots, n$ and $j = 1, \dots, m$, where $\hat{W}_{\max, i+(j-1)n} \in \mathbb{R}_+$ denotes (symmetric) element-wise projection bounds.

Finally, using (5.59) in (5.58) along with (5.57), the system error dynamics can be written as

$$\dot{e}(t) = A_r e(t) - B \tilde{W}^T(t) x(t), \quad e(0) = e_0, \quad (5.63)$$

where $\tilde{W}(t) \triangleq \hat{W}(t) - W \in \mathbb{R}^{n \times m}$. Note that the weight update law given by (5.60) can be readily derived using Lyapunov analysis by considering the Lyapunov function candidate given by (see, for example, [5–7])

$$\mathcal{V}(e, \tilde{W}) = e^T P e + \gamma^{-1} \text{tr } \tilde{W}^T \tilde{W}, \quad (5.64)$$

where differentiating (5.64) yields $\dot{\mathcal{V}}(e(t), \tilde{W}(t)) \leq -e^T(t) R e(t) \leq 0$. This guarantees that the system error state vector $e(t)$ and the weight error $\tilde{W}(t)$ are Lyapunov stable, and hence, are bounded for all $t \in \overline{\mathbb{R}}_+$. Since $x(t)$ is bounded for all $t \in \overline{\mathbb{R}}_+$, it follows from (5.63) that $\dot{e}(t)$ is bounded, and hence, $\ddot{\mathcal{V}}(e(t), \tilde{W}(t))$ is bounded for all $t \in \overline{\mathbb{R}}_+$. It then follows from Barbalat's lemma that $\lim_{t \rightarrow \infty} \dot{\mathcal{V}}(e(t), \tilde{W}(t)) = 0$, which consequently shows that $e(t) \rightarrow 0$ as $t \rightarrow \infty$. This analysis highlights that the standard model reference adaptive control formulation overviewed in this section has the capability to suppress the effect of system uncertainties, in the absence of actuator dynamics, to achieve desirable tracking performance specifications captured by (5.57).

5.2.3 Adaptive Control with Unknown Actuator Output

Building on the mathematical preliminaries overviewed in Section 5.2.2, we now present a new design procedure to ensure guaranteed stability of model reference adaptive control systems in the presence of high-order actuator dynamics with unknown outputs. For this purpose, we consider the uncertain dynamical system subject to actuator dynamics given by

$$\dot{x}(t) = Ax(t) + Bv(t), \quad x(0) = x_0. \quad (5.65)$$

In (5.65), $v(t) \in \mathbb{R}^m$ is the unknown actuator output of the high-order actuator dynamics \mathcal{G}_A given by

$$\begin{aligned} \dot{x}_c(t) &= Fx_c(t) + Gu(t), \quad x_c(0) = x_{c0}, \\ v(t) &= Hx_c(t), \end{aligned} \quad (5.66)$$

with $x_c(t) \in \mathbb{R}^p$ being the actuator state vector, $G \in \mathbb{R}^{p \times m}$ being the actuator input matrix, $H \in \mathbb{R}^{m \times p}$ being the actuator output matrix, and $F \in \mathbb{R}^{p \times p}$ being a Hurwitz matrix in Jordan form such that there exists $S \in \mathbb{R}_+^{p \times p}$ that satisfies

$$0 = F^T S + SF + I. \quad (5.67)$$

Here, without loss of much generality, we let the static gain of the actuator dynamics (5.66) be unity (i.e., $-HF^{-1}G = I$) and assume that the algebraic multiplicity of the Hurwitz matrix F is equal to its geometric multiplicity.

Next, based on Assumption 5.2.1, (5.65) can be rewritten as

$$\dot{x}(t) = A_r x(t) + B_r c(t) + B[u(t) + W^T x(t) - K_2 c(t)] + B[v(t) - u(t)]. \quad (5.68)$$

Based on the hedging approach [30, 31, 33], we now consider the (modified) reference model dynamics

$$\dot{x}_r = A_r x_r(t) + B_r c(t) + B[\hat{v}(t) - u(t)], \quad x_r(0) = x_{r0}, \quad (5.69)$$

where $\hat{v}(t) \in \mathbb{R}^m$ is an estimate of the actuator output satisfying the proposed observer dynamics of this paper given by

$$\hat{x}_c(t) = F\hat{x}_c(t) + Gu(t) + \frac{1}{\mu}S^{-1}H^T B^T P e(t), \quad \hat{x}_c(0) = \hat{x}_{c0}, \quad (5.70)$$

$$\hat{v}(t) = H\hat{x}_c(t), \quad (5.71)$$

with $\hat{x}_c(t) \in \mathbb{R}^p$ being the internal observer state vector and $\mu \in \mathbb{R}_+$. The system error dynamics then follow from the system dynamics given by (5.68) along with the adaptive control given by (5.59) and the reference model given by (5.69) as

$$\dot{e}(t) = A_r e(t) - B\tilde{W}^T(t)x(t) + B\tilde{v}(t), \quad e(0) = e_0. \quad (5.72)$$

where $\tilde{v}(t) \triangleq v(t) - \hat{v}(t) = H\tilde{x}_c(t) \in \mathbb{R}^m$ with $\tilde{x}_c(t) \triangleq x_c(t) - \hat{x}_c(t) \in \mathbb{R}^p$.

The following lemma is needed for the results in this section. For this purpose, let $\bar{\omega} \in \mathbb{R}_+$ be such that $\hat{W}_{\max, i+(j-1)n} \leq \bar{\omega}$ for all $i = 1, \dots, n$ and $j = 1, \dots, m$ and let $\underline{k} \in \mathbb{R}_+$ be such that $\underline{k} \leq k$, where k scales the eigenvalues of \mathcal{G}_A . That is, let $F \triangleq kF_0$, $H \triangleq kH_0$, $G \triangleq G_0$.

Lemma 5.2.1 *There exists a set $\kappa_1 \triangleq \{\underline{k} : \underline{k} \leq k\} \cup \{\bar{\omega} : \hat{W}_{\max, i+(j-1)n} \leq \bar{\omega}, i = 1, \dots, n, j = 1, \dots, m\}$ such that if $(\underline{k}, \bar{\omega}) \in \kappa_1$, then*

$$\mathcal{A}(\hat{W}(t), \mathcal{G}_A) = \begin{bmatrix} A_r + B\hat{W}^T(t) & BH \\ -G\hat{W}^T(t) & F \end{bmatrix} \quad (5.73)$$

is quadratically stable.

Proof. We only provide a concise sketch of the proof here. In particular, the existence of \underline{k} follows from considering and analyzing the Lyapunov inequality given by $\mathcal{A}^T(\hat{W}(t), \mathcal{G}_A)\mathcal{P} + \mathcal{P}\mathcal{A}(\hat{W}(t), \mathcal{G}_A) < 0$, $\mathcal{P} = \mathcal{P}^T > 0$ (e.g., similar in spirit to the steps taken in the proof of Lemma 3.1 of [95]). In addition, the existence of $\bar{\omega}$ follows from the fact that (5.73) is Hurwitz when $\bar{\omega} = 0$ (owing to its upper triangular structure in this case with Hurwitz matrices A_r and F on the diagonals), and hence, there must exist $\bar{\omega}$ owing to the continuity on the variations in $0 < \hat{W}_{\max, i+(j-1)n} \leq \bar{\omega}$. ■

The next theorem now presents the main result of this paper.

Theorem 5.2.1 *Consider the uncertain dynamical system given by (5.65) subject to Assumption 5.2.1, the reference model given by (5.69), the actuator dynamics given by (5.66), the adaptive feedback control law*

given by (5.59) along with the update law (5.60), and the observer dynamics given by (5.70). If $(\underline{k}, \overline{\omega}) \in \kappa_1$, then the solution $(e(t), \tilde{W}(t), x_r(t), \tilde{x}_c(t))$ of the closed-loop dynamical system is bounded and

$$\lim_{t \rightarrow \infty} e(t) = 0, \quad (5.74)$$

$$\lim_{t \rightarrow \infty} \tilde{x}_c(t) = 0. \quad (5.75)$$

Proof. To show Lyapunov stability and guarantee boundedness of the system error state $e(t)$, the weight error $\tilde{W}(t)$, and the actuator estimate error $\tilde{x}_c(t)$, consider the Lyapunov function candidate $\mathcal{V}(e, \tilde{W}, \tilde{x}_c) = e^T P e + \gamma_1^{-1} \text{tr} \tilde{W}^T \tilde{W} + \mu \tilde{x}_c^T S \tilde{x}_c$. Note that $\mathcal{V}(0, 0, 0) = 0$ and $\mathcal{V}(e, \tilde{W}, \tilde{x}_c) > 0$ for all $(e, \tilde{W}, \tilde{x}_c) \neq (0, 0, 0)$. Differentiating $\mathcal{V}(e, \tilde{W}, \tilde{x}_c)$ yields $\dot{\mathcal{V}}(e(t), \tilde{W}(t), \tilde{x}_c(t)) \leq -e^T(t) R e(t) - \mu \tilde{x}_c^T(t) \tilde{x}_c(t) \leq 0$, which guarantees the Lyapunov stability, and hence, the boundedness of the solution $(e(t), \tilde{W}(t), \tilde{x}_c(t))$. The rest of the proof follows by writing the reference model (5.69) and the observer dynamics (5.70) subject to (5.59) as

$$\dot{x}_r(t) = A_r x_r(t) + B [H \hat{x}_c(t) + \hat{W}^T(t) e(t) + \hat{W}^T(t) x_r(t)], \quad (5.76)$$

$$\dot{\hat{x}}_c(t) = F \hat{x}_c(t) - G \hat{W}^T(t) x_r(t) - G \hat{W}^T(t) e(t) + G K_2 c(t) + \frac{1}{\mu} S^{-1} H^T B^T P e(t), \quad (5.77)$$

and then using similar steps to the proof of Theorem 3.1 in [95], and hence, is omitted. \blacksquare

We now utilize LMIs to satisfy the quadratic stability of (5.73) by following a similar procedure documented in our recent works (e.g., see [102]). For this purpose, let $\overline{W}_{i_1, \dots, i_l} \in \mathbb{R}^{n \times m}$ be defined as

$$\overline{W}_{i_1, \dots, i_l} = \begin{bmatrix} (-1)^{i_1} \hat{W}_{\max, 1} & (-1)^{i_1+n} \hat{W}_{\max, 1+n} & \dots & (-1)^{i_1+(m-1)n} \hat{W}_{\max, 1+(m-1)n} \\ (-1)^{i_2} \hat{W}_{\max, 2} & (-1)^{i_2+n} \hat{W}_{\max, 2+n} & \dots & (-1)^{i_2+(m-1)n} \hat{W}_{\max, 2+(m-1)n} \\ \vdots & \vdots & \ddots & \vdots \\ (-1)^{i_n} \hat{W}_{\max, n} & (-1)^{i_n} \hat{W}_{\max, 2n} & \dots & (-1)^{i_n} \hat{W}_{\max, mn} \end{bmatrix}, \quad (5.78)$$

where $i_l \in \{1, 2\}$, $l \in \{1, \dots, mn\}$, such that $\overline{W}_{i_1, \dots, i_l}$ represents the corners of the hypercube defining the maximum variation of $\hat{W}(t)$. Utilizing the results in [96, 97], if

$$\mathcal{A}_{i_1, \dots, i_l} = \begin{bmatrix} A_r + B \overline{W}_{i_1, \dots, i_l}^T & B H \\ -G \overline{W}_{i_1, \dots, i_l}^T & F \end{bmatrix}, \quad (5.79)$$

satisfies the matrix inequality

$$\mathcal{A}_{i_1, \dots, i_l}^T \mathcal{P} + \mathcal{P} \mathcal{A}_{i_1, \dots, i_l} < 0, \quad \mathcal{P} = \mathcal{P}^T > 0, \quad (5.80)$$

for all permutations of $\overline{W}_{i_1, \dots, i_l}$, then (5.73) is quadratically stable. Since it is readily shown that (5.73) is quadratically stable for large values of k , we can cast (5.80) as a convex optimization problem and solve it using LMIs.

Here, it is important to note that the quadratic stability condition in Lemma 5.2.1, which acts as a sufficient condition for Theorem 5.2.1 showing the closed-loop model reference adaptive control system stability in the presence of high-order actuator dynamics with unknown outputs, is identical to Assumption 3 in [104], which acts as a sufficient condition for the case when the high-order actuator outputs are assumed to be known. Therefore, an important conclusion of this paper is to relax our known actuator output assumption stated in [104] by utilizing the observer dynamics (5.70) and (5.71) to estimate the unknown actuator output. In particular, the LMI analysis highlighted above will result in the same feasible region of allowable actuator dynamics regardless of whether the actuator output is known or unknown, and hence, there is no loss in relaxing the known actuator output assumption of [104].

5.2.4 Illustrative Numerical Example

To illustrate our contribution presented in Section 5.2.3, we consider the second-order system given by

$$\dot{x}(t) = \begin{bmatrix} 0 & 1 \\ 1 & 1 \end{bmatrix} x(t) + \begin{bmatrix} 0 \\ 1 \end{bmatrix} v(t), \quad (5.81)$$

with zero initial conditions. Here, let $x_1(t)$ represent the angle in radians and $x_2(t)$ represent the angular rate of change in radians per second. For the high-order actuator dynamics, we consider a single channel second-order actuator for the control input

$$F = \begin{bmatrix} 0 & 1 \\ -\omega_n^2 & -2\zeta\omega_n \end{bmatrix}, \quad G = \begin{bmatrix} 0 \\ 1 \end{bmatrix}, \quad H = \begin{bmatrix} \omega_n^2 & 0 \end{bmatrix}. \quad (5.82)$$

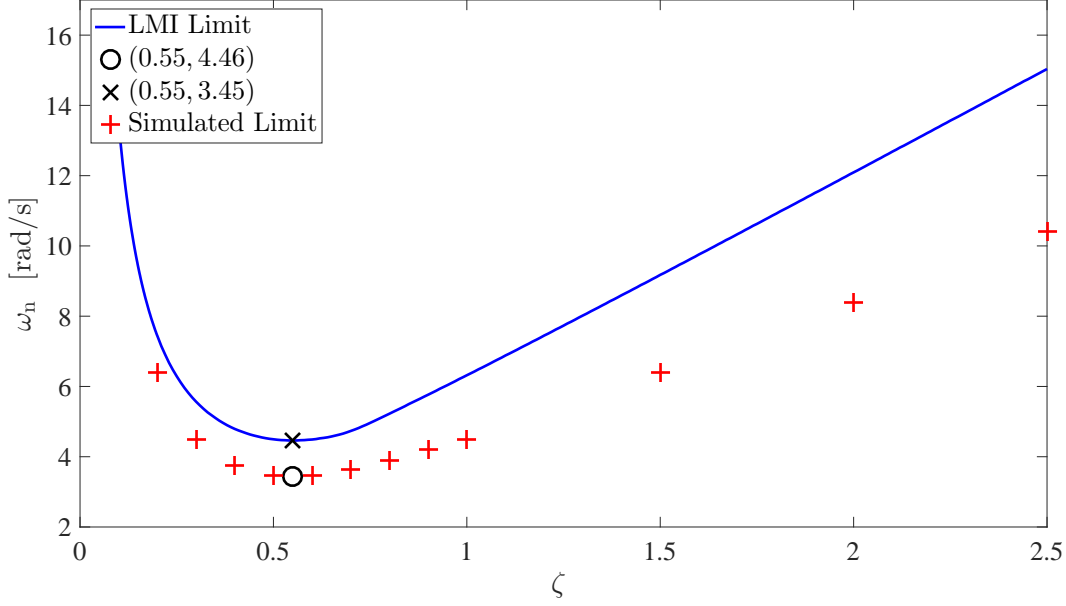


Figure 5.4: LMI calculated feasible region for actuator dynamics.

A reference model with zero initial conditions is selected with a natural frequency of $\omega_{nr} = 1.0$ rad/s and a damping ratio $\zeta_r = 0.7$, which yields

$$A_r = \begin{bmatrix} 0 & 1 \\ -1 & -1.4 \end{bmatrix}, \quad B_r = \begin{bmatrix} 0 \\ 1 \end{bmatrix}. \quad (5.83)$$

Furthermore, we use a filtered tracking command $c(t)$, set $R = I_2$ from (5.61) for the proposed adaptive controller design and set element-wise projection bounds such that $|\hat{W}(t)_{1,1}| \leq 2.1$ and $|\hat{W}(t)_{2,1}| \leq 2.5$.

Using the bounds on $\hat{W}(t)$ in the LMI analysis highlighted in Section 5.2.3, the feasible region of allowable actuator dynamics is calculated as depicted in Figure 5.4. Note that Figure 5.4 provides both the LMI calculated feasible limit as well as the feasible limit provided by the simulation results. Two points are selected to show the proposed controller performance in Figures 5.5 and 5.6. It can be seen in Figure 5.5 when the actuator dynamics are at the minimum point $(\zeta, \omega_n) = (0.55, 4.46)$, which is located on the feasible boundary, the system performances remain bounded as guaranteed by the presented theory. In Figure 5.6, we let the actuator dynamics be outside the calculated feasible region to show that the closed-loop system remains bounded until the actuator dynamics reach a value of $(\zeta, \omega_n) = (0.55, 3.45)$. This is consistent with the presented theory, as we provide an upper bound on the allowable actuator dynamics such that the closed-loop system remains bounded.

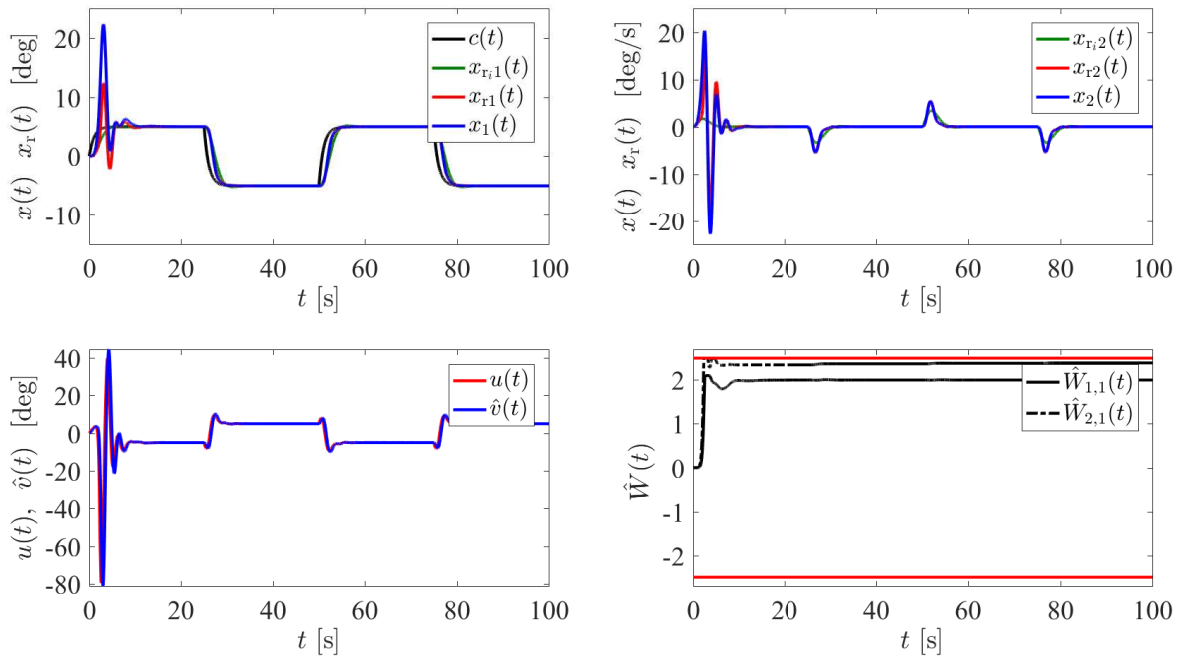


Figure 5.5: Proposed controller performance with actuator dynamics $((\zeta, \omega_n) = (0.55, 4.46))$, $\gamma_1 = 100$, $\mu = 1000$.

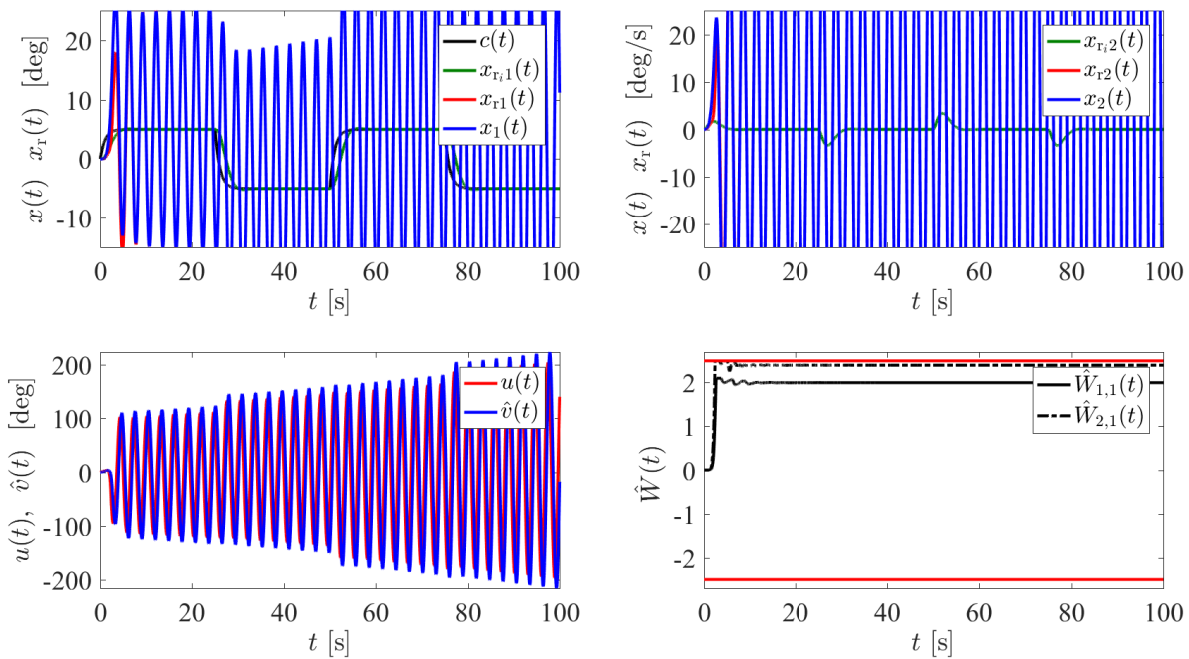


Figure 5.6: Proposed controller performance with actuator dynamics $((\zeta, \omega_n) = (0.55, 3.45))$, $\gamma_1 = 100$, $\mu = 1000$.

5.2.5 Conclusion

The purpose of this paper was to extend the recent work by the authors to the general case, where there exist high-order actuator dynamics with unknown outputs in the closed-loop model reference adaptive control systems. For this purpose, an observer architecture was proposed to provide an estimate of the unknown output of the actuator dynamics which was then used in the design of the linear matrix inequalities-based hedging framework. As a result, we were able to relax our previous known actuator output assumption while retaining the same stability condition. This in turn provides the same feasible region of allowable actuator dynamics regardless of whether the actuator output is known or unknown.

5.3 Model Reference Adaptive Control in the Presence of Actuator Dynamics with Applications to the Input Time-Delay Problem³

For computing stability limits of model reference adaptive controllers in the presence of actuator dynamics, a linear matrix inequalities-based hedging approach was recently proposed by the authors. In this paper, this approach is generalized to a general class of high-order linear time-invariant actuator dynamics with throughput term and stability of the closed-loop dynamical system is shown. As a byproduct, the proposed generalization allows the presented linear matrix inequalities-based hedging approach to be applied to the input time-delay problem through a finite-order Padé approximation. Two illustrative numerical examples are included to demonstrate the efficacy of the proposed approach.

5.3.1 Introduction

Although adaptive control theory is an effective methodology to suppress the effect of a wide class of system uncertainties, it is well known that the presence of actuator dynamics can seriously limit their stability properties. Motivated from this fact, we proposed a linear matrix inequalities-based hedging approach in a recent series of papers [95, 102–104] for computing stability limits of model reference adaptive controllers in the presence of actuator dynamics. Specifically, the hedging method modifies the ideal reference dynamics in order to allow correct adaptation that is not affected by the presence of actuator dynamics. Specifically, the stability of the closed-loop dynamical system was shown using Lyapunov theory and linear matrix inequalities were utilized to compute minimum allowable actuator bandwidth limits.

³This section is previously published in [114]. Permission is included in Appendix B.

The contribution of this paper is to generalize the linear matrix inequalities-based hedging approach to a general class of high-order linear time-invariant actuator dynamics with throughput term and show the stability of the closed-loop dynamical system. As a byproduct, the proposed generalization allows the approach to be applied to the input time-delay problem through a finite-order Padé approximation. Two illustrative numerical examples are included to demonstrate the efficacy of the proposed approach.

The notation used throughout this paper is standard. Specifically, \mathbb{R} denotes the set of real numbers, \mathbb{R}^n denotes the set of $n \times 1$ real column vectors, $\mathbb{R}^{n \times m}$ denotes the set of $n \times m$ real matrices, \mathbb{R}_+ (resp. $\overline{\mathbb{R}}_+$) denotes the set of positive (resp., nonnegative) real numbers, $\mathbb{R}_+^{n \times n}$ (resp., $\overline{\mathbb{R}}_+^{n \times n}$) denotes the set of $n \times n$ positive-definite (resp. nonnegative-definite) real matrices, $\mathbb{D}^{n \times n}$ denotes the set of $n \times n$ real matrices with diagonal scalar entries, $(\cdot)^T$ denotes the transpose operator, $(\cdot)^{-1}$ denotes the inverse operator, $\text{tr}(\cdot)$ denotes the trace operator, $\|\cdot\|_2$ denotes the Euclidian norm, $\|\cdot\|_F$ denotes the Frobenius matrix norm, $[A]_{ij}$ denotes the ij -th entry of the real matrix $A \in \mathbb{R}^{n \times m}$, $\lambda_{\min}(A)$ (resp., $\lambda_{\max}(A)$) denotes the minimum (resp., maximum) eigenvalue of the real matrix $A \in \mathbb{R}^{n \times n}$, and “ \triangleq ” denotes the equality by definition.

5.3.2 Mathematical Preliminaries

We now introduce the necessary mathematical preliminaries that are needed to develop the main results of this paper, beginning with the following definition.

Definition 5.3.1 For a convex hypercube in \mathbb{R}^n defined by $\Omega = \{\theta \in \mathbb{R}^n : (\theta_i^{\min} \leq \theta_i \leq \theta_i^{\max})_{i=1,2,\dots,n}\}$ where $(\theta_i^{\min}, \theta_i^{\max})$ represent the minimum and maximum bounds for the i^{th} component of the n -dimensional parameter vector θ . Additionally, for a sufficiently small positive constant ε , a second hypercube is defined by $\Omega_\varepsilon = \{\theta \in \mathbb{R}^n : (\theta_i^{\min} + \varepsilon \leq \theta_i \leq \theta_i^{\max} - \varepsilon)_{i=1,2,\dots,n}\}$ where $\Omega_\varepsilon \subset \Omega$. Then, the projection operator $\text{Proj} : \mathbb{R}^n \times \mathbb{R}^n \rightarrow \mathbb{R}^n$ is defined component-wise by

$$\text{Proj}(\theta, y) \triangleq \begin{cases} \left(\frac{\theta_i^{\max} - \theta_i}{\varepsilon}\right) y_i, & \text{if } \theta_i > \theta_i^{\max} - \varepsilon \text{ and } y_i > 0 \\ \left(\frac{\theta_i - \theta_i^{\min}}{\varepsilon}\right) y_i, & \text{if } \theta_i < \theta_i^{\min} + \varepsilon \text{ and } y_i < 0 \\ y_i, & \text{otherwise} \end{cases} \quad (5.84)$$

where $y \in \mathbb{R}^n$ [6].

It follows from Definition 5.3.1 that

$$(\theta - \theta^*)^T(\text{Proj}(\theta, y) - y) \leq 0, \quad \theta^* \in \Omega_\varepsilon, \quad (5.85)$$

holds [6, 82].

Note here that we use a generalization of this definition to matrices as

$$\text{Proj}_m(\Theta, Y) = (\text{Proj}(\text{col}_1(\Theta), \text{col}_1(Y)), \dots, \text{Proj}(\text{col}_m(\Theta), \text{col}_m(Y))), \quad (5.86)$$

where $\Theta \in \mathbb{R}^{n \times m}$, $Y \in \mathbb{R}^{n \times m}$, and $\text{col}_i(\cdot)$ denotes the i -th column operator. In this case, for a given Θ^* , it follows from (5.85) that

$$\text{tr} \left[(\Theta - \Theta^*)^T (\text{Proj}_m(\Theta, Y) - Y) \right] = \sum_{i=1}^m \left[\text{col}_i(\Theta - \Theta^*)^T (\text{Proj}(\text{col}_i(\Theta), \text{col}_i(Y)) - \text{col}_i(Y)) \right] \leq 0, \quad (5.87)$$

holds.

We now briefly overview the standard model reference control problem [5–7]. Specifically, consider the uncertain dynamical system given by

$$\dot{x}(t) = Ax(t) + Bu(t), \quad x(0) = x_0, \quad (5.88)$$

where $x(t) \in \mathbb{R}^n$ is the state vector available for feedback, $u(t) \in \mathbb{R}^m$ is the control input restricted to the class of admissible controls consisting of measurable functions, $A \in \mathbb{R}^{n \times n}$ is an unknown system matrix, $B \in \mathbb{R}^{n \times m}$ is a known input matrix, and the pair (A, B) is controllable.

Next, consider the reference model capturing a desired, ideal closed-loop dynamical system performance given by

$$\dot{x}_r(t) = A_r x_r(t) + B_r c(t), \quad x_r(0) = x_{r0}, \quad (5.89)$$

where $x_r(t) \in \mathbb{R}^n$ is the reference state vector, $c(t) \in \mathbb{R}^m$ is a given uniformly continuous bounded command, $A_r \in \mathbb{R}^{n \times n}$ is the Hurwitz reference model matrix, and $B_r \in \mathbb{R}^{n \times m}$ is the command input matrix. The objective

of the model reference adaptive control problem is to construct an adaptive feedback control law $u(t)$ such that the state vector $x(t)$ asymptotically follows the reference state vector $x_r(t)$.

It can be assumed, as is standard [5–7], that there exists an unknown matrix $K_1 \in \mathbb{R}^{m \times n}$ and a known matrix $K_2 \in \mathbb{R}^{m \times m}$ such that $A_r \triangleq A - BK_1$ and $B_r \triangleq BK_2$ hold. It follows that (5.88) can be written as

$$\dot{x}(t) = A_r x(t) + B_r c(t) + B[u(t) + W_1^T x(t) - K_2 c(t)], \quad (5.90)$$

where $W_1 \triangleq K_1^T \in \mathbb{R}^{n \times m}$ is unknown. Now, let the adaptive feedback control law be given by

$$u(t) = -\hat{W}_1^T(t)x(t) + K_2 c(t), \quad (5.91)$$

where $\hat{W}_1(t) \in \mathbb{R}^{n \times m}$ is the estimate of W_1 satisfying the weight update law

$$\dot{\hat{W}}_1(t) = \gamma_1 \text{Proj}_m[\hat{W}_1(t), x(t)e^T(t)PB], \quad \hat{W}_1(0) = \hat{W}_{10}, \quad (5.92)$$

with $\gamma_1 \in \mathbb{R}_+$ being the learning rate, $e(t) \triangleq x(t) - x_r(t)$ being the system error state vector, and $P \in \mathbb{R}_+^{n \times n}$ being the solution of the Lyapunov equation given by

$$0 = A_r^T P + P A_r + R, \quad (5.93)$$

$R \in \mathbb{R}_+^{n \times n}$. Note that since A_r is Hurwitz, it follows from the converse Lyapunov theory [80] that there exists a unique P satisfying (5.93) for a given R . In addition, the projection bounds are defined such that

$$|[\hat{W}_1(t)]_{ij}| \leq \hat{W}_{1, \max, i+(j-1)n}, \quad (5.94)$$

for $i = 1, \dots, n$ and $j = 1, \dots, m$, where $\hat{W}_{1, \max, i+(j-1)n} \in \mathbb{R}_+$ denotes element-wise projection bounds.

Now, using (5.91) in (5.90) along with (5.89), the system error dynamics can be written as

$$\dot{e}(t) = A_r e(t) - B\tilde{W}_1^T(t)x(t), \quad e(0) = e_0, \quad (5.95)$$

where $\tilde{W}_1(t) \triangleq \hat{W}_1(t) - W_1 \in \mathbb{R}^{n \times m}$.

The weight update law given by (5.92) can be derived using Lyapunov analysis by considering the Lyapunov function candidate given by (see, for example, [5–7])

$$\mathcal{V}(e, \tilde{W}_1) = e^T P e + \gamma_1^{-1} \text{tr} \tilde{W}_1^T \tilde{W}_1. \quad (5.96)$$

Note that $\mathcal{V}(0, 0) = 0$ and $\mathcal{V}(e, \tilde{W}_1) > 0$ for all $(e, \tilde{W}_1) \neq (0, 0)$. Now, differentiating (5.96) yields $\dot{\mathcal{V}}(e(t), \tilde{W}_1(t)) \leq -e^T(t) R e(t) \leq 0$, which guarantees that the system error state vector $e(t)$ and the weight error $\tilde{W}_1(t)$ are Lyapunov stable, and hence, are bounded for all $t \in \bar{\mathbb{R}}_+$. Since $x(t)$ is bounded for all $t \in \bar{\mathbb{R}}_+$, it follows from (5.95) that $\dot{e}(t)$ is bounded, and hence, $\ddot{\mathcal{V}}(e(t), \tilde{W}_1(t))$ is bounded for all $t \in \bar{\mathbb{R}}_+$. It then follows from Barbalat's lemma that $\lim_{t \rightarrow \infty} \dot{\mathcal{V}}(e(t), \tilde{W}_1(t)) = 0$, which consequently shows that $e(t) \rightarrow 0$ as $t \rightarrow \infty$.

Note that this highlights that the adaptive control formulation overviewed in this section has the capability to suppress the effect of system uncertainties to achieve desirable tracking performance specifications. Yet, it does not provide any guarantees in the presence actuator dynamics that appear in any practical application of adaptive controllers.

5.3.3 Adaptive Control in the Presence of High-Order Linear Time-Invariant Actuator Dynamics with Throughput Term

For the model reference adaptive control design in the presence of high-order linear time-invariant actuator dynamics with throughput term, we now generalize the linear matrix inequalities-based hedging approach of [95, 102–104]. Specifically, consider the uncertain dynamical system given by

$$\dot{x}(t) = Ax(t) + Bv(t), \quad x(0) = x_0, \quad (5.97)$$

where $v(t) \in \mathbb{R}^m$ is the actuator output of the actuator dynamics \mathcal{G}_A given by

$$\begin{aligned} \dot{x}_c(t) &= Fx_c(t) + Gu(t), \quad x_c(0) = x_{c0}, \\ v(t) &= Hx_c(t) + Ju(t), \end{aligned} \quad (5.98)$$

with $x_c(t) \in \mathbb{R}^l$ being the actuator state vector, $G \in \mathbb{R}^{l \times m}$ being the actuator input matrix, $H \in \mathbb{R}^{m \times l}$ being the actuator output matrix, $F \in \mathbb{R}^{l \times l}$ being a Hurwitz matrix, and $J \in \mathbb{R}^{m \times m}$ being the throughput matrix.

By adding and subtracting $Bu(t)$, (5.97) can be rewritten as

$$\dot{x}(t) = A_r x(t) + B_r c(t) + B[u(t) + W_1^T(t)x(t) - K_2 c(t)] + B[v(t) - u(t)]. \quad (5.99)$$

Now, based on the novel hedging approach originally proposed in [30, 31, 33], we consider the modified reference model dynamics given by

$$\dot{x}_r = A_r x_r(t) + B_r c(t) + B[v(t) - u(t)], \quad x_r(0) = x_{r0}, \quad (5.100)$$

such that with the adaptive feedback control law given by (5.91) and (5.92), the system error dynamics follows from (5.99) and (5.100) as

$$\dot{e}(t) = A_r e(t) - B\tilde{W}_1^T(t)x(t), \quad e(0) = e_0. \quad (5.101)$$

Note that (5.101) is identical to the system error dynamics given by (5.95) due to the fact that the hedging signal $B[v(t) - u(t)]$ is introduced to the ideal reference model dynamics. The next theorem establishes the stability of the closed-loop dynamical system as well as the boundedness of the modified reference model dynamics predicated on linear matrix inequalities.

Theorem 5.3.1 *Consider the uncertain dynamical system given by (5.97), the reference model given by (5.100), the actuator dynamics given by (5.98), and the adaptive feedback control law given by (5.91) along with the update law (5.92). In addition, let*

$$A(\hat{W}_1(t), \mathcal{G}_A) = \begin{bmatrix} A_r + B\hat{W}_1^T(t) - BJ\hat{W}_1^T(t) & BH \\ -G\hat{W}_1^T(t) & F \end{bmatrix}, \quad (5.102)$$

be quadratically stable. Then, the solution $(e(t), \tilde{W}_1(t), x_r(t), v(t))$ of the closed-loop dynamical system is bounded and $\lim_{t \rightarrow \infty} e(t) = 0$.

Proof. To show Lyapunov stability and guarantee boundedness of the system error state $e(t)$ and the weight error $\tilde{W}_1(t)$, consider the Lyapunov function candidate given by (5.96). Differentiating (5.96) yields $\dot{V}(e(t), \tilde{W}_1(t)) \leq -e^T(t)Re(t) \leq 0$, which guarantees the Lyapunov stability, and hence, the boundedness of the solution $(e(t), \tilde{W}_1(t))$.

To show the boundedness of $x_r(t)$ and $x_c(t)$ (and hence, $v(t)$), consider the reference model (5.100) and the actuator dynamics (5.98) subject to (5.91) as

$$\begin{aligned}\dot{x}_r(t) &= A_r x_r(t) + B_r c(t) + B [H x_c(t) + (I - J) (\hat{W}_1^T(t) x(t) - K_2 c(t))] \\ &= (A_r + B(I - J) \hat{W}_1^T(t)) x_r(t) + B H x_c(t) + B(I - J) \hat{W}_1^T(t) e(t) + B J K_2 c(t),\end{aligned}\quad (5.103)$$

$$\dot{x}_c(t) = F x_c(t) - G \hat{W}_1^T(t) x_r(t) - G \hat{W}_1^T(t) e(t) + G K_2 c(t),\quad (5.104)$$

where (5.103) and (5.104) can be rewritten in compact form as

$$\dot{\xi}(t) = \mathcal{A}(\hat{W}_1(t), \mathcal{G}_A) \xi(t) + \omega(\cdot),\quad (5.105)$$

with $\xi(t) = [x_r^T(t), x_c^T(t)]^T$ and

$$\omega(\cdot) = \begin{bmatrix} B(I - J) \hat{W}_1^T(t) e(t) + B J K_2 c(t) \\ -G \hat{W}_1^T(t) e(t) + G K_2 c(t) \end{bmatrix}.\quad (5.106)$$

Note that $\omega(\cdot)$ in (5.105) is a bounded perturbation as a result of Lyapunov stability of the pair $(e(t), \tilde{W}_1(t))$. Now, it follows that since $\omega(\cdot)$ is bounded and $\mathcal{A}(\hat{W}_1(t), \mathcal{G}_A)$ is quadratically stable, then $x_r(t)$ and $x_c(t)$ are also bounded [88]. This further implies that the actuator output $v(t)$ is bounded.

To show $\lim_{t \rightarrow \infty} e(t) = 0$, note that $x(t)$ is bounded as a consequence of the boundedness of $e(t)$ and $x_r(t)$. It now follows from (5.101) that $\dot{e}(t)$ is bounded, and hence, $\ddot{\mathcal{V}}(e(t), \tilde{W}_1(t))$ is bounded. As a consequence of the boundedness of $\ddot{\mathcal{V}}(e(t), \tilde{W}_1(t))$ and Barbalat's lemma [88], $\lim_{t \rightarrow \infty} \dot{\mathcal{V}}(e(t), \tilde{W}_1(t)) = 0$, and hence, $\lim_{t \rightarrow \infty} e(t) = 0$. ■

We now utilize linear matrix inequalities to satisfy the quadratic stability of (5.102) by following a similar procedure documented in our recent works [95, 102–104]. For this purpose, let $\bar{W}_{1_{i_1, \dots, i_l}} \in \mathbb{R}^{n \times m}$ be defined as

$$\bar{W}_{1_{i_1, \dots, i_l}} = \begin{bmatrix} (-1)^{i_1} \hat{W}_{1, \max, 1} & (-1)^{i_1+n} \hat{W}_{1, \max, 1+n} & \dots & (-1)^{i_1+(m-1)n} \hat{W}_{1, \max, 1+(m-1)n} \\ (-1)^{i_2} \hat{W}_{1, \max, 2} & (-1)^{i_2+n} \hat{W}_{1, \max, 2+n} & \dots & (-1)^{i_2+(m-1)n} \hat{W}_{1, \max, 2+(m-1)n} \\ \vdots & \vdots & \ddots & \vdots \\ (-1)^{i_n} \hat{W}_{1, \max, n} & (-1)^{i_n} \hat{W}_{1, \max, 2n} & \dots & (-1)^{i_n m} \hat{W}_{1, \max, mn} \end{bmatrix},\quad (5.107)$$

where $i_l \in \{1, 2\}$, $l \in \{1, \dots, 2^m\}$, such that $\bar{W}_{1_{i_1, \dots, i_l}}$ represents the corners of the hypercube defining the maximum variation of $\hat{W}_1(t)$. Utilizing the results in [96, 97], if

$$\mathcal{A}_{i_1, \dots, i_l} = \begin{bmatrix} A_r + B\bar{W}_{1_{i_1, \dots, i_l}}^T & -BJ\bar{W}_{1_{i_1, \dots, i_l}}^T & BH \\ & -G\bar{W}_{1_{i_1, \dots, i_l}}^T & F \end{bmatrix}, \quad (5.108)$$

satisfies the matrix inequality

$$\mathcal{A}_{i_1, \dots, i_l}^T \mathcal{P} + \mathcal{P} \mathcal{A}_{i_1, \dots, i_l} < 0, \quad \mathcal{P} = \mathcal{P}^T > 0, \quad (5.109)$$

for all permutations of $\bar{W}_{1_{i_1, \dots, i_l}}$, then (5.102) is quadratically stable. We can then cast (5.109) as a convex optimization problem and solve it effectively using linear matrix inequalities.

5.3.4 Illustrative Numerical Examples

In order to illustrate the proposed linear matrix inequalities-based hedging approach to adaptive control, we consider an application to the input time-delay problem, where for the following dynamical system given by

$$\dot{x}(t) = Ax(t) + Bu(t - \tau), \quad x(0) = x_0, \quad (5.110)$$

is considered. Note that (5.110) can be approximated in the form given by (5.97) and (5.98) using the Padé approximation for $u(t - \tau)$ term. To this end, consider the following examples.

For the first example, we consider the scalar example presented in [115] given by

$$\dot{p}(t) = L_p p(t) + L_{\delta_a} \delta_a(t), \quad (5.111)$$

which represents the roll dynamics with $p(t)$ being the roll rate in radians per second, $\delta_a(t)$ being the total differential aileron-spoiler deflection in radians, L_p being an unknown roll damping derivative, and L_{δ_a} being a known dimensional rolling moment derivative.

As in [115], we set $L_p = -0.8(\text{s}^{-1})$ and $L_{\delta_a} = 1.6(\text{s}^{-1})$ and let the reference model be

$$\dot{p}_r(t) = -2p_r(t) + 2p_{cmd}(t). \quad (5.112)$$

In addition, the projection bounds are chosen as in [115] such that $|\hat{W}_1(t)| \leq 2.7$. In the context of standard model reference adaptive control design, the maximum allowable time-delay is calculated to be $\tau^* = 0.024(s)$ in [115], where the actual time-delay is determined numerically to be around $0.38(s)$ [116]. Using the proposed linear matrix inequalities-based hedging approach of Section 5.3.3, the linear matrix inequality calculations are carried out up to the fifth order Padé approximation as shown in Figure 5.7. It can be seen from the figure that our results are much less conservative. As the order of the Padé is increased, our time-delay margin converges to $\tau^* = 0.269(s)$.

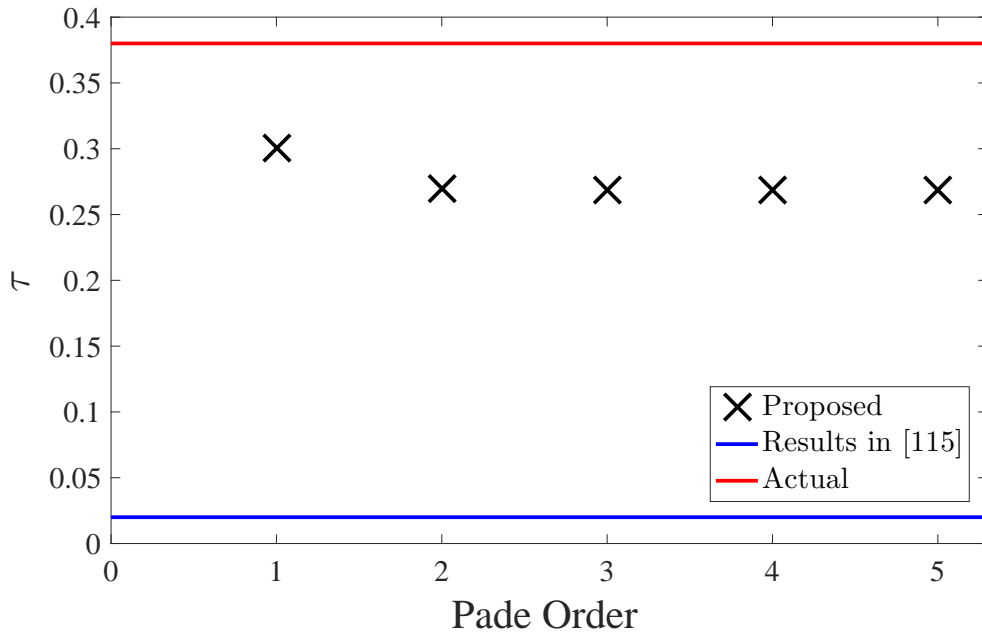


Figure 5.7: Comparison of the maximum allowable input time-delay between proposed approach of this paper and the results in [115].

For the second example, we now consider a second order dynamical system given by

$$\dot{x}(t) = \begin{bmatrix} 0 & 1 \\ 1 & 1 \end{bmatrix} x(t) + \begin{bmatrix} 0 \\ 1 \end{bmatrix} u(t - \tau), \quad x(0) = x_0. \quad (5.113)$$

We select a reference model with a natural frequency of $\omega_n = 1.0$ rad/s and a damping ratio $\zeta = 0.7$ such that

$$A_r = \begin{bmatrix} 0 & 1 \\ -1 & -1.4 \end{bmatrix}, \quad B_r = \begin{bmatrix} 0 \\ 1 \end{bmatrix}, \quad (5.114)$$

hold. Using the rectangular projection operator, the bounds on the uncertainty are set element-wise such that $|\hat{W}_1(t)_{1,1}| \leq 2.1$ and $|\hat{W}_1(t)_{2,1}| \leq 2.5$. Then using the proposed linear matrix inequalities-based hedging approach, the linear matrix inequality calculations are carried out up to the fifth order Padé approximation as shown in Figure 5.8. It can be seen from the figure that as the order of the Padé is increased, our time-delay margin converges to $\tau^* = 0.3(s)$.

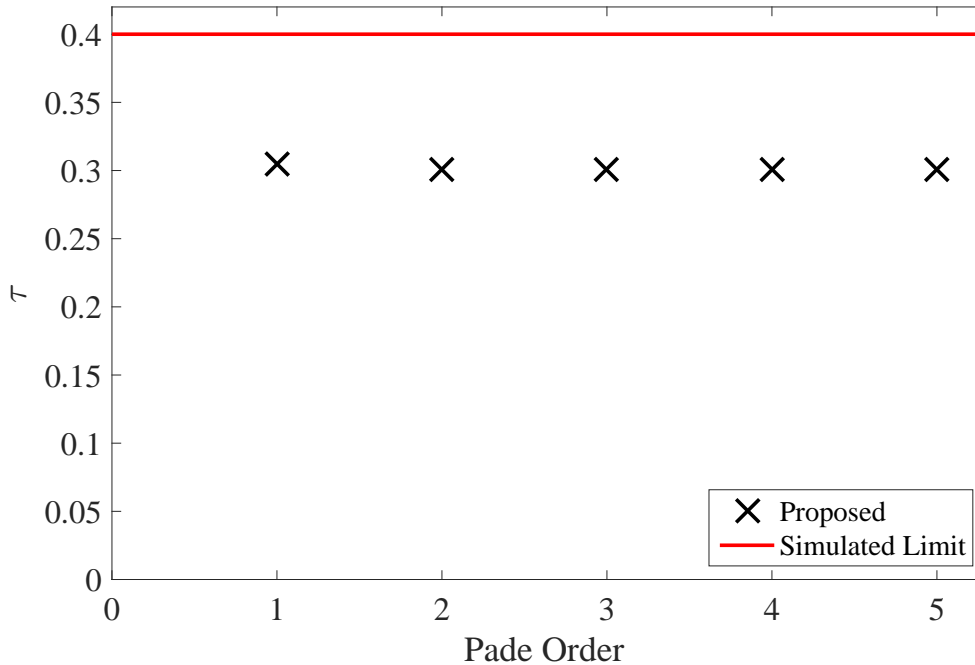


Figure 5.8: Linear matrix inequality calculated maximum allowable input time-delay.

Figures 5.9 and 5.10 show the the proposed controller performance with input time-delay. Since it is calculated that the allowable maximum time-delay margin is $\tau^* = 0.3(s)$, it is theoretically expected that the system performances are guaranteed to be bounded for time-delay values less than or equal to the calculated maximum. Figures 5.9 and 5.10 illustrate this statement, in which Figure 5.9 shows the system performance is bounded for the linear matrix inequality calculated maximum time-delay margin of $\tau^* = 0.3(s)$, and remains bounded until a time-delay value of $\tau^* = 0.4(s)$ is applied in Figure 5.10.

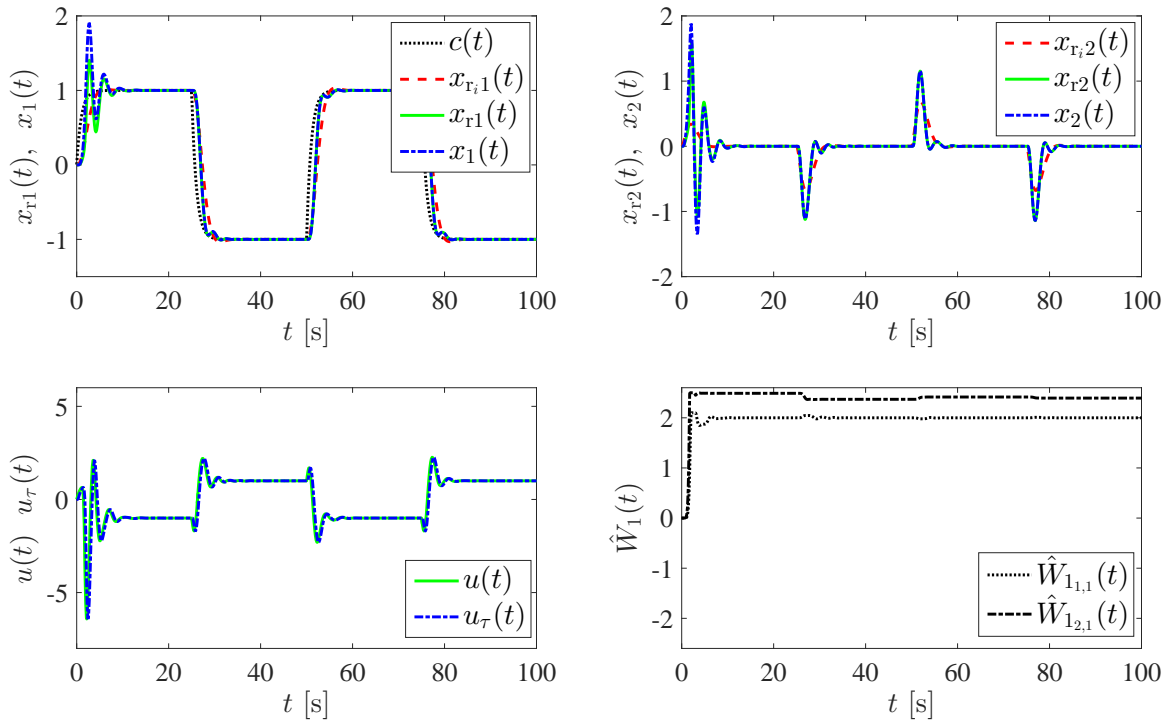


Figure 5.9: Proposed controller performance with input time-delay ($\tau^* = 0.3$ (s), $\gamma = 10$).

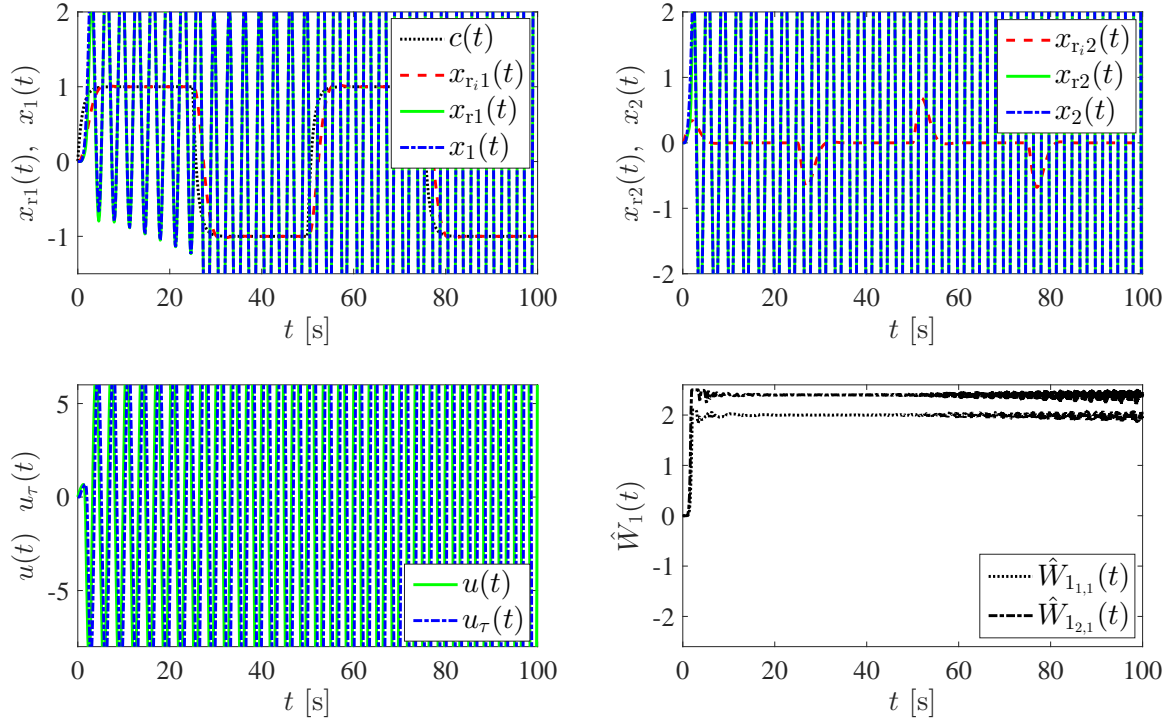


Figure 5.10: Proposed controller performance with input time-delay ($\tau^* = 0.4$ (s), $\gamma = 10$).

5.3.5 Conclusion

We generalized the linear matrix inequalities-based hedging approach of [95, 102–104] to a general class of high-order linear time-invariant actuator dynamics with throughput term and showed the stability of the closed-loop dynamical system. Through a finite-order Padé approximation, the proposed generalized allowed the presented approach to be applied to the input time-delay problem. The efficacy of the proposed approach was demonstrated through two different illustrative numerical examples.

5.4 Computing the Stability Limits of Pole-Zero Actuator Dynamics on Adaptive Control Laws for Aerospace Applications⁴

This paper illustrates an application of a linear matrix inequality-based hedging approach for model reference adaptive control in the presence of pole-zero actuator dynamics. Specifically, this approach uses a hedging signal to alter a given reference model trajectory such that adaptation is not effected by the presence of actuator dynamics, then it uses linear matrix inequalities (LMIs) to compute the stability limits of the adaptive control law as a result of the hedged reference model. In order to demonstrate the capability of the proposed approach in providing safe and predictable limits, multiple cases of pole-zero actuator dynamics are considered on the short-period dynamics of a hypersonic vehicle model, where a feasible region of safe actuation is computed for each pole-zero configuration.

5.4.1 Introduction

Stability limits of adaptive controllers in the presence of actuator dynamics is a well-known problem. In recent papers by the authors [95, 101–105, 114, 118], a new approach has been proposed using a hedged reference model and linear matrix inequalities (LMIs) to compute stability limits of adaptive controllers. In particular, we have considered a wide range of generalizations of the proposed framework, including the cases known and unknown control input, known and unknown actuator output, linear and nonlinear uncertainties, and first-order and high-order actuator dynamics. In our most recent work [118], an application to a hypersonic vehicle model is also included for first-order actuator models.

While it is possible to represent actuator models as first order dynamics using different assumptions and a reduction of order, more accurate actuator models for aerospace applications are better represented by higher order dynamics, often with a zero and multiple (usually two or three) poles. The differences between

⁴This section is previously published in [117]. The copyright is owned by the author (see Appendix B).

these models can drastically effect the closed-loop stability. Motivated from this standpoint, the purpose of this paper is to demonstrate the capability of the proposed LMI-based hedging approach to provide safe and predictable limits for a few relevant actuator models with a zero and multiple poles, as well as different control effectiveness by means of the static gain of the actuator model. Specifically, we consider multiple cases of pole-zero actuator dynamics for the short-period dynamics of a hypersonic vehicle model, where a feasible region of safe actuation is computed for each pole-zero configuration.

The notation used in this paper is fairly standard and similar to, for example, [95]. For self-containedness, note that \mathbb{R} denotes the set of real numbers, \mathbb{R}^n denotes the set of $n \times 1$ real column vectors, $\mathbb{R}^{n \times m}$ denotes the set of $n \times m$ real matrices, \mathbb{R}_+ (respectiely, $\overline{\mathbb{R}}_+$) denotes the set of positive (respectively, nonnegative) real numbers, $\mathbb{R}_+^{n \times n}$ (respectively, $\overline{\mathbb{R}}_+^{n \times n}$) denotes the set of $n \times n$ positive-definite (respectively, nonnegative-definite) real matrices, and “ \triangleq ” denotes equality by definition. In addition, we write $(\cdot)^T$ for the transpose operator and $(\cdot)^{-1}$ for the inverse operator.

5.4.2 The LMI-Based Hedging Approach for Adaptive Control: A Concise Overview

5.4.2.1 Uncertain Dynamical System with Actuator Dynamics

We now present a concise overview of the LMI-based hedging approach in the presence of actuator dynamics, where we refer to [95, 101–105, 114, 118] for details. Specifically, here we consider the uncertain dynamical system given by

$$\dot{x}_p(t) = A_p x_p(t) + B_p [v(t) + W^T x_p(t)], \quad x_p(0) = x_{p0}, \quad (5.115)$$

where $x_p(t) \in \mathbb{R}^{n_p}$ is a measurable state, $A_p \in \mathbb{R}^{n_p \times n_p}$ and $B_p \in \mathbb{R}^{n_p \times m}$ are known system matrices (with the pair (A_p, B_p) assumed to be controllable), $W \in \mathbb{R}^{n_p \times m}$ is an unknown weight matrix, and $v(t) \in \mathbb{R}^m$ is an actuator output of the actuator dynamics \mathcal{G}_A given by

$$\dot{x}_a(t) = F x_a(t) + G u(t), \quad x_a(0) = x_{a0}, \quad (5.116)$$

$$v(t) = H x_a(t), \quad (5.117)$$

with $x_a(t) \in \mathbb{R}^p$ being the actuator state vector, $G \in \mathbb{R}^{p \times m}$ being the actuator input matrix, $H \in \mathbb{R}^{m \times p}$ being the actuator output matrix, and $F \in \mathbb{R}^{p \times p}$ being a Hurwitz matrix such that there exists $S \in \mathbb{R}_+^{p \times p}$ that satisfies

$$0 = F^T S + S F + I. \quad (5.118)$$

5.4.2.2 Adaptive Control for Command Following

To address command following, let $c(t) \in \mathbb{R}^{n_c}$ be a given piecewise continuous reference command and $x_c(t) \in \mathbb{R}^{n_c}$ be the integrator state satisfying

$$\dot{x}_c(t) = E_p x_p(t) - c(t), \quad x_c(0) = x_{c0}. \quad (5.119)$$

Here, $E_p \in \mathbb{R}^{n_c \times n_p}$ allows the selection of a subset of $x_p(t)$ to follow $c(t)$. Considering (5.115) and (5.119), the augmented dynamics can be written as

$$\dot{x}(t) = \underbrace{\begin{bmatrix} A_p & 0_{n_p \times n_c} \\ E_p & 0_{n_c \times n_c} \end{bmatrix}}_A x(t) + \underbrace{\begin{bmatrix} B_p \\ 0_{n_c \times m} \end{bmatrix}}_B [v(t) + W^T x_p(t)] + \underbrace{\begin{bmatrix} 0_{n_p \times n_c} \\ -I_{n_c \times n_c} \end{bmatrix}}_{B_r} c(t), \quad x(0) = x_0, \quad (5.120)$$

where $x(t) \triangleq [x_p^T(t), x_c^T(t)]^T \in \mathbb{R}^n$, $A \in \mathbb{R}^{n \times n}$, $B \in \mathbb{R}^{n \times m}$, $B_r \in \mathbb{R}^{n \times n_c}$, and $n = n_p + n_c$. It follows by adding and subtracting $Bu(t)$ that (5.120) can be written as

$$\dot{x}(t) = Ax(t) + B_r c(t) + B[u(t) + W^T x_p(t)] + B[v(t) - u(t)]. \quad (5.121)$$

Next, let the feedback control law be given by

$$u(t) = -Kx(t) - \hat{W}^T(t)x_p(t), \quad (5.122)$$

where $K \in \mathbb{R}^{m \times n}$ is the nominal feedback gain designed such that $A_r \triangleq A - BK \in \mathbb{R}^{n \times n}$ is Hurwitz and $\hat{W}(t) \in \mathbb{R}^{n_p \times m}$ is an estimate of W satisfying the weight update law

$$\dot{\hat{W}}(t) = \gamma \text{Proj}_m [\hat{W}(t), x_p(t)e^T(t)PB], \quad \hat{W}(0) = \hat{W}_0, \quad (5.123)$$

with $\gamma \in \mathbb{R}_+$ being the learning rate, $e(t) \triangleq x(t) - x_r(t)$ being the system error state vector ($x_r(t)$ is the state vector of the reference model which will be provided shortly), and $P \in \mathbb{R}_+^{n \times n}$ being the solution of the Lyapunov equation given by

$$0 = A_r^T P + P A_r + R, \quad R \in \mathbb{R}_+^{n \times n}. \quad (5.124)$$

In (5.123), the projection operator is used, and hence, we need its definition [6].

Definition 5.4.1 Let $\Omega = \{\theta \in \mathbb{R}^n : (\theta_i^{\min} \leq \theta_i \leq \theta_i^{\max})_{i=1,2,\dots,n}\}$ be a convex hypercube in \mathbb{R}^n , where $(\theta_i^{\min}, \theta_i^{\max})$ represent the minimum and maximum bounds for the i^{th} component of the n -dimensional parameter vector θ . In addition, let $\Omega_\varepsilon = \{\theta \in \mathbb{R}^n : (\theta_i^{\min} + \varepsilon \leq \theta_i \leq \theta_i^{\max} - \varepsilon)_{i=1,2,\dots,n}\}$ be a second hypercube for a sufficiently small positive constant ε , where $\Omega_\varepsilon \subset \Omega$. With $y \in \mathbb{R}^n$, the projection operator $\text{Proj} : \mathbb{R}^n \times \mathbb{R}^n \rightarrow \mathbb{R}^n$ is then defined component-wise by

$$\text{Proj}(\theta, y) \triangleq \begin{cases} \left(\frac{\theta_i^{\max} - \theta_i}{\varepsilon}\right) y_i, & \text{if } \theta_i > \theta_i^{\max} - \varepsilon \text{ and } y_i > 0, \\ \left(\frac{\theta_i - \theta_i^{\min}}{\varepsilon}\right) y_i, & \text{if } \theta_i < \theta_i^{\min} + \varepsilon \text{ and } y_i < 0, \\ y_i, & \text{otherwise.} \end{cases} \quad (5.125)$$

In the light of Definition 5.4.1, it follows that $\text{Proj}(\theta - \theta^*)^T (\text{Proj}(\theta, y) - y) \leq 0$ (see [6, 82] for details). Note that this definition can also be generalized to matrices as $\text{Proj}_m(\Theta, Y) = (\text{Proj}(\text{col}_1(\Theta), \text{col}_1(Y)), \dots, \text{Proj}(\text{col}_m(\Theta), \text{col}_m(Y)))$, where $\Theta \in \mathbb{R}^{n \times m}$, $Y \in \mathbb{R}^{n \times m}$, and $\text{col}_i(\cdot)$ denotes i th column operator. In particular, for a given matrix Θ^* , it follows from $\text{Proj}(\theta - \theta^*)^T (\text{Proj}(\theta, y) - y) \leq 0$ that $[(\Theta - \Theta^*)^T (\text{Proj}_m(\Theta, Y) - Y)] = \sum_{i=1}^m [\text{col}_i(\Theta - \Theta^*)^T (\text{Proj}(\text{col}_i(\Theta), \text{col}_i(Y)) - \text{col}_i(Y))] \leq 0$. Now, with regard to (5.123), the projection bounds are defined such that $|\hat{W}(t)_{ij}| \leq \hat{W}_{\max, i+(j-1)n_p}$ for $i = 1, \dots, n_p$ and $j = 1, \dots, m$, where $\hat{W}_{\max, i+(j-1)n_p} \in \mathbb{R}_+$ denotes symmetric element-wise projection bounds.

Now, using (5.122) in (5.121), we can write

$$\dot{x}(t) = A_r x(t) + B_r c(t) - B \tilde{W}^T(t) x_p(t) + B[v(t) - u(t)], \quad (5.126)$$

where $\tilde{W}(t) \triangleq \hat{W}(t) - W \in \mathbb{R}^{n_p \times m}$ is the weight estimation error. Motivated by the structure of (5.126), we use the hedging approach [30, 31, 33] to design the modified reference model as

$$\dot{x}_r = A_r x_r(t) + B_r c(t) + B[v(t) - u(t)], \quad x_r(0) = x_{r0}, \quad (5.127)$$

where $x_r(t) \in \mathbb{R}^n$ is the reference state vector and $A_r \in \mathbb{R}^{n \times n}$ is the reference model matrix, such that the system error dynamics follow from (5.126) and (5.127) as

$$\dot{e}(t) = A_r e(t) - B \tilde{W}^T(t) x_p(t), \quad e(0) = e_0. \quad (5.128)$$

The following theorem (see the aforementioned papers above for proof details) presents the stability of the proposed adaptive control architecture in the presence of actuator dynamics. For this purpose, we note that $N = [I_{n_p \times n_p}, 0_{n_p \times n_c}] \in \mathbb{R}^{n_p \times n}$.

Theorem 5.4.1 Consider the uncertain dynamical system given by (5.115), the integrator dynamics given by (5.119), the actuator dynamics given by (5.116) and (5.117), the reference model given by (5.127), the feedback control law given by (5.122), and the update law given by (5.123). In addition, let

$$\mathcal{A}(\hat{W}(t), \mathcal{G}_A) = \begin{bmatrix} A + B\hat{W}^T(t)N & BH \\ -G(K + \hat{W}^T(t)N) & F \end{bmatrix} \quad (5.129)$$

be quadratically stable for all $\hat{W}(t)$ satisfying the projection based weight update law given by (5.123), then the solution $(e(t), \tilde{W}(t))$ of the closed-loop dynamical system is bounded and $\lim_{t \rightarrow \infty} e(t) = 0$.

5.4.2.3 Utilizing LMIs for Safe Adaptive Control

To satisfy the quadratic stability [97] condition in Theorem 5.4.1, we use LMIs for given projection bounds \hat{W}_{\max} on the elements of $\hat{W}(t)$. To elucidate this important point, let $\bar{W}_{i_1, \dots, i_l} \in \mathbb{R}^{n_p \times m}$ be defined as

$$\bar{W}_{i_1, \dots, i_l} = \begin{bmatrix} (-1)^{i_1} \hat{W}_{\max, 1} & (-1)^{i_1+n_p} \hat{W}_{\max, 1+n_p} & \dots & (-1)^{i_1+(m-1)n_p} \hat{W}_{\max, 1+(m-1)n_p} \\ (-1)^{i_2} \hat{W}_{\max, 2} & (-1)^{i_2+n_p} \hat{W}_{\max, 2+n_p} & \dots & (-1)^{i_2+(m-1)n_p} \hat{W}_{\max, 2+(m-1)n_p} \\ \vdots & \vdots & \ddots & \vdots \\ (-1)^{i_{n_p}} \hat{W}_{\max, n_p} & (-1)^{i_{2n_p}} \hat{W}_{\max, 2n_p} & \dots & (-1)^{i_{mn_p}} \hat{W}_{\max, mn_p} \end{bmatrix}, \quad (5.130)$$

where $i_l \in \{1, 2\}$, $l \in \{1, \dots, 2^{mn_p}\}$, such that $\bar{W}_{i_1, \dots, i_l}$ represents the corners of the hypercube defining the maximum variation of $\hat{W}(t)$, and let

$$\mathcal{A}_{i_1, \dots, i_l} = \begin{bmatrix} A + B\bar{W}_{i_1, \dots, i_l}^T N & BH \\ -G(K + \bar{W}_{i_1, \dots, i_l}^T N) & F \end{bmatrix}, \quad (5.131)$$

be the corners of the hypercube constructed from all the permutations of $\bar{W}_{i_1, \dots, i_l}$. For given actuator dynamics \mathcal{G}_A , it can then be shown that

$$\mathcal{A}_{i_1, \dots, i_l}^T \mathcal{P} + \mathcal{P} \mathcal{A}_{i_1, \dots, i_l} < 0, \quad \mathcal{P} > 0, \quad (5.132)$$

implies that $\mathcal{A}^T(\hat{W}(t), \mathcal{G}_A)\mathcal{P} + \mathcal{P}\mathcal{A}(\hat{W}(t), \mathcal{G}_A) < 0$ [96, 99]. As a consequence, one can solve the LMI given by (5.132) for all permutations of $\bar{W}_{i_1, \dots, i_l}$ to conclude the quadratic stability condition holds. Furthermore, (5.132) can be cast as a convex optimization problem to determine the feasible region for the actuator dynamics given the projection bounds \hat{W}_{\max} on the elements of $\hat{W}(t)$ which are designed based on the allowable system uncertainties.

This is important because we want to obtain a computable limit such that any actuator with dynamical characteristics captured within the computed feasible region is guaranteed to allow for safe adaptive control of the uncertain dynamical system. To do this, we need a way to start from an initial feasible point and then search in all directions of the dynamical parameters, for the feasible limit. By doing so, the entire region found through the search is guaranteed to be feasible. Besides starting from an initial feasible point, the other requirement for the search is that the parameters of the actuator dynamics are affinely parameterized such that satisfying (5.132) still implies $\mathcal{A}^T(\hat{W}(t), \mathcal{G}_A)\mathcal{P} + \mathcal{P}\mathcal{A}(\hat{W}(t), \mathcal{G}_A) < 0$ [96, 99].

With this in mind, we next show how we can affinely parameterize the actuator dynamics to fit the form of (5.132), and then search for the limit of all feasible parameter combinations thereby creating our feasible region. For this purpose, consider the actuator model given as

$$\mathcal{G}_A(s) = \frac{a_{p-1}s^{p-1} + a_{p-2}s^{p-2} + \dots + a_1s + a_0}{s^p + b_{p-1}s^{p-1} + \dots + b_1s + b_0}, \quad (5.133)$$

which can be written in controllable canonical form as (5.116) and (5.117) with the matrices

$$F = \begin{bmatrix} 0 & 1 & 0 & \dots & 0 \\ 0 & 0 & 1 & \dots & 0 \\ \vdots & \vdots & \vdots & \ddots & \vdots \\ 0 & 0 & 0 & \dots & 1 \\ -b_0 & -b_1 & -b_2 & \dots & -b_{p-1} \end{bmatrix}, \quad G = \begin{bmatrix} 0 \\ 0 \\ \vdots \\ 0 \\ 1 \end{bmatrix}, \quad H = \begin{bmatrix} a_0 & a_1 & a_2 & \dots & a_{p-1} \end{bmatrix}. \quad (5.134)$$

Note here that we use the controllable canonical form of $\mathcal{G}_A(s)$ to keep the term $-G(K + \bar{W}_{i_1, \dots, i_l}^T N)$ in (5.131) affine. Now, since we are interested in determining how the parameters a_k and b_k , $k = 0, 1, \dots, p-1$ of the actuator matrices, can be varied from initial feasible values such that (5.132) still holds, we let $a_k \triangleq a_k^{\text{feas}} - \delta a_k$ and $b_k \triangleq b_k^{\text{feas}} - \delta b_k$, where a_k^{feas} and b_k^{feas} indicate the initial feasible values (i.e., the actuator is sufficiently “fast” for these values) and δa_k and δb_k are the variation in the parameters such that we can

incrementally decrease from the feasible starting point. It then follows that the matrices F and H in (5.134) can be written as

$$\begin{aligned}
 F = & \underbrace{\begin{bmatrix} 0 & 1 & 0 & \dots & 0 \\ 0 & 0 & 1 & \dots & 0 \\ \vdots & \vdots & \vdots & \ddots & \vdots \\ 0 & 0 & 0 & \dots & 1 \\ -b_0^{\text{feas}} & -b_1^{\text{feas}} & -b_2^{\text{feas}} & \dots & -b_{p-1}^{\text{feas}} \end{bmatrix}}_{F^{\text{feas}}} + \delta b_0 \underbrace{\left[\begin{array}{c|c} \mathbf{0}_{(p-1) \times 1} & \mathbf{0}_{(p-1) \times (p-1)} \\ \hline 1 & \mathbf{0}_{1 \times (p-1)} \end{array} \right]}_{F_0} \\
 & + \delta b_1 \underbrace{\left[\begin{array}{c|c} \mathbf{0}_{(p-1) \times 2} & \mathbf{0}_{(p-2) \times (p-2)} \\ \hline 0 & 1 \end{array} \right]}_{F_1} + \dots + \delta b_{p-1} \underbrace{\left[\begin{array}{c|c} \mathbf{0}_{(p-1) \times (p-1)} & \mathbf{0}_{(p-1) \times 1} \\ \hline \mathbf{0}_{1 \times (p-1)} & 1 \end{array} \right]}_{F_{p-1}} \quad (5.135)
 \end{aligned}$$

$$\begin{aligned}
 H = & \underbrace{\begin{bmatrix} a_0^{\text{feas}} & a_1^{\text{feas}} & a_2^{\text{feas}} & \dots & a_{p-1}^{\text{feas}} \end{bmatrix}}_{H^{\text{feas}}} + \delta a_0 \underbrace{\begin{bmatrix} -1 & 0 & \dots & 0 \end{bmatrix}}_{H_0} \\
 & + \delta a_1 \underbrace{\begin{bmatrix} 0 & -1 & \dots & 0 \end{bmatrix}}_{H_1} + \dots + \delta a_{p-1} \underbrace{\begin{bmatrix} 0 & 0 & \dots & -1 \end{bmatrix}}_{H_{p-1}}. \quad (5.136)
 \end{aligned}$$

Using (5.135) and (5.136) we can reconstruct (5.131) as

$$\mathcal{A}_{i_1, \dots, i_l} = \underbrace{\begin{bmatrix} A + B\bar{W}_{i_1, \dots, i_l}^T N & BH^{\text{feas}} \\ -G(K + \bar{W}_{i_1, \dots, i_l}^T N) & F^{\text{feas}} \end{bmatrix}}_{\mathcal{A}_{i_1, \dots, i_l}^{\text{feas}}} + \sum_{k=0}^{p-1} \delta a_k \begin{bmatrix} \mathbf{0}_{n \times n} & BH_k \\ \mathbf{0}_{p \times n} & \mathbf{0}_{p \times p} \end{bmatrix} + \sum_{k=0}^{p-1} \delta b_k \begin{bmatrix} \mathbf{0}_{n \times n} & \mathbf{0}_{n \times p} \\ \mathbf{0}_{p \times n} & F_k \end{bmatrix}. \quad (5.137)$$

Now using the parameterized form given by (5.137), we start the search from initial feasible values a_k^{feas} and b_k^{feas} , $k = 0, 1, \dots, p-1$, with $\delta a_k = 0$ and $\delta b_k = 0$, $k = 0, 1, \dots, p-1$, such that all initial corners of the hypercube constructed from all the permutations of $\bar{W}_{i_1, \dots, i_l}$ (i.e. $\mathcal{A}_{i_1, \dots, i_l}^{\text{feas}}$) satisfy (5.132). Then the search is conducted to find the largest variations in δa_k and δb_k , $k = 0, 1, \dots, p-1$ such that (5.132) is still satisfied. To further elucidate the proposed approach, Algorithm Feasible Region Search describes this process to compute this feasible region of a_k and b_k parameters of the actuator dynamics, where the optimization is carried out using YALMIP [119], but other solvers can also be used [120].

Algorithm 1 Feasible Region Search

Data: $A, B, K, N, \hat{W}_{\max, i+(j-1)n_p}, a_k^{\text{feas}}, b_k^{\text{feas}}, \epsilon_{\text{tol}}$

Result: a_k, b_k

```
for  $\delta a_0 = 0 : \epsilon_{\text{tol}} : a_0^{\text{feas}}$  do
  for  $\delta a_1 = 0 : \epsilon_{\text{tol}} : a_1^{\text{feas}}$  do
    :
    for  $\delta a_{p-1} = 0 : \epsilon_{\text{tol}} : a_{p-1}^{\text{feas}}$  do
      for  $\delta b_0 = 0 : \epsilon_{\text{tol}} : b_0^{\text{feas}}$  do
        for  $\delta b_1 = 0 : \epsilon_{\text{tol}} : b_1^{\text{feas}}$  do
          :
          for  $\delta b_{p-1} = 0 : \epsilon_{\text{tol}} : b_{p-1}^{\text{feas}}$  do
            if  $\mathcal{A}_{i_1, \dots, i_l}^T \mathcal{P} + \mathcal{P} \mathcal{A}_{i_1, \dots, i_l} < 0$  and  $\mathcal{P} > 0$  then
              | Continue
            else
              | Break
            end
          end
           $a_k = a_k^{\text{feas}} - \delta a_k, k = 0, 1, \dots, p-1$ 
           $b_k = b_k^{\text{feas}} - \delta b_k, k = 0, 1, \dots, p-1$ 
          Save  $(a_0, a_1, \dots, a_{p-1}, b_0, b_1, \dots, b_{p-1})$ 
        end
      end
    end
  end
end
end
end
```

Now, using the above LMI analysis and search algorithm, we are able to compute feasible regions for the actuator dynamics such that safe adaptation is guaranteed. In the next section, we use this method to compute the limits for higher order actuator models for the control of the short-period dynamics of a hypersonic vehicle model.

5.4.3 Evaluation of LMI-Based Hedging Approach for Adaptive Control of a Hypersonic Vehicle Model with Pole-Zero Actuator Dynamics

To elucidate our proposed approach to the actuator dynamics problem, we provide the following application to a hypersonic vehicle. Consider the uncertain hypersonic vehicle short-period dynamics given by

$$\dot{x}_p(t) = \begin{bmatrix} -2.39 \times 10^{-1} & 1 \\ 4.26 & -1.19 \times 10^{-1} \end{bmatrix} x_p(t) + \begin{bmatrix} -1.33 \times 10^{-4} \\ -1.84 \times 10^{-1} \end{bmatrix} (v(t) + W^T x_p(t)), \quad (5.138)$$

with zero initial conditions and the state vector being defined as $x_p(t) = [\alpha(t), q(t)]^T$, where $\alpha(t)$ denotes the angle-of-attack and $q(t)$ denotes the pitch rate. The uncertainty is considered to be $W = [-100 \ 0.01]^T$ such that it dominantly and excessively effects the stability derivative $C_{m\alpha}$. Specifically, the value -100 creates a 400% increase in $C_{m\alpha}$, destabilizing the nominal closed-loop system, whereas the second value 0.01 can be considered to be small since it will not effect the closed-loop performance of the hypersonic vehicle which is lightly damped. In addition, $v(t)$ is the actuator output of the actuator dynamics which we represent in the frequency domain as

$$V(s) = \mathcal{G}_A(s)\Delta_e(s), \quad (5.139)$$

where $\Delta_e(s)$ denotes the elevator deflection command. Linear quadratic regulator (LQR) theory [91] is used to design the nominal controller for the proposed control design, with $E_p = [1, 0]$ such that a desired angle-of-attack command is followed. The controller gain matrix K is obtained using the highlighted augmented formulation, along with the weighting matrices $Q = \text{diag}[2000, 25, 400000]$ to penalize the states and $R = 12.5$ to penalize the control input, resulting in the gain matrix $K = \begin{bmatrix} -135.9 & -37.7 & -178.9 \end{bmatrix}$, which has a desirable 60.4° phase margin and a crossover frequency of 6.75 Hz. In addition, we set the element-wise projection bounds as $|[\hat{W}(t)]_{1,1}| \leq 105$ and $|[\hat{W}(t)]_{2,1}| \leq 0.1$, such that we obtain the permutations defining the maximum variation of $\hat{W}(t)$ as

$$\bar{W}_1 = \begin{bmatrix} 105 \\ 0.1 \end{bmatrix}, \bar{W}_2 = \begin{bmatrix} -105 \\ 0.1 \end{bmatrix}, \bar{W}_3 = \begin{bmatrix} 105 \\ -0.1 \end{bmatrix}, \text{ and } \bar{W}_4 = \begin{bmatrix} -105 \\ -0.1 \end{bmatrix}.$$

Using all the permutations of $\bar{W}_i, i = 1, \dots, 4$ the corners of the hypercube are then constructed as

$$\mathcal{A}_i = \begin{bmatrix} A + B\bar{W}_i^T N & BH \\ -G(K + \bar{W}_i^T N) & F \end{bmatrix}, \quad i = 1, \dots, 4. \quad (5.140)$$

The purpose of the rest of this section is to analyze the effect of different actuator dynamics on the allowable feasible region for safe adaptive control. In light of this, the information above is all that is necessary to conduct the LMI analysis highlighted in Section 5.4.2.3 such that the feasible region can be computed using Algorithm 1 Feasible Region Search. Even though time response simulations of the controller performance are not included in this analysis, it should be noted that the selected feedback gain matrix K is tuned for desirable nominal control performance and the uncertainty given by W deteriorates the nominal controller performance such that the proposed adaptive controller is necessary for extracting a desirable performance from the uncertain dynamical system. For additional details including time response simulations of the performance of the proposed control design, the reader is directed to [118]. To thoroughly analyze the effect on the feasible region by higher order actuator dynamics, we divide this section into three subsections in which we first consider a second order actuator model, then add a zero to this second order model, and finally add a pole along with the zero such that the final actuator model considered is a third order system with one zero and three poles.

5.4.3.1 Computing Limits for Second Order Actuator Dynamics

In this subsection, we begin with a second order actuator model which is then be used as a baseline for comparison with the actuator models presented in the remaining subsections. For this purpose, consider the actuator dynamics given in the frequency domain as

$$\mathcal{G}_A(s) = \frac{K_a \omega_n^2}{s^2 + 2\zeta \omega_n s + \omega_n^2}, \quad (5.141)$$

where K_a is the static gain, ω_n is the natural frequency, and ζ is the damping ratio. It follows that (5.141) can be written as in (5.116) and (5.117) with

$$F = \begin{bmatrix} 0 & 1 \\ -\omega_n^2 & -2\zeta \omega_n \end{bmatrix}, \quad G = \begin{bmatrix} 0 \\ 1 \end{bmatrix}, \quad H = \begin{bmatrix} K_a \omega_n^2 & 0 \end{bmatrix}. \quad (5.142)$$

In order to use Algorithm 1 Feasible Region Search, it is necessary for (5.142) to be affinely parameterized. For this purpose, let $a_0 = b_0 = \omega_n^2$ and $b_1 = 2\zeta\omega_n$, where the static gain K_a is not included in a_0 to more conveniently visualize its effect. This is done by fixing K_a at different values and then running the search algorithm for the remaining parameters and plotting the resulting 2-D figure. Since $a_0 = b_0$, the F and H actuator matrices in (5.142) can be written as

$$F = \underbrace{\begin{bmatrix} 0 & 1 \\ -b_0^{\text{feas}} & -b_1^{\text{feas}} \end{bmatrix}}_{F^{\text{feas}}} + \delta b_0 \underbrace{\begin{bmatrix} 0 & 0 \\ 1 & 0 \end{bmatrix}}_{F_1} + \delta b_1 \underbrace{\begin{bmatrix} 0 & 0 \\ 0 & 1 \end{bmatrix}}_{F_2}, \quad (5.143)$$

$$H = \underbrace{\begin{bmatrix} K_a b_0^{\text{feas}} & 0 \end{bmatrix}}_{H^{\text{feas}}} + \delta b_0 \underbrace{\begin{bmatrix} -K_a & 0 \end{bmatrix}}_{H_1} + \delta b_1 \underbrace{\begin{bmatrix} 0 & 0 \end{bmatrix}}_{H_2}. \quad (5.144)$$

Furthermore, the corners of the hypercube given by (5.140) can now be represented as

$$\mathcal{A}_i = \begin{bmatrix} A + B\bar{W}_i^T & BH^{\text{feas}} \\ -G(K + \bar{W}_i^T N) & F^{\text{feas}} \end{bmatrix} + \delta b_0 \begin{bmatrix} 0_{3 \times 3} & BH_1 \\ 0_{2 \times 3} & F_1 \end{bmatrix} \delta b_1 \begin{bmatrix} 0_{3 \times 3} & BH_2 \\ 0_{2 \times 3} & F_2 \end{bmatrix}. \quad (5.145)$$

Now, starting at the initial feasible values $b_0^{\text{feas}} = 8100$ and $b_1^{\text{feas}} = 270$ (i.e., $\omega_n = 90$ and $\zeta = 1.5$) we use Algorithm 1 Feasible Region Search to obtain the feasible region of b_0 and b_1 , and then map it back to ω_n and ζ (i.e., $\omega_n = \sqrt{b_0}$ and $\zeta = \frac{b_1}{2\sqrt{b_0}}$). The resulting feasible region of allowable actuator dynamics is shown in Figure 5.11 with different fixed static gain K_a values between 0.65 and 3.0. Specifically, it can be concluded from the figure that any actuator with dynamical characteristics above all the computed limits can be used for safe adaptive control of the considered hypersonic vehicle in the respective range of static gain values. For example, if the actuator considered has the pair $(\zeta, \omega_n) = (0.55, 30)$, it can be concluded that safe actuation is guaranteed for $K_a \in [0.65, 3.0]$. Furthermore, it can be seen from the figure that when $K_a < 1$ ($K_a = 1$ is indicated by the black dashed trace), the feasible region gets smaller due to the more dramatic increase in necessary ω_n values. In addition, it is evident that the feasible regions also decreases when $K_a > 1$, such that $K_a = 1$ can be concluded to be the optimum static gain value in that it provides the largest feasible region.

It should be noted that another way to investigate this problem is by considering the uncertainty in the static gain K_a as part of an unknown control effectiveness which would then be used to build the corners

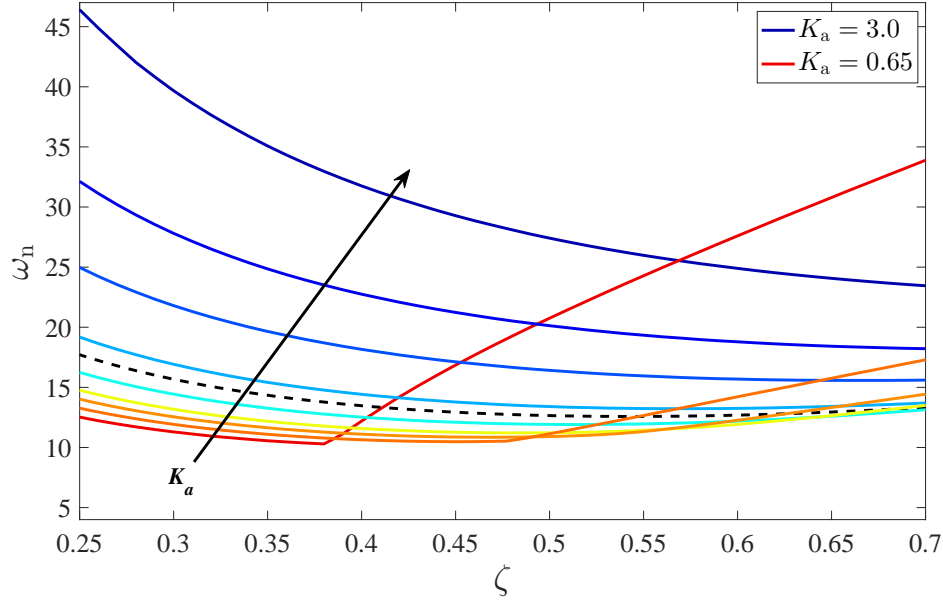


Figure 5.11: LMI calculated feasible region for second order actuator dynamics with $K_a \in [0.65, 3.0]$. The black dashed trace indicates $K_a = 1.0$.

of the hypercube for the LMI analysis. In this case, the architecture considered in [95, 103] which includes an unknown control effectiveness could be used to determine the feasible region.

5.4.3.2 Computing Limits for Second Order Actuator Dynamics with One Zero

We now add a zero to the second order actuator model from Section 5.4.3.1 and assume unity static gain

$$\mathcal{G}_A(s) = \frac{\omega_n^2(\lambda_1 s + 1)}{s^2 + 2\zeta\omega_n s + \omega_n^2}, \quad (5.146)$$

where $-\lambda_1^{-1}$ is the added zero. It follows that (5.146) can be written in controllable canonical form with

$$F = \begin{bmatrix} 0 & 1 \\ -\omega_n^2 & -2\zeta\omega_n \end{bmatrix}, \quad G = \begin{bmatrix} 0 \\ 1 \end{bmatrix}, \quad H = \begin{bmatrix} \omega_n^2 & \lambda_1\omega_n^2 \end{bmatrix}. \quad (5.147)$$

As in Section 5.4.3.1, for visual convenience, we plot the feasible region of (ζ, ω_n) for different fixed values of the added zero. With this in mind, we again let $b_0 = \omega_n^2$ and $b_1 = 2\zeta\omega_n$ and write the parameterized matrices

$$F = \underbrace{\begin{bmatrix} 0 & 1 \\ -b_0^{\text{feas}} & -b_1^{\text{feas}} \end{bmatrix}}_{F^{\text{feas}}} + \delta b_0 \underbrace{\begin{bmatrix} 0 & 0 \\ 1 & 0 \end{bmatrix}}_{F_1} + \delta b_1 \underbrace{\begin{bmatrix} 0 & 0 \\ 0 & 1 \end{bmatrix}}_{F_2}, \quad (5.148)$$

$$H = \underbrace{\begin{bmatrix} b_0^{\text{feas}} & \lambda_1 b_0^{\text{feas}} \end{bmatrix}}_{H^{\text{feas}}} + \delta b_0 \underbrace{\begin{bmatrix} -1 & -\lambda_1 \end{bmatrix}}_{H_1} + \delta b_1 \underbrace{\begin{bmatrix} 0 & 0 \end{bmatrix}}_{H_2}. \quad (5.149)$$

such that the corners of the hypercube can be constructed as in (5.145). Starting at the initial feasible values $b_0^{\text{feas}} = 8100$ and $b_1^{\text{feas}} = 270$ (i.e., $\omega_n = 90$ and $\zeta = 1.5$), Algorithm 1 Feasible Region Search is used to find the feasible region of b_0 and b_1 for three different zero values (i.e., $\lambda_1 = 1.0, 0.5, 0.1$). The corresponding feasible regions of ω_n and ζ values are shown in Figure 5.12, such that any actuator in an aircraft with characteristics above these feasible regions is guaranteed to provide safe adaptation. It can be seen that as the zero moves further left from the imaginary axis, the feasible region gets smaller. In addition, points are included to show where instability is reached in simulation to estimate the conservatism of the computed limit provide by the proposed approach.

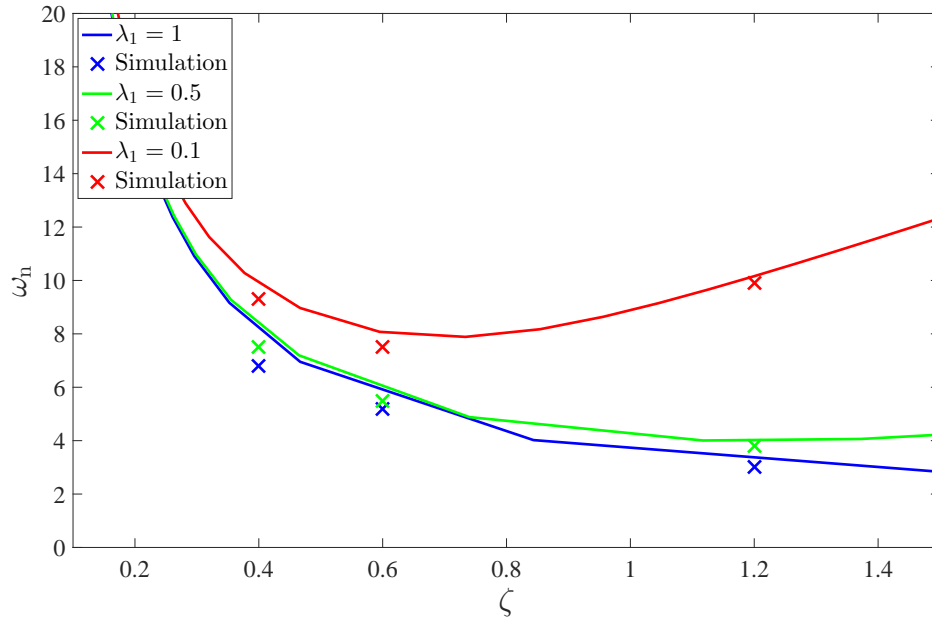


Figure 5.12: LMI calculated feasible region for second order actuator dynamics with additional zero.

5.4.3.3 Computing Limits for Third Order Actuator Dynamics with One Zero and Three Poles

For this example, a pole is added to the actuator model from Section 5.4.3.2 such that the resulting actuator model is third order. For this purpose, consider the actuator dynamics given in the frequency domain as

$$\mathcal{G}_A(s) = \frac{\omega_n^2(\lambda_1 s + 1)}{(\lambda_2 s + 1)(s^2 + 2\zeta\omega_n s + \omega_n^2)}, \quad (5.150)$$

where $-\lambda_2^{-1}$ is the added pole. In controllable canonical form, (5.150) can be written as in (5.116) and (5.117) with

$$F = \begin{bmatrix} 0 & 1 & 0 \\ 0 & 0 & 1 \\ -\frac{\omega_n^2}{\lambda_2} & -\omega_n^2 - \frac{2\zeta\omega_n}{\lambda_2} & -2\zeta\omega_n - \frac{1}{\lambda_2} \end{bmatrix}, \quad G = \begin{bmatrix} 0 \\ 0 \\ 1 \end{bmatrix}, \quad H = \begin{bmatrix} \frac{\omega_n^2}{\lambda_2} & \frac{\lambda_1\omega_n^2}{\lambda_2} & 0 \end{bmatrix}. \quad (5.151)$$

Again for convenience in displaying the results, we fix λ_1 and λ_2 to obtain the feasible region of ζ and ω_n values. For this purpose, we use each of the three zeros considered in the previous section, with three different poles, and then the feasible region is computed. To use Algorithm 1 Feasible Region Search let $b_0 = \omega_n^2$ and $b_1 = 2\zeta\omega_n$ such that the parameterized actuator matrices F and H follow as

$$F = \begin{bmatrix} 0 & 1 & 0 \\ 0 & 0 & 1 \\ -\frac{1}{\lambda_2}b_0^{\text{feas}} & -(b_0^{\text{feas}} + \frac{1}{\lambda_2}b_1^{\text{feas}}) & -(b_1^{\text{feas}} + \frac{1}{\lambda_2}) \end{bmatrix} + \delta b_0 \begin{bmatrix} 0 & 0 & 0 \\ 0 & 0 & 0 \\ \frac{1}{\lambda_2} & 1 & 0 \end{bmatrix} + \delta b_1 \begin{bmatrix} 0 & 0 & 0 \\ 0 & 0 & 0 \\ 0 & \frac{1}{\lambda_2} & 1 \end{bmatrix}, \quad (5.152)$$

$$H = \begin{bmatrix} \frac{1}{\lambda_2}b_0^{\text{feas}} & \frac{\lambda_1}{\lambda_2}b_0^{\text{feas}} & 0 \end{bmatrix} + \delta b_0 \begin{bmatrix} -\frac{1}{\lambda_2} & -\frac{\lambda_1}{\lambda_2} & 0 \end{bmatrix} + \delta b_1 \begin{bmatrix} 0 & 0 & 0 \end{bmatrix}. \quad (5.153)$$

such that the corners of the hypercube can be constructed as

$$A_i = \begin{bmatrix} A + B\bar{W}_i^T & BH^{\text{feas}} \\ -G(K + \bar{W}_i^T N) & F^{\text{feas}} \end{bmatrix} + \delta b_0 \begin{bmatrix} 0_{3 \times 3} & BH_1 \\ 0_{3 \times 3} & F_1 \end{bmatrix} \delta b_1 \begin{bmatrix} 0_{3 \times 3} & BH_2 \\ 0_{3 \times 3} & F_2 \end{bmatrix}. \quad (5.154)$$

Starting at the initial feasible values $b_0^{\text{feas}} = 8100$ and $b_1^{\text{feas}} = 270$ (i.e., $\omega_n = 90$ and $\zeta = 1.5$), Algorithm 1 Feasible Region Search is used to find the feasible region of b_0 and b_1 and then mapped back to ω_n and ζ as shown in Figures 5.13–5.15. It can be seen that the location of the third pole, effects the allowable variation in ω_n and ζ . For instance, in Figure 5.13, when λ_2 is large (i.e., the pole is closer to the imaginary axis), larger ζ values require drastically large ω_n values whereas when λ_2 gets smaller (i.e., the pole moves further away from the imaginary axis), smaller ω_n values can be tolerated for the respective ζ values. Similar arguments can be made from Figures 5.14 and 5.15. In addition, simulations were run to determine at what values the system yields unbounded trajectories. These points are included to estimate the conservatism of the proposed approach.

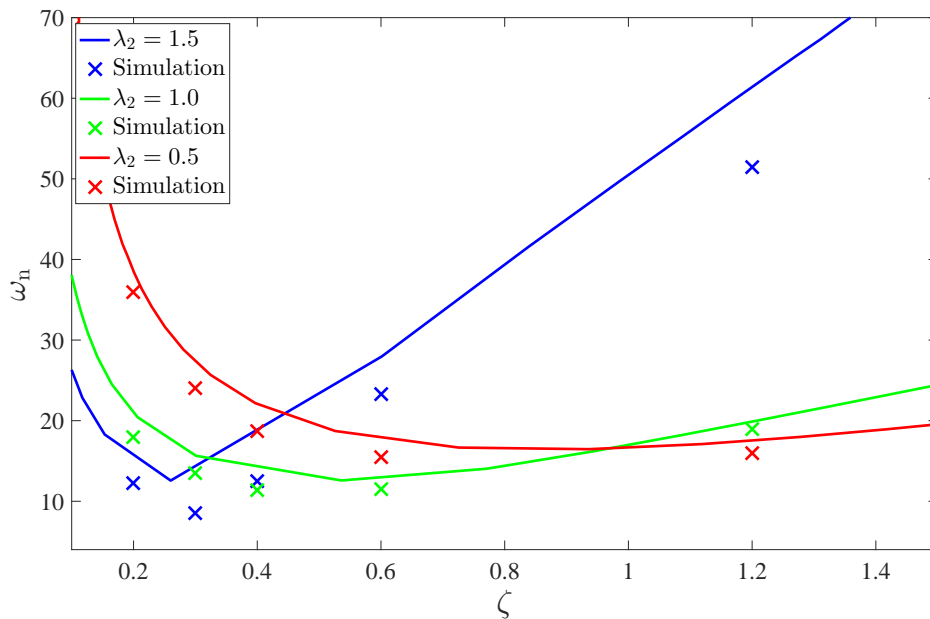


Figure 5.13: LMI calculated feasible region for third order actuator dynamics with one zero ($\lambda_1 = 1.0$) and three poles.

In addition, Figures 5.16–5.20 are included to show the performance of the proposed approach. Specifically, Figure 5.16 shows the feasible region computed by Algorithm 1 Feasible Region Search for the case with the added zero at $\lambda_1 = 1.0$ and the third pole at $\lambda_2 = 0.5$ from Figure 5.13. Additional data points with different ζ and ω_n values have been included with the LMI computed limit, with the simulation results provided in Figures 5.17 – 5.20. In particular, Figure 5.17 shows the reference model performance for data points 1-5 which are all contained within or on the feasible limit. This shows approximately where the performance of the reference model deteriorates when compared to a sufficiently “fast” actuator (i.e.,

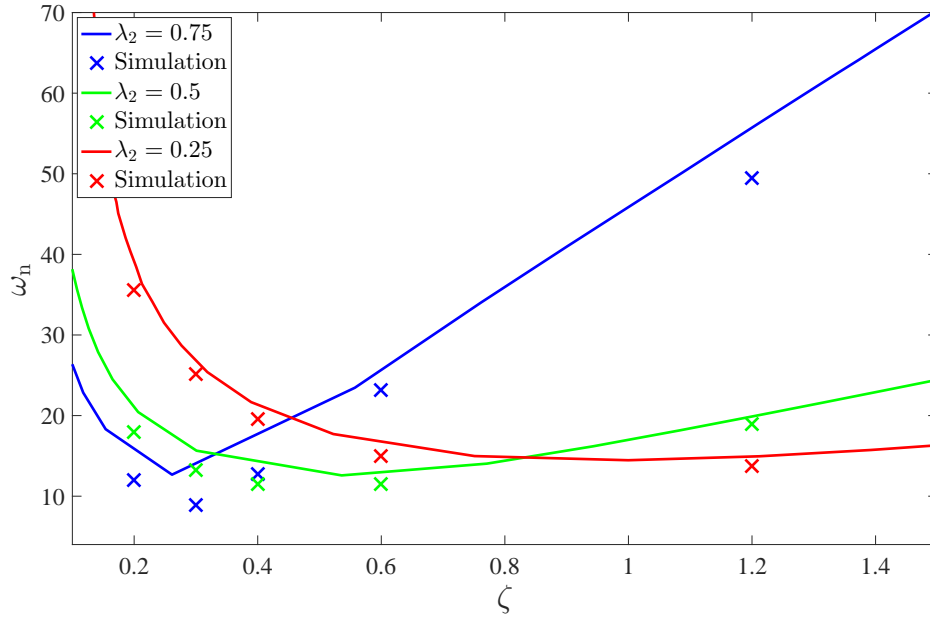


Figure 5.14: LMI calculated feasible region for third order actuator dynamics with one zero ($\lambda_1 = 0.5$) and three poles.

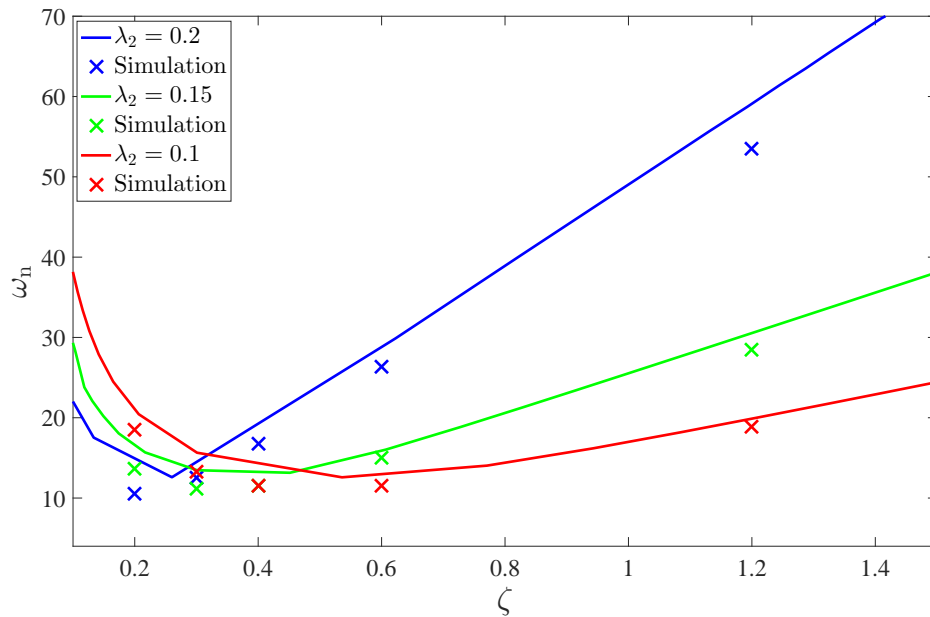


Figure 5.15: LMI calculated feasible region for third order actuator dynamics with one zero ($\lambda_1 = 0.1$) and three poles.

data point 1 representing $(\zeta, \omega_n) = (0.53, 60)$). As seen in the figure, the angle-of-attack trajectory does not change considerably between the different (ζ, ω_n) values, whereas the pitch rate has different degrees of oscillation in the transient portion. It was found that as the value of ζ increased, a larger value of ω_n was

required for more desirable reference model performance. Lastly, Figures 5.18–5.20 show the state tracking and control performance for data points 1,2, and 6 from Figure 5.16. It can be seen from Figures 5.18 and 5.19 that the state tracking and control performance deteriorate slightly between the sufficiently “fast” actuator given by $(\zeta, \omega_n) = (0.53, 60)$ and the dynamics at the feasible limit given by $(\zeta, \omega_n) = (0.53, 18.7)$. This is to be expected since the reference model performance is effected as actuator becomes “slower” as seen in Figure 5.17. The point of instability is then reached at $(\zeta, \omega_n) = (0.53, 16.7)$ as seen by the unbounded trajectories in Figure 5.20.

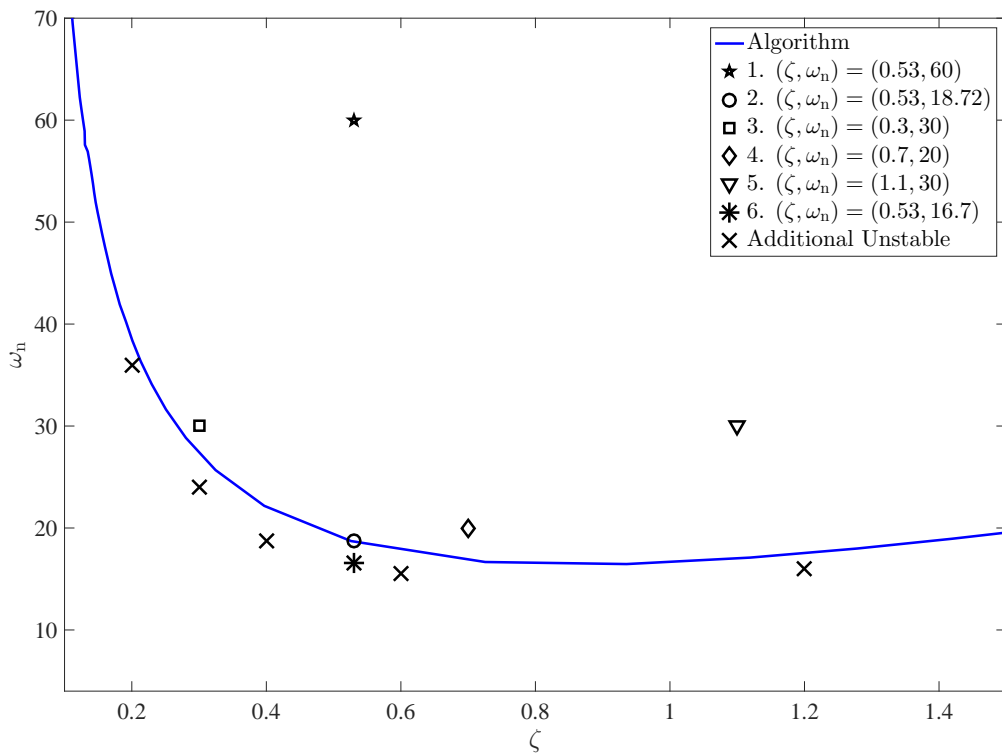


Figure 5.16: LMI feasible region with additional simulation points for third order actuator model from Figure 5.13 with $\lambda_1 = 1.0$ and $\lambda_2 = 0.5$.

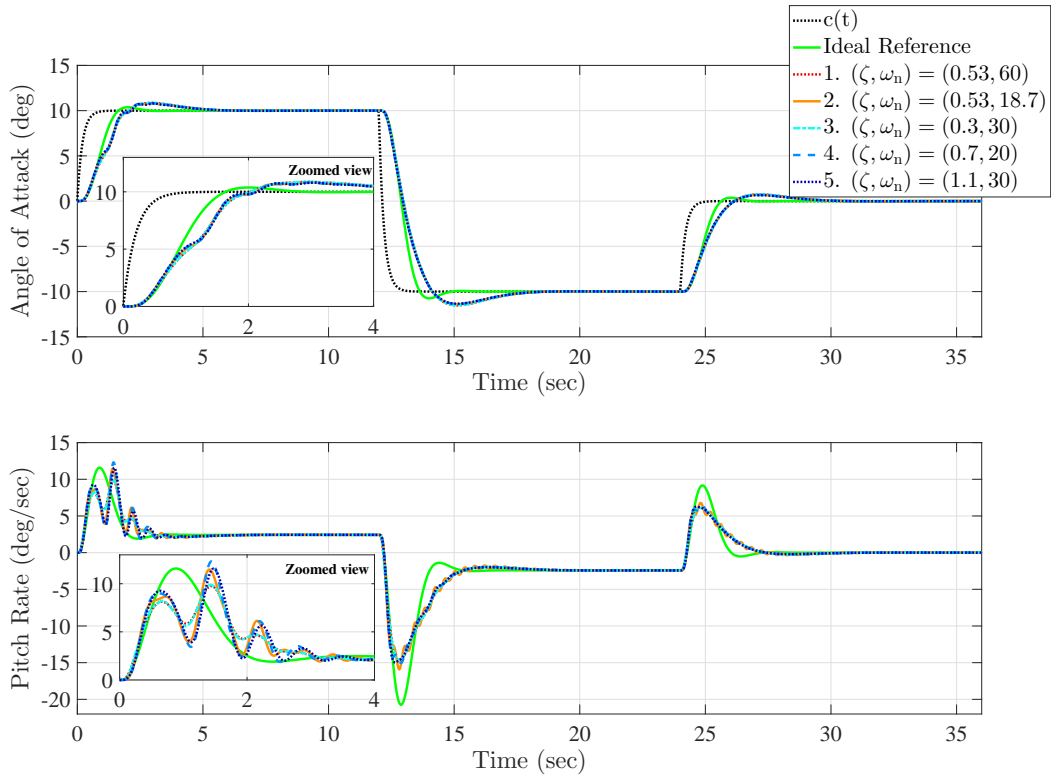


Figure 5.17: Reference model performance for data points 1-5 of Figure 5.16.

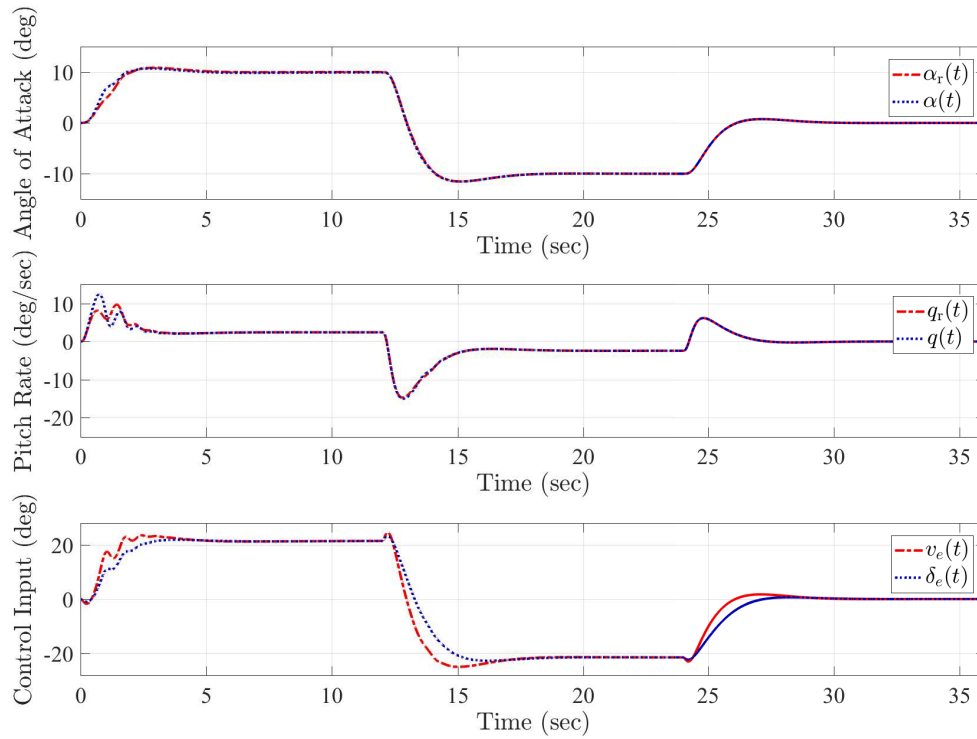


Figure 5.18: State tracking and controller performance for data point 1 (i.e., $(\zeta, \omega_n) = (0.53, 60)$) of Figure 5.16.

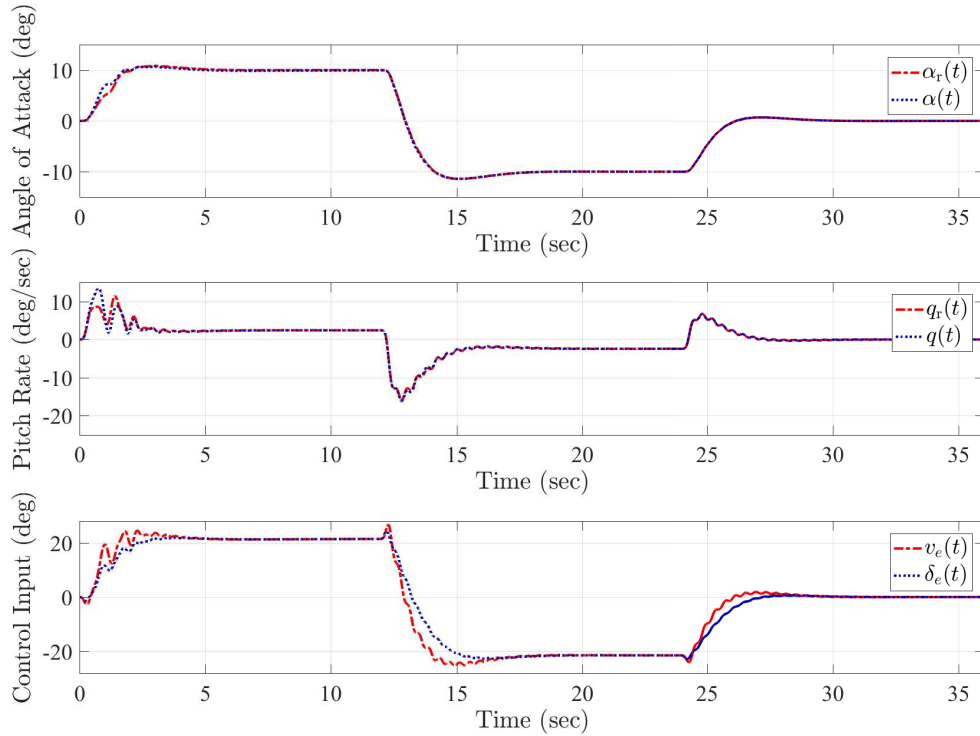


Figure 5.19: State tracking and controller performance for data point 2 (i.e., $(\zeta, \omega_n) = (0.53, 18.7)$) of Figure 5.16.

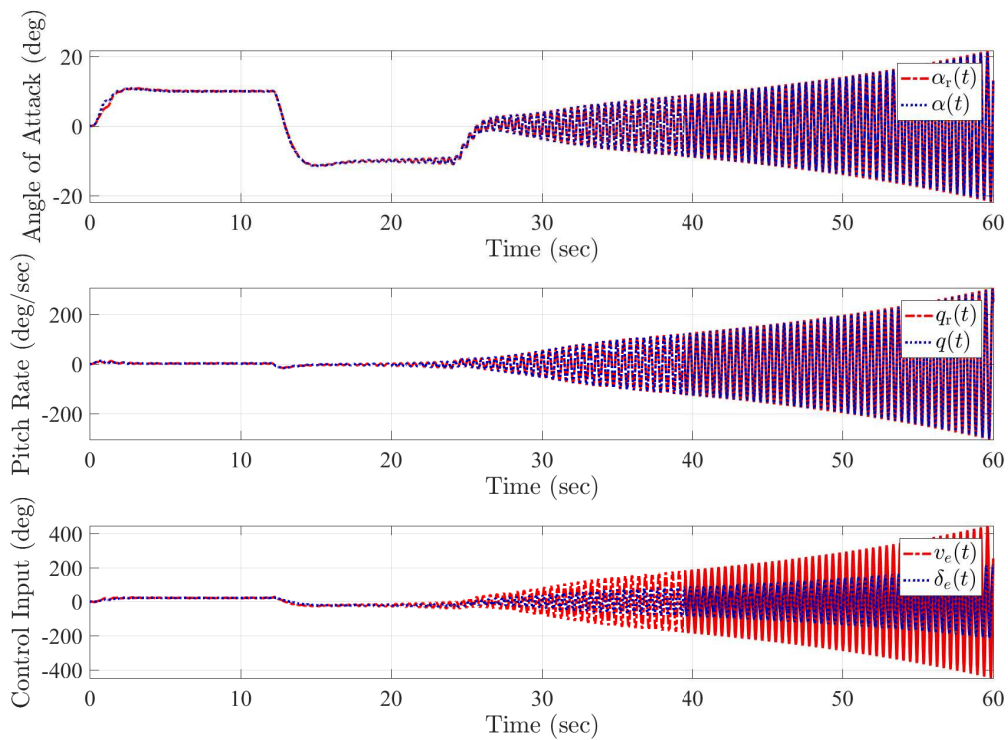


Figure 5.20: State tracking and controller performance for data point 6 (i.e., $(\zeta, \omega_n) = (0.53, 16.7)$) of Figure 5.16.

5.4.4 Conclusion

In this paper, an LMI-based hedging approach for model reference adaptive control in the presence of high-order actuator dynamics was applied to the short-period dynamics of a hypersonic vehicle model subject to pole-zero actuator dynamics. It was shown that the proposed approach has the ability to provide a feasible region of safe actuation limits for different high order actuator models with varying pole and zero locations as well as different static gain values.

CHAPTER 6: EXPANDED REFERENCE MODELS FOR UNCERTAIN DYNAMICAL SYSTEMS WITH ACTUATOR DYNAMICS: STABILITY, PERFORMANCE, AND ROBUSTNESS

For uncertain dynamical systems with actuator dynamics, this paper presents a new adaptive control architecture using expanded reference models. Specifically, the proposed adaptive control architecture allows the trajectories of the uncertain dynamical system to follow the trajectories of the expanded reference model that are shown to remain predictably close to the trajectories of the ideal reference model, which captures a desired closed-loop system performance, as compared to a well-respected approach. In addition, we utilize a command governor architecture with the proposed expanded reference model in order to achieve asymptotic convergence of the expanded reference model trajectories to those of the ideal reference model such that the desired closed-loop system performance can be captured. We then incorporate an estimation of the actuator bandwidth for providing robustness of the proposed adaptive control architecture against possible uncertainties in the actuator bandwidths. Finally, we analyze the stability of the proposed adaptive control architecture and its generalizations using linear matrix inequalities and Lyapunov theory, and also present a numerical hypersonic vehicle example for illustrating the efficacy of our contributions.

6.1 Introduction

6.1.1 Motivation and Background

The design of a model reference adaptive control algorithm has three major components — a reference model, an update law, and a feedback control law [3, 4]. Specifically, a desired closed-loop system performance is captured by the reference model. The system error between the state (respectively, output) of this model and the state (respectively, output) of the uncertain dynamical system is used to drive the update law online. This then allows the control law to adapt its feedback gains using the information received from the update law for suppressing the system error. The promising feature of this control algorithm is its ability to achieve desired levels of system performance without excessively relying on dynamical models of the

system being controlled. Therefore, it can effectively guarantee certain levels of system performance in the presence of system uncertainties (see, for example, [5–7, 93]).

While addressing system uncertainties, the presence of unmodeled dynamics are often neglected in the design of model reference adaptive control algorithms (see, for example, [8–12] and references therein). A practically unavoidable form of unmodeled dynamics is the actuator dynamics that is present in any physical system. In particular, if the bandwidths of each actuator channel are not sufficiently fast, then the closed-loop system trajectories may not behave close to the reference model trajectories and, importantly, the stability of the closed-loop system can be lost. Furthermore, additional verification steps are necessary to show the allowable bandwidth range of the actuator dynamics for safety-critical and human-in-the-loop applications such that the adaptive control algorithms correctly suppress the system uncertainties [95].

The authors of [58] investigate how slow the actuator dynamics need to become before the closed-loop stability is negatively effected for a scalar system. In addition, they then propose different modifications to the control law to provide additional robustness when the actuator dynamics are not sufficiently fast. The authors of [30–33] propose a well-respected practical approach in the aerospace engineering field known as (pseudo-control) hedging. In particular, based on a given reference model capturing a desired closed-loop dynamical system performance, the hedging approach alters the trajectories of this model enabling adaptive control laws to be designed such that their stability is not affected by the presence of actuator dynamics. Furthermore, the results documented in [95, 117, 118] present theoretical generalizations to this approach, where linear matrix inequalities (LMIs) are used to show that correct adaptation in the presence of actuator dynamics is only feasible under certain stability limits. Specifically, considering the actuator dynamics of interest, when the solution to the resulting LMIs is feasible, then stability of the closed-loop dynamical system is guaranteed. While the hedging approach is a well-adopted technique with applications to aircraft [30–34, 121], spacecraft [122], helicopters [123], and missiles [124]), the stability guarantees as shown in [95, 117, 118] are limited to achieving bounded controlled system trajectories around a neighborhood of the given ideal reference model that captures a desired closed-loop system performance.

6.1.2 Contribution and Notation

The contributions of this paper can be stated as follows. First, we present a new adaptive control architecture using expanded reference models for uncertain dynamical systems with actuator dynamics. The proposed adaptive control architecture allows the trajectories of the uncertain dynamical system to

follow the trajectories of the expanded reference model, which are shown to remain predictably close to the trajectories of the ideal reference model as compared with the hedging approach. Second, we utilize a new command governor architecture developed for the proposed expanded reference model for the purpose of achieving asymptotic convergence of the expanded reference model trajectories to those of the ideal reference model such that the desired closed-loop system performance can be captured. Third, we incorporate an estimation of the actuator bandwidth for providing robustness against possible uncertainties in the bandwidths of actuator channels. Finally, we analyze the stability of the proposed adaptive control architecture and its generalizations using linear matrix inequalities and Lyapunov theory, and also present a numerical hypersonic vehicle example for illustrating the efficacy of our contributions.

It should also be noted that two preliminary conference versions of this paper appeared in [125, 126]. The present paper significantly goes beyond these preliminary conference papers in the sense that *i)* neither [125] nor [126] consider uncertainty in the control effectiveness and the present work does, *ii)* a command governor architecture is implemented in the present paper such that asymptotic convergence to the ideal reference model is guaranteed and neither [125] nor [126] can achieve this, and *iii)* this present work considers uncertainty in the actuator bandwidth for a multi-input case whereas [126] only considered a single control channel. In addition, this paper provides additional motivation and discussion on the proposed expanded reference model design including comparisons to the hedging approach as well as detailed proofs.

Throughout this paper, we use \mathbb{R} for the set of real numbers, \mathbb{R}^n for the set of $n \times 1$ real column vectors, $\mathbb{R}^{n \times m}$ for the set of $n \times m$ real matrices, \mathbb{R}_+ (respectively, $\overline{\mathbb{R}}_+$) for the set of positive (respectively, nonnegative) real numbers, $\mathbb{R}_+^{n \times n}$ (respectively, $\overline{\mathbb{R}}_+^{n \times n}$) for the set of $n \times n$ positive-definite (respectively, nonnegative-definite) real matrices, $\mathbb{D}^{n \times n}$ for the set of $n \times n$ real matrices with diagonal scalar entries, $0_{n \times m}$ for the $m \times m$ matrix of all zeros, I_n for the $n \times n$ identity matrix, and “ \triangleq ” for the equality by definition. We also write $(\cdot)^T$ for the transpose operator, $(\cdot)^{-1}$ for the inverse operator, $\text{tr}(\cdot)$ for the trace operator, $\mathcal{L}\{\cdot\}$ for the Laplace transform operator, and \mathbf{e}_i for the standard basis for $i = 1, \dots, n$.

6.2 Problem Formulation

In this section, we introduce the problem considered throughout this paper. For this purpose, consider the uncertain dynamical system given by

$$\dot{x}(t) = Ax(t) + B(\Lambda v(t) + W^T x(t)), \quad x(0) = x_0, \quad (6.1)$$

where $x(t) \in \mathbb{R}^n$ is an available (i.e., measurable) state vector and $v(t) \in \mathbb{R}^m$ is the actuator output of the actuator dynamics satisfying

$$\dot{v}(t) = -M(v(t) - u(t)), \quad v(0) = v_0, \quad (6.2)$$

with $u(t) \in \mathbb{R}^m$ being the control signal (i.e., the input of the actuator dynamics) and $M \in \mathbb{R}^{m \times m} \cap \mathbb{D}^{m \times m}$ is constructed of diagonal entries $m_{i,i} > 0$, $i = 1, \dots, m$ that represent the actuator bandwidth of each control channel. In addition, $A \in \mathbb{R}^{n \times n}$ is a known system matrix, $B \in \mathbb{R}^{n \times m}$ is a known control input matrix, $W \in \mathbb{R}^{n \times m}$ is an unknown weight matrix, and $\Lambda \in \mathbb{R}_+^{m \times m} \cap \mathbb{D}^{m \times m}$ is an unknown control effectiveness matrix that can be parameterized as

$$\Lambda = I_m + \delta\Lambda, \quad (6.3)$$

where $\delta\Lambda \in \mathbb{R}^{m \times m} \cap \mathbb{D}^{m \times m}$ is unknown¹. Throughout this paper, we make the standard assumption that the pair (A, B) is controllable.

Next, consider the reference model capturing a desired (i.e., ideal) closed-loop dynamical system performance given by

$$\dot{x}_r(t) = A_r x_r(t) + B_r c(t), \quad x_r(0) = x_{r0}, \quad (6.4)$$

where $x_r(t) \in \mathbb{R}^n$ is the reference state vector, $A_r \in \mathbb{R}^{n \times n}$ is the Hurwitz reference model matrix, $B_r \in \mathbb{R}^{n \times m}$ is the command input matrix, and $c(t) \in \mathbb{R}^m$ is the desired uniformly continuous smooth and bounded reference command. In the classical sense, the objective of the model reference adaptive control problem is to design an adaptive feedback control law such that the state vector $x(t)$ at least closely follows the reference state vector $x_r(t)$ in the presence of system uncertainties captured by the unknown matrices “ W ” and “ $\delta\Lambda$ ” that appear in (6.1) and (6.3).

6.2.1 Actuators with Sufficiently Fast Dynamics

If the actuator dynamics given by (6.2) are sufficiently fast, then it is common practice to neglect their presence. In this case, (6.1) becomes

¹The parameterized form of the unknown control effectiveness given by (6.3) is fairly adopted in literature (see, for example, [95, 127–129])

$$\dot{x}(t) = Ax(t) + B((I_m + \delta\Lambda)u(t) + W^T x(t)), \quad x(0) = x_0. \quad (6.5)$$

In this approximate form, the control channel has direct access to the system uncertainties; hence, a standard model reference adaptive control architecture can be easily implemented to suppress the system uncertainties. To elucidate this well-known point and be self-contained, let the feedback control law be given as in [95] by²

$$u(t) = -(I_m + \delta\hat{\Lambda}(t))^{-1}(\hat{W}^T(t)x(t) + K_1x(t) - K_2c(t)), \quad (6.6)$$

where $K_1 \in \mathbb{R}^{m \times n}$ and $K_2 \in \mathbb{R}^{m \times m}$ are the nominal feedback and feedforward gain matrices designed such that $A_r \triangleq A - BK_1$ and $B_r \triangleq BK_2$ hold. Furthermore, $\hat{W}(t) \in \mathbb{R}^{n \times m}$ and $\delta\hat{\Lambda}(t) \in \mathbb{R}^{m \times m}$ are the (online) estimates of W and $\delta\Lambda$ respectively satisfying the weight update laws

$$\dot{\hat{W}}(t) = \gamma \text{Proj}_m[\hat{W}(t), x(t)e^T(t)PB], \quad \hat{W}(0) = \hat{W}_0, \quad (6.7)$$

$$\delta\dot{\hat{\Lambda}}(t) = \alpha \text{Proj}_m[\delta\hat{\Lambda}(t), B^T P e(t)u^T(t)], \quad \delta\hat{\Lambda}(0) = \delta\hat{\Lambda}_0, \quad (6.8)$$

where $\gamma \in \mathbb{R}_+$ and $\alpha \in \mathbb{R}_+$ are learning rate gains, $P \in \mathbb{R}_+^{n \times n}$ is a solution of the Lyapunov equation $0 = A_r^T P + P A_r + R$, $R \in \mathbb{R}_+^{n \times n}$, and $e(t) \triangleq x(t) - x_r(t)$ is the system error state vector³. Using (6.4), (6.5), and (6.6), the system error dynamics can then be written as

$$\dot{e}(t) = A_r e(t) - B(\tilde{W}^T(t)x(t) + \delta\tilde{\Lambda}(t)u(t)), \quad e(0) = e_0, \quad (6.9)$$

where $\tilde{W}(t) \triangleq \hat{W}(t) - W \in \mathbb{R}^{n \times m}$ and $\delta\tilde{\Lambda}(t) \triangleq \delta\hat{\Lambda}(t) - \delta\Lambda \in \mathbb{R}^{m \times m}$.

From (6.9), the weight update laws (6.7) and (6.8) can be easily derived using the Lyapunov function $\mathcal{V}(e, \tilde{W}, \delta\tilde{\Lambda}) = e^T P e + \gamma^{-1} \text{tr} \tilde{W}^T \tilde{W} + \alpha^{-1} \text{tr} \delta\tilde{\Lambda}^T \delta\tilde{\Lambda}$ [5–7]. Specifically, from the time derivative of this Lyapunov function, i.e., $\dot{\mathcal{V}}(e(t), \tilde{W}(t)) \leq -e^T(t) R e(t) \leq 0$, one can conclude the boundedness of the solution $(e(t), \tilde{W}(t), \delta\tilde{\Lambda}(t))$ as well as $\lim_{t \rightarrow \infty} \dot{\mathcal{V}}(e(t), \tilde{W}(t), \delta\tilde{\Lambda}(t)) = 0$, where the latter results from Barbalat's lemma [88]. This consequently shows that $e(t) \rightarrow 0$ as $t \rightarrow \infty$, thereby achieving the classical objective of the model reference adaptive control problem.

²To ensure (6.6) is implementable, the projection bounds for the estimate of $\delta\hat{\Lambda}(t)$ in (6.8) can be defined such that $I_m + \delta\hat{\Lambda}(t)$ is invertible (see, for example, [95, 127, 130, 131]).

³Details on the projection operator are given in Appendix A

6.2.2 Actuators without Sufficiently Fast Dynamics

For many real-world engineering applications, especially for safety-critical applications, when the actuator dynamics given by (6.2) are not sufficiently fast, one must consider (6.1) and (6.2) together in order to correctly represent the uncertain dynamical system to be controlled. This in turn implies the control channel cannot directly access the system uncertainties for the purpose of suppressing their presence; hence, the closed-loop stability characteristics of the model reference adaptive control architecture overviewed in Section 6.2.1 no longer hold. To address this challenge, a well-respected approach in the aerospace engineering field is the (pseudo-control) hedging method [30–33] (also see [95, 117, 118] and references therein). In particular, this method alters the “ideal” reference model trajectory given by (6.4) with a hedging term to allow for “correct” adaptation in the presence of actuator dynamics. In this case, the (altered) reference model is given by

$$\dot{x}_r(t) = \underbrace{A_r x_r(t) + B_r c(t)}_{\text{Ideal Reference Model}} + \underbrace{B(v(t) - u(t))}_{\text{Hedging Term}}, \quad x_r(0) = x_{r0}. \quad (6.10)$$

Now, as in [95], let the feedback control law be given by

$$u(t) = -K_1 x(t) + K_2 c(t) - \hat{W}^T(t)x(t) - \delta \hat{\Lambda}(t)v(t), \quad (6.11)$$

where $K_1 \in \mathbb{R}^{n \times m}$ and $K_2 \in \mathbb{R}^{m \times m}$ are defined the same as in Section 6.2.1, $\hat{W}(t) \in \mathbb{R}^{n \times m}$ satisfies the weight update law given by (6.7), and $\delta \hat{\Lambda}(t) \in \mathbb{R}^{m \times m}$ satisfies the weight update law given by

$$\delta \dot{\hat{\Lambda}}(t) = \alpha \text{Proj}_m[\delta \hat{\Lambda}(t), B^T P e(t)v^T(t)], \quad \delta \hat{\Lambda}(0) = \delta \hat{\Lambda}_0. \quad (6.12)$$

It follows from adding and subtracting “ $Bu(t)$ ” in (6.1) and using (6.11), the uncertain dynamical system can be written as

$$\dot{x}(t) = A_r x(t) + B_r c(t) - B(\tilde{W}^T(t)x(t) + \delta \tilde{\Lambda}(t)v(t)) + B(v(t) - u(t)). \quad (6.13)$$

The error dynamics then follow from (6.10) and (6.13) as

$$\dot{e}(t) = A_r e(t) - B(\tilde{W}^T(t)x(t) + \delta \tilde{\Lambda}(t)v(t)), \quad e(0) = e_0. \quad (6.14)$$

By considering the Lyapunov candidate function in Section 6.2.1 and using (6.7), (6.12), and (6.14) one can show the Lyapunov stability; hence, boundedness of the solution $(e(t), \bar{W}(t), \delta\tilde{\Lambda}(t))$. To conclude $e(t) \rightarrow 0$ as $t \rightarrow \infty$, the boundedness of the modified reference model given by (6.10) is necessary. As shown in [95], one can augment the reference model dynamics given by (6.10) and the actuator dynamics given by (6.2) as

$$\begin{bmatrix} \dot{x}_r(t) \\ \dot{v}(t) \end{bmatrix} = \underbrace{\begin{bmatrix} A + B\hat{W}^T(t) & B(I_m + \delta\hat{\Lambda}(t)) \\ -M(K_1 + \hat{W}^T(t)) & -M(I_m + \delta\hat{\Lambda}(t)) \end{bmatrix}}_{\mathcal{A}(\hat{W}(t), \delta\hat{\Lambda}(t))} \begin{bmatrix} x_r(t) \\ v(t) \end{bmatrix} + \underbrace{\begin{bmatrix} B(K + \hat{W}^T(t))e(t) \\ M(K_2c(t) - (K + \hat{W}^T(t))e(t)) \end{bmatrix}}_{\omega(\cdot)}. \quad (6.15)$$

Since $\omega(\cdot)$ is a bounded perturbation, one can conclude that $x_r(t)$ and $v(t)$ are bounded provided that $\mathcal{A}(\hat{W}(t), \delta\hat{\Lambda}(t))$ is quadratically stable (i.e., $\mathcal{A}^T(\hat{W}(t), \delta\hat{\Lambda}(t))\mathcal{P} + \mathcal{P}\mathcal{A}(\hat{W}(t), \delta\hat{\Lambda}(t)) < 0$, $\mathcal{P} = \mathcal{P}^T > 0$). This condition can be satisfied using LMIs (we refer to [95] for details). Now one can conclude that $e(t) \rightarrow 0$ as $t \rightarrow \infty$ by application of Barbalat's lemma [88] once again achieving the classical objective of the model reference adaptive control problem, but now for the presence of actuator dynamics through the alteration of the ideal reference model dynamics with the hedging term.

6.2.3 Objectives of the Paper

Now, as overviewed in Section 6.2.2, the hedging approach [30–33, 95, 117, 118] is a way to address the challenge resulting from the presence of actuator dynamics in uncertain dynamical systems. However, by altering the trajectory of the ideal reference model with the hedging term, one introduces additional transient terms to the reference model. One important transient term introduced is the system error signal $e(t)$ that appears inside the term $\omega(\cdot)$ of (6.15) (see also Remark 6.3.2). This particular transient term is important, because while it is guaranteed that the system error asymptotically vanishes, it is not known, without conservatism, how the transients of $e(t)$ behave such that the trajectory of the the hedged reference model can deviate from the ideal reference model trajectory in an unpredictable fashion.

The objectives of this paper can now be stated as follows: Consider the uncertain dynamical system given by (6.1) with the actuator dynamics given by (6.2). Design an adaptive control architecture such that:

- i) The trajectories of the uncertain dynamical system follow the trajectories of a desired expanded reference model, where this model does not include the effect from the system error $e(t)$ (Section 6.3);
- ii) Convergence to the ideal reference model given by (6.4) can be guaranteed (Section 6.4);
- iii) Robustness to uncertainty in the actuator bandwidths M is obtained (Section 6.5).

6.3 Expanded Reference Models for Uncertain Dynamical Systems with Actuator Dynamics

We now introduce the proposed adaptive control architecture that allows for trajectories of the uncertain dynamical system given by (6.1) to follow the trajectories of a desired reference model not including the transients of the system error $e(t)$. For this purpose, we consider an actuator model⁴ and design an expanded reference model as

$$\underbrace{\begin{bmatrix} \dot{x}_r(t) \\ \dot{v}_r(t) \end{bmatrix}}_{z_r(t)} = \underbrace{\begin{bmatrix} A + B\hat{W}^T(t) & B(I_m + \delta\hat{\Lambda}(t)) \\ -M(K_1 + \hat{W}^T(t)) & -M(I_m + \delta\hat{\Lambda}(t)) \end{bmatrix}}_{F_r(\hat{W}(t), \delta\hat{\Lambda}(t))} \underbrace{\begin{bmatrix} x_r(t) \\ v_r(t) \end{bmatrix}}_{z_r(t)} + \underbrace{\begin{bmatrix} 0_{n \times m} \\ MK_2 \end{bmatrix}}_{G_r} c(t) \quad (6.16)$$

where $K_1 \in \mathbb{R}^{m \times n}$ and $K_2 \in \mathbb{R}^{m \times m}$ are the nominal gains designed such that $A_r = A - BK_1$ is Hurwitz, $B_r = BK_2$ with K_2 being nonsingular, and $-EA_r^{-1}B_r = I$ with $E \in \mathbb{R}^{m \times n}$ being a matrix that allows a user to select a subset $x(t)$ to follow $c(t)$. In addition, $\hat{W}(t) \in \mathbb{R}^{n \times m}$ and $\delta\hat{\Lambda}(t) \in \mathbb{R}^{m \times m} \cap \mathbb{D}^{m \times m}$ are the estimates of W and $\delta\Lambda$ respectively for which the weight update laws are introduced later^{5,6}.

⁴The assumed knowledge of the actuator bandwidth of the actuator model is relaxed in Section 6.5. Because, in real-world applications, this bandwidth may not be precisely known but it is usually known with some error tolerance.

⁵While the reference model design in [132] is similar in spirit to the proposed expanded reference model, one significant difference however is that the reference model matrix in [132] is designed using a matching condition assumption, where some of the matrices used to construct the reference model matrix also include the system uncertainties such that it may not always be possible to obtain an appropriate reference model matrix without explicit information of the system. In contrast, the expanded reference model proposed in this paper, is shown to be purely constructed of known matrices and known signals. In addition, the weight update law in [132] includes the actuator bandwidth m (scalar case) in the input matrix, whereas the proposed weight update laws in this paper do not. This is important, because if the actuator bandwidth is sufficiently large, the weight update law in [132] will produce a high gain adaptation effect (high-frequency oscillations in the control signal) which can cause instability through excited unmodeled dynamics or violated rate saturation limits.

⁶Stability of the proposed expanded reference model is addressed in Theorem 6.3.1.

Remark 6.3.1 The hedged reference model dynamics in (6.15) can be equivalently written as

$$\begin{bmatrix} \dot{x}_r(t) \\ \dot{v}(t) \end{bmatrix} = \underbrace{\begin{bmatrix} A + B\hat{W}^T(t) & B(I_m + \delta\hat{\Lambda}(t)) \\ -M(K_1 + \hat{W}^T(t)) & -M(I_m + \delta\hat{\Lambda}(t)) \end{bmatrix}}_{\mathcal{A}(\hat{W}(t), \delta\hat{\Lambda}(t))} \begin{bmatrix} x_r(t) \\ v(t) \end{bmatrix} + \underbrace{\begin{bmatrix} 0_{n \times m} \\ MK_2 \end{bmatrix}}_{\mathcal{B}_r} c(t) + \underbrace{\begin{bmatrix} B(K_1 + \hat{W}^T(t))e(t) \\ -(K_1 + \hat{W}^T(t))e(t) \end{bmatrix}}_{\phi(e(t))}. \quad (6.17)$$

Since the proposed expanded reference model given by (6.16) does not contain the additional $\phi(e(t))$ term as in (6.17), it is not be effected by the unpredictable transients of the system error. Thus, the proposed architecture does not significantly alter the trajectories from the ideal reference model as compared with the hedging approach. In fact, the structure of the expanded reference model given by (6.16) is intuitive (see the next remark).

Remark 6.3.2 The proposed expanded reference model given by (6.16) approximates the ideal reference model dynamics given by (6.4) as the actuator bandwidths become large. To elucidate this in a simple setting, without loss of generality, consider the scalar control input case as

$$\dot{x}_r(t) = (A + B\hat{W}^T(t))x_r(t) + B(1 + \delta\hat{\lambda}(t))v_r(t), \quad (6.18)$$

$$\dot{v}_r(t) = -m(K_1 + \hat{W}^T(t))x_r(t) - m(1 + \delta\hat{\lambda}(t))v_r(t) + mK_2c(t). \quad (6.19)$$

In the Laplace domain with zero initial conditions, (6.19) can be written as

$$V_r(s) = \frac{\Phi(s)}{m^{-1}s + 1}, \quad (6.20)$$

where $\Phi(s) = \mathcal{L} \left\{ -(K_1 + \hat{W}^T(t))x_r(t) - \delta\hat{\lambda}(t)v_r(t) + K_2c(t) \right\}$. In addition, one can equivalently write (6.18) as

$$\begin{aligned} \dot{x}_r(t) &= (A - BK_1)x_r(t) + BK_2c(t) + B(v_r(t) + (K_1 + \hat{W}^T(t))x_r(t) + \delta\hat{\lambda}(t)v_r(t) - K_2c(t)) \\ &= A_r x_r(t) + B_r c(t) + B(v_r(t) - \phi(t)), \end{aligned} \quad (6.21)$$

or in the Laplace domain with zero initial conditions as

$$sX_r(s) = A_r X_r(s) + B_r C(s) + B(V_r(s) - \Phi(s)). \quad (6.22)$$

Now, using (6.20) in (6.22) it follows that

$$sX_r(s) = A_r X_r(s) + B_r C(s) + B \left[\frac{1}{m^{-1}s + 1} - 1 \right] \Phi(s), \quad (6.23)$$

such that one can make the intuitive argument as m , the actuator bandwidth, becomes large, the reference model dynamics given by (6.18) and (6.19) closely approximates the ideal reference model dynamics given by (6.4) (i.e. $\dot{x}_r(t) = A_r x_r(t) + B_r c(t)$) owing to the fact that the term in brackets of (6.23) becomes small as m becomes large. This presents the intuition behind the structure of the expanded reference model given by (6.16).

Next, to achieve tracking of the expanded reference model (6.16), let the feedback control law be given by

$$u(t) = -K_1 x(t) + K_2 c(t) - \hat{W}^T(t) x(t) - \delta \hat{\Lambda}(t) v(t), \quad (6.24)$$

where $\hat{W}(t)$ satisfies the weight update law

$$\dot{\hat{W}}(t) = \gamma \text{Proj}_m [\hat{W}(t), x(t) \tilde{z}^T(t) \mathcal{P} B^*], \quad \hat{W}(0) = \hat{W}_0, \quad (6.25)$$

with $\gamma \in \mathbb{R}_+$ being the learning rate, $\tilde{z}(t) = [e^T(t), \tilde{v}^T(t)]^T \in \mathbb{R}^{n+m}$ being the augmented error of the system error state vector $e(t) \in \mathbb{R}^n$ and the actuator output error $\tilde{v}(t) \triangleq v(t) - v_r(t) \in \mathbb{R}^m$, $\mathcal{P} \in \mathbb{R}_+^{(n+m) \times (n+m)}$ being a solution of a matrix inequality for which further details are given below, and $B^* = [B^T, 0_{m \times m}]^T \in \mathbb{R}^{(n+m) \times m}$. In addition, the projection bounds are defined such that $\hat{w}_{\min, i+(j-1)n} \leq [\hat{W}(t)]_{ij} \leq \hat{w}_{\max, i+(j-1)n}$, for $i = 1, \dots, n$ and $j = 1, \dots, m$. Moreover, $\delta \hat{\Lambda}(t)$ is constructed from the elemental weight update laws

$$\delta \hat{\lambda}_i(t) = \alpha_i \text{Proj} [\delta \hat{\lambda}_i(t), v_i(t) \tilde{z}^T(t) \mathcal{P} B^* \mathbf{e}_i], \quad \delta \hat{\lambda}_i(0) = \delta \hat{\lambda}_{i0}, \quad i = 1, \dots, m, \quad (6.26)$$

where $\alpha_i \in \mathbb{R}_+$ are the learning rates for each respective element, $v_i(t)$ is the i^{th} element of the actuator output vector, and \mathbf{e}_i is the standard basis for $i = 1, \dots, m$. Note here that by elementally updating we can set $\delta \hat{\Lambda}(t) \triangleq \text{diag}([\delta \hat{\lambda}_1(t), \delta \hat{\lambda}_2(t), \dots, \delta \hat{\lambda}_m(t)])$ to estimate the uncertain diagonal elements of $\delta \Lambda$. The elemental projection bounds are defined such that $\delta \hat{\lambda}_{i, \min} \leq \delta \hat{\lambda}_i(t) \leq \delta \hat{\lambda}_{i, \max}$, for $i = 1, \dots, m$. The definition of the projection operator [6] used in the weight update laws is given the Appendix A.

Now, using (6.24) in (6.2) and adding and subtracting $B\hat{W}^T(t)x(t)$ and $B\delta\hat{\Lambda}(t)v(t)$ to (6.1) we can write the uncertain dynamical system and the actuator dynamics as

$$\dot{x}(t) = (A + B\hat{W}^T(t))x(t) + B(I_m + \delta\hat{\Lambda}(t))v(t) + B(\tilde{W}^T(t)x(t) + \delta\tilde{\Lambda}(t)v(t)), \quad (6.27)$$

$$\dot{v}(t) = -M(K_1 + \hat{W}^T(t))x(t) - M(I_m + \delta\hat{\Lambda}(t))v(t) + MK_2c(t), \quad (6.28)$$

which can be written in compact form as

$$\dot{z}(t) = F_r(\hat{W}(t), \delta\hat{\Lambda}(t))z(t) + G_r c(t) - B^*(\tilde{W}^T(t)x(t) + \delta\tilde{\Lambda}(t)v(t)). \quad (6.29)$$

where $z(t) \triangleq [x^T(t), v^T(t)]^T$, $\tilde{W}(t) = \hat{W}(t) - W \in \mathbb{R}^{n \times m}$, and $\delta\tilde{\Lambda}(t) = \delta\hat{\Lambda}(t) - \delta\Lambda \in \mathbb{R}^{m \times m} \cap \mathbb{D}^{m \times m}$. Defining the augmented error $\tilde{z}(t) \triangleq z(t) - z_r(t)$, the following error dynamics can be written from (6.29) and (6.16) as

$$\dot{\tilde{z}}(t) = F_r(\hat{W}(t), \delta\hat{\Lambda}(t))\tilde{z}(t) - B^*(\tilde{W}^T(t)x(t) + \delta\tilde{\Lambda}(t)v(t)), \quad \tilde{z}(0) = \tilde{z}_0, \quad (6.30)$$

which, owing to the diagonal structure of $\delta\tilde{\Lambda}(t)$, can be equivalently rewritten as

$$\dot{\tilde{z}}(t) = F_r(\hat{W}(t), \delta\hat{\Lambda}(t))\tilde{z}(t) - B^*\left(\tilde{W}^T(t)x(t) + \sum_{i=1}^m \mathbf{e}_i \delta\tilde{\lambda}_i(t)v_i(t)\right), \quad \tilde{z}(0) = \tilde{z}_0. \quad (6.31)$$

The following assumption, which captures the fundamental interplay between the allowable system uncertainties and actuator dynamics, is necessary for the feasibility of the model reference adaptive control in the presence of actuator dynamics (also see (6.39) in the proof of Theorem 6.3.1 later).

Assumption 6.3.1 *The matrix given by*

$$\mathcal{A}(\hat{W}(t), \delta\hat{\Lambda}(t), \varepsilon) = \begin{bmatrix} A + B\hat{W}^T(t) + \frac{\varepsilon}{2}I_n & B(I_m + \delta\hat{\Lambda}(t)) \\ -M(K_1 + \hat{W}^T(t)) & -M(I_m + \delta\hat{\Lambda}(t)) + \frac{\varepsilon}{2}I_m \end{bmatrix}, \quad (6.32)$$

with $\varepsilon \in \mathbb{R}_+$ being a design parameter, is quadratically stable.

Remark 6.3.3 *By definition, (6.32) is quadratically stable if and only if there exists a $\mathcal{P} > 0$ such that $\mathcal{A}^T(\hat{W}(t), \delta\hat{\Lambda}(t), \varepsilon)\mathcal{P} + \mathcal{P}\mathcal{A}(\hat{W}(t), \delta\hat{\Lambda}(t), \varepsilon) < 0$ holds [97, 98]. Using LMIs, we can satisfy the quadratic*

stability of (6.32) for given projection bounds \hat{W}_{\max} and $\delta\hat{\lambda}_{\max}$ for the elements of $\hat{W}(t)$ and $\delta\hat{\Lambda}(t)$ respectively, the bandwidths of the actuator dynamics M , and the design parameter ε . For this purpose, let $\overline{W}_{i_1, \dots, i_f} \in \mathbb{R}^{n \times m}$ be defined as

$$\overline{W}_{i_1, \dots, i_f} = \begin{bmatrix} i_1 \hat{w}_{\max,1} + (1-i_1) \hat{w}_{\min,1} & i_{1+n} \hat{w}_{\max,1+n} + (1-i_{1+n}) \hat{w}_{\min,1+n} \\ i_2 \hat{w}_{\max,2} + (1-i_2) \hat{w}_{\min,2} & i_{2+n} \hat{w}_{\max,2+n} + (1-i_{2+n}) \hat{w}_{\min,2+n} \\ \vdots & \vdots \\ i_n \hat{w}_{\max,n} + (1-i_n) \hat{w}_{\min,n} & i_{2n} \hat{w}_{\max,2n} + (1-i_{2n}) \hat{w}_{\min,2n} \\ \dots & i_{1+(m-1)n} \hat{w}_{\max,1+(m-1)n} + (1-i_{1+(m-1)n}) \hat{w}_{\min,1+(m-1)n} \\ \dots & i_{2+(m-1)n} \hat{w}_{\max,2+(m-1)n} + (1-i_{2+(m-1)n}) \hat{w}_{\min,2+(m-1)n} \\ \dots & \vdots \\ \dots & i_{mn} \hat{w}_{\max,mn} + (1-i_{mn}) \hat{w}_{\min,mn} \end{bmatrix}, \quad (6.33)$$

where $i_f \in \{0,1\}$, $f \in \{1, \dots, 2^{mn}\}$, such that $\overline{W}_{i_1, \dots, i_f}$ represents the corners of the hypercube defining the variation of $\hat{W}(t)$, and

$$\overline{\delta\Lambda}_{i_1, \dots, i_g} = \text{diag} \left([i_1 \delta\hat{\lambda}_{\max,1} + (1-i_1) \delta\hat{\lambda}_{\min,1}, \dots, i_m \delta\hat{\lambda}_{\max,m} + (1-i_m) \delta\hat{\lambda}_{\min,m}] \right), \quad (6.34)$$

where $i_g \in \{0,1\}$, $g \in \{1, \dots, 2^m\}$, such that $\overline{\delta\Lambda}_{i_1, \dots, i_g}$ represents the corners of the hypercube defining the variation of $\delta\hat{\Lambda}(t)$. Now, let

$$\mathcal{A}_{i_1, \dots, i_h} = \begin{bmatrix} A + B \overline{W}_{i_1, \dots, i_f}^T + \frac{\varepsilon}{2} I_n & B(I_m + \overline{\delta\Lambda}_{i_1, \dots, i_g}) \\ -M(K_1 + \overline{W}_{i_1, \dots, i_f}^T) & -M(I_m + \overline{\delta\Lambda}_{i_1, \dots, i_g}) + \frac{\varepsilon}{2} I_m \end{bmatrix}, \quad (6.35)$$

where $h \in \{1, \dots, 2^m + 2^{mn}\}$ be the corners of the hypercube constructed from all the permutations of $\overline{W}_{i_1, \dots, i_f}$ and $\overline{\delta\Lambda}_{i_1, \dots, i_g}$. For a given M , it can then be shown that

$$\mathcal{A}_{i_1, \dots, i_h}^T \mathcal{P} + \mathcal{P} \mathcal{A}_{i_1, \dots, i_h} < 0, \quad \mathcal{P} > 0, \quad (6.36)$$

implies that $\mathcal{A}^T(\hat{W}(t), \delta\hat{\Lambda}(t), \varepsilon)\mathcal{P} + \mathcal{P}\mathcal{A}(\hat{W}(t), \delta\hat{\Lambda}(t), \varepsilon) < 0$ [96, 99]; thus, one can solve the LMI given by (6.36) to calculate \mathcal{P} , which is then used in the weight update laws (6.25) and (6.26).

Now that Assumption 6.3.1 can be satisfied through the use of LMIs as shown in Remark 6.3.3, we are ready to state the following theorem.

Theorem 6.3.1 Consider the uncertain dynamical system given by (6.1), the actuator dynamics given by (6.2), the expanded reference model given by (6.16), the feedback control law given by (6.24), and the update laws given by (6.25) and (6.26). Under Assumption 6.3.1, the solution $(\tilde{z}(t), \tilde{W}(t), \delta\tilde{\Lambda}(t))$ of the closed-loop dynamical system is bounded, $\lim_{t \rightarrow \infty} e(t) = 0$, and $\lim_{t \rightarrow \infty} \tilde{v}(t) = 0$.

Proof. To show the Lyapunov stability; hence, the boundedness of the solution $(\tilde{z}(t), \tilde{W}(t), \delta\tilde{\Lambda}(t))$, consider the Lyapunov function candidate given by

$$\mathcal{V}(\tilde{z}, \tilde{W}, \delta\tilde{\Lambda}) = \tilde{z}^T \mathcal{P} \tilde{z} + \gamma^{-1} \text{tr} \tilde{W}^T \tilde{W} + \sum_{i=1}^m \alpha_i^{-1} \delta \tilde{\lambda}_i^2. \quad (6.37)$$

Note that $\mathcal{V}(0, 0, 0) = 0$ and $\mathcal{V}(\tilde{z}, \tilde{W}, \delta\tilde{\Lambda}) > 0$ for all $(\tilde{z}, \tilde{W}, \delta\tilde{\Lambda}) \neq (0, 0, 0)$. Differentiating (6.37) along the closed-loop system trajectories and using (6.25) and (6.26) yields

$$\begin{aligned} \dot{\mathcal{V}}(\tilde{z}(t), \tilde{W}(t), \delta\tilde{\Lambda}(t)) &= 2\tilde{z}^T(t) \mathcal{P} \left(F_r(\hat{W}(t), \delta\hat{\Lambda}(t)) \tilde{z}(t) - B^* \tilde{W}^T(t) x(t) - B^* \sum_{i=1}^m \mathbf{e}_i \delta \tilde{\lambda}_i(t) v_i(t) \right) \\ &\quad + 2\gamma^{-1} \text{tr} \tilde{W}^T(t) \dot{\hat{W}}(t) + 2 \sum_{i=1}^m \alpha_i^{-1} \delta \tilde{\lambda}_i(t) \delta \dot{\tilde{\lambda}}_i(t) \\ &= \tilde{z}^T(t) \left(F_r^T(\hat{W}(t), \delta\hat{\Lambda}(t)) \mathcal{P} + \mathcal{P} F_r(\hat{W}(t), \delta\hat{\Lambda}(t)) \right) \tilde{z}(t) \\ &\quad - 2\tilde{z}^T(t) \mathcal{P} B^* \tilde{W}^T(t) x(t) + 2\gamma^{-1} \text{tr} \tilde{W}^T(t) \dot{\hat{W}}(t) \\ &\quad - 2\tilde{z}^T(t) \mathcal{P} B^* (\mathbf{e}_1 \delta \tilde{\lambda}_1(t) v_1(t) + \mathbf{e}_2 \delta \tilde{\lambda}_2(t) v_2(t) + \dots + \mathbf{e}_m \delta \tilde{\lambda}_m(t) v_m(t)) \\ &\quad + 2(\alpha_1^{-1} \delta \tilde{\lambda}_1(t) \delta \dot{\tilde{\lambda}}_1(t) + \alpha_2^{-1} \delta \tilde{\lambda}_2(t) \delta \dot{\tilde{\lambda}}_2(t) + \dots + \alpha_m^{-1} \delta \tilde{\lambda}_m(t) \delta \dot{\tilde{\lambda}}_m(t)) \\ &= \tilde{z}^T(t) \left(F_r^T(\hat{W}(t), \delta\hat{\Lambda}(t)) \mathcal{P} + \mathcal{P} F_r(\hat{W}(t), \delta\hat{\Lambda}(t)) \right) \tilde{z}(t) \\ &\quad + 2\gamma^{-1} \text{tr} \tilde{W}^T(t) \left(\dot{\hat{W}}(t) - \gamma x(t) \tilde{z}^T(t) \mathcal{P} B^* \right) \\ &\quad + 2 \sum_{i=1}^m \alpha_i^{-1} \delta \tilde{\lambda}_i(t) (\delta \dot{\tilde{\lambda}}_i(t) - \alpha_i v_i(t) \tilde{z}^T(t) \mathcal{P} B^* \mathbf{e}_i) \\ &\leq \tilde{z}^T(t) \left(F_r^T(\hat{W}(t), \delta\hat{\Lambda}(t)) \mathcal{P} + \mathcal{P} F_r(\hat{W}(t), \delta\hat{\Lambda}(t)) \right) \tilde{z}(t). \end{aligned} \quad (6.38)$$

By adding and subtracting $\frac{\varepsilon}{2}I$, it follows that (6.38) can be equivalently written as

$$\begin{aligned}
& \dot{V}(\tilde{z}(t), \tilde{W}(t), \delta\tilde{\Lambda}(t)) \\
& \leq \tilde{z}^T(t) \left(\left(F_r(\hat{W}(t), \delta\hat{\Lambda}(t)) + \frac{\varepsilon}{2} I_{n+m} \right)^T \mathcal{P} + \mathcal{P} \left(F_r(\hat{W}(t), \delta\hat{\Lambda}(t)) + \frac{\varepsilon}{2} I_{n+m} \right) \right) \tilde{z}(t) - \varepsilon \tilde{z}^T(t) \mathcal{P} \tilde{z}(t) \\
& = \tilde{z}^T(t) \left(\mathcal{A}^T(\hat{W}(t), \delta\hat{\Lambda}(t), \varepsilon) \mathcal{P} + \mathcal{P} \mathcal{A}(\hat{W}(t), \delta\hat{\Lambda}(t), \varepsilon) \right) \tilde{z}(t) - \varepsilon \tilde{z}^T(t) \mathcal{P} \tilde{z}(t). \tag{6.39}
\end{aligned}$$

Since $\mathcal{A}(\hat{W}(t), \delta\hat{\Lambda}(t), \varepsilon)$ is quadratically stable by Assumption 6.3.1 (satisfied using LMIs, see Remark 6.3.3), it follows further from (6.39) that $\dot{V}(\tilde{z}(t), \tilde{W}(t), \delta\tilde{\Lambda}(t)) \leq -\varepsilon \tilde{z}^T(t) \mathcal{P} \tilde{z}(t) \leq 0$, which guarantees the boundedness of the solution $(\tilde{z}(t), \tilde{W}(t), \delta\tilde{\Lambda}(t))$.

To conclude $\lim_{t \rightarrow \infty} e(t) = 0$ and $\lim_{t \rightarrow \infty} \tilde{v}(t) = 0$ it is necessary to show that $x_r(t)$ is bounded. From Assumption 6.3.1, it follows that $\mathcal{A}^T(\hat{W}(t), \delta\hat{\Lambda}(t), \varepsilon) \mathcal{P} + \mathcal{P} \mathcal{A}(\hat{W}(t), \delta\hat{\Lambda}(t), \varepsilon) < 0$, which can be equivalently written as $F_r^T(\hat{W}(t), \delta\hat{\Lambda}(t)) \mathcal{P} + \mathcal{P} F_r(\hat{W}(t), \delta\hat{\Lambda}(t)) < -\varepsilon \mathcal{P} < 0$, and hence, $F_r(\hat{W}(t), \delta\hat{\Lambda}(t))$ is quadratically stable. Since $F_r(\hat{W}(t), \delta\hat{\Lambda}(t))$ is quadratically stable and $G_{rc}(t)$ is bounded, it follows that $x_r(t)$ and $v_r(t)$ are bounded. It follows that $\ddot{V}(\tilde{z}(t), \hat{W}(t), \delta\hat{\Lambda}(t))$ is bounded⁷ such that from Barbalat's lemma [88] it can be concluded that $\lim_{t \rightarrow \infty} \dot{V}(\tilde{z}(t), \hat{W}(t), \delta\hat{\Lambda}(t)) = 0$; hence, $\lim_{t \rightarrow \infty} e(t) = 0$ and $\lim_{t \rightarrow \infty} \tilde{v}(t) = 0$. ■

As discussed in Remark 6.3.1, the proposed adaptive control architecture can improve the performance as compared to the hedging approach by removing the transients of the system error $e(t)$ from the proposed expanded reference model. In addition, as shown in Theorem 6.3.1, the trajectories of the uncertain dynamical system follow the trajectories of the desired reference model. Yet, like the hedging approach but without depending on the system error, the proposed expanded reference model still alters the ideal reference model given by (6.4) (especially when the actuator bandwidths are small, see Remark 6.3.2), such that the trajectories can still be modified from the trajectories which capture the desired closed-loop dynamical system performance. In the next section, we show that the proposed expanded reference model can be guaranteed to converge to the ideal reference model given by (6.4) such that the desired closed-loop dynamical system performance can be captured by the uncertain dynamical system.

6.4 A Command Governor Architecture for Performance Guarantees

In this section, we provide guarantees on the performance of the proposed adaptive control architecture. This is done by implementing a command governor architecture in the expanded reference model presented in the previous section such that its trajectories converge, in a predictable fashion, to the

⁷Additional details and discussion on the boundedness of $\ddot{V}(\cdot)$ are given in Remark 6.4.1.

trajectories of the ideal reference model⁸. Now, we augment the expanded reference model given by (6.16) with a command governor architecture as

$$\dot{z}_r(t) = F_r(\hat{W}(t), \delta\hat{\Lambda}(t))z_r(t) + G_r c_g(t) \quad (6.40)$$

$$c_g(t) = c(t) + D\xi(t), \quad (6.41)$$

where $c(t) \in \mathbb{R}^m$ is the uniformly continuous smooth and bounded reference command used in (6.4) and (6.16) (since $c(t)$ is a user-defined smooth function, we implicitly assume that $\dot{c}(t)$ is bounded as well as available) and $D\xi(t) \in \mathbb{R}^m$ is a command governor signal with $D \triangleq K_2^{-1}M^{-1} \in \mathbb{R}^{m \times m}$ and $\xi(t) \in \mathbb{R}^m$ being the command governor output given by

$$\xi(t) = (I_m + \delta\hat{\Lambda}(t))^{-1}(-\mu\rho(t) - \phi_1(t)) - \phi_2(t), \quad (6.42)$$

where $\mu \in \mathbb{R}_+$ is the command governor gain, $\rho \in \mathbb{R}^m$ is the command governor state vector

$$\rho(t) \triangleq (K_1 + \hat{W}^T(t))x_r(t) + (I_m + \delta\hat{\Lambda}(t))v_r(t) - K_2c(t). \quad (6.43)$$

In addition, a backstepping-like approach is used to design the command governor signals⁹

$$\begin{aligned} \phi_1(t) &\triangleq (K_1 + \hat{W}^T(t)) \left((A + B\hat{W}^T(t))x_r(t) + B(I_m + \delta\hat{\Lambda}(t))v_r(t) \right) - K_2\dot{c}(t) \\ &\quad + \delta\dot{\hat{\Lambda}}(t)v_r(t) + \dot{\hat{W}}^T(t)x_r(t) \\ &= (K_1 + \hat{W}^T(t)) \left((A + B\hat{W}^T(t))x_r(t) + B(I_m + \delta\hat{\Lambda}(t))v_r(t) \right) - K_2\dot{c}(t) \\ &\quad + \text{diag} \left(\left[\alpha_i \text{Proj} \left[\delta\hat{\lambda}_i(t), v_i(t)\tilde{z}^T(t)\mathcal{P}B^*e_i \right] \right] \right) v_r(t) \\ &\quad + \gamma \left(\text{Proj}_m \left[\hat{W}(t), x(t)\tilde{z}^T(t)\mathcal{P}B^* \right] \right)^T x_r(t), \quad i = 1, \dots, m, \end{aligned} \quad (6.44)$$

$$\phi_2(t) \triangleq -M(K_1 + \hat{W}^T(t))x_r(t) - M(I_m + \delta\hat{\Lambda}(t))v_r(t) + MK_2c(t). \quad (6.45)$$

⁸A command governor architecture is also used by the authors in [81] to improve transient performance and [19] for dynamical systems with unmatched uncertainties. The implementation of the proposed command governor architecture in this paper is however different from these in that we use it with the reference model to improve its performance in the presence of actuator dynamics. We also refer to the survey paper [133] for more applications of command governors (also referred to as reference shaping techniques) for both adaptive and non-adaptive control architectures.

⁹We refer to the proof of Theorem 6.4.1 and particularly (6.55)–(6.57) for how (6.44) and (6.45) are designed.

It should be noted that $K_1 \in \mathbb{R}^{m \times n}$ and $K_2 \in \mathbb{R}^{m \times m}$ are the same nominal control gains given in Section 6.3, $\hat{W} \in \mathbb{R}^{n \times m}$ satisfies the weight update law given by (6.25), and $\delta \hat{\Lambda}(t) \triangleq \text{diag}([\delta \hat{\lambda}_1(t), \delta \hat{\lambda}_2(t), \dots, \delta \hat{\lambda}_m(t)])$ satisfies the elemental update laws given by (6.26). The only additional modification is to the feedback control law now given by

$$u(t) = -K_1 x(t) + K_2 c_g(t) - \hat{W}^T(t)x(t) - \delta \hat{\Lambda}(t)v(t), \quad (6.46)$$

to achieve tracking of the command governor based expanded reference model given by (6.40).

As in Section 6.3, by adding and subtracting $B\hat{W}^T(t)x(t)$ and $B\delta \hat{\Lambda}(t)v(t)$ to (6.1) and now using (6.46) in (6.2), we can write the augmented uncertain dynamical system and actuator dynamics in compact form as

$$\dot{z}(t) = F_r(\hat{W}(t), \delta \hat{\Lambda}(t))z(t) + G_r c_g(t) - B^*(\tilde{W}^T(t)x(t) + \delta \tilde{\Lambda}(t)v(t)). \quad (6.47)$$

It then follows from (6.40) and (6.47) that the system error dynamics can be given identically as (6.30) (equivalently written as (6.31)).

Lemma 6.4.1 *Consider the uncertain dynamical system given by (6.1), the actuator dynamics given by (6.2), the expanded reference model given by (6.40), the feedback control law given by (6.46), and the update laws given by (6.25) and (6.26). Under Assumption 6.3.1, the solution $(\tilde{z}(t), \tilde{W}(t), \delta \tilde{\Lambda}(t))$ of the closed-loop dynamical system is bounded.*

Proof. Owing to the modification to the feedback control law given by (6.46) resulting in the same system error dynamics as in Section 6.3, the proof follows as the first part of the proof for Theorem 6.3.1. As a brief review of this, consider the Lyapunov function candidate given by (6.37). Differentiation of (6.37) and application of (6.25) and (6.26) results in $\dot{V}(\tilde{z}(t), \tilde{W}(t), \delta \tilde{\Lambda}(t)) \leq -\varepsilon \tilde{z}^T(t) \mathcal{P} \tilde{z}(t) \leq 0$, which guarantees the Lyapunov stability, and hence, the boundedness of the solution $(\tilde{z}(t), \tilde{W}(t), \delta \tilde{\Lambda}(t))$. ■

Remark 6.4.1 *As in the proof of Theorem 6.3.1, it is necessary to show the proposed expanded reference model given by (6.40) is bounded. This is because in order to use Barbalat's lemma [88] to show that $\lim_{t \rightarrow \infty} \dot{V}(\tilde{z}(t), \hat{W}(t), \delta \hat{\Lambda}(t)) = 0$, and hence, $\lim_{t \rightarrow \infty} e(t) = 0$ and $\lim_{t \rightarrow \infty} \tilde{v}(t) = 0$, one still needs to show that $\dot{V}(\tilde{z}(t), \tilde{W}(t), \delta \tilde{\Lambda}(t))$ is bounded. To elucidate this point, note that it follows from the proofs of Theorem*

6.3.1 and Lemma 6.4.1 that one can write

$$\begin{aligned}
\dot{V}(\tilde{z}(t), \tilde{W}(t), \delta\hat{\Lambda}(t)) &= -2\epsilon\tilde{z}^T(t)\mathcal{P}\dot{\tilde{z}}(t) \\
&= -2\epsilon\tilde{z}^T(t)\mathcal{P}\left(F_r(\hat{W}(t), \delta\hat{\Lambda}(t))\tilde{z}(t) - B^*\left(\tilde{W}^T(t)e(t) + \delta\tilde{\Lambda}(t)\tilde{v}(t)\right)\right. \\
&\quad \left.- B^*\left(\tilde{W}^T(t)x_r(t) + \delta\tilde{\Lambda}(t)v_r(t)\right)\right), \tag{6.48}
\end{aligned}$$

where at first, it is not yet known that $x_r(t)$ and $v_r(t)$ are bounded due to the expanded reference models considered in (6.16) (for Theorem 6.3.1) and (6.40) (for Lemma 6.4.1). As shown in the proof of Theorem 6.3.1, it is relatively straightforward to show boundedness of the expanded reference model given by (6.16) under Assumption 6.3.1, which implies the quadratic stability of $F_r(\hat{W}(t), \delta\hat{\Lambda}(t))$, and owing to the boundedness of the term “ $G_r c(t)$ ”; thus one can use Barbalat’s lemma to conclude the proof. This is where the analysis will differ for the modified expanded reference model given by (6.40), since it now includes the command governor architecture in the term “ $G_r c_g(t)$ ”.

Motivated by the discussion in Remark 6.4.1, we now show that the proposed implementation of the command governor architecture not only ensures boundedness of the expanded reference model given by (6.40), but also guarantees that the trajectories of the expanded reference model given in (6.40) asymptotically converges to the trajectories of the ideal reference model given by (6.4), capturing the desired closed-loop system performance. For this purpose, we restate the ideal reference model dynamics given by (6.4) with new notation as

$$\dot{x}_r(t) = A_r x_r(t) + B_r c(t), \quad x_r(0) = x_{r0}, \tag{6.49}$$

where $x_r(t) \in \mathbb{R}^n$ is the ideal reference model state. In addition, we define $\tilde{x}_r(t) \triangleq x_r(t) - x_r(t)$ to be the error between the modified reference model and the ideal reference model states.

Theorem 6.4.1 *Consider the uncertain dynamical system given by (6.1), the actuator dynamics given by (6.2), the ideal reference model given by (6.49), the modified expanded reference model given by (6.40), the command governor architecture given by (6.41), (6.42), (6.43), (6.44), and (6.45), the feedback control law given by (6.46), and the update laws given by (6.25) and (6.26). Under Assumption 6.3.1, then $(x_r(t), v_r(t))$ are bounded, $\lim_{t \rightarrow \infty} \tilde{x}_r(t) = 0$, $\lim_{t \rightarrow \infty} \rho(t) = 0$, $\lim_{t \rightarrow \infty} e(t) = 0$, and $\lim_{t \rightarrow \infty} \tilde{v}(t) = 0$.*

Proof. We first write the modified expanded reference model given by (6.40) in its augmented form as

$$\underbrace{\begin{bmatrix} \dot{x}_r(t) \\ \dot{v}_r(t) \end{bmatrix}}_{\dot{z}_r(t)} = \underbrace{\begin{bmatrix} A + B\hat{W}^T(t) & B(I_m + \delta\hat{\Lambda}(t)) \\ -M(K_1 + \hat{W}^T(t)) & -M(I_m + \delta\hat{\Lambda}(t)) \end{bmatrix}}_{F_r(\hat{W}(t), \delta\hat{\Lambda}(t))} \underbrace{\begin{bmatrix} x_r(t) \\ v_r(t) \end{bmatrix}}_{z_r(t)} + \underbrace{\begin{bmatrix} 0_{n \times m} \\ MK_2 \end{bmatrix}}_{G_r} c_g(t). \quad (6.50)$$

Considering the $x_r(t)$ dynamics, we add and subtract the terms “ $BK_1x_r(t)$ ” and “ $BK_2c(t)$ ” such that one can write

$$\begin{aligned} \dot{x}_r(t) &= (A - BK_1)x_r(t) + BK_2c(t) + B\left(K_1x_r(t) - K_2c(t) + \hat{W}^T(t)x_r(t) + (I_m + \delta\hat{\Lambda}(t))v_r(t)\right) \\ &= A_rx_r(t) + B_r c(t) + B\left((K_1 + \hat{W}^T(t))x_r(t) + (I_m + \delta\hat{\Lambda}(t))v_r(t) - K_2c(t)\right), \end{aligned} \quad (6.51)$$

which can be equivalently written using (6.43) as

$$\dot{x}_r(t) = A_rx_r(t) + B_r c(t) + B\rho(t). \quad (6.52)$$

Now, it follows from (6.49) and (6.52) that the reference model error dynamics between the ideal reference model and the proposed modified reference model can be given by

$$\dot{\tilde{x}}_r(t) = A_r\tilde{x}_r(t) + B\rho(t). \quad (6.53)$$

From (6.53), if we can show $\rho(t) \rightarrow 0$ as $t \rightarrow \infty$, then the modified reference model trajectories will converge to the ideal reference model trajectories. In light of this, we differentiate $\rho(t)$ in time to obtain the following dynamics

$$\dot{\rho}(t) = \dot{W}^T(t)x_r(t) + (K_1 + \hat{W}^T(t))\dot{x}_r(t) - K_2\dot{c}(t) + \delta\dot{\Lambda}(t)v_r(t) + (I_m + \delta\hat{\Lambda}(t))\dot{v}_r(t). \quad (6.54)$$

Using the $x_r(t)$ and $v_r(t)$ dynamics of (6.50) in (6.54) yields

$$\begin{aligned} \dot{\rho}(t) &= \dot{W}^T(t)x_r(t) + (K_1 + \hat{W}^T(t))\left((A + B\hat{W}^T(t))x_r(t) + B(I_m + \delta\hat{\Lambda}(t))v_r(t)\right) - K_2\dot{c}(t) + \delta\dot{\Lambda}(t)v_r(t) \\ &\quad + (I_m + \delta\hat{\Lambda}(t))\left[-M(K_1 + \hat{W}^T(t))x_r(t) - M(I_m + \delta\hat{\Lambda}(t))v_r(t) + MK_2 + \xi(t)\right]. \end{aligned} \quad (6.55)$$

Using the command governor signal (6.42) in (6.55) gives the following

$$\begin{aligned}\dot{\rho}(t) &= \hat{W}^T(t)x_r(t) + (K_1 + \hat{W}^T(t)) \left((A + B\hat{W}^T(t))x_r(t) + B(I_m + \delta\hat{\Lambda}(t))v_r(t) \right) - K_2\dot{c}(t) + \delta\hat{\Lambda}(t)v_r(t) \\ &\quad + (I_m + \delta\hat{\Lambda}(t)) \left[-M(K_1 + \hat{W}^T(t))x_r(t) - M(I_m + \delta\hat{\Lambda}(t))v_r(t) + MK_2 - \phi_2(t) \right] \\ &\quad - \mu\rho(t) - \phi_1(t)\end{aligned}\tag{6.56}$$

where applying the signals (6.44) and (6.45) results in the following dynamics

$$\dot{\rho}(t) = -\mu\rho(t).\tag{6.57}$$

Now, using (6.53) and (6.57), the error dynamics between the reference models can be written compactly as

$$\underbrace{\begin{bmatrix} \dot{\tilde{x}}_r(t) \\ \dot{\rho}(t) \end{bmatrix}}_{\chi_r(t)} = \underbrace{\begin{bmatrix} A_r & B \\ 0_{m \times n} & -\mu I_m \end{bmatrix}}_{\mathcal{A}_r} \underbrace{\begin{bmatrix} \tilde{x}_r(t) \\ \rho(t) \end{bmatrix}}_{\chi_r(t)}.\tag{6.58}$$

Since A_r is Hurwitz, $\mu > 0$, and \mathcal{A}_r is in upper triangular form, $\lim_{t \rightarrow \infty} \tilde{x}_r(t) = 0$ and $\lim_{t \rightarrow \infty} \rho(t) = 0$ are immediate.

Finally, since $x_{r_1}(t)$ is bounded and $x_r(t) = \tilde{x}_r(t) + x_{r_1}(t)$, it follows that $x_r(t)$ is bounded, and since x_r is bounded and $\rho(t)$ is bounded, and owing to the projection based weight update laws, $\hat{W}(t)$ and $\delta\hat{\Lambda}(t)$ are both bounded, and since the input command $c(t)$ is bounded, it follows from (6.43) that $v_r(t)$ is bounded. Now, as a consequence of Lemma 6.4.1, $\tilde{z}(t)$, $\tilde{W}(t)$ and $\delta\tilde{\Lambda}(t)$ are all bounded, such that it can now be concluded that $\dot{V}(\tilde{z}(t), \tilde{W}(t), \delta\tilde{\Lambda}(t))$ as given by (6.48) is bounded. Barbalat's lemma [88] can now be used to conclude that $\lim_{t \rightarrow \infty} \dot{V}(\tilde{z}(t), \tilde{W}(t), \delta\tilde{\Lambda}(t)) = 0$, and hence, $\lim_{t \rightarrow \infty} e(t) = 0$ and $\lim_{t \rightarrow \infty} \tilde{v}(t) = 0$. ■

Remark 6.4.2 *The performance guarantees obtained in this section can be seen from the augmented dynamics given by (6.58), which show that the modified expanded reference model trajectories converge to the ideal reference model trajectories when*

$$\chi_r(t) = e^{\mathcal{A}_r t} \chi_r(0),\tag{6.59}$$

vanishes, where it is well known that the rate of convergence depends on the maximum eigenvalue of \mathcal{A}_r . Moreover, if $\chi_r(0) = 0$ can be selected, then $\chi_r(t) = 0$ for all time and the modified expanded reference model trajectories exactly capture the desired closed-loop system performance of the ideal reference model. It should be noted here that since the ideal reference model dynamics are solely used for analysis purposes, one can trivially select $x_{r,0} = x_{r0}$ such that with $\rho(0) = 0$ it follows that $\chi_r(0) = 0$ holds.

Remark 6.4.3 From Theorem 6.4.1, since $\lim_{t \rightarrow \infty} e(t) = 0$ (meaning that the uncertain dynamical system trajectories asymptotically converge to the modified expanded reference model trajectories) and $\lim_{t \rightarrow \infty} \tilde{x}_r(t) = 0$ (meaning the modified expanded reference model trajectories converge to the ideal reference model trajectories) then asymptotic convergence between the uncertain dynamical system and ideal reference model trajectories is achieved.

At this point, the proposed adaptive control architecture using expanded reference models is shown to allow for convergence of the trajectories of the uncertain dynamical system to the trajectories of a desired reference model, where the desired reference model does not include the unpredictable effect from the transients of the system error $e(t)$, and can also be modified to further guarantee convergence to the ideal reference model given by (6.4) (also given by (6.49)). Yet, the construction of the proposed expanded reference model designs require knowledge of the actuator bandwidths which may not always be possible. For this reason, the next section relaxes this condition to allow for a more robust design in the presence of unknown actuator bandwidths.

6.5 Robustness of Expanded Reference Model Architecture to Unknown Actuator Bandwidths

In this section, we consider the case in which the actuator bandwidths are not completely known such that the proposed expanded reference model needs to be redesigned using an estimate of the unknown part allowing for a more robust architecture. For this purpose, we parameterize the actuator bandwidth matrix such that (6.2) is now given by

$$\dot{v}(t) = -(M_0 + \delta M)(v(t) - u(t)), \quad v(0) = v_0, \quad (6.60)$$

where $M_0 \in \mathbb{R}_+^{m \times m} \cap \mathbb{D}^{m \times m}$ represents a known part of the actuator bandwidths and $\delta M \in \mathbb{R}^{m \times m} \cap \mathbb{D}^{m \times m}$ represents the unknown variations in the actuator bandwidths.

To obtain the same performance guarantees as Section 6.4, we again augment a command governor architecture with the expanded reference model now given by

$$\underbrace{\begin{bmatrix} \dot{x}_r(t) \\ \dot{v}_r(t) \end{bmatrix}}_{z_r(t)} = \underbrace{\begin{bmatrix} A + B\hat{W}^T(t) & B(I_m + \delta\hat{\Lambda}(t)) \\ -(M_0 + \delta\hat{M}(t))(K_1 + \hat{W}^T(t)) & -(M_0 + \delta\hat{M}(t))(I_m + \delta\hat{\Lambda}(t)) \end{bmatrix}}_{F_r(\hat{W}(t), \delta\hat{\Lambda}(t), \delta\hat{M}(t))} \underbrace{\begin{bmatrix} x_r(t) \\ v_r(t) \end{bmatrix}}_{z_r(t)} + \underbrace{\begin{bmatrix} 0_{n \times m} \\ (M_0 + \delta\hat{M}(t))K_2 \end{bmatrix}}_{G_r(\delta\hat{M}(t))} c_g(t), \quad (6.61)$$

where $\delta\hat{M}(t) \in \mathbb{R}^{m \times m} \cap \mathbb{D}^{m \times m}$ is an estimate of δM constructed from the elemental weight update laws

$$\delta\dot{\hat{m}}_i(t) = -\beta_i \text{Proj}[\delta\hat{m}_i(t), \sigma_i(\cdot)\bar{z}^T(t)\mathcal{P}G\mathbf{e}_i], \quad \delta\hat{m}_i(0) = \delta\hat{m}_{i0}, \quad i = 1, \dots, m, \quad (6.62)$$

where $\beta_i \in \mathbb{R}_+$ is the learning rate for the respective estimates, $\sigma_i(\cdot)$ is the i^{th} element of the vector resulting from the feedback given by $\sigma(\cdot) \triangleq (I_m + \delta\hat{\Lambda}(t))v(t) + (K_1 + \hat{W}^T(t))x(t) - K_2c_g(t) \in \mathbb{R}^m$, $G = [0_{m \times n}, I_{m \times m}]^T \in \mathbb{R}^{(n+m) \times m}$, and \mathbf{e}_i is the standard basis for $i = 1, \dots, m$ as in the previous section. Note here again by elementally updating we can set $\delta\hat{m}(t) \triangleq \text{diag}([\delta\hat{m}_1(t), \delta\hat{m}_2(t), \dots, \delta\hat{m}_m(t)])$. The elemental projection bounds are defined such that $\delta\hat{m}_{i,\min} \leq \delta\hat{m}_i(t) \leq \delta\hat{m}_{i,\max}$, for $i = 1, \dots, m$.

In (6.61), the signal $c_g(t)$ is given by

$$c_g(t) = c(t) + D(t)\xi(t), \quad (6.63)$$

where $c(t) \in \mathbb{R}^m$ is the uniformly continuous smooth and bounded reference command used in the previous sections (again, since $c(t)$ is a user-defined smooth function, we implicitly assume that $\dot{c}(t)$ is bounded as well as available), $D(t) \triangleq K_2^{-1}(M_0 + \delta\hat{M}(t))^{-1} \in \mathbb{R}^{m \times m}$. Note here that in practice, the nominal known part of the actuator bandwidth M_0 is larger than the variation given by δM such that one can select the projection bounds on $\delta\hat{M}(t)$ to ensure $(M_0 + \delta\hat{M}(t))^{-1}$ is implementable. Similar to Section 6.4, the command governor output $\xi(t) \in \mathbb{R}^m$ is given by

$$\xi(t) = (I_m + \delta\hat{\Lambda}(t))^{-1}(-\mu\rho(t) - \phi_1^*(t)) - \phi_2^*(t), \quad (6.64)$$

where $\mu \in \mathbb{R}_+$ is the command governor gain, $\rho(t) \in \mathbb{R}^m$ is the command governor state given by (6.43), $\phi_1^*(t) = \phi_1(t) \in \mathbb{R}^m$ with $\phi_1(t)$ given by (6.44), and the signal $\phi_2^*(t) \in \mathbb{R}^m$ satisfies¹⁰

$$\begin{aligned} \phi_2(t) \triangleq & -(M_0 + \delta\hat{M}(t))(K_1 + \hat{W}^T(t))x_r(t) - (M_0 + \delta\hat{M}(t))(I_m + \delta\hat{\Lambda}(t))v_r(t) \\ & + (M_0 + \delta\hat{M}(t))K_2c(t). \end{aligned} \quad (6.65)$$

In addition, it should be noted that $K_1 \in \mathbb{R}^{m \times n}$ and $K_2 \in \mathbb{R}^{m \times m}$ are the same nominal control gains given in Sections 6.3 and 6.4, $\hat{W} \in \mathbb{R}^{n \times m}$ satisfies the weight update law given by (6.25), and $\delta\hat{\Lambda}(t) \triangleq \text{diag}([\delta\hat{\lambda}_1(t), \delta\hat{\lambda}_2(t), \dots, \delta\hat{\lambda}_m(t)])$ satisfies the elemental update law given by (6.26), and the feedback control law is given by (6.46).

By adding and subtracting $B\hat{W}^T(t)x(t)$ and $B\delta\hat{\Lambda}(t)v(t)$ to (6.1), adding and subtracting $\delta\hat{M}(t) \cdot (v(t) - u(t))$ to (6.60), and using (6.46), we can write the augmented uncertain dynamical system and actuator dynamics in compact form as

$$\begin{aligned} \dot{z}(t) = & F_r(\hat{W}(t), \delta\hat{\Lambda}(t), \delta\hat{M}(t))z(t) + G_r(\delta\hat{M}(t))c_g(t) \\ & - B^*(\tilde{W}^T(t)x(t) + \delta\tilde{\Lambda}(t)v(t)) + G\delta\tilde{M}(t)\sigma(\cdot), \end{aligned} \quad (6.66)$$

where $\delta\tilde{M}(t) \triangleq \delta\hat{M}(t) - \delta M$. It then follows from (6.61) and (6.66) that the system error dynamics can be given as

$$\dot{\tilde{z}}(t) = F_r(\hat{W}(t), \delta\hat{\Lambda}(t), \delta\hat{M}(t))\tilde{z}(t) - B^*(\tilde{W}^T(t)x(t) + \delta\tilde{\Lambda}(t)v(t)) + G\delta\tilde{M}(t)\sigma(\cdot) \quad \tilde{z}(0) = \tilde{z}_0. \quad (6.67)$$

In addition, owing to the diagonal structure of $\delta\tilde{\Lambda}(t)$ and $\delta\tilde{M}(t)$, (6.67) can be equivalently written

$$\dot{\tilde{z}}(t) = F_r(\hat{W}(t), \delta\hat{\Lambda}(t), \delta\hat{M}(t))\tilde{z}(t) - B^* \left(\tilde{W}^T(t)x(t) + \sum_{i=1}^m \mathbf{e}_i \delta\tilde{\lambda}_i(t)v_i(t) \right) + G \sum_{i=1}^m \mathbf{e}_i \delta\tilde{m}_i(t)\sigma_i(\cdot). \quad (6.68)$$

The following assumption, which is a slightly modified version of Assumption 6.3.1, is necessary for the results in this section.

¹⁰Here we refer to the proof of Theorem 6.5.1 and particularly (6.79) and (6.80) for how $\phi_1^*(t)$ and $\phi_2^*(t)$ are designed for this section.

Assumption 6.5.1 *The matrix given by*

$$\mathcal{A}(\hat{W}(t), \delta\hat{\Lambda}(t), \delta\hat{M}(t), \varepsilon) = \begin{bmatrix} A + B\hat{W}^T(t) + \frac{\varepsilon}{2}I_n & B(I_m + \delta\hat{\Lambda}(t)) \\ -(M_0 + \delta\hat{M}(t))(K_1 + \hat{W}^T(t)) & -(M_0 + \delta\hat{M}(t))(I_m + \delta\hat{\Lambda}(t)) + \frac{\varepsilon}{2}I_m \end{bmatrix}, \quad (6.69)$$

with $\varepsilon \in \mathbb{R}_+$ being a design parameter, is quadratically stable.

Remark 6.5.1 *As shown in Section 6.3, we can similarly use LMIs to satisfy the quadratic stability of (6.69), for given projection bounds \hat{W}_{\max} , $\delta\hat{\Lambda}_{\max}$, and $\delta\hat{m}_{\max}$, on the elements of $\hat{W}(t)$, $\delta\hat{\Lambda}(t)$, and $\delta\hat{M}(t)$ respectively, for the known parts of the actuator bandwidths given by M_0 , and for the design parameter ε . For this purpose, we first write (6.69) as*

$$\mathcal{A}(\cdot) = \begin{bmatrix} A + B\hat{W}^T(t) + \frac{\varepsilon}{2}I_n \\ -M_0K_1 - M_0\hat{W}^T(t) - \delta\hat{M}(t)K_1 - \delta\hat{M}(t)\hat{W}^T(t) \\ \dots \\ B(I_m + \delta\hat{\Lambda}(t)) \\ -M_0 - M_0\delta\hat{\Lambda}(t) - \delta\hat{M}(t) - \delta\hat{M}(t)\delta\hat{\Lambda}(t) + \frac{\varepsilon}{2}I_m \end{bmatrix}. \quad (6.70)$$

Now, let $\bar{W}_{i_1, \dots, i_f} \in \mathbb{R}^{n \times m}$ be defined as (6.33) and $\bar{\delta\Lambda}_{i_1, \dots, i_g} \in \mathbb{R}^{m \times m} \cap \mathbb{D}^{m \times m}$ be defined as (6.34) to represent the corners of the hypercubes defining the variation of $\hat{W}(t)$ and $\delta\hat{\Lambda}(t)$ respectively. Similarly, let $\bar{\delta M}_{i_1, \dots, i_h}$ be defined as

$$\bar{\delta M}_{i_1, \dots, i_h} = \text{diag} \left([i_1 \delta\hat{m}_{\max, 1} + (1 - i_1) \delta\hat{m}_{\min, 1}, \dots, i_m \delta\hat{m}_{\max, m} + (1 - i_m) \delta\hat{m}_{\min, m}] \right), \quad (6.71)$$

where $i_h \in \{0, 1\}$, $h \in \{1, \dots, 2^m\}$, such that $\bar{\delta M}_{i_1, \dots, i_h}$ represents the corners of the hypercube defining the variation of $\delta\hat{M}(t)$. In addition, due to the product terms of $\delta\hat{M}(t)\hat{W}^T(t)$ and $\delta\hat{M}(t)\delta\hat{\Lambda}(t)$ in (6.70), let the variations of $\Omega(t) \triangleq \delta\hat{M}(t)\hat{W}^T(t)$ and $\Pi(t) \triangleq \delta\hat{M}(t)\delta\hat{\Lambda}(t)$ be respectively defined as $\bar{\Omega}_{i_1, \dots, i_r} = \bar{\delta M}_{i_1, \dots, i_h} \bar{W}_{i_1, \dots, i_f}$ and $\bar{\Pi}_{i_1, \dots, i_s} = \bar{\delta M}_{i_1, \dots, i_h} \bar{\delta\Lambda}_{i_1, \dots, i_g}$, where $r \in \{1, \dots, 2^{m^2+n}\}$ and $s \in \{1, \dots, 2^{m+1}\}$. Then

$$\mathcal{A}_{i_1, \dots, i_p} = \begin{bmatrix} A + B\bar{W}_{i_1, \dots, i_f}^T + \frac{\varepsilon}{2}I_n \\ -M_0K_1 - M_0\bar{W}_{i_1, \dots, i_f}^T - \bar{\delta M}_{i_1, \dots, i_h}K_1 - \bar{\Omega}_{i_1, \dots, i_r} \end{bmatrix}$$

$$\dots \begin{bmatrix} B(I_m + \overline{\delta\Lambda}_{i_1, \dots, i_g}) \\ -M_0 - M_0 \overline{\delta\Lambda}_{i_1, \dots, i_g} - \overline{\delta M}_{i_1, \dots, i_h} - \overline{\Pi}_{i_1, \dots, i_s} + \frac{\varepsilon}{2} I_m \end{bmatrix}, \quad (6.72)$$

represents the corners of the hypercube constructed from all the permutations of $\overline{W}_{i_1, \dots, i_f}$, $\overline{\delta\Lambda}_{i_1, \dots, i_g}$, $\overline{\delta M}_{i_1, \dots, i_h}$, $\overline{\Omega}_{i_1, \dots, i_r}$, and $\overline{\Pi}_{i_1, \dots, i_s}$. For a given M_0 , it can then be shown that

$$\mathcal{A}_{i_1, \dots, i_p}^T \mathcal{P} + \mathcal{P} \mathcal{A}_{i_1, \dots, i_p} < 0, \quad \mathcal{P} > 0, \quad (6.73)$$

implies that $\mathcal{A}^T(\hat{W}(t), \delta\hat{\Lambda}(t), \delta\hat{M}(t), \varepsilon) \mathcal{P} + \mathcal{P} \mathcal{A}(\hat{W}(t), \delta\hat{\Lambda}(t), \delta\hat{M}(t), \varepsilon) < 0$ [96, 99]; thus, one can solve the LMI given by (6.73) to calculate \mathcal{P} , which is then used in the weight update laws (6.25), (6.26), and (6.62).

Now that Assumption 6.5.1 can be satisfied through the use of LMIs as shown in Remark 6.5.1, we are ready to state the following theorem.

Theorem 6.5.1 Consider the uncertain dynamical system given by (6.1), the actuator dynamics given by (6.60), the ideal reference model given by (6.49), the expanded reference model given by (6.61), the command governor architecture given by (6.63), (6.64), (6.43), (6.44), and (6.65), the feedback control law given by (6.46), and the update laws given by (6.25), (6.26), (6.62). Under Assumption 6.5.1, the solution $(\tilde{z}(t), \tilde{W}(t), \delta\tilde{\Lambda}(t), \delta\tilde{M}(t))$ of the closed-loop dynamical system is bounded, $\lim_{t \rightarrow \infty} \tilde{x}_r(t) = 0$, $\lim_{t \rightarrow \infty} \rho(t) = 0$, $\lim_{t \rightarrow \infty} e(t) = 0$, and $\lim_{t \rightarrow \infty} \tilde{v}(t) = 0$.

Proof. To show the Lyapunov stability; hence, the boundedness of the solution $(\tilde{z}(t), \tilde{W}(t), \delta\tilde{\Lambda}(t), \delta\tilde{M}(t))$, consider the Lyapunov function candidate given by

$$\mathcal{V}(\tilde{z}, \tilde{W}, \delta\tilde{\Lambda}, \delta\tilde{M}) = \tilde{z}^T \mathcal{P} \tilde{z} + \gamma^{-1} \text{tr} \tilde{W}^T \tilde{W} + \sum_{i=1}^m \alpha_i^{-1} \delta\tilde{\lambda}_i^2 + \sum_{i=1}^m \beta_i^{-1} \delta\tilde{m}_i^2. \quad (6.74)$$

Note that $\mathcal{V}(0, 0, 0, 0) = 0$ and $\mathcal{V}(\tilde{z}, \tilde{W}, \delta\tilde{\Lambda}, \delta\tilde{M}) > 0$ for all $(\tilde{z}, \tilde{W}, \delta\tilde{\Lambda}, \delta\tilde{M}) \neq (0, 0, 0, 0)$. Differentiating (6.74) along the closed-loop system trajectories and using (6.25), (6.26), (6.62) yields

$$\begin{aligned}
& \dot{V}(\tilde{z}(t), \tilde{W}(t), \delta\tilde{\Lambda}(t), \delta\tilde{M}(t)) \\
&= 2\tilde{z}^T(t)\mathcal{P}\left(F_r(\hat{W}(t), \delta\hat{\Lambda}(t), \delta\hat{M}(t))\tilde{z}(t) - B^*\tilde{W}^T(t)x(t) - B^*\sum_{i=1}^m \mathbf{e}_i\delta\tilde{\lambda}_i(t)v_i(t)\right. \\
&\quad \left.+ G\sum_{i=1}^m \mathbf{e}_i\delta\tilde{m}_i(t)\sigma_i(\cdot)\right) + 2\gamma^{-1}\text{tr}\tilde{W}^T(t)\dot{\hat{W}}(t) + 2\sum_{i=1}^m \alpha_i^{-1}\delta\tilde{\lambda}_i(t)\delta\dot{\lambda}_i(t) \\
&\quad + 2\sum_{i=1}^m \beta_i^{-1}\delta\tilde{m}_i(t)\delta\dot{m}_i(t) \\
&= \tilde{z}^T(t)\left(F_r^T(\hat{W}(t), \delta\hat{\Lambda}(t), \delta\hat{M}(t))\mathcal{P} + \mathcal{P}F_r(\hat{W}(t), \delta\hat{\Lambda}(t), \delta\hat{M}(t))\right)\tilde{z}(t) \\
&\quad - 2\tilde{z}^T(t)\mathcal{P}B^*\tilde{W}^T(t)x(t) + 2\gamma^{-1}\text{tr}\tilde{W}^T(t)\dot{\hat{W}}(t) \\
&\quad - 2\tilde{z}^T(t)\mathcal{P}B^*(\mathbf{e}_1\delta\tilde{\lambda}_1(t)v_1(t) + \mathbf{e}_2\delta\tilde{\lambda}_2(t)v_2(t) + \dots + \mathbf{e}_m\delta\tilde{\lambda}_m(t)v_m(t)) \\
&\quad + 2(\alpha_1^{-1}\delta\tilde{\lambda}_1(t)\delta\dot{\lambda}_1(t) + \alpha_2^{-1}\delta\tilde{\lambda}_2(t)\delta\dot{\lambda}_2(t) + \dots + \alpha_m^{-1}\delta\tilde{\lambda}_m(t)\delta\dot{\lambda}_m(t)) \\
&\quad + 2\tilde{z}^T(t)\mathcal{P}G(\mathbf{e}_1\delta\tilde{m}_1(t)\sigma_1(\cdot) + \mathbf{e}_2\delta\tilde{m}_2(t)\sigma_2(\cdot) + \dots + \mathbf{e}_m\delta\tilde{m}_m(t)\sigma_m(\cdot)) \\
&\quad + 2(\beta_1^{-1}\delta\tilde{m}_1(t)\delta\dot{m}_1(t) + \beta_2^{-1}\delta\tilde{m}_2(t)\delta\dot{m}_2(t) + \dots + \beta_m^{-1}\delta\tilde{m}_m(t)\delta\dot{m}_m(t)) \\
&= \tilde{z}^T(t)\left(F_r^T(\hat{W}(t), \delta\hat{\Lambda}(t), \delta\hat{M}(t))\mathcal{P} + \mathcal{P}F_r(\hat{W}(t), \delta\hat{\Lambda}(t), \delta\hat{M}(t))\right)\tilde{z}(t) \\
&\quad + 2\gamma^{-1}\text{tr}\tilde{W}^T(t)\left(\dot{\hat{W}}(t) - \gamma x(t)\tilde{z}^T(t)\mathcal{P}B^*\right) \\
&\quad + 2\sum_{i=1}^m \alpha_i^{-1}\delta\tilde{\lambda}_i(t)(\delta\dot{\lambda}_i(t) - \alpha_i v_i(t)\tilde{z}^T(t)\mathcal{P}B^*\mathbf{e}_i) \\
&\quad + 2\sum_{i=1}^m \beta_i^{-1}\delta\tilde{m}_i(t)(\delta\dot{m}_i(t) + \beta_i\sigma_i(\cdot)\tilde{z}^T(t)\mathcal{P}G\mathbf{e}_i) \\
&\leq \tilde{z}^T(t)\left(F_r^T(\hat{W}(t), \delta\hat{\Lambda}(t), \delta\hat{M}(t))\mathcal{P} + \mathcal{P}F_r(\hat{W}(t), \delta\hat{\Lambda}(t), \delta\hat{M}(t))\right)\tilde{z}(t). \tag{6.75}
\end{aligned}$$

Following similar steps as the proof of Theorem 6.3.1, one can show under Assumption 6.5.1 (satisfied using LMIs, see Remark 6.5.1), that (6.75) reduces to $\dot{V}(\tilde{z}(t), \tilde{W}(t), \delta\tilde{\Lambda}(t), \delta\tilde{M}(t)) \leq -\varepsilon\tilde{z}^T(t)\mathcal{P}\tilde{z}(t) \leq 0$, which guarantees the boundedness of the solution $(\tilde{z}(t), \tilde{W}(t), \delta\tilde{\Lambda}(t), \delta\tilde{M}(t))$.

Now, following similar steps as the proof of Theorem 6.4.1, by adding and subtracting the terms “ $BK_1x_r(t)$ ” and “ $BK_2c(t)$ ” to the $x_r(t)$ dynamics of the expanded reference model given by (6.61) we can write

$$\dot{x}_r(t) = A_r x_r(t) + B_r c(t) + B\rho(t). \tag{6.76}$$

From (6.49) and (6.76) the reference model error dynamics can be given as

$$\dot{\tilde{x}}_r(t) = A_r \tilde{x}_r(t) + B\rho(t). \tag{6.77}$$

Differentiating $\rho(t)$ in time, we obtain the following dynamics

$$\dot{\rho}(t) = \dot{\hat{W}}^T(t)x_r(t) + (K_1 + \hat{W}^T(t))\dot{x}_r(t) - K_2\dot{c}(t) + \delta\dot{\hat{\Lambda}}(t)v_r(t) + (I_m + \delta\hat{\Lambda}(t))\dot{v}_r(t), \quad (6.78)$$

and using the $x_r(t)$ and $v_r(t)$ dynamics of (6.61) in (6.78) yields

$$\begin{aligned} \dot{\rho}(t) = & \dot{\hat{W}}^T(t)x_r(t) + (K_1 + \hat{W}^T(t)) \left((A + B\hat{W}^T(t))x_r(t) + B(I_m + \delta\hat{\Lambda}(t))v_r(t) \right) - K_2\dot{c}(t) + \delta\dot{\hat{\Lambda}}(t)v_r(t) \\ & + (I_m + \delta\hat{\Lambda}(t)) \left[-(M_0 + \delta\hat{M}(t))(K_1 + \hat{W}^T(t))x_r(t) - (M_0 + \delta\hat{M}(t))(I_m + \delta\hat{\Lambda}(t))v_r(t) \right. \\ & \left. + (M_0 + \delta\hat{M}(t))K_2 + \xi(t) \right]. \end{aligned} \quad (6.79)$$

Using the command governor signal (6.64) in (6.79) gives the following

$$\begin{aligned} \dot{\rho}(t) = & \dot{\hat{W}}^T(t)x_r(t) + (K_1 + \hat{W}^T(t)) \left((A + B\hat{W}^T(t))x_r(t) + B(I_m + \delta\hat{\Lambda}(t))v_r(t) \right) - K_2\dot{c}(t) + \delta\dot{\hat{\Lambda}}(t)v_r(t) \\ & + (I_m + \delta\hat{\Lambda}(t)) \left[-(M_0 + \delta\hat{M}(t))(K_1 + \hat{W}^T(t))x_r(t) - (M_0 + \delta\hat{M}(t))(I_m + \delta\hat{\Lambda}(t))v_r(t) \right. \\ & \left. + (M_0 + \delta\hat{M}(t))K_2 - \phi_2^*(t) \right] - \mu\rho(t) - \phi_1^*(t) \end{aligned} \quad (6.80)$$

where applying the signals (6.44) and (6.65), (6.80) reduces to $\dot{\rho}(t) = -\mu\rho(t)$, such that the dynamics can be augmented with (6.77) as

$$\begin{bmatrix} \dot{\tilde{x}}_r(t) \\ \dot{\rho}(t) \end{bmatrix} = \begin{bmatrix} A_r & B \\ 0_{m \times n} & -\mu I_m \end{bmatrix} \begin{bmatrix} \tilde{x}_r(t) \\ \rho(t) \end{bmatrix}. \quad (6.81)$$

Since A_r is Hurwitz, $\mu > 0$, and (6.81) is in upper triangular form, $\lim_{t \rightarrow \infty} \tilde{x}_r(t) = 0$ and $\lim_{t \rightarrow \infty} \rho(t) = 0$ are immediate.

Finally, since $x_{r_i}(t)$ is bounded and $x_r(t) = \tilde{x}_r(t) + x_{r_i}(t)$, then $x_r(t)$ is bounded, and since x_r is bounded and $\rho(t)$ is bounded, and owing to the projection based weight update laws, $\hat{W}(t)$, $\delta\hat{\Lambda}(t)$, and $\delta\hat{M}(t)$ are all bounded, and since the input command $c(t)$ is bounded, it follows from (6.43) that $v_r(t)$ is bounded. In addition, from the Lyapunov stability of the solution $(\tilde{z}(t), \tilde{W}(t), \delta\tilde{\Lambda}(t), \delta\tilde{M}(t))$ we know $\tilde{z}(t)$, $\tilde{W}(t)$, $\delta\tilde{\Lambda}(t)$, and $\delta\tilde{M}(t)$ are all bounded, such that it can now be concluded that $\dot{V}(\tilde{z}(t), \tilde{W}(t), \delta\tilde{\Lambda}(t), \delta\tilde{M}(t))$ is bounded. By Barbalat's lemma [88], $\lim_{t \rightarrow \infty} \dot{V}(\tilde{z}(t), \tilde{W}(t), \delta\tilde{\Lambda}(t), \delta\tilde{M}(t)) = 0$; hence, $\lim_{t \rightarrow \infty} e(t) = 0$ and $\lim_{t \rightarrow \infty} \tilde{v}(t) = 0$. ■

Remark 6.5.2 *The conclusions noted in Remarks 6.4.2 and 6.4.3 can be made here as well, but now for the case in which the actuator bandwidths are unknown.*

The next section considers an application to a hypersonic vehicle, where we apply the most general form of the proposed adaptive control architecture given in this section.

6.6 Illustrative Example

To elucidate our proposed approach to the actuator dynamics problem, we provide the following application to a hypersonic vehicle. Specifically, consider the uncertain hypersonic vehicle longitudinal dynamics given by the short-period approximation as

$$\dot{x}(t) = \underbrace{\begin{bmatrix} -2.39 \times 10^{-1} & 1 \\ 4.26 & -1.19 \times 10^{-1} \end{bmatrix}}_A x(t) + \underbrace{\begin{bmatrix} -1.33 \times 10^{-4} \\ -1.84 \times 10^{-1} \end{bmatrix}}_B (\lambda v(t) + W^T x(t)), \quad (6.82)$$

with zero initial conditions and the state vector being defined as $x(t) = [\alpha(t), q(t)]^T$, where $\alpha(t)$ denotes the angle-of-attack and $q(t)$ denotes the pitch rate. The uncertainty is considered to be $W = [-100 \ .01]^T$ such that it dominantly effects the stability derivative C_{m_α} . Specifically, the value -100 creates a 400% increase in C_{m_α} , destabilizing the nominal closed-loop system, whereas the second value 0.01 can be considered to be small since it does not significantly effect the closed-loop performance of the hypersonic vehicle, which is lightly damped. In addition, the control effectiveness $\lambda = 1 + \delta\lambda$, with $\delta\lambda$ being the unknown variation, is considered to be 25% deficient such that $\delta\lambda = -0.25$. The actuator output $v(t)$ is given by the actuator dynamics

$$\dot{v}(t) = -m(v(t) - u(t)), \quad (6.83)$$

where $u(t)$ denotes the elevator deflection command and m is the actuator bandwidth which is scalar since we are considering a single input control channel. The actuator bandwidth is $m = 10 \pm 0.25$ rad/sec, such that it can be parameterized as $m = m_0 + \delta m$, with $m_0 = 10$ rad/sec and $\delta m \in [-0.25, 0.25]$ rad/sec. For this example, we set the unknown portion as $\delta m = -0.25$ rad/sec such that there is less available bandwidth than the assumed m_0 value.

Linear quadratic regulator theory [91] is used to design the nominal controller for both the proposed control design and a hedging based control design (for comparison purposes). The feedback gain matrix K_1 is designed such that $A_r = A - BK_1$ is Hurwitz using the weighting matrices $Q = \text{diag}([5 \times 10^5 \ 10^3])$ to penalize the states and $R = 25$ to penalize the control input, resulting in $K_1 = -[156.3459, 40.9615]$ that has a desirable 65.4° phase margin and a crossover frequency of 7.95 rad/sec. The feedforward gain K_2 is designed such that the desired angle-of-attack position $\alpha(t)$ is followed. For this purpose, using $E = [1, 0]$, the gain K_2 is calculated as $K_2 = -(EA_r^{-1}B)^{-1} = -143.2845$. The desired angle-of-attack command in degrees is generated using $c(t) = 2\sin(0.5t)$. In addition, the same learning gains are used for both controllers given by $\Gamma = 10^3$, $\alpha = 10$, and $\beta = 10$. For hedging based control design, the solution to $A_r^T P + PA_r + R_1 = 0$ is calculated with $R_1 = \text{diag}[10^3, 10^3]$ (selected as in [118], in which it was appropriately tuned for desirable performance). In the proposed controller we use the feasible solution \mathcal{P} from the LMI analysis in Remark 6.5.1 which can be obtained for the consider example set-up and with the selected elemental projection bounds given by $-105 \leq [\hat{W}(t)]_1 \leq 0$, $0 \leq [\hat{W}(t)]_2 \leq 0.1$, $-0.2625 \leq \delta \hat{\lambda}(t) \leq 0$, and $|\delta \hat{m}(t)| \leq 0.2625$.

Figures 6.1 and 6.2 highlight the performance guarantees discussed in Remark 6.4.2 (and Remark 6.5.2). In particular, Figure 6.1 shows the convergence of the proposed expanded reference model trajectories to the ideal reference model trajectories for different values of μ . From Remark 6.4.2 and for the considered example set-up we have

$$\mathcal{A}_r = \begin{bmatrix} -0.2599 & 0.9946 & -0.0001 \\ -24.5199 & -7.6583 & -0.1841 \\ 0 & 0 & -\mu \end{bmatrix}. \quad (6.84)$$

For the three different values of μ shown in Figure 6.1, the resulting rates of convergence matched to the μ value follow as $(\mu = 0.5, \lambda_{\max}(\mathcal{A}_r) = -0.5)$, $(\mu = 1.0, \lambda_{\max}(\mathcal{A}_r) = -1.0)$, and $(\mu = 10, \lambda_{\max}(\mathcal{A}_r) = -3.9591)$. These correspond to the approximately 8 sec, 4 sec, and 1 sec convergence times depicted in Figure 6.1. Furthermore, Figure 6.2 shows the case in which the initial conditions are zero and the proposed expanded reference model trajectories captures the ideal reference model trajectories exactly.

Figures 6.3 and 6.4 compare the control performance between the proposed adaptive control architecture using expanded reference models augmented with a command governor architecture and a hedging

based adaptive control architecture. Specifically, it can be seen in Figure 6.3 that the proposed expanded reference model trajectories identically capture the ideal reference model trajectories (i.e., $\chi_r(0) = 0$) whereas due to the transients of the system error signal $e(t)$, the hedged reference model trajectories deviate from the ideal reference model trajectories. The actual state trajectories of the uncertain hypersonic vehicle also converge to the expanded reference model trajectories (hence the ideal reference model trajectories) for the proposed adaptive control architecture quicker than the hedging based adaptive control architecture. In addition, Figure 6.4 shows that the magnitude of the applied adaptive control signal and actuator output is less for the proposed adaptive control architecture as opposed to the hedging based adaptive control architecture.

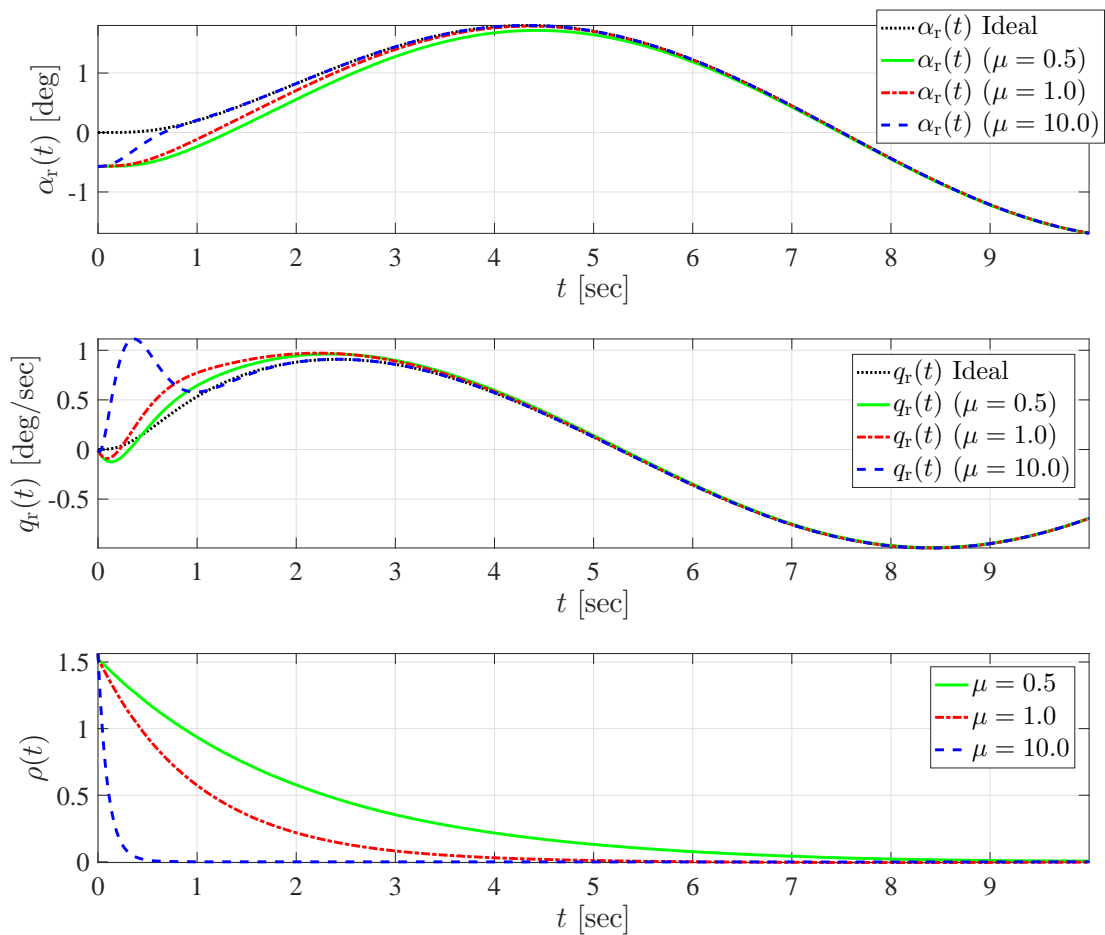


Figure 6.1: Convergence of expanded reference model trajectories to the ideal reference model trajectories for different rates of convergence.

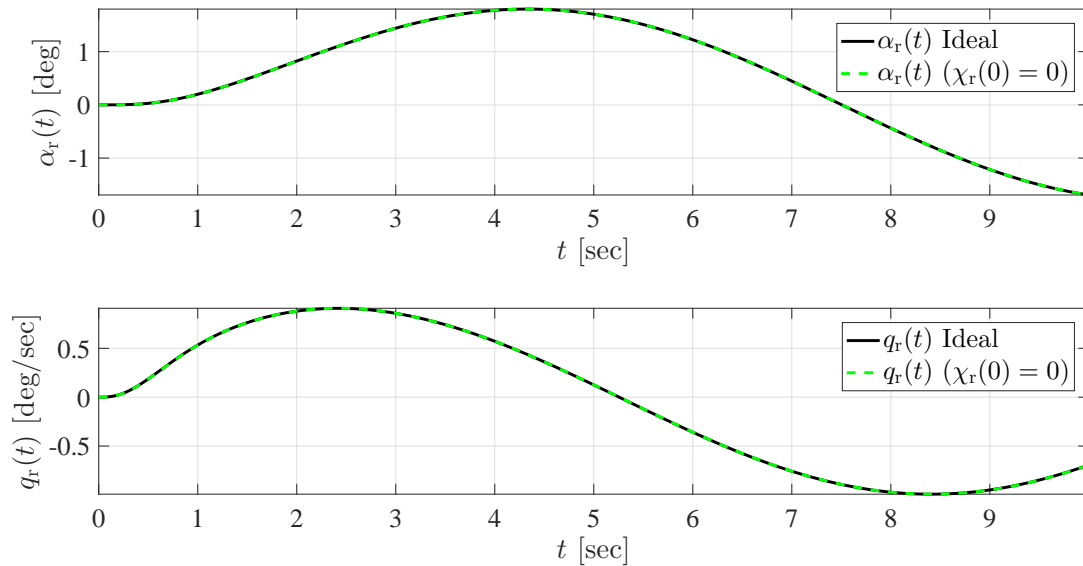


Figure 6.2: Expanded reference model trajectories exactly capturing the ideal reference model trajectories for zero initial conditions.

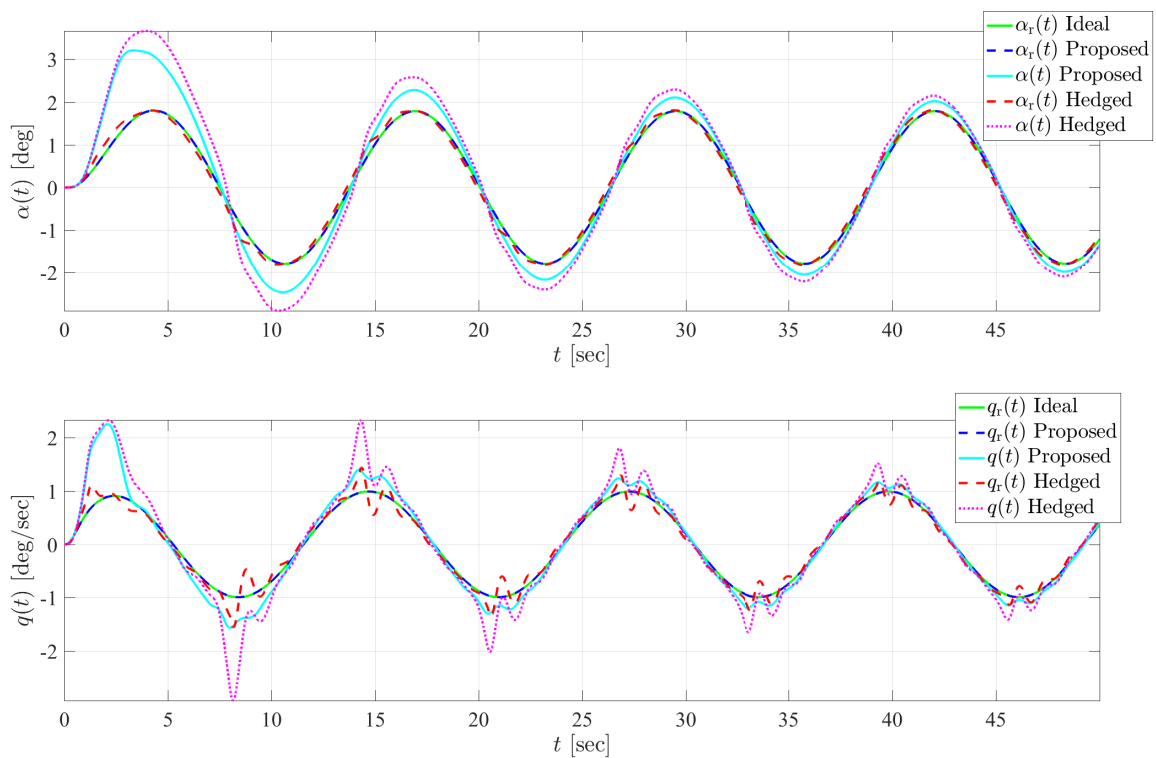


Figure 6.3: Comparison of the proposed expanded reference model control performance and a hedging based control performance.

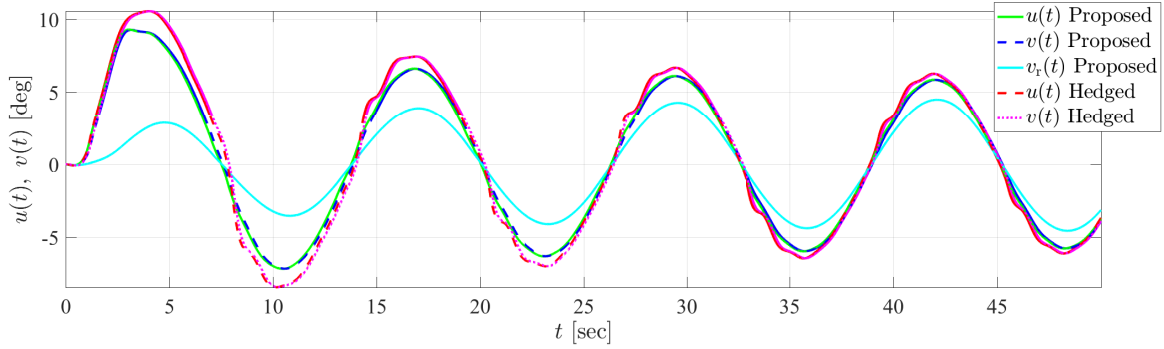


Figure 6.4: Control inputs and actuator outputs for Figure 6.3.

6.7 Conclusion

In this paper, we documented a new model reference adaptive control architecture for uncertain dynamical systems with actuator dynamics. We first showed that the trajectories of the expanded reference model remain predictably close to the trajectories of the ideal reference model as compared to the hedging approach, and we then show that asymptotic convergence to the ideal reference model trajectories is guaranteed by utilizing a new command governor architecture developed for the proposed expanded reference model. In order to achieve a robust implementation in the presence of possible uncertainties in the bandwidths of actuator channels, we also redesigned the expanded reference model with the estimate of actuator bandwidths. Finally, a numerical application to a hypersonic vehicle model elucidated our contributions and presented comparisons with the hedging approach.

CHAPTER 7: DECENTRALIZED ADAPTIVE ARCHITECTURES FOR CONTROL OF LARGE-SCALE ACTIVE-PASSIVE MODULAR SYSTEMS WITH STABILITY AND PERFORMANCE GUARANTEES^{1,2}

Decentralized control of large-scale active-passive modular systems is considered in this paper. The considered class of large-scale systems consist of physically interconnected and generally heterogeneous modules, where local control signals can only be applied to a subset of these modules (i.e., *active* modules) and the rest do not admit any control signals (i.e., *passive* modules). Specifically, based on a set-theoretic model reference adaptive control approach predicated on restricted potential functions, we design and analyze decentralized command following control laws for each active module such that they can effectively perform their tasks in the presence of unknown physical interconnections between modules and module-level system uncertainties. The key feature of our framework allows the system error trajectories of the active modules to be contained within a-priori, user-defined compact sets. Thus, they are guaranteed to achieve strict performance guarantees, where this is of paramount importance for practical applications. In addition to our theoretical findings and research contributions, the efficacy of the proposed decentralized adaptive control architecture is demonstrated in an illustrative numerical example.

7.1 Introduction

The design and implementation of decentralized architectures for controlling complex large-scale systems is a nontrivial control engineering task involving the consideration of components interacting with the physical processes to be controlled. Specifically, large-scale systems are characterized by a large number of highly-coupled heterogeneous components exchanging matter, energy, or information and have become ubiquitous given the recent advances in embedded sensor and computation technologies. Examples of such systems include but are not limited to network systems, power systems, communication systems, process control systems, water systems, highway systems, and air traffic control systems (see, for example, [59, 60]

¹This chapter is previously published in [134]. Permission is included in Appendix B.

²This chapter is a by-product of consulting work. Permission is included in Appendix B.

and references therein). An important class of large-scale systems is *modular systems* in which there exists a physical interconnection between modules. A major challenge in the control of modular systems is associated with the unknown physical interconnections between modules and module-level system uncertainties.

Although fixed-gain robust control design approaches (see, for example, [1, 135]) can be used to handle the unknown physical interconnections and module-level system uncertainties, they require the knowledge of bounds resulting from uncertainty parameterizations. However, characterization of these bounds is not a trivial task especially for complex large-scale systems due to practical constraints involving time and cost. To this end, the authors of [61–72] propose notable decentralized, partially decentralized, or distributed adaptive control approaches, where their approaches have the ability to learn and suppress the effect of such uncertainties, require less modeling information than do fixed-gain robust control approaches, and significantly reduce the design and implementation of control architectures. Therefore, the adaptive nature of these approaches provides an effective control design methodology for large-scale modular systems.

More specifically, the authors of [61–66] consider decentralized adaptive control approaches, where no communication (i.e., information exchange) is allowed between the modules. The authors of [67–71] consider partially decentralized adaptive control approaches in that they require every local controller to access the desired closed-loop system trajectories of all other modules. This may not be feasible in practice for highly-complex large-scale modular systems. Nevertheless, these approaches guarantee stability of the overall large-scale modular system without necessarily making global assumptions. Departing from these results, the authors of [72] proposed a distributed adaptive control approach with strict performance guarantees, where only neighboring modules are allowed to communicate with each other. While this approach does not require any global communication, it still requires modules to communicate with each other through a graph topology and this may not always be feasible for certain practical applications of large-scale modular systems. Another approach that gives strict performance guarantees is [73], where the authors utilize an adaptive backstepping scheme.

It is of practical importance to note that the approaches documented in [61–73] require all modules of a large-scale system to be controlled. However, this may not be possible especially for highly complex large-scale modular systems. For example, there may exist a specific subset of modules in practice that cannot be accessed or some of the modules can be subject to actuator failures in that it may not be possible to drive such modules through control signals. In this case, the set of modules that cannot be driven by control signals affect the others as unmodeled dynamics, which often have asymptotically stable unperturbed

dynamics. Although there are a few approaches that consider decentralized adaptive control of large-scale modular systems in the presence of unmodeled dynamics [136–139], these approaches do not necessarily achieve strict performance guarantees on the overall closed-loop large-scale system. Throughout this paper, we use the phrase *active modules* for the modules subject to local control signals and the phrase *passive modules* for the modules that do not admit any control signals; therefore, they act as unmodeled dynamics to the active modules in the sense of [136–139].

The overarching *contribution* of this paper is a new decentralized adaptive control architecture for large-scale active-passive modular systems. Specifically, based on a set-theoretic adaptive control approach predicated on restricted potential functions, we design and analyze decentralized command following control laws for each active module such that they can effectively perform their tasks in the presence of unknown physical interconnections between modules and module-level system uncertainties. The key feature of our framework allows the system error trajectories of the active modules to be contained within a-priori, user-defined compact sets. Thus, they are guaranteed to achieve strict performance guarantees, where this is of paramount importance for practical applications. In addition to our theoretical findings and research contributions, the efficacy of the proposed decentralized adaptive control architecture is also demonstrated in an illustrative numerical example. Finally, a preliminary version of this paper appeared in [140]. The present paper considerably goes beyond this version by providing comprehensive proofs of the main results, a new and more challenging illustrative numerical example, and additional motivation and remarks on the proposed decentralized adaptive control architecture for large-scale active-passive modular systems.

The *notation* used in this paper is fairly standard. Specifically, \mathbb{R} denotes the set of real numbers, \mathbb{R}^n denotes the set of $n \times 1$ real column vectors, $\mathbb{R}^{n \times m}$ denotes the set of $n \times m$ real matrices, \mathbb{R}_+ (resp. $\overline{\mathbb{R}}_+$) denotes the set of positive (resp. non-negative-definite) real numbers, $\mathbb{R}_+^{n \times n}$ (resp. $\overline{\mathbb{R}}_+^{n \times n}$) denotes the set of $n \times n$ positive-definite (resp. non-negative-definite) real matrices, $\mathbb{D}^{n \times n}$ denotes the set of $n \times n$ real matrices with diagonal scalar entries, $(\cdot)^T$ denotes transpose, $(\cdot)^{-1}$ denotes inverse, $\text{tr}(\cdot)$ denotes the trace operator, $\|\cdot\|_2$ denotes the Euclidian norm, $\|\cdot\|_F$ denotes the Frobenius matrix norm, “ \triangleq ” denotes equality by definition, and $\lambda_{\min}(A)$ (resp. $\lambda_{\max}(A)$) denotes the minimum (resp. maximum) eigenvalue of the Hermitian matrix A .

The *organization* of this paper is as follows. Section 7.2 introduces the problem formulation of the large-scale active-passive modular systems. Section 7.3 presents the proposed decentralized adaptive control, while Section 7.4 provides the stability and performance guarantees of the proposed controller.

An illustrative numerical example is provided in Section 7.5 to demonstrate the efficacy of the proposed approach and conclusions are summarized in Section 7.6. It should be also noted for completeness that a set-theoretic architecture is utilized in the previous work by the authors [72, 74]. However, the results of [72] is in the context of distributed adaptive control; hence, the considered modules communicate with each other through a graph topology as discussed above. Moreover, [72] does not consider the presence of passive modules, which do exist in practice as also discussed above. Finally, the results of [74] is based on the results in [72] and it is not at all in the context of large-scale active-passive modular systems.

7.2 Problem Formulation

The problem formulation for the decentralized control of large-scale active-passive modular systems is introduced in this section. To this end, we start with the following necessary definition utilized throughout this paper³.

Definition 7.2.1 Consider a large-scale modular system with N modules. Let $N_A \leq N$ of the N modules be subject to control signals and let the rest $N_P \leq N$ of the N modules be not subject to any control signal, where $N = N_A + N_P$. We then refer to the N_A modules that are subject to control signals as active modules and the rest N_P of the N modules as passive modules.

We next consider the uncertain large-scale active-passive modular system \mathcal{G} comprised of $N_A \leq N$ active modules given by

$$\mathcal{G}_{A_i} : \dot{x}_i(t) = A_i x_i(t) + B_i [\Lambda_i u_i(t) + \alpha_i(x(t)) + \beta_i(z(t))], \quad x_i(0) = x_{i0}, \quad (7.1)$$

for $i = 1, \dots, N_A$, and $N_P \leq N$ passive modules given by

$$\mathcal{G}_{P_i} : \dot{z}_i(t) = F_i z_i(t) + G_i \delta_i(x(t)), \quad z_i(0) = z_{i0}, \quad (7.2)$$

for $i = 1, \dots, N_P$. In (7.1), $x_i(t) \in \mathbb{R}^{n_i}$ is the state vector of the active modules available for feedback, $u_i(t) \in \mathbb{R}^{m_i}$ is the control signal applied to the active modules, $A_i \in \mathbb{R}^{n_i \times n_i}$ is an unknown system matrix and $B_i \in \mathbb{R}^{n_i \times m_i}$ is a known control input matrix such that the pair (A_i, B_i) is controllable, and $\Lambda_i \in \mathbb{R}_+^{m_i \times m_i} \cap \mathbb{D}^{m_i \times m_i}$

³Note that Definition 7.2.1 is consistent with the active-passive notion introduced in [141–146], where it is *not* related with the *passivity theory* appearing in the control systems literature (see, for example, [147]).

is an unknown control effectiveness matrix with positive entries on its diagonal. In addition, $z_i(t) \in \mathbb{R}^{p_i}$ is the state vector of the passive modules and $F_i \in \mathbb{R}^{p_i \times p_i}$ and $G_i \in \mathbb{R}^{p_i \times q_i}$ are unknown matrices appearing in (7.2). Furthermore, $\alpha_i : \overline{\mathbb{R}}_+ \times \mathbb{R}^{n_1+n_2+\dots+n_{N_A}} \rightarrow \mathbb{R}^{m_i}$ represents the unknown physical interconnections between active modules, $\beta_i : \overline{\mathbb{R}}_+ \times \mathbb{R}^{p_1+p_2+\dots+p_{N_P}} \rightarrow \mathbb{R}^{m_i}$ represents the effect on the active modules from their unknown physical interconnections with the passive modules, and $\delta_i : \overline{\mathbb{R}}_+ \times \mathbb{R}^{n_1+n_2+\dots+n_{N_A}} \rightarrow \mathbb{R}^{q_i}$ represents the effect on the passive modules from their unknown physical interconnections with the active modules. Finally, note that $x(t) \triangleq [x_1^T(t), x_2^T(t), \dots, x_{N_A}^T(t)]^T$ and $z(t) \triangleq [z_1^T(t), z_2^T(t), \dots, z_{N_P}^T(t)]^T$.

Remark 7.2.1 *To elucidate the large-scale active-passive modular system setup introduced in (7.1) and (7.2), consider the example in Figure 7.1, which depicts a cutout of an aircraft with multiple controllable flap surfaces along its wing allowing for flexible wing shaping [148–152]. In this representative example, imagine that all flaps are connected through a flexible membrane and that a fault has occurred in flaps 3, 4, and 6, such that they no longer receive a control input, but still affect flaps 1, 2, and 5. In this case, flaps 1, 2, and 5 are considered as active modules, \mathcal{G}_{A_i} , $i = 1, 2, 3$, subject to decentralized controllers given by \mathcal{C}_{A_i} , $i = 1, 2, 3$. The active modules are interconnected with two passive modules \mathcal{G}_{P_i} , $i = 1, 2$ (flaps 3, 4, and 6, where flaps 3 and 4 are combined as \mathcal{G}_{P_1} , such that it is augmented in the sense that it consists of two separate interconnected passive modules grouped as one passive module). In this setup, the active module \mathcal{G}_{A_1} (flap 1) is interconnected with the active module \mathcal{G}_{A_2} (flap 2); hence, it only has the unknown interconnection depicted by $\alpha_1(x)$. The active module \mathcal{G}_{A_2} (flap 2) is interconnected with both the active module \mathcal{G}_{A_1} (flap 1) and the augmented passive module \mathcal{G}_{P_1} ; hence, it has the unknown interconnections depicted by $\alpha_2(x)$ and $\beta_2(z)$. The same arguments can be made for the other modules used in this example. For another representative example, see the mechanical system setup utilized in the illustrative numerical example of Section 7.5.*

Remark 7.2.2 *The large-scale active-passive modular system setup introduced in (7.1) and (7.2) captures a large-scale system \mathcal{G} subject to unmodeled dynamics in the sense of [136–139], as discussed earlier. To see this, consider Figure 7.2 as an example, where each active module is interconnected with a passive module representing unmodeled dynamics for these active modules.*

Consistent with the decentralized adaptive control literature (see, for example, [61–63, 66, 68]), we make the following assumption for the large-scale active-passive modular system setup introduced in (7.1) and (7.2).

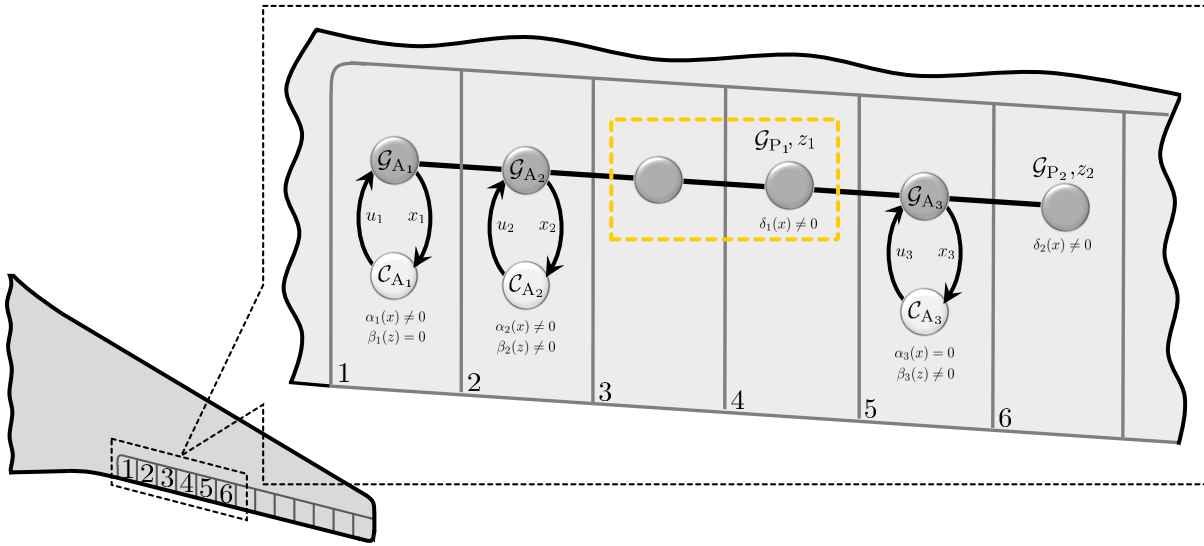


Figure 7.1: A large-scale modular system representation of wing shaping aircraft in Remark 7.2.1, where thick lines represent unknown physical interconnections between the modules.

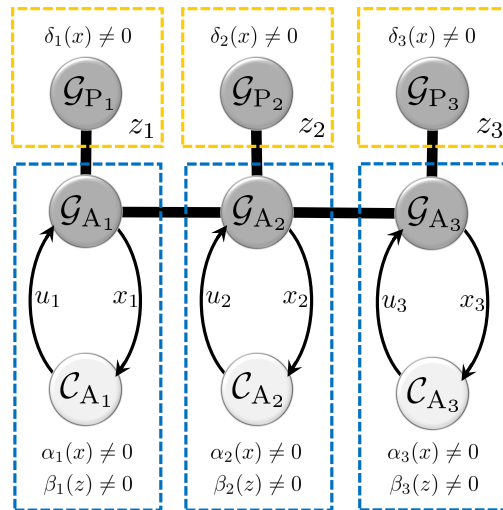


Figure 7.2: A large-scale modular system in Remark 7.2.2 with active modules (blue boxes) and passive modules (yellow boxes), where thick lines represent unknown physical interconnections between the modules.

Assumption 7.2.1 The nonlinear functions α_i , β_i , and δ_i appearing in (7.1) and (7.2) satisfy

$$\|\alpha_i(x(t))\|_2 \leq \alpha_i^* \sum_{j=1}^{N_A} \|x_j(t)\|_2, \quad \alpha_i^* > 0, \quad (7.3)$$

$$\|\beta_i(z(t))\|_2 \leq \beta_i^* \sum_{j=1}^{N_P} \|z_j(t)\|_2, \quad \beta_i^* > 0, \quad (7.4)$$

$$\|\delta_i(x(t))\|_2 \leq \delta_i^* \sum_{j=1}^{N_A} \|x_j(t)\|_2, \quad \delta_i^* > 0, \quad (7.5)$$

respectively, where α_i^* , β_i^* , and δ_i^* denote unknown constants.

For the feasibility of a decentralized control solution for the large-scale active-passive modular system setup introduced in (7.1) and (7.2), the following assumption is necessary and standard.

Assumption 7.2.2 The system matrices of the passive modules, F_i , which appear in the dynamics given by (7.2), are Hurwitz.

Remark 7.2.3 As a direct consequence of Assumption 7.2.2, there exist constants ξ_{1i} and ξ_{2i} such that

$$\|z_i(t)\|_2 \leq \xi_{1i} + \xi_{2i} \|\delta_i(x(t))\|_2. \quad (7.6)$$

This can be seen by rewriting the passive module dynamics given by (7.2) as

$$z_i(t) = e^{F_i t} z_{i0} + \int_0^t e^{F_i(t-\tau)} G_i \delta_i(x(\tau)) d\tau. \quad (7.7)$$

It now follows from [80] that $z_i(t)$ can be bounded by

$$\begin{aligned} \|z_i(t)\|_2 &\leq \kappa_{1i} e^{-\kappa_{2i} t} \|z_{i0}\|_2 + \int_0^t \kappa_{1i} e^{-\kappa_{2i}(t-\tau)} \|G_i\|_F \|\delta_i(x(\tau))\|_2 d\tau \\ &\leq \kappa_{1i} e^{-\kappa_{2i} t} \|z_{i0}\|_2 + \frac{\kappa_{1i} \|G_i\|_F}{\kappa_{2i}} \sup_{0 \leq \tau \leq t} \|\delta_i(x(\tau))\|_2, \end{aligned} \quad (7.8)$$

where $\kappa_{1i} > 0$ and $0 < \kappa_{2i} < -\rho(F_i)$, $\rho(F_i) \triangleq \max \{\operatorname{Re} \lambda_i : \lambda_i \in \operatorname{spec}(F_i)\}$. Noting that for an arbitrary vector $v(t)$, $\|v(t)\|_\infty = \sup_t |v(t)|$ and $\|v(t)\|_\infty \leq \|v(t)\|_2$ are true, we can further bound (7.8) by

$$\begin{aligned} \|z_i(t)\|_2 &\leq \kappa_{1i} e^{-\kappa_{2i} t} \|z_{i0}\|_2 + \frac{\kappa_{1i} \|G_i\|_F}{\kappa_{2i}} \|\delta_i(x(t))\|_\infty \\ &\leq \kappa_{1i} e^{-\kappa_{2i} t} \|z_{i0}\|_2 + \frac{\kappa_{1i} \|G_i\|_F}{\kappa_{2i}} \|\delta_i(x(t))\|_2. \end{aligned} \quad (7.9)$$

Finally, since the exponentially decaying function $e^{-\kappa_{2i}t}$ has a maximum of 1 at $t = 0$, we can let $\xi_{1i} \triangleq \kappa_{1i} \|z_{i0}\|_2$ and $\xi_{2i} \triangleq \frac{\kappa_{1i} \|G_i\|_F}{\kappa_{2i}}$ and arrive at the result in (7.6).

To capture a desired closed-loop dynamical system performance for each active module, consider the reference model for active modules given by

$$\mathcal{G}_{A_{ri}} : \quad \dot{x}_{ri}(t) = A_{ri}x_{ri}(t) + B_{ri}c_i(t), \quad x_{ri}(0) = x_{ri0}, \quad (7.10)$$

for $i = 1, \dots, N_A$, where $x_{ri}(t) \in \mathbb{R}^{n_i}$ is the reference state vector, $c_i(t) \in \mathbb{R}^{m_i}$ is a given uniformly continuous bounded command, $A_{ri} \in \mathbb{R}^{n_i \times n_i}$ is the Hurwitz reference model matrix, and $B_{ri} \in \mathbb{R}^{n_i \times m_i}$ is the command input matrix. Since $c_i(t)$ is bounded, it follows that $\|x_{ri}(t)\|_2 \leq x_{ri}^*$ for $i = 1, \dots, N_A$, with x_{ri}^* being the upper bound for each active module reference model. We now make the following classical assumption in adaptive control literature (see, for example, [6]).

Assumption 7.2.3 *There exist gain matrices $K_{1i} \in \mathbb{R}^{m_i \times n_i}$ and $K_{2i} \in \mathbb{R}^{m_i \times m_i}$ such that $A_{ri} \triangleq A_i - B_i K_{1i}$ and $B_{ri} \triangleq B_i K_{2i}$ hold.*

Note that (7.1) can now be rewritten using Assumption 7.2.3 as

$$\dot{x}_i(t) = A_{ri}x_i(t) + B_{ri}c_i(t) + B_i\Lambda_i[u_i(t) + W_i^T\sigma_i(x_i(t), c_i(t))] + B_i[\alpha_i(x(t)) + \beta_i(z(t))], \quad (7.11)$$

where $W_i \triangleq [\Lambda_i^{-1}K_{1i}, -\Lambda_i^{-1}K_{2i}]^T \in \mathbb{R}^{(n_i+m_i) \times m_i}$ is an unknown weight matrix and $\sigma_i(x_i(t), c_i(t)) \triangleq [x_i^T(t), c_i^T(t)]^T \in \mathbb{R}^{n_i+m_i}$ is a known basis function. In addition, the error dynamics for the active modules follow from (7.10) and (7.11) as

$$\dot{e}_i(t) = A_{ri}e_i(t) + B_i\Lambda_i[u_i(t) + W_i^T\sigma_i(x_i(t), c_i(t))] + B_i[\alpha_i(x(t)) + \beta_i(z(t))], \quad (7.12)$$

where $e_i(t) \triangleq x_i(t) - x_{ri}(t)$ is the system error for the active modules.

The *decentralized control problem* considered in this paper is now stated as follows. Subject to Assumptions 7.2.1, 7.2.2, and 7.2.3, consider the large-scale modular system given by (7.1) and (7.2) with N_A active modules and N_P passive modules. We aim at designing local control signals for each active module such that the active module trajectories follow reference model trajectories, the system error trajectories are restricted to a-priori, user-defined compact sets enforcing strict performance guarantees, and stability of

the overall closed-loop large-scale system involving not only active modules but also passive modules is achieved. For this purpose, the next section introduces the proposed *set-theoretic decentralized adaptive control architecture*.

7.3 Decentralized Adaptive Control for Active-Passive Modular Systems

To address command following in the presence of unknown physical interconnections between active and passive modules and module-level system uncertainties, this section proposes a set-theoretic decentralized control architecture for the modular system presented in Section 7.2. To this end, we start with the following necessary definitions.

Definition 7.3.1 Consider a convex hypercube in the form

$$\Omega_0 = \{ \theta_0 \in \mathbb{R}^s : (\theta_{0i}^{\min} \leq \theta_{0i} \leq \theta_{0i}^{\max})_{i=1,2,\dots,s} \}, \quad (7.13)$$

where $\Omega_0 \in \mathbb{R}^s$, and θ_{0i}^{\min} and θ_{0i}^{\max} respectively represent the minimum and maximum bounds for the i^{th} component of the s -dimensional parameter vector θ_0 (we set $\theta_{0i}^{\min} = -\theta_{0i}^{\max}$ for the results of this paper without loss of generality). Furthermore, for a sufficiently small positive constant v_0 , consider another hypercube in the form

$$\Omega_v = \{ \theta_0 \in \mathbb{R}^s : (\theta_{0i}^{\min} + v_0 \leq \theta_{0i} \leq \theta_{0i}^{\max} - v_0)_{i=1,2,\dots,s} \}, \quad (7.14)$$

where $\Omega_v \subset \Omega$. The projection operator $\text{Proj} : \mathbb{R}^s \times \mathbb{R}^s \rightarrow \mathbb{R}^s$ is then defined component-wise by

$$\text{Proj}(\theta, y) \triangleq \begin{cases} \left(\frac{\theta_{0i}^{\max} - \theta_{0i}}{v_0} \right) y_i, & \text{if } \theta_{0i} > \theta_{0i}^{\max} - v_0 \text{ and } y_i > 0, \\ \left(\frac{\theta_{0i} - \theta_{0i}^{\min}}{v_0} \right) y_i, & \text{if } \theta_{0i} < \theta_{0i}^{\min} + v_0 \text{ and } y_i < 0, \\ y_i, & \text{otherwise,} \end{cases}$$

where $y \in \mathbb{R}^s$.

Remark 7.3.1 As it is known, it follows from Definition 7.3.1 that

$$(\theta_0 - \theta_0^*)^T (\text{Proj}(\theta_0, y) - y) \leq 0, \quad (7.15)$$

holds for $\theta_0 \in \Omega_0$ and $y \in \mathbb{R}^s$ [6]. Throughout the paper, we also use the generalization of (7.15) to matrices as $\text{Proj}_m(\Theta, Y) = (\text{Proj}(\text{col}_1(\Theta), \text{col}_1(Y)), \dots, \text{Proj}(\text{col}_m(\Theta), \text{col}_m(Y)))$, where $\Theta \in \mathbb{R}^{n \times m}$, $Y \in \mathbb{R}^{n \times m}$, and $\text{col}_i(\cdot)$ denotes the i -th column operator. In this case, for a given matrix Θ^* ,

$$\text{tr} \left[(\Theta - \Theta^*)^T (\text{Proj}_m(\Theta, Y) - Y) \right] = \sum_{i=1}^m \left[\text{col}_i(\Theta - \Theta^*)^T (\text{Proj}(\text{col}_i(\Theta), \text{col}_i(Y)) - \text{col}_i(Y)) \right] \leq 0 \quad (7.16)$$

follows as a consequence of (7.15).

Definition 7.3.2 For a given vector $y \in \mathbb{R}^s$, the tangent hyperbolic function is defined by

$$\tanh(y^T) \triangleq [\tanh(y(1)), \dots, \tanh(y(s))]^T \in \mathbb{R}^s. \quad (7.17)$$

Definition 7.3.3 Let $\|y\|_H = \sqrt{y^T H y}$ be a weighted Euclidean norm, where $y \in \mathbb{R}^s$ is a real column vector and $H \in \mathbb{R}_+^{s \times s}$. We define $\phi(\|y\|_H)$, $\phi: \mathbb{R}^s \rightarrow \mathbb{R}$, to be a restricted potential function (barrier Lyapunov function) defined on the set

$$\mathcal{D}_\varepsilon \triangleq \{y: \|y\|_H \in [0, \varepsilon)\}, \quad (7.18)$$

with $\varepsilon \in \mathbb{R}_+$ being an a priori, user-defined constant, if the following statements hold [74]:

- If $\|y\|_H = 0$, then $\phi(\|y\|_H) = 0$.
- If $y \in \mathcal{D}_\varepsilon$ and $\|y\|_H \neq 0$, then $\phi(\|y\|_H) > 0$.
- If $\|y\|_H \rightarrow \varepsilon$, then $\phi(\|y\|_H) \rightarrow \infty$.
- $\phi(\|y\|_H)$ is continuously differentiable on \mathcal{D}_ε .
- If $y \in \mathcal{D}_\varepsilon$, then $\phi_d(\|y\|_H) > 0$, where $\phi_d(\|y\|_H) \triangleq \frac{d\phi(\|y\|_H)}{d\|y\|_H^2}$.
- If $y \in \mathcal{D}_\varepsilon$, then $2\phi_d(\|y\|_H)\|y\|_H^2 - \phi(\|y\|_H) > 0$.

Remark 7.3.2 As noted in [74], Definition 7.3.3 generalizes the definition of the restricted potential functions (barrier Lyapunov functions) used by the authors of [72, 153–157]. For example, a candidate restricted potential function satisfying the conditions of Definition 7.3.3 has the form

$$\phi(\|y\|_H) = \frac{\|y\|_H^2}{\varepsilon - \|y\|_H}, \quad y \in \mathcal{D}_\varepsilon. \quad (7.19)$$

To achieve command following in the presence of unknown physical interconnections between active and passive modules and module-level system uncertainties, we propose the set-theoretic decentralized adaptive control architecture constructed using restricted potential functions for the active modules \mathcal{G}_{A_i} as

$$\mathcal{C}_{A_i} : u_i(t) = -\hat{W}_i^T(t)\sigma_i(x_i(t), c_i(t)) - \hat{\psi}_i(t)\tanh(\phi_d(\|e_i(t)\|_{P_i})e_i^T(t)P_iB_i) - \hat{\theta}_i(t)B_i^T P_i e_i(t), \quad (7.20)$$

where $\hat{W}_i(t) \in \mathbb{R}^{n_i \times m_i}$ is an estimate of W_i satisfying the projection operator-based weight update law

$$\dot{\hat{W}}_i(t) = \gamma_i \text{Proj}_m [\hat{W}_i(t), \phi_d(\|e_i(t)\|_{P_i})\sigma_i(x_i(t), c_i(t))e_i^T(t)P_iB_i], \quad \hat{W}_i(0) = \hat{W}_{i0}, \quad (7.21)$$

which also includes restricted potential functions, where $\gamma_i \in \mathbb{R}_+$ is the learning rate gain and $\phi_d(\|e_i(t)\|_{P_i})$ can be viewed as an error dependent learning rate. Moreover, $\hat{\psi}_i(t)$ and $\hat{\theta}_i(t)$ are projection operator-based adaptive terms satisfying

$$\dot{\hat{\psi}}_i(t) = \mu_i \text{Proj} [\hat{\psi}_i(t), \phi_d(\|e_i(t)\|_{P_i})e_i^T(t)P_iB_i \tanh(\phi_d(\|e_i(t)\|_{P_i})e_i^T(t)P_iB_i)], \quad (7.22)$$

$$\hat{\psi}_i(0) = \hat{\psi}_{i0} \in \overline{\mathbb{R}}_+,$$

$$\dot{\hat{\theta}}_i(t) = \eta_i \text{Proj} [\hat{\theta}_i(t), \phi_d(\|e_i(t)\|_{P_i})\|B_i^T P_i e_i(t)\|_2^2], \quad (7.23)$$

$$\hat{\theta}_i(0) = \hat{\theta}_{i0} \in \overline{\mathbb{R}}_+,$$

with $\mu_i \in \mathbb{R}_+$ and $\eta_i \in \mathbb{R}_+$ being design parameters. Note that since $\hat{\psi}_i(0) \in \overline{\mathbb{R}}_+$ and $\hat{\theta}_i(0) \in \overline{\mathbb{R}}_+$, then $\hat{\psi}_i(t) \in \overline{\mathbb{R}}_+$ and $\hat{\theta}_i(t) \in \overline{\mathbb{R}}_+$ respectively hold. In (7.21), (7.22), and (7.23), $P_i \in \mathbb{R}_+^{n_i \times n_i}$ is a solution of the Lyapunov equation

$$0 = A_{ri}^T P_i + P_i A_{ri} + R_i, \quad (7.24)$$

with $R_i \in \mathbb{R}_+^{n_i \times n_i}$. Since A_{ri} is Hurwitz, note that from the converse Lyapunov theory [80] that there exists a unique P_i satisfying (7.24) for a given R_i . Finally, we select the projection bounds for (7.21), (7.22), and (7.23) to respectively satisfy

$$|[\hat{W}_i(t)]_{jk_i}| \leq \hat{W}_{i, \max, j_i+(k_i-1)n_i}, \quad j_i = 1, \dots, n_i \text{ and } k_i = 1, \dots, m_i, \quad (7.25)$$

$$0 \leq \hat{\psi}_i(t) \leq \psi_i \rho_{1i}, \quad \psi_i \triangleq \frac{\bar{\xi}_i}{\lambda_{\min}(\Lambda_i)}, \quad \rho_{1i} > 1, \quad (7.26)$$

$$0 \leq \hat{\theta}_i(t) \leq \theta_i \rho_{2i}, \quad \theta_i \triangleq \frac{\xi_{2i}^* l_i N_A}{2\lambda_{\min}(\Lambda_i)}, \quad \rho_{2i} > 1, \quad (7.27)$$

where $\hat{W}_{i,\max,j_i+(k_i-1)n_i} \in \mathbb{R}_+$ denotes element-wise projection bounds, $\psi_i \rho_{1i}$ and $\theta_i \rho_{2i}$ respectively denote the projection bounds for the adaptive terms given by (7.22) and (7.23) with ρ_{1i} and ρ_{2i} being free design variables and $\bar{\xi}_i \in \mathbb{R}_+$ and $\xi_{2i}^* \in \mathbb{R}_+$ to be defined later, and $l_i \in \mathbb{R}_+$ is another free design variable⁴.

7.4 Stability and Performance Guarantees

In this section, we present the stability analysis and establish strict performance guarantees of the set-theoretic decentralized control architecture proposed in Section 7.3. For this purpose, we first state the system error dynamics for the active modules \mathcal{G}_{A_i} as

$$\begin{aligned} \dot{e}_i(t) = & A_{r_i} e_i(t) - B_i \Lambda_i \left[\tilde{W}_i^T(t) \sigma_i(x_i(t), c_i(t)) + \tilde{\psi}_i(t) \tanh(\phi_d(\|e_i(t)\|_{P_i})) e_i^T(t) P_i B_i \right. \\ & \left. + \hat{\theta}_i(t) B_i^T P_i e_i(t) \right] + B_i (\alpha_i(x(t)) + \beta_i(z(t))), \end{aligned} \quad (7.28)$$

as a consequence of using (7.20) in (7.12), where $\tilde{W}_i(t) \triangleq \hat{W}_i(t) - W_i$. We then define $x_{r_{\max}} = \max_i \{x_{r_i}^*\}$, $\tilde{\psi}_i(t) \triangleq \hat{\psi}_i(t) - \psi_i$, $\tilde{\theta}_i(t) \triangleq \hat{\theta}_i(t) - \theta_i$, $\xi_{2i}^* \triangleq \alpha_i^* + \beta_i^* N_P \max_j \{ \xi_{2j} \delta_j^* \}$, and $\bar{\xi}_i \triangleq \beta_i^* N_P \cdot \max_j \{ \xi_{1j} \} + \xi_{2i}^* N_A \cdot x_{r_{\max}}$. The next theorem presents the main result of this section.

Theorem 7.4.1 *Consider the uncertain large-scale modular system \mathcal{G} comprised of interconnected active modules, \mathcal{G}_{A_i} , and passive modules, \mathcal{G}_{P_i} , described by (7.1) and (7.2), respectively, subject to Assumptions 7.2.1, 7.2.2, and 7.2.3. Additionally, consider the active module reference models given by (7.10) and control laws given by (7.20), along with the update laws (7.21), (7.22), and (7.23). If $\|e_{i0}\|_{P_i} < \varepsilon_i$, then the solution $(e_i(t), \tilde{W}_i(t), \tilde{\psi}_i(t), \tilde{\theta}_i(t), z_i(t))$ of the closed-loop dynamical large-scale modular system \mathcal{G} is bounded, where the active module system errors strictly satisfy the a-priori given, user-defined worst-case performance bounds given by*

$$\|e_i(t)\|_{P_i} < \varepsilon_i, \quad t \in \bar{\mathbb{R}}_+. \quad (7.29)$$

Proof. To show boundedness of the closed-loop dynamics of the active modules \mathcal{G}_{A_i} , consider the energy function $\mathcal{V}_i : \mathcal{D}_{e_i} \times \mathbb{R}^{\dim(\tilde{W}_i)} \times \mathbb{R}^{\dim(\tilde{\psi}_i)} \times \mathbb{R}^{\dim(\tilde{\theta}_i)} \rightarrow \bar{\mathbb{R}}_+$ given by

$$\begin{aligned} \mathcal{V}_i(e_i(t), \tilde{W}_i(t), \tilde{\psi}_i(t), \tilde{\theta}_i(t)) = & \phi(\|e_i(t)\|_{P_i}) + \gamma_i^{-1} \text{tr} \left(\tilde{W}_i(t) \Lambda_i^{\frac{1}{2}} \right)^T \left(\tilde{W}_i(t) \Lambda_i^{\frac{1}{2}} \right) \\ & + (\mu_i^{-1} \tilde{\psi}_i^2(t) + \eta_i^{-1} \tilde{\theta}_i^2(t)) \lambda_{\min}(\Lambda_i), \end{aligned} \quad (7.30)$$

⁴As standard in the adaptive control literature, one can choose all projection bounds to be sufficiently large without requiring strict knowledge of the bounds on the unknown parameters.

where $\mathcal{D}_{e_i} \triangleq \{e_i(t) : \|e_i(t)\|_{P_i} < \varepsilon_i\}$ and $\dim(\tilde{W}_i)$, $\dim(\tilde{\psi}_i)$, and $\dim(\tilde{\theta}_i)$ denote the dimensions of \tilde{W}_i , $\tilde{\psi}_i$, and $\tilde{\theta}_i$, respectively. Note that $\mathcal{V}_i(0,0,0,0) = 0$, $\mathcal{V}_i(e_i, \tilde{W}_i, \tilde{\psi}_i, \tilde{\theta}_i) > 0$ for all $(e_i, \tilde{W}_i, \tilde{\psi}_i, \tilde{\theta}_i) \neq (0,0,0,0)$, and

$$\begin{aligned} \frac{d\phi(\|e_i(t)\|_{P_i})}{dt} &= \frac{d\phi(\|e_i(t)\|_{P_i})}{d\|e_i(t)\|_{P_i}^2} \frac{d\|e_i(t)\|_{P_i}^2}{dt} \\ &= 2\phi_d(\|e_i(t)\|_{P_i}) e_i^T(t) P_i \dot{e}_i(t). \end{aligned} \quad (7.31)$$

Now, differentiating (7.30) and using (7.21) yields

$$\begin{aligned} \dot{\mathcal{V}}_i(e_i(t), \tilde{W}_i(t), \tilde{\psi}_i(t), \tilde{\theta}_i(t)) &= 2\phi_d(\|e_i(t)\|_{P_i}) e_i^T(t) P_i \dot{e}_i(t) + 2\gamma_i^{-1} \text{tr} \tilde{W}_i^T(t) \dot{\tilde{W}}_i(t) \Lambda_i + 2 \left(\mu_i^{-1} \tilde{\psi}_i(t) \dot{\tilde{\psi}}_i(t) + \eta_i^{-1} \tilde{\theta}_i(t) \dot{\tilde{\theta}}_i(t) \right) \lambda_{\min}(\Lambda_i) \\ &= -\phi_d(\|e_i(t)\|_{P_i}) e_i^T(t) R_i e_i(t) - 2\phi_d(\|e_i(t)\|_{P_i}) e_i^T(t) P_i B_i \tilde{W}_i^T(t) \sigma_i(x_i(t), c_i(t)) \\ &\quad - 2\hat{\psi}_i(t) \phi_d(\|e_i(t)\|_{P_i}) e_i^T(t) P_i B_i \Lambda_i \tanh(\phi_d(\|e_i(t)\|_{P_i}) e_i^T(t) P_i B_i) \\ &\quad - 2\hat{\theta}_i(t) \phi_d(\|e_i(t)\|_{P_i}) e_i^T(t) P_i B_i \Lambda_i B_i^T P_i e_i(t) + 2\phi_d(\|e_i(t)\|_{P_i}) e_i^T(t) P_i B_i (\alpha_i(x(t)) + \beta_i(z(t))) \\ &\quad + 2\text{tr} \tilde{W}_i^T(t) \text{Proj}_m[\hat{W}_i(t), \phi_d(\|e_i(t)\|_{P_i}) \sigma_i(x_i(t), c_i(t)) e_i^T(t) P_i B_i] \Lambda_i \\ &\quad + 2 \left(\mu_i^{-1} \tilde{\psi}_i(t) \dot{\tilde{\psi}}_i(t) + \eta_i^{-1} \tilde{\theta}_i(t) \dot{\tilde{\theta}}_i(t) \right) \lambda_{\min}(\Lambda_i) \\ &\leq -\phi_d(\|e_i(t)\|_{P_i}) e_i^T(t) R_i e_i(t) - 2\hat{\psi}_i(t) \phi_d(\|e_i(t)\|_{P_i}) e_i^T(t) P_i B_i \Lambda_i \tanh(\phi_d(\|e_i(t)\|_{P_i}) e_i^T(t) P_i B_i) \\ &\quad - 2\hat{\theta}_i(t) \phi_d(\|e_i(t)\|_{P_i}) e_i^T(t) P_i B_i \Lambda_i B_i^T P_i e_i(t) + 2\phi_d(\|e_i(t)\|_{P_i}) e_i^T(t) P_i B_i (\alpha_i(x(t)) + \beta_i(z(t))) \\ &\quad + 2 \left(\mu_i^{-1} \tilde{\psi}_i(t) \dot{\tilde{\psi}}_i(t) + \eta_i^{-1} \tilde{\theta}_i(t) \dot{\tilde{\theta}}_i(t) \right) \lambda_{\min}(\Lambda_i). \end{aligned} \quad (7.32)$$

As a direct consequence of the projection operator-based update laws for $\hat{\psi}_i(t)$ and $\hat{\theta}_i(t)$, the inequalities

$$\begin{aligned} &-2\hat{\psi}_i(t) \phi_d(\|e_i(t)\|_{P_i}) e_i^T(t) P_i B_i \Lambda_i \tanh(\phi_d(\|e_i(t)\|_{P_i}) e_i^T(t) P_i B_i) \\ &\leq -2\hat{\psi}_i(t) \phi_d(\|e_i(t)\|_{P_i}) e_i^T(t) P_i B_i \lambda_{\min}(\Lambda_i) \tanh(\phi_d(\|e_i(t)\|_{P_i}) e_i^T(t) P_i B_i), \end{aligned} \quad (7.33)$$

and

$$-2\hat{\theta}_i(t) \phi_d(\|e_i(t)\|_{P_i}) e_i^T(t) P_i B_i \Lambda_i B_i^T P_i e_i(t) \leq -2\hat{\theta}_i(t) \phi_d(\|e_i(t)\|_{P_i}) \lambda_{\min}(\Lambda_i) \|B_i^T P_i e_i(t)\|_2^2, \quad (7.34)$$

hold. Now, we can write (7.32) with (7.33) and (7.34) as

$$\begin{aligned}
& \dot{\mathcal{V}}_i(e_i(t), \tilde{W}_i(t), \tilde{\psi}_i(t), \tilde{\theta}_i(t)) \\
& \leq -\phi_d(\|e_i(t)\|_{P_i}) \lambda_{\min}(R_i) \|e_i(t)\|_2^2 + 2\phi_d(\|e_i(t)\|_{P_i}) \|B_i^T P_i e_i(t)\|_2 \|\alpha_i(x(t)) + \beta_i(z(t))\|_2 \\
& \quad - 2\tilde{\psi}_i(t) \phi_d(\|e_i(t)\|_{P_i}) e_i^T(t) P_i B_i \lambda_{\min}(\Lambda_i) \tanh(\phi_d(\|e_i(t)\|_{P_i}) e_i^T(t) P_i B_i) \\
& \quad - 2\hat{\theta}_i(t) \phi_d(\|e_i(t)\|_{P_i}) \lambda_{\min}(\Lambda_i) \|B_i^T P_i e_i(t)\|_2^2 + 2\left(\mu_i^{-1} \tilde{\psi}_i(t) \dot{\tilde{\psi}}_i(t) + \eta_i^{-1} \tilde{\theta}_i(t) \dot{\tilde{\theta}}_i(t)\right) \lambda_{\min}(\Lambda_i). \quad (7.35)
\end{aligned}$$

Next, note that

$$\begin{aligned}
& 2\phi_d(\|e_i(t)\|_{P_i}) \|B_i^T P_i e_i(t)\|_2 \|\alpha_i(x(t)) + \beta_i(z(t))\|_2 \\
& \leq 2\phi_d(\|e_i(t)\|_{P_i}) \|B_i^T P_i e_i(t)\|_2 \left[\|\alpha_i(x(t))\|_2 + \|\beta_i(z(t))\|_2 \right] \\
& \leq 2\phi_d(\|e_i(t)\|_{P_i}) \|B_i^T P_i e_i(t)\|_2 \left[\alpha_i^* \sum_{j=1}^{N_A} \|x_j(t)\|_2 + \beta_i^* \sum_{j=1}^{N_P} \|z_j(t)\|_2 \right] \\
& \leq 2\phi_d(\|e_i(t)\|_{P_i}) \|B_i^T P_i e_i(t)\|_2 \left[\alpha_i^* \sum_{j=1}^{N_A} \|x_j(t)\|_2 + \beta_i^* \sum_{j=1}^{N_P} \left(\xi_{1,j} + \xi_{2,j} \delta_j^* \sum_{k=1}^{N_A} \|x_k(t)\|_2 \right) \right] \\
& \leq 2\phi_d(\|e_i(t)\|_{P_i}) \|B_i^T P_i e_i(t)\|_2 \left[\beta_i^* N_P \max_j \{ \xi_{1,j} \} + \xi_{2i}^* \sum_{j=1}^{N_A} \|x_j(t)\|_2 \right] \\
& \leq 2\phi_d(\|e_i(t)\|_{P_i}) \|B_i^T P_i e_i(t)\|_2 \left[\beta_i^* N_P \max_j \{ \xi_{1,j} \} + \xi_{2i}^* \sum_{j=1}^{N_A} (\|e_j(t)\|_2 + \|x_{rj}(t)\|_2) \right] \\
& \leq 2\phi_d(\|e_i(t)\|_{P_i}) \|B_i^T P_i e_i(t)\|_2 \left[\beta_i^* N_P \max_j \{ \xi_{1,j} \} + \xi_{2i}^* N_A \max_i \{ x_{ri} \} + \xi_{2i}^* \sum_{j=1}^{N_A} \|e_j(t)\|_2 \right] \\
& = 2\phi_d(\|e_i(t)\|_{P_i}) \|B_i^T P_i e_i(t)\|_2 \bar{\xi}_i + \phi_d(\|e_i(t)\|_{P_i}) \xi_{2i}^* \sum_{j=1}^{N_A} 2 \|B_i^T P_i e_i\|_2 \|e_j(t)\|_2. \quad (7.36)
\end{aligned}$$

In addition, using Young's inequality [14] for the second term in (7.36) gives

$$\begin{aligned}
& \phi_d(\|e_i(t)\|_{P_i}) \xi_{2i}^* \sum_{j=1}^{N_A} 2 \|B_i^T P_i e_i(t)\|_2 \|e_j(t)\|_2 \\
& \leq \phi_d(\|e_i(t)\|_{P_i}) \xi_{2i}^* \sum_{j=1}^{N_A} \left(l_i \|B_i^T P_i e_i(t)\|_2^2 + \frac{1}{l_i} \|e_j(t)\|_2^2 \right) \\
& = \phi_d(\|e_i(t)\|_{P_i}) \xi_{2i}^* N_A l_i \|B_i^T P_i e_i(t)\|_2^2 + \frac{\phi_d(\|e_i(t)\|_{P_i}) \xi_{2i}^*}{l_i} \sum_{j=1}^{N_A} \|e_j(t)\|_2^2. \quad (7.37)
\end{aligned}$$

Now, using (7.36) with (7.37) in (7.35) yields

$$\begin{aligned}
& \dot{\mathcal{V}}_i(e_i(t), \tilde{W}_i(t), \tilde{\Psi}_i(t), \tilde{\Theta}_i(t)) \\
& \leq -\phi_d(\|e_i(t)\|_{P_i}) \lambda_{\min}(R_i) \|e_i(t)\|_2^2 + 2\phi_d(\|e_i(t)\|_{P_i}) \|B_i^T P_i e_i(t)\|_2 \bar{\xi}_i \\
& \quad + \phi_d(\|e_i(t)\|_{P_i}) \xi_{2i}^* N_A l_i \|B_i^T P_i e_i(t)\|_2^2 + \frac{\phi_d(\|e_i(t)\|_{P_i}) \xi_{2i}^*}{l_i} \sum_{j=1}^{N_A} \|e_j(t)\|_2^2 \\
& \quad - 2\tilde{\Psi}_i(t) \phi_d(\|e_i(t)\|_{P_i}) e_i^T(t) P_i B_i \lambda_{\min}(\Lambda_i) \tanh(\phi_d(\|e_i(t)\|_{P_i}) e_i^T(t) P_i B_i) \\
& \quad - 2\hat{\Theta}_i(t) \phi_d(\|e_i(t)\|_{P_i}) \lambda_{\min}(\Lambda_i) \|B_i^T P_i e_i(t)\|_2^2 + 2\left(\mu_i^{-1} \tilde{\Psi}_i(t) \dot{\tilde{\Psi}}_i(t) + \eta_i^{-1} \tilde{\Theta}_i(t) \dot{\hat{\Theta}}_i(t)\right) \lambda_{\min}(\Lambda_i) \\
& = -\phi_d(\|e_i(t)\|_{P_i}) \lambda_{\min}(R_i) \|e_i(t)\|_2^2 + \frac{\phi_d(\|e_i(t)\|_{P_i}) \xi_{2i}^*}{l_i} \sum_{j=1}^{N_A} \|e_j(t)\|_2^2 \\
& \quad + 2\lambda_{\min}(\Lambda_i) \Psi_i \left[\|\phi_d(\|e_i(t)\|_{P_i}) B_i^T P_i e_i(t)\|_2 - \phi_d(\|e_i(t)\|_{P_i}) e_i^T(t) P_i B_i \tanh(\phi_d(\|e_i(t)\|_{P_i}) \right. \\
& \quad \cdot e_i^T(t) P_i B_i) \left. \right] + 2\mu_i^{-1} \tilde{\Psi}_i \left[\dot{\tilde{\Psi}}_i(t) - \mu_i \phi_d(\|e_i(t)\|_{P_i}) e_i^T P_i B_i \tanh(\phi_d(\|e_i(t)\|_{P_i}) e_i^T P_i B_i) \right] \lambda_{\min}(\Lambda_i) \\
& \quad + 2\eta_i^{-1} \tilde{\Theta}_i \left[\dot{\hat{\Theta}}_i(t) - \eta_i \phi_d(\|e_i(t)\|_{P_i}) \|B_i^T P_i e_i^T(t)\|_2^2 \right] \lambda_{\min}(\Lambda_i). \tag{7.38}
\end{aligned}$$

Owing to the nature of using the tangent hyperbolic function,

$$\|\phi_d(\|e_i(t)\|_{P_i}) B_i^T P_i e_i(t)\|_2 - \phi_d(\|e_i(t)\|_{P_i}) e_i^T(t) P_i B_i \tanh(\phi_d(\|e_i(t)\|_{P_i}) e_i^T(t) P_i B_i) \leq \mathcal{L}_i, \tag{7.39}$$

holds [158], where $\mathcal{L}_i = 0.2785$ for all $i = 1, 2, \dots, N_A$. Using this along with (7.22) and (7.23) in (7.38) yields

$$\begin{aligned}
& \dot{\mathcal{V}}_i(e_i(t), \tilde{W}_i(t), \tilde{\Psi}_i(t), \tilde{\Theta}_i(t)) \\
& \leq -\phi_d(\|e_i(t)\|_{P_i}) \lambda_{\min}(R_i) \|e_i(t)\|_2^2 + \frac{\phi_d(\|e_i(t)\|_{P_i}) \xi_{2i}^*}{l_i} \sum_{j=1}^{N_A} \|e_j(t)\|_2^2 + 2\lambda_{\min}(\Lambda_i) \Psi_i \mathcal{L}_i. \tag{7.40}
\end{aligned}$$

Consider the aggregated energy function for the active modules $\mathcal{V}(\cdot) = \sum_{i=1}^{N_A} \mathcal{V}_i(\cdot)$, which results in

$$\begin{aligned}
\dot{\mathcal{V}}(\cdot) & \leq \sum_{i=1}^{N_A} \left[-\phi_d(\|e_i(t)\|_{P_i}) \lambda_{\min}(R_i) \|e_i(t)\|_2^2 + \frac{\phi_d(\|e_i(t)\|_{P_i}) \xi_{2i}^*}{l_i} \sum_{j=1}^{N_A} \|e_j(t)\|_2^2 + 2\lambda_{\min}(\Lambda_i) \Psi_i \mathcal{L}_i \right] \\
& = -\sum_{i=1}^{N_A} \phi_d(\|e_i(t)\|_{P_i}) \left[\lambda_{\min}(R_i) - \sum_{j=1}^{N_A} \frac{\xi_{2j}^*}{l_j} \right] \|e_i(t)\|_2^2 + \sum_{i=1}^{N_A} 2\lambda_{\min}(\Lambda_i) \Psi_i \mathcal{L}_i. \tag{7.41}
\end{aligned}$$

Using the inequality $\lambda_{\min}(P_i) \|e_i(t)\|_2^2 \leq e_i^T(t)P_i e_i(t) \leq \lambda_{\max}(P_i) \|e_i(t)\|_2^2$, one can write (7.41) as

$$\begin{aligned} \dot{\mathcal{V}}(\cdot) &\leq -\sum_{i=1}^{N_A} \phi_d(\|e_i(t)\|_{P_i}) \frac{1}{\lambda_{\max}(P_i)} \left[\lambda_{\min}(R_i) - \sum_{j=1}^{N_A} \frac{\xi_{2j}^*}{l_j} \right] e_i^T(t)P_i e_i(t) + \sum_{i=1}^{N_A} 2\lambda_{\min}(\Lambda_i) \psi_i \mathcal{L}_i \\ &= -\sum_{i=1}^{N_A} \left(\frac{1}{2} \rho_i \phi(\|e_i(t)\|_{P_i}) + \rho_i \left(\phi_d(\|e_i(t)\|_{P_i}) \cdot e_i^T(t)P_i e_i(t) - \frac{1}{2} \phi(\|e_i(t)\|_{P_i}) \right) \right) \\ &\quad + \sum_{i=1}^{N_A} 2\lambda_{\min}(\Lambda_i) \psi_i \mathcal{L}_i \end{aligned} \quad (7.42)$$

where $\rho_i = \frac{1}{\lambda_{\max}(P_i)} \left[\lambda_{\min}(R_i) - \sum_{j=1}^{N_A} \frac{\xi_{2j}^*}{l_j} \right]$. Noting from Definition 7.3.3 that $\phi_d(\|e_i(t)\|_{P_i}) e_i^T(t)P_i e_i(t) - \frac{1}{2} \phi(\|e_i(t)\|_{P_i}) > 0$, (7.42) can be written as

$$\begin{aligned} \dot{\mathcal{V}}(\cdot) &\leq -\sum_{i=1}^{N_A} \frac{1}{2} \rho_i \left(\phi(\|e_i(t)\|_{P_i}) + \gamma_i^{-1} \text{tr} \left(\tilde{W}_i(t) \Lambda_i^{\frac{1}{2}} \right)^T \left(\tilde{W}_i(t) \Lambda_i^{\frac{1}{2}} \right) + (\mu_i^{-1} \tilde{\psi}_i^2(t) + \eta_i^{-1} \tilde{\theta}_i^2(t)) \lambda_{\min}(\Lambda_i) \right) \\ &\quad + \sum_{i=1}^{N_A} \left(\frac{1}{2} \rho_i \left(\gamma_i^{-1} \text{tr} \left(\tilde{W}_i(t) \Lambda_i^{\frac{1}{2}} \right)^T \left(\tilde{W}_i(t) \Lambda_i^{\frac{1}{2}} \right) + (\mu_i^{-1} \tilde{\psi}_i^2(t) + \eta_i^{-1} \tilde{\theta}_i^2(t)) \lambda_{\min}(\Lambda_i) \right) \right. \\ &\quad \left. + 2\lambda_{\min}(\Lambda_i) \psi_i \mathcal{L}_i \right) \\ &\leq -a_{\min} \mathcal{V}(\cdot) + b_{\max}, \end{aligned} \quad (7.43)$$

where $a_{\min} = \min_i \left\{ \frac{1}{2} \rho_i \right\}$ and

$$b_{\max} = N_A \max_i \left\{ \left(\frac{1}{2} \rho_i (\gamma_i^{-1} \omega_i^{*2} \lambda_{\max}(\Lambda_i) + (\mu_i^{-1} \psi_i^{*2} + \eta_i^{-1} \theta_i^{*2}) \lambda_{\min}(\Lambda_i)) + 2\lambda_{\min}(\Lambda_i) \psi_i \mathcal{L}_i \right) \right\}, \quad (7.44)$$

with $\|\tilde{W}_i(t)\|_{\mathbb{F}} \leq \omega_i^*$, $|\tilde{\psi}_i(t)| \leq \psi_i^*$, and $|\tilde{\theta}_i(t)| \leq \theta_i^*$. From (7.43), $\mathcal{V}(e(t), \tilde{W}(t), \tilde{\psi}(t), \tilde{\theta}(t))$ is upper bounded by $\mathcal{V}_{\max} \triangleq \max \left\{ \mathcal{V}_0, \frac{b_{\max}}{a_{\min}} \right\}$, where $\mathcal{V}_0 \triangleq N_A \max_i \mathcal{V}(e_i(0), \tilde{W}_i(0), \tilde{\psi}_i(0), \tilde{\theta}_i(0))$. Now from $\mathcal{V}(\cdot) = \sum_{i=1}^{N_A} \mathcal{V}_i(\cdot)$, it follows that $\mathcal{V}_i(e_i(t), \tilde{W}_i(t), \tilde{\psi}_i(t), \tilde{\theta}_i(t)) \leq \mathcal{V}_{\max}$, $i = 1, 2, \dots, N_A$, resulting in $\phi(\|e_i(t)\|_{P_i}) \leq \mathcal{V}_{\max}$, $i = 1, 2, \dots, N_A$, and hence, the strict performance bound on the active modules given by (7.29) is now immediate. Furthermore, $\mathcal{V}_i(e_i(t), \tilde{W}_i(t), \tilde{\psi}_i(t), \tilde{\theta}_i(t)) \leq \mathcal{V}_{\max}$, $i = 1, 2, \dots, N_A$, implies the solution of the closed-loop active module dynamics, $(e_i(t), \tilde{W}_i(t), \tilde{\psi}_i(t), \tilde{\theta}_i(t))$, is bounded. As a direct consequence of the boundedness of $e_i(t)$, $i = 1, 2, \dots, N_A$, it follows that $x_i(t)$, $i = 1, 2, \dots, N_A$, is also bounded. From Assumption 7.2.2, F_i , $i = 1, 2, \dots, N_P$, is Hurwitz, and hence, $z_i(t)$, $i = 1, 2, \dots, N_P$, is bounded. The boundedness of the overall closed-loop large-scale active-passive modular system \mathcal{G} is now immediate. ■

Remark 7.4.1 From the solution of the inequality (7.43) given by

$$\mathcal{V}(\cdot) \leq \mathcal{V}_0 e^{-a_{\min} t} + \frac{b_{\max}}{a_{\min}} (1 - e^{-a_{\min} t}), \quad (7.45)$$

it follows that $\lim_{t \rightarrow \infty} \mathcal{V}(\cdot) \leq \frac{b_{\max}}{a_{\min}}$. This upper bound on the trajectories of $\mathcal{V}(\cdot)$ as $t \rightarrow \infty$, can be made small by increasing the adaptation gains γ_i , μ_i , and η_i . In addition, it should be noted that the one can either judiciously choose R_i in the Lyapunov equation (7.24) to obtain a different solution P_i or use an optimization process [159] to design P_i to improve the enforcing of the performance bound $\|e_i(t)\| < \varepsilon_i$.

Remark 7.4.2 As a result of the strict performance bound enforced on the active module \mathcal{G}_{Λ_i} error given by (7.29), it follows as in [74] that upper bounds can be enforced on the state signal $x_i(t)$ and the control signal $u_i(t)$. For this purpose, it follows from $e_i(t) \triangleq x_i(t) - x_{ri}(t)$ that

$$\begin{aligned} \|x_i(t)\|_2 &= \|e_i(t) + x_{ri}(t)\|_2 \\ &\leq \|e_i(t)\|_2 + \|x_{ri}(t)\|_2 \\ &\leq \frac{\varepsilon_i}{\sqrt{\lambda_{\min}(P_i)}} + x_{ri}^*, \end{aligned} \quad (7.46)$$

and from (7.20) that

$$\begin{aligned} \|u_i(t)\|_2 &= \left\| -\hat{W}_i^T(t) \sigma_i(x_i(t), c_i(t)) - \hat{\psi}_i(t) \tanh(\phi_d(\|e_i(t)\|_{P_i})) e_i^T(t) P_i B_i - \hat{\theta}_i(t) B_i^T P_i e_i(t) \right\|_2 \\ &\leq \omega^* \|\sigma_i(x_i(t), c_i(t))\|_2 + \psi_i \rho_{1i} + \theta_i \rho_{2i} \|B_i^T P_i\|_F \|e_i(t)\|_2, \end{aligned} \quad (7.47)$$

where $\|\hat{W}_i(t)\|_F \leq \omega^*$ holds owing to the projection bounds on each element, with $\omega^* \in \mathbb{R}_+$. Since $\sigma_i(x_i(t), c_i(t)) = [x_i^T(t), c_i^T(t)]^T$, it follows that $\|\sigma_i(x_i(t), c_i(t))\|_2^2 = \|x_i(t)\|_2^2 + \|c_i(t)\|_2^2 \leq (\|x_i(t)\|_2 + \|c_i(t)\|_2)^2$; hence, $\|\sigma_i(x_i(t), c_i(t))\|_2 \leq \|x_i(t)\|_2 + \|c_i(t)\|_2$, such that the bound on $u_i(t)$ can be further given as

$$\begin{aligned} \|u_i(t)\|_2 &\leq \omega^* (\|x_i(t)\|_2 + \|c_i(t)\|_2) + \psi_i \rho_{1i} + \theta_i \rho_{2i} \|B_i^T P_i\|_F \frac{\varepsilon_i}{\sqrt{\lambda_{\min}(P_i)}} \\ &\leq \omega^* \left(\frac{\varepsilon_i}{\sqrt{\lambda_{\min}(P_i)}} + x_{ri}^* + \|c_i(t)\|_2 \right) + \psi_i \rho_{1i} + \theta_i \rho_{2i} \|B_i^T P_i\|_F \frac{\varepsilon_i}{\sqrt{\lambda_{\min}(P_i)}} \\ &= \frac{\varepsilon_i}{\sqrt{\lambda_{\min}(P_i)}} (\omega^* + \theta_i \rho_{2i} \|B_i^T P_i\|_F) + \omega^* (x_{ri}^* + \|c_i(t)\|_2) + \psi_i \rho_{1i}. \end{aligned} \quad (7.48)$$

Now, if one is interested in applying a state and/or control dependent function such as a cost function (e.g., to minimize drag as in [151, 152]), the corresponding function is bounded owing to the performance bound enforced by the proposed control design. As an example, consider the cost function for each active module i given by

$$J_i = \frac{1}{2} \left(x_i^T(t) Q_i x_i(t) + u_i^T(t) R_i u_i(t) \right). \quad (7.49)$$

This can be bounded using (7.46) and (7.48) as follows

$$\begin{aligned} J_i &\leq \frac{1}{2} \left(\lambda_{\min}(Q_i) \|x_i(t)\|_2 + \lambda_{\min}(R_i) \|u_i(t)\|_2 \right) \\ &\leq \frac{1}{2} \left(\lambda_{\min}(Q_i) \left(\frac{\varepsilon_i}{\sqrt{\lambda_{\min}(P_i)}} + x_{ii}^* \right) + \lambda_{\min}(R_i) \left(\frac{\varepsilon_i}{\sqrt{\lambda_{\min}(P_i)}} (\omega^* + \theta_i \rho_{2i} \|B_i^T P_i\|_F) \right. \right. \\ &\quad \left. \left. + \omega^* (x_{ii}^* + \|c_i(t)\|_2) + \psi_i \rho_{1i} \right) \right). \end{aligned} \quad (7.50)$$

It is then possible to reduce the bound on the cost function to some extent by the selection of the a-priori, user-defined performance bound ε_i .

Remark 7.4.3 In the case one is not interested in command following, but instead the simpler stabilization case is considered, the control architecture given in Section 7.3 can be modified to stabilize the large-scale modular system given by (7.1) and (7.2). For this purpose, the control architecture given by (7.20), (7.21), (7.22), (7.23) is redefined as

$$u_i(t) = -\hat{W}_i^T(t) x_i(t) - \hat{\psi}_i(t) \tanh(\phi_d(\|x_i(t)\|_{P_i}) x_i^T(t) P_i B_i) - \hat{\theta}_i(t) B_i^T P_i x_i(t) - \hat{\theta}_i(t) B_i^T P_i x_i(t), \quad (7.51)$$

$$\dot{\hat{W}}_i(t) = \gamma_i \text{Proj}_m [\hat{W}_i(t), \phi_d(\|x_i(t)\|_{P_i}) x_i(t) x_i^T(t) P_i B_i], \quad (7.52)$$

$$\dot{\hat{\psi}}_i(t) = \mu_i \text{Proj} [\hat{\psi}_i(t), \phi_d(\|x_i(t)\|_{P_i}) x_i^T(t) P_i B_i \tanh(\phi_d(\|x_i(t)\|_{P_i}) x_i^T(t) P_i B_i)], \quad (7.53)$$

$$\dot{\hat{\theta}}_i(t) = \eta_i \text{Proj} [\hat{\theta}_i(t), \phi_d(\|x_i(t)\|_{P_i}) \|B_i^T P_i x_i(t)\|_2^2], \quad (7.54)$$

with $\hat{W}_i(0) = \hat{W}_{i0}$, $\hat{\psi}_i(0) = \hat{\psi}_{i0} \in \overline{\mathbb{R}}_+$, and $\hat{\theta}_i(0) = \hat{\theta}_{i0} \in \overline{\mathbb{R}}_+$. Then, by considering the energy function

$$\begin{aligned} \mathcal{V}_i(x_i(t), \tilde{W}_i(t), \tilde{\psi}_i(t), \tilde{\theta}_i(t)) &= \phi(\|x_i(t)\|_{P_i}) + \gamma_i^{-1} \text{tr} \left(\tilde{W}_i(t) \Lambda_i^{\frac{1}{2}} \right)^T \left(\tilde{W}_i(t) \Lambda_i^{\frac{1}{2}} \right) \\ &\quad + (\mu_i^{-1} \tilde{\psi}_i^2(t) + \eta_i^{-1} \tilde{\theta}_i^2(t)) \lambda_{\min}(\Lambda_i), \end{aligned} \quad (7.55)$$

and following similar steps as the proof of Theorem 7.4.1, one can conclude that the solution $(x_i(t), \tilde{W}_i(t), \tilde{\Psi}_i(t), \tilde{\theta}_i(t), z_i(t))$ of the closed-loop dynamical large-scale modular system \mathcal{G} is bounded and the active module states strictly satisfy the given user-defined worst-case performance bound given by $\|x_i(t)\|_{P_i} < \varepsilon_i$, $t \in \bar{\mathbb{R}}_+$.

7.5 Illustrative Numerical Example

In this section, we present a numerical example to illustrate the efficacy of the proposed adaptive decentralized control architecture. For this purpose, consider the uncertain dynamical large-scale system depicted in Figure 7.3, which has four active modules and one passive module.

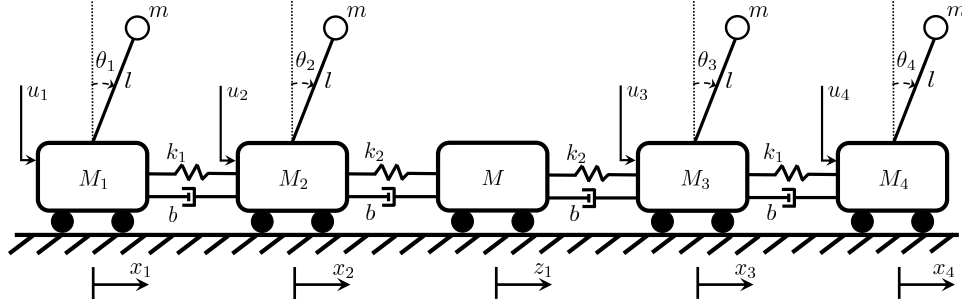


Figure 7.3: An interconnected large-scale system consisting of five carts.

The active modules have the following dynamics

$$\begin{bmatrix} \dot{\theta}_i(t) \\ \ddot{\theta}_i(t) \\ \dot{x}_i(t) \\ \ddot{x}_i(t) \end{bmatrix} = \begin{bmatrix} 0 & 1 & 0 & 0 \\ \frac{(M_i+m_0)g}{M_i l} & 0 & \frac{k_1}{M_i l} & \frac{b}{M_i l} \\ 0 & 0 & 0 & 1 \\ \frac{m_0 g}{M_i} & 0 & -\frac{k_1}{M_i} & -\frac{b}{M_i} \end{bmatrix} \begin{bmatrix} \theta_i(t) \\ \dot{\theta}_i(t) \\ x_i(t) \\ \dot{x}_i(t) \end{bmatrix} + \begin{bmatrix} 0 \\ -\frac{1}{M_i l} \\ 0 \\ \frac{1}{M_i} \end{bmatrix} (\Lambda_i u_i(t) + \alpha_i(x(t))), \quad (7.56)$$

$$\begin{bmatrix} \dot{\theta}_i(t) \\ \ddot{\theta}_i(t) \\ \dot{x}_i(t) \\ \ddot{x}_i(t) \end{bmatrix} = \begin{bmatrix} 0 & 1 & 0 & 0 \\ \frac{(M_i+m_0)g}{M_i l} & 0 & \frac{k_1+k_2}{M_i l} & \frac{2b}{M_i l} \\ 0 & 0 & 0 & 1 \\ \frac{m_0 g}{M_i} & 0 & -\frac{(k_1+k_2)}{M_i} & -\frac{2b}{M_i} \end{bmatrix} \begin{bmatrix} \theta_i(t) \\ \dot{\theta}_i(t) \\ x_i(t) \\ \dot{x}_i(t) \end{bmatrix} + \begin{bmatrix} 0 \\ -\frac{1}{M_i l} \\ 0 \\ \frac{1}{M_i} \end{bmatrix} (\Lambda_i u_i(t) + \alpha_i(x(t)) + \beta_i(z(t))), \quad (7.57)$$

where (7.56) is for active carts $i = 1, 4$ and (7.57) is for active carts $i = 2, 3$. The unknown physical interconnections between active modules are given by

$$\begin{aligned}\alpha_1(x(t)) &= k_1 x_2(t) + b \dot{x}_2(t), \\ \alpha_2(x(t)) &= k_1 x_1(t) + b \dot{x}_1(t), \\ \alpha_3(x(t)) &= k_1 x_4(t) + b \dot{x}_4(t), \\ \alpha_4(x(t)) &= k_1 x_3(t) + b \dot{x}_3(t),\end{aligned}$$

and the unknown physical interconnections with the passive module are given by

$$\beta_i(x(t)) = k_2 z_1(t) + b \dot{z}_1(t), \quad i = 2, 3.$$

In addition, the passive module has the following dynamics

$$\dot{z}_1(t) = \begin{bmatrix} 0 & 1 \\ -\frac{2k_2}{M} & -\frac{2b}{M} \end{bmatrix} z_1(t) + \begin{bmatrix} 0 \\ \frac{1}{M} \end{bmatrix} \delta(x(t)). \quad (7.58)$$

The unknown physical interconnection with the active modules is given by

$$\delta(x(t)) = k_2 (x_2(t) + x_3(t)) + b (\dot{x}_2(t) + \dot{x}_3(t)).$$

For this example, all the cart masses are known as $M_1 = M_4 = 1.0$ (kg), $M_2 = M_3 = 3.0$ (kg), and $M = 5.0$ (kg), each pendulum has a length $l = 2$ (m) with a mass $m = 0.5$ (kg), and $g = 9.81$ (m/s²) is the gravitational constant. In addition, the spring constant and damper coefficient are unknown but for simulation purposes we let $k_1 = 1.0$ (N · m⁻¹), $k_2 = 2.0$ (N · m⁻¹), and $b = 1.0$ (N · sec · m⁻¹), and the unknown control effectiveness is set as $\Lambda_i = 0.5$, $i = 1, 2, 3, 4$.

For this example, we set the command signal for each active module to follow as $c_i = \sin(\omega_i t)$, where $\omega_i = 0.1$, for $i = 1, 2, 3, 4$, and we set $R_i = I_2$ for the proposed adaptive decentralized control for the active modules. Linear quadratic regulation theory [91] is used to design the nominal feedback control gain K_{1i} , for $i = 1, 2, 3, 4$. Through tuning, we select the weighting matrices $Q = \text{diag}[0.1, 1, 10, 5]$ to penalize the states and $R = 1$ to penalize the control input such that we obtain $K_{1i} = \begin{bmatrix} -69. & -29.0 & -4.3 & -7.3 \end{bmatrix}$, for $i = 1, 4$, and $K_{1i} = \begin{bmatrix} -120.8 & -52.3 & -7.4 & -10.1 \end{bmatrix}$, for $i = 2, 3$, to design the Hurwitz reference models A_{ri} , for $i = 1, 2, 3, 4$. A pre-filter design is used such that a desired cart position $x_i(t)$ is followed. For this purpose, using $C = [0, 0, 1, 0]$, the gain K_{2i} is calculated as $K_{2i} = -(C(A_i - B_i K_{1i})^{-1} B_i)^{-1} = -3.3$,

for $i = 1, 4$ and $K_{2i} = -4.4$, for $i = 2, 3$. Finally, using the rectangular projection operator, bounds on the uncertainty are set element-wise to be 5% greater than each uncertain element of $W_i = [\Lambda_i^{-1}K_{1i}, -\Lambda_i^{-1}K_{2i}]^T$ for $i = 1, 2, 3, 4$, and we set $0 \leq \hat{\psi}_i(t) \leq 100$ and $0 \leq \hat{\theta}_i(t) \leq 100$, for $i = 1, 2, 3, 4$. The learning gains are set as $\gamma_i = 1$, for $i = 1, 2, 3, 4$, and the gains for the robustifying terms are set as $\mu_i = 10$ and $\eta_i = 10$, for $i = 1, 2, 3, 4$.

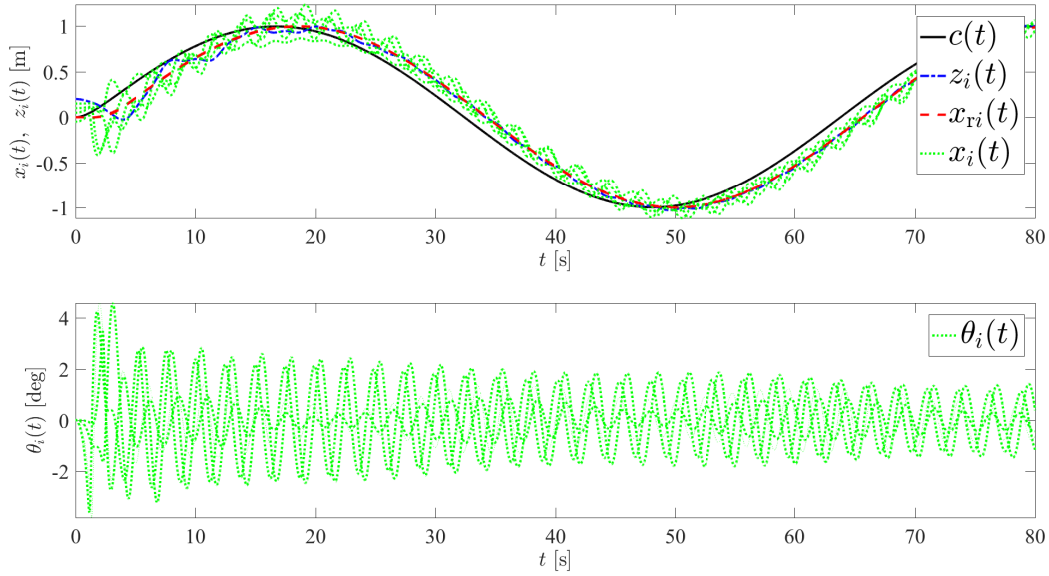


Figure 7.4: Position tracking and pendulum stabilization of the proposed adaptive decentralized controller with the performance bound $\varepsilon_i = 1.0$.

Figures 7.4–7.7 show the performance of the interconnected cart system for different performance bounds ε_i . Specifically, a performance bound of $\varepsilon_i = 1.0$ is used in Figures 7.4 and 7.5 and then reduced to $\varepsilon_i = 0.5$ in Figures 7.6 and 7.7. It can be seen in Figures 7.4 and 7.6 that all the active modules approximately follow the reference model trajectory and passive module remains bounded, where the performance is improved from Figure 7.4 to Figure 7.6 due to the more strictly enforced performance bound ε_i . Figures 7.5 and 7.7 show the change in the error dependent learning gain $\phi_d(\|e_i(t)\|_{P_i})$ to prevent the violation of ε_i as the active modules follow the reference model trajectory. This is consistent with the presented theory in that the violation of ε_i is prevented as the error dependent learning gain increases.

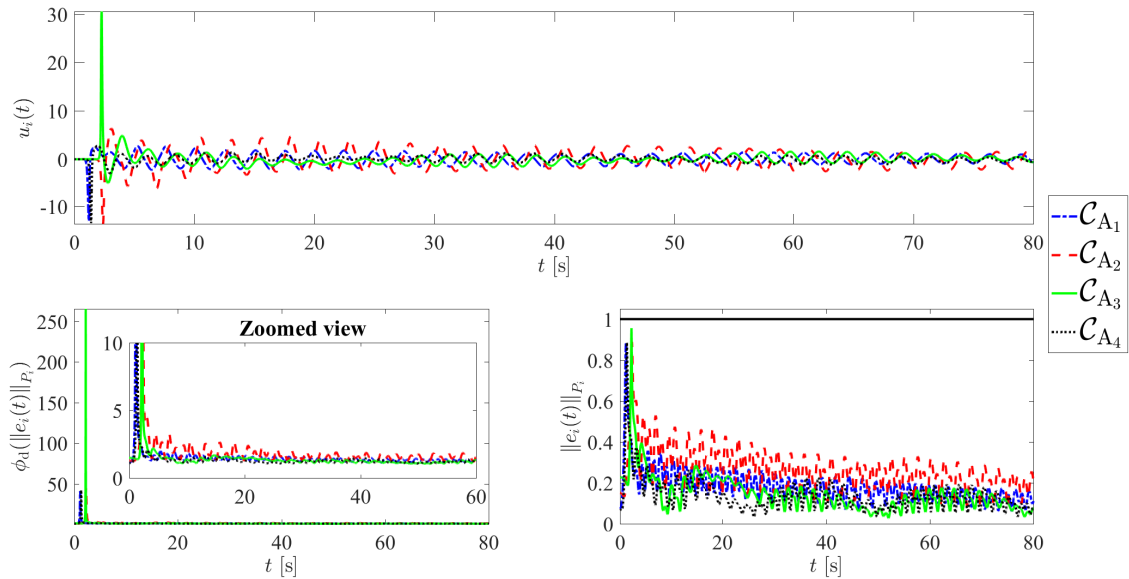


Figure 7.5: Proposed adaptive decentralized control performance, error dependent learning gain, and weighted norm of the active module system with the performance bound $\varepsilon_i = 1.0$.

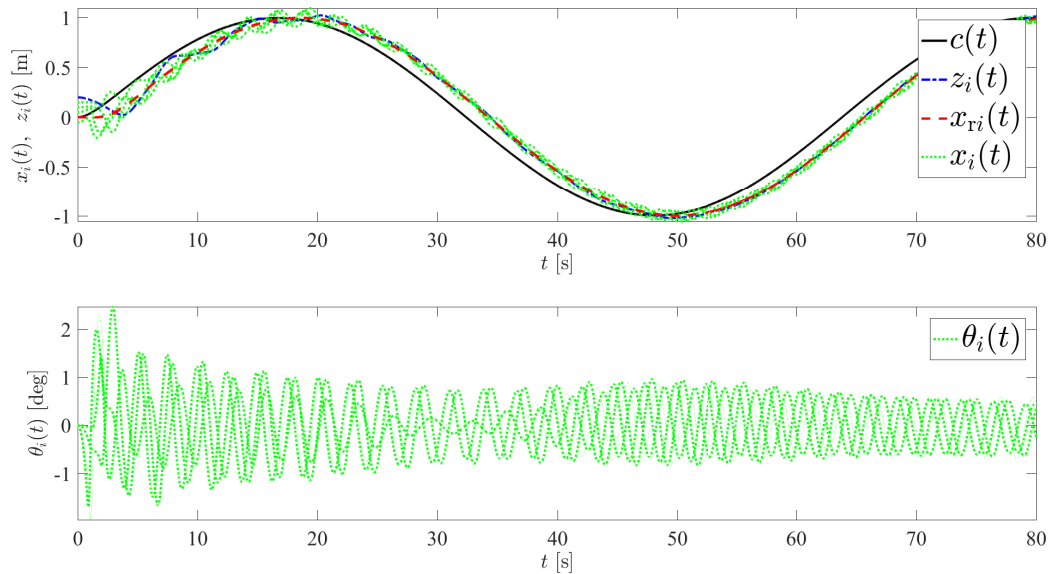


Figure 7.6: Position tracking and pendulum stabilization of the proposed adaptive decentralized controller with the performance bound $\varepsilon_i = 0.5$.

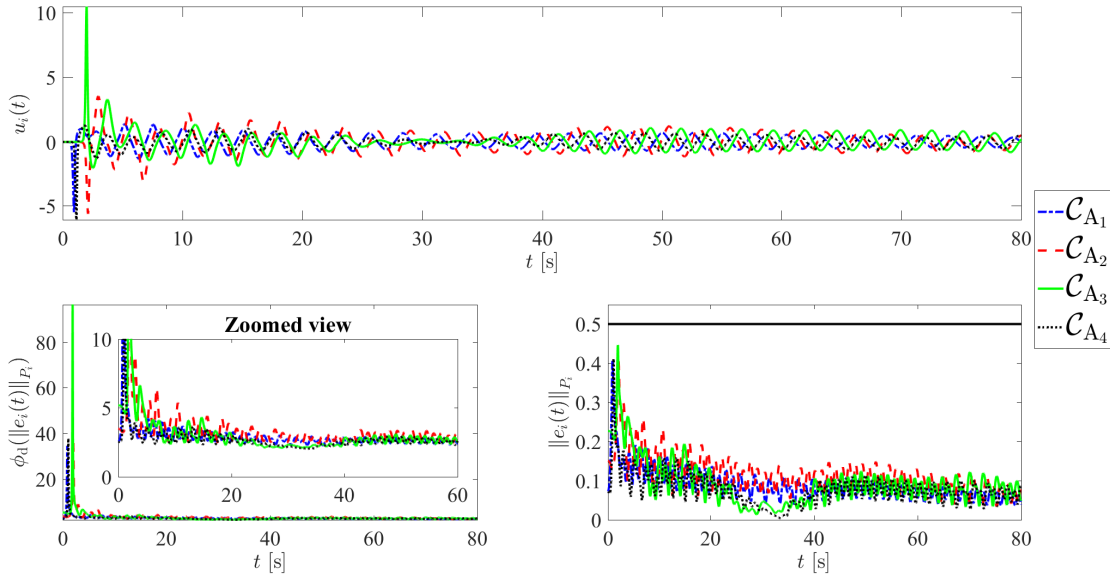


Figure 7.7: Proposed adaptive decentralized control performance, error dependent learning gain, and weighted norm of the active module system with the performance bound $\varepsilon_i = 0.5$.

To investigate the effect of the passive module dynamics on the ability of the active modules to be properly controlled, while enforcing a performance bound of $\varepsilon_i = 0.5$, the mass of the passive cart is changed. In particular, Figures 7.8 and 7.9 show the proposed decentralized control performance when the mass of the passive module is decreased to $M = 0.1$ (kg), whereas in Figures 7.10 and 7.11, the mass is increased to $M = 25$ (kg). As expected by intuition, when the mass of the passive module is small, its motion is dominantly effected by the movement of the active modules next to it. This can be seen from Figure 7.8 in which the passive module position trajectory closely follows the trajectories of the active modules. On the other hand, when the mass of the passive module is large as in Figure 7.10, the motion of the passive module dominates that of the active modules. This is evident from the periodic-like trajectory of the active modules as they closely track the reference model trajectory, but are effected by the movement of the passive module. Note that in either case in which the passive module effects the active modules, the performance bound $\varepsilon_i = 0.5$ is not violated by the active modules.

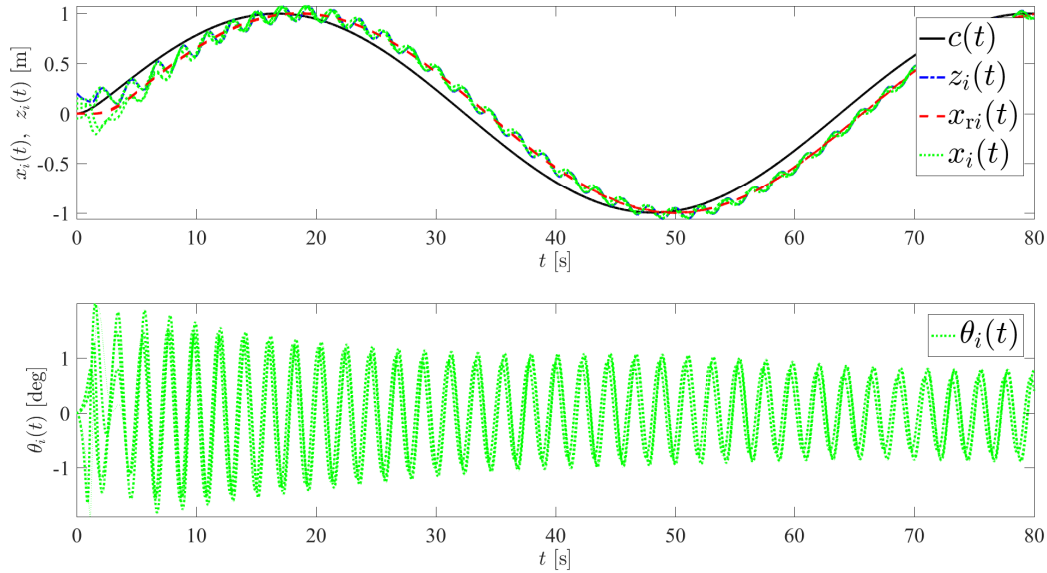


Figure 7.8: Position tracking and pendulum stabilization of the proposed adaptive decentralized controller with the mass of the passive module decreased to $M = 0.1$ (kg).

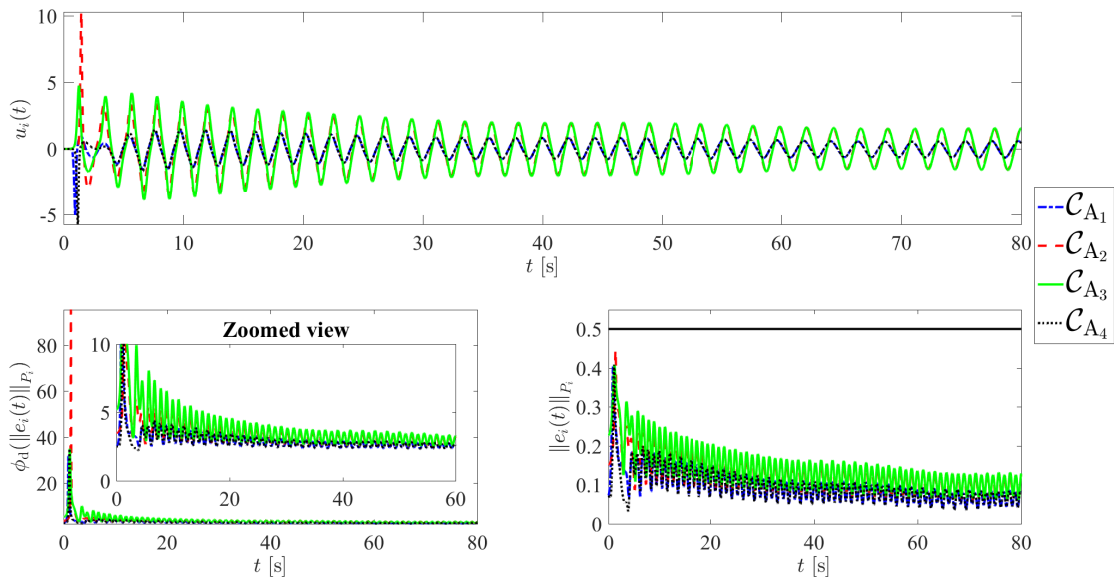


Figure 7.9: Proposed adaptive decentralized control performance, error dependent learning gain, and weighted norm of the active module system with the mass of the passive module decreased to $M = 0.1$ (kg).

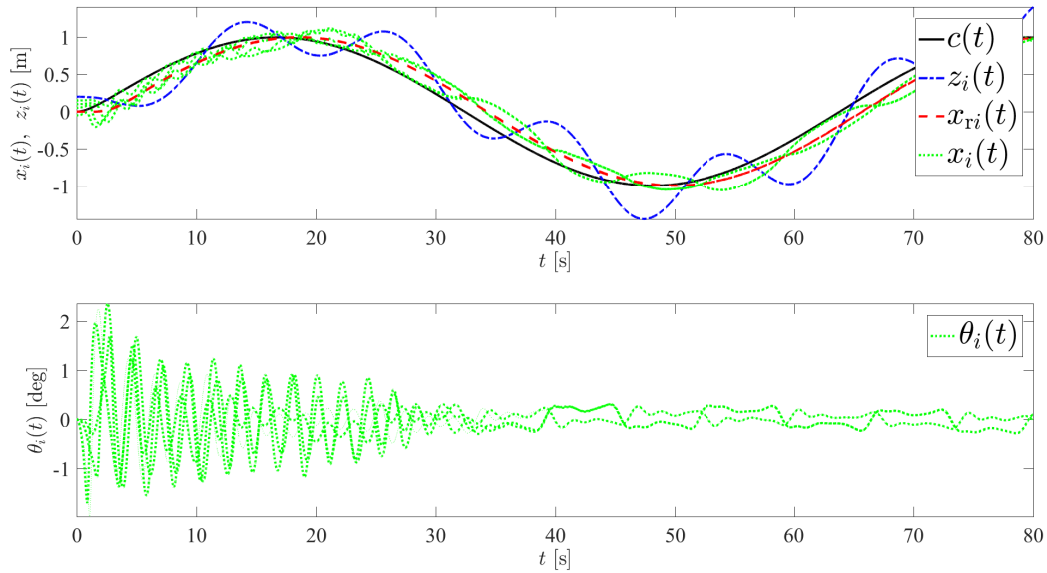


Figure 7.10: Position tracking and pendulum stabilization of the proposed adaptive decentralized controller with the mass of the passive module increased to $M = 25$ (kg).

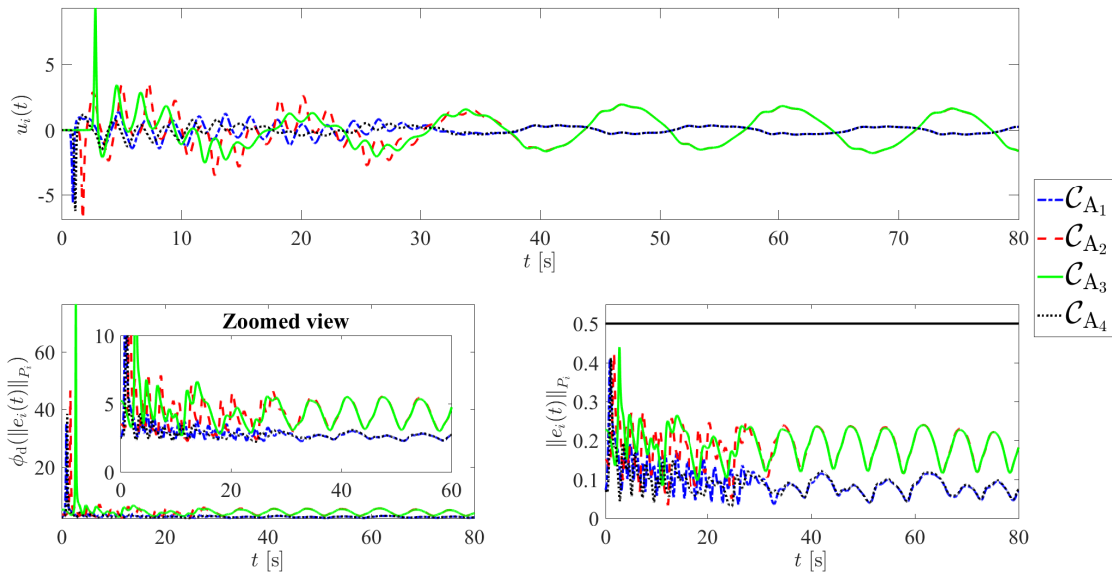


Figure 7.11: Proposed adaptive decentralized control performance, error dependent learning gain, and weighted norm of the active module system with the mass of the passive module increased to $M = 25$ (kg).

7.6 Conclusion

In the presence of unknown physical interconnections between active and passive modules and module-level system uncertainties, the design and implementation of decentralized architectures for the control of complex large-scale systems is a nontrivial control engineering task. Motivated from this standpoint, we proposed a new decentralized command following architecture for unknown large-scale active-passive modular systems and showed stability of the overall closed-loop system using a set-theoretic adaptive approach predicated on restricted potential functions. The key feature of our methodology was to restrict the system error trajectories such that they are guaranteed to stay within user-defined limits even in the presence of the unmodeled dynamics resulting from the passive modules. An illustrative numerical example demonstrated the efficacy of the proposed framework. Finally, while the results of this paper consider fixed performance bounds for each active module, this can be generalized to the case in which the performance bound is time-varying (i.e., $\varepsilon(t)$) by using recent results [160] proposed for sole systems. This extension allows for the initial tracking error $e(0)$ to be large and then converge to a small region defined by $\varepsilon(t)$.

CHAPTER 8: ON ADAPTIVE CONTROL OF UNACTUATED DYNAMICAL SYSTEMS THROUGH INTERCONNECTIONS WITH STABILITY AND PERFORMANCE GUARANTEES^{1,2}

This paper studies control and performance enforcement for a class of uncertain dynamical systems consisting of actuated and unactuated portions that are physically interconnected to each other (Figure 8.1). Performance guarantees are enforced on not only the actuated portion of the interconnected dynamics but also the unactuated portion via the proposed adaptive control approach, where this is accomplished through the physical interconnection with the actuated portion of the dynamics. Specifically, the proposed approach stabilizes the overall interconnected system in the presence of unknown physical interconnections as well as system uncertainties. For enforcing performance guarantees, a set-theoretic model reference adaptive control approach is used to restrict the respective system error trajectories of the actuated and unactuated dynamics inside a-priori, user-defined compact sets. In addition, the proposed approach utilizes linear matrix inequalities to verify stability of appropriate control parameters as well as the allowable system uncertainties and unknown physical interconnections. Finally, the efficacy of the proposed approach is demonstrated with an example.

8.1 Introduction

In this paper, we study a class of dynamical systems that is characterized by two (or more) sets of uncertain dynamics with an unknown physical interconnection between these dynamics (Figure 8.1). In particular, only a portion of the resulting interconnected dynamics is actuated (G_1 in Figure 8.1) while the other portion is unactuated (G_2 in Figure 8.1). A motivating example for the considered class of dynamical systems includes slung-load systems (see, for example, [161–168]), where a helicopter is actuated with a physical connection to the load that is unactuated. In the above work, the dynamics of the load affect the stability and achievable performance of the overall slung-load system, where the objective is then is to

¹This chapter has been submitted to the *IEEE Conference on Decision and Control*.

²This chapter is a by-product of consulting work. Permission is included in Appendix B.

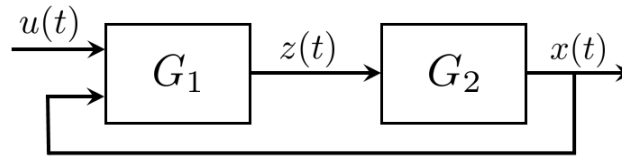


Figure 8.1: Block diagram representation of the open-loop interconnected uncertain dynamical system setup considered in this paper with $u(t)$, $z(t)$, and $x(t)$ respectively denoting the control signal applied to G_1 , the state vector of G_1 , and the state vector of G_2 .

design control laws for load damping such that the slung-load system remains stable and has some degree of desirable performance. However, no performance guarantees are made for the load itself, which is desirable in safety-critical scenarios such as precision load placement or navigation through densely obstructed areas.

The system behavior discussed above also falls under a class of underactuated mechanical systems, which are defined as systems with more degrees of freedom than there are actuators. A vast amount of literature already exists considering the control of underactuated mechanical systems (see, for example, [169–181], and references therein as well as [182–184] that use the terminology of super-articulated mechanical systems). In addition to the motivating example of slung-load systems, underactuated mechanical systems include unactuated fuel slosh dynamics in spacecraft [175, 176], robot manipulators including flexible joints and flexible links [172, 174, 177, 179, 182, 185], multibody mobile robots (i.e., car with trailer) [169, 186], inverted pendulums on carts [182, 187], bipedal walking [180, 181], and crane systems [188, 189]. Different control approaches used in these works include feedback linearization [174–176, 179], open-loop vibrational control of unactuated joints [177], and backstepping [182, 185, 186]. To handle uncertainties, several adaptive control methods have been studied [187, 189–194].

The authors of [190] consider the fact that uncertainties in underactuated systems do not satisfy a linear-in-parameter property. By using an extended dynamic model with a normal form augmentation, the parameter linearity is recovered such that a parameter adaptive control law can then be implemented to suppress the effect of the system uncertainties. While an important step, only stabilization of the entire underactuated system is considered without any consideration for the performance of the unactuated dynamics. Similarly, [192] proposes an adaptive control for underactuated systems that avoids the linear-in-parameter property by not using detailed model information, but instead using estimated model parameters. The resulting control allows for the actuated degrees of freedom to track desired trajectories, while the unactuated dynamics are considered as unmodeled dynamics. It is also shown in [192] that performance bounds can be computed and improved by increasing adaptation rate; however, no guarantees can be made to

enforce this without judiciously choosing the adaptation rate. Performance bounds are also only considered for the actuated degrees of freedom.

The authors in [191] design an adaptive variable structure set-point control law to drive all states of an underactuated robot system to desired values in the presence of parameterized uncertainties, where it is discussed that system performance can be improved by proper selection of controller gains. In [187], the authors propose an adaptive control law using fuzzy logic for an inverted pendulum set-up. Similarly, an adaptive fuzzy logic based control law is proposed in [193] utilizing a hierarchical structure of sliding surfaces to drive tracking errors to zero. Furthermore, performance bounds on the tracking error are computed (but not enforced). The authors of [194] propose a combined adaptive supervisory control along with a Lyapunov-based tracking control law to obtain a uniform ultimate bound result on the tracking error, where this bound can be made arbitrarily small through selection of the control parameters. In [188] and an adaptive extension [189], a form of performance guarantees are considered. In particular, both consider an overhead crane system where a motion planning method is used to keep the swing angle of the load attached to the crane within certain constraints; however, they only consider stabilization of the attached load where our approach allows for command following of the unactuated dynamics (i.e., load in the sense of the crane system). Moreover, our approach is proposed here in a more general form such that it could be applied to other underactuated systems, while [188, 189] are specific for the crane system considered.

The contribution of this paper is an adaptive control architecture for uncertain dynamical systems subject to interconnected actuated and unactuated dynamics with performance guarantees enforced to both dynamics. The control and performance enforcement of the unactuated dynamics is accomplished through the physical interconnection with the actuated dynamics, where the proposed control is applied to stabilize the overall interconnected system in the presence of unknown physical interconnections as well as uncertainties in both the actuated and unactuated dynamics. The performance guarantees are enforced using a set-theoretic model reference adaptive control approach³ such that the respective system error trajectories of the actuated and unactuated dynamics are restricted to stay inside user-defined compact sets. In addition, the proposed approach uses linear matrix inequalities (LMIs) to verify stability of appropriate control parameters as well as the allowable system uncertainties and unknown physical interconnections. An example is included to demonstrate the efficacy of the proposed approach.

³Note that a set-theoretic adaptive control architecture is utilized in the prior work of the authors [72, 74, 134, 140, 195]; however, they are not applicable as-they-are to the problem considered in this paper (see Section 8.2).

8.2 Problem Formulation

We start with introducing the class of interconnected uncertain dynamical systems considered in this paper⁴

$$\dot{x}(t) = Ax(t) + B[Jz(t) + W_u^T x(t)], \quad x(0) = x_0, \quad (8.1)$$

$$\dot{z}(t) = Fz(t) + G[u(t) + Hx(t) + W_a^T z(t)], \quad z(0) = z_0, \quad (8.2)$$

where (8.1) is the unactuated portion of the interconnected system and (8.2) is the actuated portion. In (8.1) and (8.2), $x(t) \in \mathbb{R}^n$ is the state vector of the unactuated dynamics available for feedback $z(t) \in \mathbb{R}^p$ is the state vector of the actuated dynamics available for feedback, and $u(t) \in \mathbb{R}^q$ is the control signal applied to the actuated dynamics. In addition, $A \in \mathbb{R}^{n \times n}$ and $B \in \mathbb{R}^{n \times m}$ are a known system matrix and a known input matrix, respectively, for the unactuated dynamics such that the pair (A, B) is controllable, and $F \in \mathbb{R}^{p \times p}$ and $G \in \mathbb{R}^{p \times q}$ are a known system matrix and a known control input matrix, respectively, for the actuated dynamics such that the pair (F, G) is controllable. Furthermore, $W_u \in \mathbb{R}^{n \times m}$ and $W_a \in \mathbb{R}^{p \times q}$ are unknown weight matrices respectively representing uncertainty in the unactuated and actuated dynamics, $J \in \mathbb{R}^{m \times p}$ represents the effect on the unactuated dynamics from the unknown physical interconnection with the actuated dynamics, and $H \in \mathbb{R}^{q \times n}$ represents the effect on the actuated dynamics from the unknown physical interconnection with the unactuated dynamics, where we consider these unknown physical interconnections to be parameterized as

$$H = H_0 + H_\Delta, \quad (8.3)$$

$$J = J_0 + J_\Delta, \quad (8.4)$$

with $H_0 \in \mathbb{R}^{q \times n}$ and $J_0 \in \mathbb{R}^{m \times p}$ consisting of known coefficients of the physical interconnection and $H_\Delta \in \mathbb{R}^{q \times n}$ and $J_\Delta \in \mathbb{R}^{m \times p}$ consisting of the unknown coefficients of the physical interconnection.

Remark 8.2.1 Under nominal conditions (i.e., $J_\Delta = 0$, $H_\Delta = 0$, $W_u = 0$, $W_a = 0$), (8.1) and (8.2) reduce to

$$\dot{x}(t) = Ax(t) + BJ_0 z(t), \quad (8.5)$$

$$\dot{z}(t) = Fz(t) + G[u(t) + H_0 x(t)]. \quad (8.6)$$

In this form, a possible selection of the control signal is $u(t) = -K_1 z(t) + K_2 u_1(t) - H_0 x(t)$, where $K_1 \in \mathbb{R}^{q \times p}$ is designed such that $F - GK_1$ is Hurwitz, $K_2 \in \mathbb{R}^{q \times m}$, and $u_1(t) \in \mathbb{R}^m$ is an additional control signal to be

⁴To elucidate the interconnected uncertain dynamical system setup presented in (8.1) and (8.2), consider the open-loop block diagram in Figure 8.1. In this block diagram, G_1 represents the actuated dynamics receiving a control signal $u(t)$ as well as the unactuated state signal $x(t)$ through physical interconnection with G_2 , where G_2 represents the unactuated dynamics receiving the actuated state signal $z(t)$ through the physical interconnection.

applied to the unactuated dynamics. With this control signal, one can write (8.5) and (8.6) equivalently as

$$\dot{x}(t) = Ax(t) + Bv(t), \quad (8.7)$$

$$\dot{z}(t) = (F - GK_1)z(t) + GK_2u_1(t), \quad (8.8)$$

$$v(t) = J_0z(t). \quad (8.9)$$

By choosing (the pre-filter gain) K_2 as $-J_0(F - GK_1)^{-1}GK_2 = I$, one can design the remaining control signal $u_1(t)$, for example, to stabilize (8.7). To see this, consider an equivalent form of (8.7) given by

$$\dot{x}(t) = Ax(t) + Bu_1(t) + B(v(t) - u_1(t)). \quad (8.10)$$

If K_1 is selected such that the system in (8.8) and (8.9) is sufficiently fast and since $-J_0(F - GK_1)^{-1}GK_2 = I$, then one would expect $u_1(t) = -L_1x(t)$, $L_1 \in \mathbb{R}^{m \times n}$, with $A - BL_1$ being Hurwitz to stabilize (8.10), where in this case $\lim_{t \rightarrow \infty}(v(t) - u_1(t)) = 0$ can be concluded⁵.

Remark 8.2.2 The nominal case discussed in Remark 8.2.1 simplifies the problem such that one can also augment the dynamics in (8.7)-(8.9) and write them as

$$\begin{bmatrix} \dot{x}(t) \\ \dot{z}(t) \end{bmatrix} = \begin{bmatrix} A & BJ_0 \\ 0 & F - GK_1 \end{bmatrix} \begin{bmatrix} x(t) \\ z(t) \end{bmatrix} + \begin{bmatrix} 0 \\ GK_2 \end{bmatrix} u_1(t). \quad (8.11)$$

As already discussed, this is an easier problem to solve using linear control theory. However, due to the presence of uncertainties in both the actuated and unactuated dynamics and the unknown physical interconnections in the considered dynamics given by (8.1) and (8.2), the control problem becomes more complex. To see this, we similarly augment the dynamics in (8.1) and (8.2) yielding

$$\begin{bmatrix} \dot{x}(t) \\ \dot{z}(t) \end{bmatrix} = \begin{bmatrix} A & BJ_0 \\ GH_0 & F \end{bmatrix} \begin{bmatrix} x(t) \\ z(t) \end{bmatrix} + \begin{bmatrix} 0 \\ G \end{bmatrix} (u(t) + H_\Delta x(t) + W_a^T z(t)) + \begin{bmatrix} B \\ 0 \end{bmatrix} (J_\Delta z(t) + W_u^T x(t)). \quad (8.12)$$

From (8.12), the challenge of this ‘‘augment the dynamics’’ approach is that the uncertainty in the term ‘‘ $J_\Delta z(t) + W_u^T x(t)$ ’’ is unmatched, meaning that there is no access to the control channel to suppress this uncertainty with standard model reference adaptive control architectures. While there are some approaches

⁵We refer to Section 8.4 and specifically Remark 8.4.1 for the analytical condition predicated on LMIs to verify overall closed-loop system stability based on the aforementioned design gain.

to handle unmatched uncertainties in the context of model reference adaptive control (see, for example, [5, 7, 18, 82, 196]), they involve additional complexity; hence, they are not adopted in the context of this paper.

Remark 8.2.3 From Remark 8.2.1, the dynamics given by (8.7)-(8.9) can also be interpreted as an “actuator dynamics” problem, where (8.7) represents the system dynamics and (8.8) and (8.9) represent the actuator dynamics. If there are uncertainties in the system dynamics (i.e., $W_u^T x(t) \neq 0$), this becomes a non-trivial problem for model reference adaptive control since the presence of the actuator dynamics prevent the direct suppression of the uncertainties through the control channel (unmatched uncertainties as discussed in Remark 8.2.2). On this subject, a practical approach referred to as hedging is proposed by the authors of [30–33] to allow for correct adaptation in the presence of actuator dynamics. Furthermore, the work in [95, 101–105, 114, 118] propose significant contributions to the hedging approach and make use of LMIs to provide sufficient stability conditions. While these approaches are promising for the application of adaptive control to uncertain dynamical systems with actuator dynamics, the interconnected uncertain dynamical system considered in this paper includes additional complexity owing to the uncertainties in the actuated dynamics and unknown physical interconnections that are not considered in [30–33, 95, 101–105, 114, 118].

The adaptive control problem considered in this paper is now stated as follows: Consider the interconnected uncertain dynamical system given by (8.1) and (8.2). Design a control signal for the actuated dynamics given by (8.2) such that a) trajectories of the actuated dynamics follow the trajectories of a desired reference model, b) the trajectories of the unactuated dynamics given by (8.1) follow the trajectories of a desired reference model, c) the respective system error trajectories of the actuated and unactuated dynamics are restricted to a-priori, user-defined compact sets enforcing performance guarantees. For this purpose, the next section introduces the proposed set-theoretic adaptive control architecture.

8.3 Adaptive Control for Unactuated Dynamics Through Interconnections

In this section, we propose a set-theoretic adaptive control architecture for the interconnected uncertain dynamical system presented in Section 8.2 such that command following of the unactuated dynamics is achieved. To begin with, we provide the following necessary definition [74].

Definition 8.3.1 Let $\|y\|_M = \sqrt{y^T M y}$ be a weighted Euclidean norm, where $y \in \mathbb{R}^s$ is a real column vector and $M \in \mathbb{R}_+^{s \times s}$. We define $\phi(\|y\|_M)$, $\phi : \mathbb{R}^s \rightarrow \mathbb{R}$, to be a restricted potential function (barrier Lyapunov

function) defined on the set $\mathcal{D}_\varepsilon \triangleq \{y : \|y\|_M \in [0, \varepsilon]\}$ with $\varepsilon \in \mathbb{R}_+$ being an a priori, user-defined constant, if the following statements hold: i) If $\|y\|_M = 0$, then $\phi(\|y\|_M) = 0$. ii) If $y \in \mathcal{D}_\varepsilon$ and $\|y\|_M \neq 0$, then $\phi(\|y\|_M) > 0$. iii) If $\|y\|_M \rightarrow \varepsilon$, then $\phi(\|y\|_M) \rightarrow \infty$. iv) $\phi(\|y\|_M)$ is continuously differentiable on \mathcal{D}_ε . v) If $y \in \mathcal{D}_\varepsilon$, then $\phi_d(\|y\|_M) > 0$, where $\phi_d(\|y\|_M) \triangleq \frac{d\phi(\|y\|_M)}{d\|y\|_M^2}$. vi) If $y \in \mathcal{D}_\varepsilon$, then $2\phi_d(\|y\|_M)\|y\|_M^2 - \phi(\|y\|_M) > 0$ ^{6,7}.

Now, consider the interconnected uncertain dynamical system given by (8.1) and (8.2) with (8.3) and (8.4) as

$$\dot{x}(t) = Ax(t) + B[(J_0 + J_\Delta)z(t) + W_u^T x(t)], \quad (8.13)$$

$$\dot{z}(t) = Fz(t) + G[u(t) + (H_0 + H_\Delta)x(t) + W_a^T z(t)]. \quad (8.14)$$

The remainder of this section is divided into two subsections. In Section 8.3.1, we design the proposed control law as it applies to the actuated dynamics given by (8.14) and in Section 8.3.2 we address how the unactuated dynamics given by (8.13) can be controlled by the physical interconnection to the actuated dynamics.

8.3.1 Control Design for Actuated Dynamics

To control the actuated dynamics in the presence of system uncertainties and unknown physical interconnections with the unactuated dynamics, consider the adaptive control given by

$$u(t) = -K_1 z(t) + K_2 u_1(t) - (H_0 + \hat{H}_\Delta(t))x(t) - \hat{W}_a^T(t)z(t), \quad (8.15)$$

where $K_1 \in \mathbb{R}^{q \times p}$ is designed such that $F_r \triangleq F - GK_1$ is Hurwitz, $K_2 \in \mathbb{R}^{q \times m}$ is designed such that $-J_0(F - GK_1)^{-1}GK_2 = I$, and $u_1(t) \in \mathbb{R}^m$ is an additional control signal to be applied to the unactuated dynamics which is designed in the next section. In addition, $\hat{H}_\Delta(t) \in \mathbb{R}^{q \times n}$ and $\hat{W}_a(t) \in \mathbb{R}^{p \times q}$ are the estimates of H_Δ and W_a satisfying the respective weight update laws given by

$$\dot{\hat{H}}_\Delta(t) = \alpha \text{Proj}_m[\hat{H}_\Delta(t), \phi_d(\|\tilde{z}(t)\|_S) G^T S \tilde{z}(t) x^T(t)], \quad \hat{H}_\Delta(0) = \hat{H}_{\Delta 0}, \quad (8.16)$$

⁶The last condition vi) is shown in [74] to be necessary when the system uncertainties are time-varying such that a bounded result is obtained for the closed-loop system stability. While we do not consider the actuated and unactuated system uncertainties to be time-varying in the theoretical development of this paper, we include this final condition on the restricted potential function such that our results can be readily extended for the practical case in which the uncertainties are time-varying.

⁷As considered in [72, 74, 134, 140, 195], a candidate restricted potential function that satisfies all the conditions stated in Definition 8.3.1 has the form $\phi(\|y\|_M) = \|y\|_M^2 / (\varepsilon - \|y\|_M)$, $y \in \mathcal{D}_\varepsilon$.

$$\dot{\hat{W}}_a(t) = \gamma_a \text{Proj}_m [\hat{W}_a(t), \phi_d(\|\tilde{z}(t)\|_S) z(t) \tilde{z}^T(t) S G], \quad \hat{W}_a(0) = \hat{W}_{a0}, \quad (8.17)$$

where $\alpha \in \mathbb{R}_+$ and $\gamma_a \in \mathbb{R}_+$ are learning rates, $\phi_d(\|\tilde{z}(t)\|_S)$ can be considered as an error dependent learning gain, $S \in \mathbb{R}_+^{p \times p}$ is a solution of the Lyapunov equation $0 = F_r^T S + S F_r + I$, and $\tilde{z}(t) \triangleq z(t) - z_r(t)$ is the system error of the actuated dynamics with $z_r(t) \in \mathbb{R}^p$ being the reference state vector satisfying the reference model dynamics that capture a desired closed-loop dynamical system performance motivated by Remark 8.2.1 and given by⁸

$$\dot{z}_r(t) = F_r z_r(t) + G_r u_1(t), \quad z_r(0) = z_{r0}, \quad (8.18)$$

with $G_r = G K_2 \in \mathbb{R}^{p \times m}$ being the reference model input matrix⁹.

8.3.2 Control Design to Account for Unactuated Dynamics

In this section, the remaining control signal $u_1(t)$ is designed to allow for command following of the unactuated dynamics. It is applied to the actuated dynamics for the purpose of controlling the unactuated dynamics through the physical interconnection of the two dynamics. To accomplish this, we start by adding and subtracting the term “ $Bu_1(t)$ ” to unactuated dynamics such that (8.13) can be rewritten as

$$\dot{x}(t) = Ax(t) + B[u_1(t) + J_\Delta z(t) + W_u^T x(t)] + B[J_0 z(t) - u_1(t)]. \quad (8.19)$$

Now, let the additional control signal be given by

$$u_1(t) = -L_1 x(t) + L_2 c(t) - \hat{J}_\Delta(t) z(t) - \hat{W}_u^T(t) x(t), \quad (8.20)$$

where $L_1 \in \mathbb{R}^{m \times n}$ is designed such that $A_r \triangleq A - B L_1$ is Hurwitz, $L_2 \in \mathbb{R}^{m \times m}$ is a feedforward gain, and $c(t) \in \mathbb{R}^m$ is a given uniformly continuous bounded command. In addition, $\hat{J}_\Delta(t) \in \mathbb{R}^{m \times p}$ and $\hat{W}_u(t) \in \mathbb{R}^{n \times m}$ are the estimates of J_Δ and W_u satisfying the respective weight update laws given by

$$\dot{\hat{J}}_\Delta(t) = \beta \text{Proj}_m [\hat{J}_\Delta(t), \phi_d(\|e(t)\|_p) B^T P e(t) z^T(t)], \quad \hat{J}_\Delta(0) = \hat{J}_{\Delta 0}, \quad (8.21)$$

$$\dot{\hat{W}}_u(t) = \gamma_u \text{Proj}_m [\hat{W}_u(t), \phi_d(\|e(t)\|_p) x(t) e^T(t) P B], \quad \hat{W}_u(0) = \hat{W}_{u0}, \quad (8.22)$$

⁸Stability of the considered reference model is addressed in the proof of Theorem 8.4.1 (also see the LMI analysis in Remark 8.4.1).

⁹In (8.16) and (8.17), a rectangular projection operator is used (see [6, 82] for more details) such that the element-wise projection bounds $|\hat{H}_\Delta(t)_{ij}| \leq \hat{H}_{\Delta, \max, i+(j-1)q}$, $i = 1, \dots, q$, $j = 1, \dots, n$, $|\hat{W}_a(t)_{ij}| \leq \hat{W}_{a, \max, i+(j-1)p}$, $i = 1, \dots, p$, $j = 1, \dots, q$, are respectively satisfied.

where $\beta \in \mathbb{R}_+$ and $\gamma_u \in \mathbb{R}_+$ are learning rates, $\phi_d(\|e(t)\|_p)$ can be considered as an error dependent learning gain, $P \in \mathbb{R}_+^{n \times n}$ is a solution of the Lyapunov equation $0 = A_r^T P + P A_r + I$, and $e(t) \triangleq x(t) - x_r(t)$ is the system error of the unactuated dynamics with $x_r(t) \in \mathbb{R}^n$ being the reference state vector satisfying the following reference model dynamics based on the hedging approach [30–33, 95, 101–105, 114, 118],

$$\dot{x}_r(t) = A_r x_r(t) + B_r c(t) + B[J_0 z(t) - u_1(t)], \quad x_r(0) = x_{r0}, \quad (8.23)$$

with $B_r = B L_2 \in \mathbb{R}^{n \times m}$ being the reference model input matrix¹⁰.

8.4 Stability and Performance Guarantees

We now present the stability analysis and establish performance guarantees of the adaptive control method proposed in Section 8.3 for the actuated and unactuated dynamics. For this purpose, we first state the actuated system error dynamics resulting from (8.14), (8.15), and (8.18), as

$$\dot{\tilde{z}}(t) = F_r \tilde{z}(t) - G \tilde{H}_\Delta(t) x(t) - G \tilde{W}_a^T(t) z(t), \quad \tilde{z}(0) = \tilde{z}_0, \quad (8.24)$$

where $\tilde{H}_\Delta(t) \triangleq \hat{H}_\Delta(t) - H_\Delta \in \mathbb{R}^{q \times n}$ and $\tilde{W}_a(t) \triangleq \hat{W}_a(t) - W_a \in \mathbb{R}^{p \times q}$ and the unactuated system error dynamics resulting from (8.19), (8.20), and (8.23), as

$$\dot{e}(t) = A_r e(t) - B \tilde{J}_\Delta(t) z(t) - B \tilde{W}_u^T(t) x(t), \quad e(0) = e_0, \quad (8.25)$$

where $\tilde{J}_\Delta(t) \triangleq \hat{J}_\Delta(t) - J_\Delta \in \mathbb{R}^{m \times p}$ and $\tilde{W}_u(t) \triangleq \hat{W}_u(t) - W_u \in \mathbb{R}^{n \times m}$. The following assumption is necessary for the remaining results in this paper.

Assumption 8.4.1 *The matrix*

$$\mathcal{A}(\hat{J}_\Delta(t), \hat{W}_u(t)) = \begin{bmatrix} A + B \hat{W}_u^T(t) & B(J_0 + \hat{J}_\Delta(t)) \\ -G_r(L_1 + \hat{W}_u^T(t)) & F_r - G_r \hat{J}_\Delta(t) \end{bmatrix}, \quad (8.26)$$

*is quadratically stable*¹¹.

¹⁰In (8.21) and (8.22), a rectangular projection operator is used such that the element-wise projection bounds $|\hat{J}_\Delta(t)_{ij}| \leq \hat{J}_{\Delta, \max, i+(j-1)m}$, $i = 1, \dots, m$, $j = 1, \dots, p$, $|\hat{W}_u(t)_{ij}| \leq \hat{W}_{u, \max, i+(j-1)n}$, $i = 1, \dots, n$, $j = 1, \dots, m$, are respectively satisfied.

¹¹Remark 8.4.1 addresses how this assumption can be satisfied using LMIs.

Theorem 8.4.1 Consider the interconnected uncertain dynamical system described by (8.1) and (8.2), the reference models given by (8.18) and (8.23), and the control laws given by (8.15) and (8.20) with the update laws (8.16), (8.17), (8.21), and (8.22). If $\|\tilde{z}_0\|_S < \varepsilon_{\tilde{z}}$ and $\|e_0\|_P < \varepsilon_e$, then under Assumption 8.4.1, the solution $(\tilde{z}(t), e(t), \tilde{H}_\Delta(t), \tilde{W}_a(t), \tilde{J}_\Delta(t), \tilde{W}_u(t))$ of the closed-loop interconnected dynamical system is bounded, $\lim_{t \rightarrow \infty} \tilde{z}(t) = 0$, and $\lim_{t \rightarrow \infty} e(t) = 0$. In addition, the actuated and unactuated system errors strictly satisfy the a-priori given, user-defined performance bounds respectively given by

$$\|\tilde{z}(t)\|_S < \varepsilon_{\tilde{z}}, \quad t \in \overline{\mathbb{R}}_+, \quad (8.27)$$

$$\|e(t)\|_P < \varepsilon_e, \quad t \in \overline{\mathbb{R}}_+. \quad (8.28)$$

Proof. To show boundedness of the closed-loop interconnected dynamical system, consider the energy function $\mathcal{V} : \mathcal{D}_{\varepsilon_{\tilde{z}}} \times \mathcal{D}_{\varepsilon_e} \times \mathbb{R}^{\dim(\tilde{H}_\Delta)} \times \mathbb{R}^{\dim(\tilde{W}_a)} \times \mathbb{R}^{\dim(\tilde{J}_\Delta)} \times \mathbb{R}^{\dim(\tilde{W}_u)} \rightarrow \overline{\mathbb{R}}_+$ given by

$$\begin{aligned} \mathcal{V}(\tilde{z}, e, \tilde{H}_\Delta, \tilde{W}_a, \tilde{J}_\Delta, \tilde{W}_u) &= \phi(\|\tilde{z}\|_S) + \phi(\|e\|_P) + \alpha^{-1} \text{tr} \tilde{H}_\Delta^T \tilde{H}_\Delta + \gamma_a^{-1} \text{tr} \tilde{W}_a^T \tilde{W}_a \\ &\quad + \beta^{-1} \text{tr} \tilde{J}_\Delta^T \tilde{J}_\Delta + \gamma_u^{-1} \text{tr} \tilde{W}_u^T \tilde{W}_u, \end{aligned} \quad (8.29)$$

where $\mathcal{D}_{\varepsilon_{\tilde{z}}} \triangleq \{\tilde{z}(t) : \|\tilde{z}(t)\|_P < \varepsilon_{\tilde{z}}\}$ and $\mathcal{D}_{\varepsilon_e} \triangleq \{e(t) : \|e(t)\|_P < \varepsilon_e\}$, and $\mathbb{R}^{\dim(\tilde{H}_\Delta)}$, $\mathbb{R}^{\dim(\tilde{W}_a)}$, $\mathbb{R}^{\dim(\tilde{J}_\Delta)}$, and $\mathbb{R}^{\dim(\tilde{W}_u)}$ denote the dimensions of \tilde{H}_Δ , \tilde{W}_a , \tilde{J}_Δ , and \tilde{W}_u respectively¹².

Differentiating (8.29) yields

$$\begin{aligned} \dot{\mathcal{V}}(\tilde{z}(t), e(t), \tilde{H}_\Delta(t), \tilde{W}_a(t), \tilde{J}_\Delta(t), \tilde{W}_u(t)) &= 2\phi_d(\|\tilde{z}(t)\|_S) \tilde{z}^T(t) S \dot{\tilde{z}}(t) + 2\phi_d(\|e(t)\|_P) e^T(t) P \dot{e}(t) + 2\alpha^{-1} \text{tr} \tilde{H}_\Delta^T(t) \dot{\tilde{H}}_\Delta(t) \\ &\quad + 2\gamma_a^{-1} \text{tr} \tilde{W}_a^T(t) \dot{\tilde{W}}_a(t) + 2\beta^{-1} \text{tr} \tilde{J}_\Delta^T(t) \dot{\tilde{J}}_\Delta(t) + 2\gamma_u^{-1} \text{tr} \tilde{W}_u^T(t) \dot{\tilde{W}}_u(t) \\ &= -\phi_d(\|\tilde{z}(t)\|_S) \|\tilde{z}(t)\|^2 - \phi_d(\|e(t)\|_P) \|e(t)\|^2 - 2\phi_d(\|\tilde{z}(t)\|_S) \tilde{z}^T(t) S G \tilde{H}_\Delta(t) x(t) \\ &\quad - 2\phi_d(\|\tilde{z}(t)\|_S) \tilde{z}^T(t) S G \tilde{W}_a^T(t) z(t) - 2\phi_d(\|e(t)\|_P) e^T(t) P B \tilde{J}_\Delta(t) z(t) \\ &\quad - 2\phi_d(\|e(t)\|_P) e^T(t) P B \tilde{W}_u^T(t) x(t) + 2\alpha^{-1} \text{tr} \tilde{H}_\Delta^T(t) \dot{\tilde{H}}_\Delta(t) + 2\gamma_a^{-1} \text{tr} \tilde{W}_a^T(t) \dot{\tilde{W}}_a(t) \\ &\quad + 2\beta^{-1} \text{tr} \tilde{J}_\Delta^T(t) \dot{\tilde{J}}_\Delta(t) + 2\gamma_u^{-1} \text{tr} \tilde{W}_u^T(t) \dot{\tilde{W}}_u(t). \end{aligned} \quad (8.30)$$

Using (8.16), (8.17), (8.21), and (8.22), (8.30) reduces to

$$\dot{\mathcal{V}}(\cdot) \leq -\phi_d(\|\tilde{z}(t)\|_S) \|\tilde{z}(t)\|^2 - \phi_d(\|e(t)\|_P) \|e(t)\|^2 \leq 0, \quad (8.31)$$

¹²Note that $\mathcal{V}(0, 0, 0, 0, 0, 0) = 0$, $\mathcal{V}(\tilde{z}, e, \tilde{H}_\Delta, \tilde{W}_a, \tilde{J}_\Delta, \tilde{W}_u) > 0$ for all $(\tilde{z}, e, \tilde{H}_\Delta, \tilde{W}_a, \tilde{J}_\Delta, \tilde{W}_u) \neq (0, 0, 0, 0, 0, 0)$, and $d\phi(\|\tilde{z}(t)\|_S)/dt = 2\phi_d(\|\tilde{z}(t)\|_S) \tilde{z}^T(t) S \dot{\tilde{z}}(t)$, $d\phi(\|e(t)\|_P)/dt = 2\phi_d(\|e(t)\|_P) e^T(t) P \dot{e}(t)$.

which guarantees the Lyapunov stability, and hence, the boundedness of the solution $(\tilde{z}(t), e(t), \tilde{H}_\Delta(t), \tilde{W}_a(t), \tilde{J}_\Delta(t), \tilde{W}_u(t))$.

To reach the conclusion that $\lim_{t \rightarrow \infty} \tilde{z}(t) = 0$ and $\lim_{t \rightarrow \infty} e(t) = 0$, we first show the boundedness of the reference model signals $z_r(t)$ and $x_r(t)$. For this purpose, using (8.20), (8.18) and (8.23) can be written in compact form as

$$\dot{\theta}(t) = \mathcal{A}(\hat{J}_\Delta(t), \hat{W}_u(t))\theta(t) + \omega(\cdot), \quad (8.32)$$

where $\theta(t) = [x_r^T(t), z_r^T(t)]^T$ and

$$\omega(\cdot) = \begin{bmatrix} B[(J_0 + \hat{J}_\Delta(t))\tilde{z}(t) + (L_1 + \hat{W}_u^T(t))e(t)] \\ G_r[L_2c(t) - \hat{J}_\Delta(t)\tilde{z}(t) - (L_1 + \hat{W}_u^T(t))e(t)] \end{bmatrix}. \quad (8.33)$$

It follows from the Lyapunov stability of the solution $(\tilde{z}(t), e(t), \tilde{H}_\Delta(t), \tilde{W}_a(t), \tilde{J}_\Delta(t), \tilde{W}_u(t))$ that $\omega(\cdot)$ in (8.32) is a bounded perturbation. Since $\omega(\cdot)$ is bounded and $\mathcal{A}(\hat{J}_\Delta(t), \hat{W}_u(t))$ is quadratically stable by Assumption 8.4.1, it follows that $x_r(t)$ and $z_r(t)$ are bounded [88]. Moreover, $z(t)$ and $x(t)$ are bounded as a consequence of the boundedness of the respective signals $\tilde{z}(t)$, $z_r(t)$, $e(t)$, and $x_r(t)$, such that from (8.24) and (8.25), $\dot{\tilde{z}}(t)$ and $\dot{e}(t)$ are also bounded. Now, from the proof of Theorem 5.3 in [72], $\lim_{t \rightarrow \infty} \tilde{z}(t) = 0$ and $\lim_{t \rightarrow \infty} e(t) = 0$. Finally, (8.31) implies that $\mathcal{V}(\tilde{z}(t), e(t), \tilde{H}_\Delta(t), \tilde{W}_a(t), \tilde{J}_\Delta(t), \tilde{W}_u(t)) \leq \mathcal{V}_{\max}$, where $\mathcal{V}_{\max} \triangleq \mathcal{V}(\tilde{z}(0), e(0), \tilde{H}_\Delta(0), \tilde{W}_a(0), \tilde{J}_\Delta(0), \tilde{W}_u(0))$. It then follows that $\phi(\|\tilde{z}(t)\|_S) \leq \mathcal{V}_{\max}$ and $\phi(\|e(t)\|_P) \leq \mathcal{V}_{\max}$, and hence, the performance bounds respectively given by (8.27) and (8.28) are immediate. ■

Remark 8.4.1 *Similar to [95, 101–105, 114, 118], we now use LMIs to satisfy the quadratic stability [97] of (8.26) for given projection bounds $\hat{J}_{\Delta, \max}$ and $\hat{W}_{u, \max}$ on the elements of $\hat{J}_\Delta(t)$ and $\hat{W}_u(t)$, respectively. To elucidate this point, let $\bar{J}_{\Delta, i_1, \dots, i_l} \in \mathbb{R}^{m \times p}$ and $\bar{W}_{u, i_1, \dots, i_l} \in \mathbb{R}^{n \times m}$ be respectively defined as*

$$\bar{J}_{\Delta, i_1, \dots, i_f} = \begin{bmatrix} (-1)^{i_1} \hat{J}_{\Delta, \max, 1} & (-1)^{i_1+m} \hat{J}_{\Delta, \max, 1+m} & \dots & (-1)^{i_1+(p-1)m} \hat{J}_{\Delta, \max, 1+(p-1)m} \\ (-1)^{i_2} \hat{J}_{\Delta, \max, 2} & (-1)^{i_2+m} \hat{J}_{\Delta, \max, 2+m} & \dots & (-1)^{i_2+(p-1)m} \hat{J}_{\Delta, \max, 2+(p-1)m} \\ \vdots & \vdots & \ddots & \vdots \\ (-1)^{i_m} \hat{J}_{\Delta, \max, m} & (-1)^{i_2m} \hat{J}_{\Delta, \max, 2m} & \dots & (-1)^{i_{pm}} \hat{J}_{\Delta, \max, pm} \end{bmatrix}, \quad (8.34)$$

$$\bar{W}_{u,i_1,\dots,i_g} = \begin{bmatrix} (-1)^{i_1} \hat{W}_{u,\max,1} & (-1)^{i_1+n} \hat{W}_{u,\max,1+n} & \dots & (-1)^{i_1+(m-1)n} \hat{W}_{u,\max,1+(m-1)n} \\ (-1)^{i_2} \hat{W}_{u,\max,2} & (-1)^{i_2+n} \hat{W}_{u,\max,2+n} & \dots & (-1)^{i_2+(m-1)n} \hat{W}_{u,\max,2+(m-1)n} \\ \vdots & \vdots & \ddots & \vdots \\ (-1)^{i_n} \hat{W}_{u,\max,n} & (-1)^{i_n+n} \hat{W}_{u,\max,2n} & \dots & (-1)^{i_n+mn} \hat{W}_{u,\max,mn} \end{bmatrix}, \quad (8.35)$$

where $i_f \in \{1, 2\}$, $f \in \{1, \dots, 2^{pm}\}$, such that $\bar{J}_{\Delta, i_1, \dots, i_f}$ represents the corners of the hypercube defining the maximum variation of $\hat{J}_{\Delta}(t)$, and $i_g \in \{1, 2\}$, $g \in \{1, \dots, 2^{mn}\}$, such that $\bar{W}_{u, i_1, \dots, i_g}$ represents the corners of the hypercube defining the maximum variation of $\hat{W}_u(t)$. Then, let

$$\mathcal{A}_{i_1, \dots, i_h} = \begin{bmatrix} A + B\bar{W}_{u, i_1, \dots, i_g}^T & B(J_0 + \bar{J}_{\Delta, i_1, \dots, i_f}) \\ -G_r(L_1 + \bar{W}_{u, i_1, \dots, i_g}^T) & F_r - G_r\bar{J}_{\Delta, i_1, \dots, i_f} \end{bmatrix}, \quad (8.36)$$

where $h \in \{1, \dots, 2^{(pm+mn)}\}$, be the corners of the hypercube constructed from all the permutations of $\bar{J}_{\Delta, i_1, \dots, i_f}$ and $\bar{W}_{u, i_1, \dots, i_g}$. By proper selection of K_1 in $F_r = F - GK_1$ and L_1 , it can then be shown that

$$\mathcal{A}_{i_1, \dots, i_h}^T \mathcal{P} + \mathcal{P} \mathcal{A}_{i_1, \dots, i_h} < 0, \quad \mathcal{P} > 0, \quad (8.37)$$

implies that $\mathcal{A}^T(\hat{J}_{\Delta}(t), \hat{W}_u(t)) \mathcal{P} + \mathcal{P} \mathcal{A}(\hat{J}_{\Delta}(t), \hat{W}_u(t)) < 0$ [96, 99]; thus, one can solve the LMI given by (8.37) to ensure Assumption 8.4.1 is satisfied.

The performance bounds on the unactuated dynamics from Theorem 8.4.1 are “strict” in relation to the reference model given by (8.23). Since this reference model alters the trajectory of the ideal reference model dynamics given by

$$\dot{x}_r^{\text{id}}(t) = A_r x_r^{\text{id}}(t) + B_r c(t), \quad x_r^{\text{id}}(0) = x_{r0}^{\text{id}}, \quad (8.38)$$

where $x_r^{\text{id}}(t) \in \mathbb{R}^n$ is the ideal reference state (which is bounded by $\|x_r^{\text{id}}(t)\|_2 \leq x_r^*$ for a bounded reference command $\|c(t)\|_2 \leq c^*$), it is also necessary to analyze the distance between the unactuated dynamical system and this ideal reference model. This is also considered to be important in other works in which an ideal reference model has been modified (see, for example, [118, 197]). For this purpose, we define $\tilde{x}_r(t) \triangleq x_r(t) - x_r^{\text{id}}(t)$ as the error between the reference model given by (8.23) and the ideal reference (8.38).

Next, note that

$$\begin{aligned}\|x(t) - x_r^{\text{id}}(t)\|_2 &= \|e(t) + \tilde{x}_r(t)\|_2 \\ &\leq \|e(t)\|_2 + \|\tilde{x}_r(t)\|_2,\end{aligned}\quad (8.39)$$

implying that decreasing the bounds on both error signals will effectively decrease the distance between the unactuated dynamical system trajectory and the ideal reference model trajectory.

Remark 8.4.2 The performance bounds given by (8.27) and (8.28) can also be written as

$$\|\tilde{z}(t)\|_2 < \frac{\varepsilon_z}{\sqrt{\lambda_{\min}(S)}}, \quad (8.40)$$

$$\|e(t)\|_2 < \frac{\varepsilon_e}{\sqrt{\lambda_{\min}(P)}}, \quad (8.41)$$

respectively. From (8.41), we can enforce part of (8.39) through the a-priori, user-defined bound ε_e .

The next theorem shows the bound on $\|\tilde{x}_r(t)\|_2$ also depends on the enforced performance bounds.

Theorem 8.4.2 Consider the reference model for the actuated dynamics given by (8.18), the reference model for the unactuated dynamics given by (8.23), and the ideal reference model given by (8.38) subject to the control signal given by (8.20) and the update laws (8.21) and (8.22). Under Assumption 8.4.1, the upper bound for $\|\tilde{x}_r(t)\|_2$ is given by

$$\|\tilde{x}_r(t)\|_2 \leq \sqrt{\frac{\lambda_{\max}(\mathcal{P})}{\lambda_{\min}(\mathcal{P})}} \Theta^*, \quad (8.42)$$

where

$$\Theta^* \triangleq 2\rho^{-1} \|\mathcal{P}B\|_F \left[\psi^* \left(\frac{\varepsilon_e}{\sqrt{\lambda_{\min}(P)}} + x_r^* \right) + \phi^* \left(\frac{\varepsilon_z}{\sqrt{\lambda_{\min}(S)}} \right) + \|L_2\|_F c^* \right]. \quad (8.43)$$

Proof. Consider the reference model error dynamics obtained from the reference model (8.23) and the ideal reference model (8.38) subject to the control signal (8.20) given by

$$\begin{aligned}\dot{\tilde{x}}_r(t) &= A_r \tilde{x}_r(t) + B[J_0 z(t) - u_1(t)] \\ &= (A + B\hat{W}_u^T(t))\tilde{x}_r(t) + B(J_0 + \hat{J}_\Delta(t))z_r(t) + B[(L_1 + \hat{W}_u^T(t))e(t) \\ &\quad + (J_0 + \hat{J}_\Delta(t))\tilde{z}(t) + (L_1 + \hat{W}_u^T(t))x_r^{\text{id}}(t) - L_2 c(t)].\end{aligned}\quad (8.44)$$

In addition, the reference model (8.18) subject to (8.20) can be written as

$$\begin{aligned}\dot{z}_r(t) &= F_r z_r(t) - G_r(L_1 + \hat{W}_u^T(t))\tilde{x}_r(t) - G_r[(L_1 + \hat{W}_u^T(t))e(t) \\ &\quad + (J_0 + \hat{J}_\Delta(t))\tilde{z}(t) + (L_1 + \hat{W}_u^T(t))x_r^{\text{id}}(t) - L_2 c(t)].\end{aligned}\quad (8.45)$$

Now, it follows that (8.44) and (8.45) can be written in compact form as

$$\dot{\xi}(t) = \mathcal{A}(\hat{J}_\Delta(t), \hat{W}_u(t))\xi(t) + \mathcal{B}\kappa(\cdot), \quad (8.46)$$

with $\xi(t) = [\tilde{x}_r^T(t), z_r^T(t)]^T$, $\mathcal{B} = [B^T, -G_r^T]^T$, and

$$\kappa(\cdot) = (L_1 + \hat{W}_u^T(t))e(t) + (J_0 + \hat{J}_\Delta(t))\tilde{z}(t) + (L_1 + \hat{W}_u^T(t))x_r^{\text{id}}(t) - L_2 c(t). \quad (8.47)$$

Note that $\kappa(\cdot)$ is bounded as a result of Theorem 8.4.1 and the boundedness of the ideal reference model (8.38). This bound can be written as

$$\begin{aligned}\|\kappa(\cdot)\|_2 &= \|(L_1 + \hat{W}_u^T(t))e(t) + (J_0 + \hat{J}_\Delta(t))\tilde{z}(t) + (L_1 + \hat{W}_u^T(t))x_r^{\text{id}}(t) - L_2 c(t)\|_2 \\ &\leq \psi^*(\|e(t)\|_2 + x_r^*) + \phi^* \|\tilde{z}(t)\|_2 + \|L_2\|_F c^*,\end{aligned}\quad (8.48)$$

where $\|L_1 + \hat{W}_u^T(t)\|_F \leq \psi^*$ and $\|J_0 + \hat{J}_\Delta(t)\|_F \leq \phi^*$. Using the enforced performance bounds given by (8.40) and (8.41), (8.48) can be further bounded as

$$\|\kappa(\cdot)\|_2 \leq \psi^* \left(\frac{\varepsilon_e}{\sqrt{\lambda_{\min}(P)}} + x_r^* \right) + \phi^* \frac{\varepsilon_z}{\sqrt{\lambda_{\min}(S)}} + \|L_2\|_F c^*, \quad (8.49)$$

Next, it follows from the quadratic stability of $\mathcal{A}(\hat{J}_\Delta(t), \hat{W}_u(t))$ by Assumption 8.4.1 and compactness that there exists a $\rho \in \mathbb{R}_+$ such that

$$\mathcal{A}^T(\hat{J}_\Delta(t), \hat{W}_u(t))\mathcal{P} + \mathcal{P}\mathcal{A}(\hat{J}_\Delta(t), \hat{W}_u(t)) + \rho I \leq 0. \quad (8.50)$$

Now, consider the positive-definite energy function

$$\mathcal{V}(\xi) = \xi^T \mathcal{P} \xi, \quad (8.51)$$

where differentiation and use of (8.46) yields

$$\begin{aligned}
\dot{\mathcal{V}}(\xi(t)) &= 2\xi^T(t)\mathcal{P}\dot{\xi}(t) \\
&= \xi^T(t)[\mathcal{A}^T(\hat{J}_\Delta(t), \hat{W}_u(t))\mathcal{P} + \mathcal{P}\mathcal{A}(\hat{J}_\Delta(t), \hat{W}_u(t))]\xi(t) + 2\xi^T(t)\mathcal{P}\mathcal{B}\kappa(\cdot). \quad (8.52)
\end{aligned}$$

Furthermore, using (8.49) and (8.50), one can write (8.52) as

$$\begin{aligned}
\dot{\mathcal{V}}(\xi(t)) &\leq -\rho\|\xi(t)\|_2^2 + 2\|\xi(t)\|_2\|\mathcal{P}\mathcal{B}\|_F\|\kappa(\cdot)\|_2 \\
&\leq -\rho\|\xi(t)\|_2^2 + 2\|\xi(t)\|_2\|\mathcal{P}\mathcal{B}\|_F\left[\psi^*\left(\frac{\varepsilon_e}{\sqrt{\lambda_{\min}(\mathcal{P})}} + x_r^*\right) + \phi^*\frac{\varepsilon_z}{\sqrt{\lambda_{\min}(\mathcal{S})}} + \|L_2\|_F c^*\right] \\
&= -\|\xi(t)\|_2(\|\xi(t)\|_2 - \Theta^*), \quad (8.53)
\end{aligned}$$

and hence, $\dot{\mathcal{V}}(\xi(t)) < 0$ outside the compact set $\Omega = \{\xi : \|\xi(t)\|_2 \leq \Theta^*\}$.

Next, it follows that $\mathcal{V}(\xi)$ is upper and lower bounded by $\lambda_{\min}(\mathcal{P})\|\xi(t)\|_2^2 \leq \mathcal{V}(\xi) \leq \lambda_{\max}(\mathcal{P})\|\xi(t)\|_2^2$, and since $\|\tilde{x}_r(t)\|_2^2 \leq \|\xi(t)\|_2^2$ it follows that

$$\lambda_{\min}(\mathcal{P})\|\tilde{x}_r(t)\|_2^2 \leq \lambda_{\max}(\mathcal{P})\|\xi(t)\|_2^2 \leq \lambda_{\max}(\mathcal{P})\Theta^{*2}. \quad (8.54)$$

Division of both sides of (8.54) by $\lambda_{\min}(\mathcal{P})$ and then taking the square root results in (8.42). ■

Remark 8.4.3 From Theorem 8.4.2, one can reduce the bound on $\|\tilde{x}_r(t)\|_2$ through the selection of the a-priori, user-defined performance bounds in (8.27) and (8.28). It then follows from Theorems 8.4.1 and 8.4.2 as well as the discussion in Remark 8.4.2 that performance guarantees can be effectively enforced between the unactuated dynamical system trajectories and the ideal reference model trajectories.

Remark 8.4.4 The reference model of the actuated system given by (8.18) already represents the ideal dynamics. It is designed to match the ideal case discussed in Remark 8.2.1 such that the additional control signal $u_1(t)$ can be “passed” through to the unactuated dynamics by means of the physical interconnection. For this reason, a similar analysis as in Theorem 8.4.2 is not performed here.

8.5 Illustrative Numerical Example

We now present a numerical example to illustrate the efficacy of the proposed set-theoretic adaptive control architecture. For this purpose, consider the interconnected uncertain dynamical system depicted in Figure 8.2, which has an actuated cart interconnected to an unactuated cart with an inverted pendulum. The

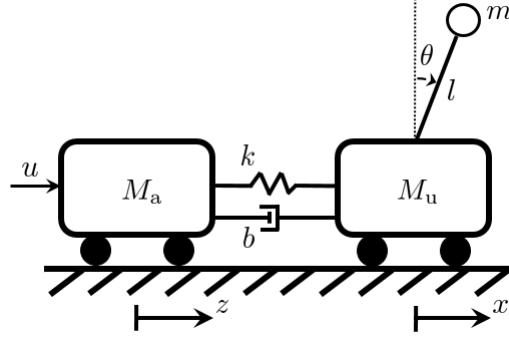


Figure 8.2: An interconnected system with an actuated cart physically connected to an unactuated cart with inverted pendulum.

dynamics for the interconnected system in Figure 8.2 can be given by

$$\begin{aligned}
 \begin{bmatrix} \dot{\theta}(t) \\ \ddot{\theta}(t) \\ \dot{x}(t) \\ \ddot{x}(t) \end{bmatrix} &= \begin{bmatrix} 0 & 1 & 0 & 0 \\ \frac{(M_u+m)g}{M_u l} & 0 & \frac{k_0}{M_u l} & \frac{b_0}{M_u l} \\ 0 & 0 & 0 & 1 \\ \frac{mg}{M_u} & 0 & -\frac{k_0}{M_u} & -\frac{b_0}{M_u} \end{bmatrix} \begin{bmatrix} \theta(t) \\ \dot{\theta}(t) \\ x(t) \\ \dot{x}(t) \end{bmatrix} + \begin{bmatrix} 0 \\ -\frac{1}{M_u l} \\ 0 \\ \frac{1}{M_u} \end{bmatrix} \left(([k_0, b_0] + [\delta k, \delta b]) \begin{bmatrix} z(t) \\ \dot{z}(t) \end{bmatrix} \right. \\
 &\quad \left. + [-\delta k, -\delta b] \begin{bmatrix} x(t) \\ \dot{x}(t) \end{bmatrix} \right), \tag{8.55}
 \end{aligned}$$

$$\begin{aligned}
 \begin{bmatrix} \dot{z}(t) \\ \ddot{z}(t) \end{bmatrix} &= \begin{bmatrix} 0 & 1 \\ -\frac{k_0}{M_a} & -\frac{b_0}{M_a} \end{bmatrix} \begin{bmatrix} z(t) \\ \dot{z}(t) \end{bmatrix} + \begin{bmatrix} 0 \\ \frac{1}{M_a} \end{bmatrix} \left(u(t) + ([k_0, b_0] + [\delta k, \delta b]) \begin{bmatrix} x(t) \\ \dot{x}(t) \end{bmatrix} \right. \\
 &\quad \left. + [-\delta k, -\delta b] \begin{bmatrix} z(t) \\ \dot{z}(t) \end{bmatrix} \right). \tag{8.56}
 \end{aligned}$$

For this example, the cart masses are known as $M_a = 10.0$ (kg) and $M_u = 5.0$ (kg), the pendulum has a length of $l = 3$ (m) with a mass $m = 1.0$ (kg), and $g = 9.81$ (m/s^2) is the gravitational constant. In addition, the spring constant $k = k_0 + \delta k$ has a known nominal value of $k_0 = 5.0$ ($\text{N} \cdot \text{m}^{-1}$) with δk representing unknown variation and the damper coefficient $b = b_0 + \delta b$ has a known nominal value of $b_0 = 2.0$ ($\text{N} \cdot \text{sec} \cdot \text{m}^{-1}$) with δb representing unknown variation. For the simulation, δk is set to 1.0 and δb is set to 0.5. Furthermore, we initialize the actuated cart at $z_0 = [0.1, 0]^T$ and the unactuated cart at $x_0 = [0.1, 0, 0.1, 0]$ and apply a step command signal for the unactuated cart.

Linear quadratic regulation theory [91] is used to design the nominal feedback control gains K_1 and L_1 for the actuated and unactuated carts respectively. Through tuning, we select the weighting matrices $Q_a = \text{diag}[600, 50]$ to penalize the states of the actuated cart and $R_a = 25$ to penalize the control input $u(t)$, such that we obtain $K_1 = [117.6, 58.0]$ and design the Hurwitz reference model F_r for the actuated cart. For the unactuated cart, we select $Q_u = \text{diag}[0.1, 1, 10, 1]$ to penalize its states and $R_u = 1.2^{-1}$ to penalize the control input $u_1(t)$ such that we obtain $L_1 = [-186.7, -97.6, -10.8, -11.8]$ for the unactuated cart, which is used to design its Hurwitz reference model matrix A_r . The feedforward gain K_2 is designed such that $-J_0(F - GK_1)^{-1}GK_2 = 1$, where $J_0 = [k_0, b_0]$, which results in $K_2 = 24.5$. Similarly, a pre-filter is used such that a desired unactuated cart position $x(t)$ is followed. For this purpose, using $C = [0, 0, 1, 0]$, the gain L_2 is calculated as $L_2 = -(C(A - BL_1)^{-1}B)^{-1} = -5.8$. Finally, using the rectangular projection operator, bounds on the uncertainties are set element-wise to be 10% greater than each uncertain element of $W_a = W_u = [-\delta k, -\delta b]^T$ and $H_\Delta = J_\Delta = [\delta k, \delta b]$. The learning gains are set as $\gamma_a = \gamma_u = \alpha = \beta = 1$, such that we solely focus on the ability of the error dependent learning gains $\phi_d(\|\tilde{z}(t)\|_S)$ and $\phi_d(\|e(t)\|_P)$ to enforce the performance bounds which are set to $\varepsilon_z = \varepsilon_e = 0.25$.

The feasibility of the control parameters and system uncertainties is first verified using the LMI analysis discussed in Remark 8.4.1. With a feasible solution, the proposed adaptive control is implemented, which results in the performance shown in Figures 8.3 and 8.4. In particular, Figure 8.3 shows that the position of the unactuated cart properly follows the reference model trajectory, while the pendulum remains properly inverted. Figure 8.4 shows that the performance bounds on the actuated and unactuated carts are enforced for all time. The initial conditions of the carts start just within the user-defined bound such that the error dependent gain is larger to prevent violation of the performance bound. As the command is applied and the carts follow the command, the performance guarantee remains enforced.

8.6 Conclusion

We proposed an adaptive control architecture for interconnected uncertain dynamical systems to control and enforce performance bounds on not only the actuated dynamics but also the unactuated dynamics using the physical interconnection. It was shown that stability and enforced performance guarantees of the interconnected system are obtained using a set-theoretic adaptive control architecture predicated on restricted potential functions. As a result, the system error trajectories of the actuated and unactuated dynamics were shown to be restricted and stay within user-defined limits even in the presence of uncer-

tainties in both the actuated and unactuated dynamics as well as unknown physical interconnections. It was also shown through application of LMIs that the stability of the selected control parameters and allowable interconnected system uncertainties could be verified.

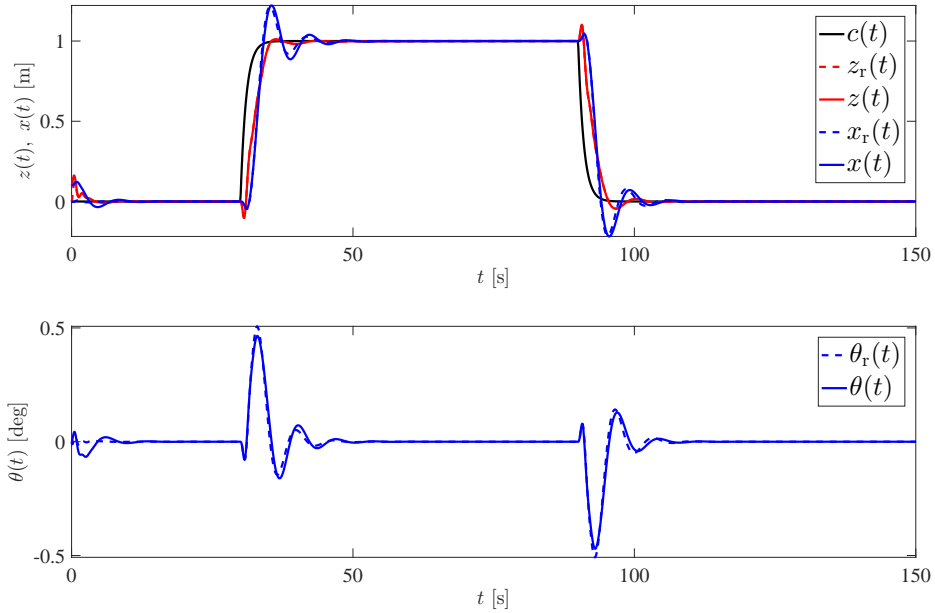


Figure 8.3: Proposed set-theoretic adaptive control performance for interconnected actuated and unactuated carts.

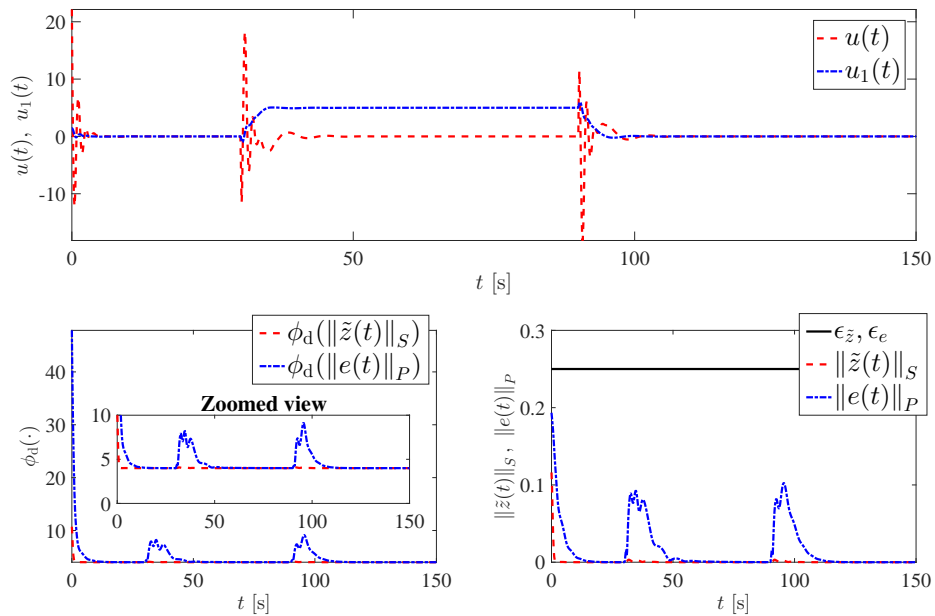


Figure 8.4: Control signals, error dependent learning gains, and enforced performance bounds.

CHAPTER 9: CONCLUDING REMARKS AND FUTURE RESEARCH

9.1 Concluding Remarks

The intent of this dissertation has been to present new model reference adaptive control architectures with stability, performance, and robustness considerations, to address challenges related to the verification of adaptive control systems. Specifically, the proposed architectures allow for improved transient performance as well as enforced performance guarantees, trajectory following of nonlinear reference models, correct adaptation in the presence of actuator dynamics, and control of large-scale interconnected modular systems.

To address the challenges in improving the transient performance, first an approach using artificial basis functions was presented. These artificial basis functions are constructed using a gradient optimization procedure such that they can improve the transient response of an adaptively controlled system, and hence, can be used to achieve predictable closed-loop system performance. This is then extended to a direct uncertainty minimization approach that uses modification terms in the adaptive control law and the update law to suppress the effect of system uncertainty on the transient system response for improved system performance. In addition, the use of a varying gain on the modification term was shown to keep the system error approximately within a-priori given, user-defined error performance bounds. This was then generalized further to incorporate a nonlinear reference model to better capture the desired closed-loop system performance for a class of nonlinear uncertain dynamical systems.

For the adaptive control of uncertain dynamical systems in the presence of high-order actuator dynamics, an LMI-based hedging approach was presented. Specifically, the proposed approach modifies the ideal reference model dynamics using the hedging method to allow correct adaptation that is not affected by the presence of actuator dynamics. The stability of this modified reference model coupled with the actuator dynamics was analyzed using tools and methods from Lyapunov stability, matrix mathematics, and LMIs. In addition, the distance between the uncertain dynamical system and the ideal (i.e., unmodified) reference model dynamics was also analyzed and it was remarked that this distance either can be made small by increasing the learning gain and the bandwidth of the actuator dynamics or asymptotically vanishes when

the uncertain dynamical system is driven by constant reference commands. This approach was further generalized for the cases in which the system uncertainties are nonlinear, the actuator output is unknown, and the actuator dynamics contain an additional throughput term with an application to the input time-delay problem. In addition, a detailed presentation of the algorithm used to compute the high-order actuator dynamics parameters was included with an application to a hypersonic vehicle model subject to pole-zero actuator dynamics. Finally, to go beyond the hedging approach for actuator dynamics that can only guarantee bounded trajectories in the neighborhood of the ideal reference model trajectories, a new model reference adaptive control architecture using expanded reference models was proposed. It was shown that the trajectories of the expanded reference model remain predictably close to the trajectories of the ideal reference model as compared to the hedging approach. In addition, it was shown that asymptotic convergence to the ideal reference model trajectories can be guaranteed using a new command governor architecture developed for the proposed expanded reference model. Moreover, to achieve a robust implementation in the presence of possible uncertainties in the bandwidths of actuator channels, the expanded reference model was redesigned with the estimate of actuator bandwidths.

For the control of large-scale interconnected modular systems a new decentralized adaptive control architecture was proposed using a set-theoretic adaptive approach predicated on restricted potential functions. The key feature of this methodology was to restrict the system error trajectories of the active modules such that they are guaranteed to stay within user-defined limits even in the presence of the unmodeled dynamics resulting from the passive modules. This was then extended to control and enforce performance bounds on not only the actuated dynamics (active module) but also the unactuated dynamics (passive module) using the physical interconnection. Finally, it was also shown through application of LMIs that the stability of the selected control parameters and allowable interconnected system uncertainties could be verified.

9.2 Future Research

There are several possible research directions that can be considered for each result in this dissertation. Since each architecture proposed assumes fully measurable states, one global direction is to extend to the case in which there is limited state information (i.e., output feedback adaptive control). In addition, more experimentation could be conducted to further show the effectiveness of the proposed results in real-world scenarios and bridge the gap between theory and practice. One such possible experimental result for the

work in Chapter 7 is an application to a small scale morphing wing aircraft. Additional experimentation could also include application of the performance oriented architectures to unmanned aerial vehicles.

For the actuator dynamics problem, a large amount of work has already gone into the LMI-based hedging approach including several generalizations as documented in Chapters 4 and 5. The improved architecture proposed in Chapter 6 is a more recent result, and hence, only considers, first order actuators, linear uncertainties, and known actuator outputs. Possible research directions would then be to extend the work in Chapter 6 to consider high-order actuator dynamics, nonlinear uncertainties, and unknown actuator outputs. Since the expanded reference model with the command governor architecture has been shown to capture the ideal reference model trajectories (and the LMI-based hedging approach cannot), these extensions would make this the most general approach for adaptive control systems subject to actuator dynamics.

While the results in Chapter 7 and 8 consider fixed performance bounds, this can be generalized to the case in which the performance bound is time-varying (i.e., $\varepsilon(t)$) by using recent results [160] proposed for sole systems. This extension allows for the initial tracking error $e(0)$ to be large and then converge to a small region defined by $\varepsilon(t)$. Finally, as noted in Section 1, addressing the challenges presented by actuator nonlinearities is another possible research direction. Currently, the author has preliminary work on this using the expanded reference model architecture for uncertain dynamical systems with both actuator dynamics and actuator amplitude saturation limits [198].

REFERENCES

- [1] K. Zhou and J. C. Doyle, *Essentials of robust control*, vol. 180. Upper Saddle River, NJ: Prentice Hall, 1998.
- [2] S. Skogestad and I. Postlethwaite, *Multivariable feedback control: Analysis and design*, vol. 2. New York, NY: Wiley, 2007.
- [3] H. P. Whitaker, J. Yamron, and A. Kezer, *Design of Model Reference Control Systems for Aircraft*. Cambridge, MA: Instrumentation Laboratory, Massachusetts Institute of Technology, 1958.
- [4] P. V. Osburn, H. P. Whitaker, and A. Kezer, "New developments in the design of adaptive control systems," *Institute of Aeronautical Sciences*, 1961.
- [5] K. S. Narendra and A. M. Annaswamy, *Stable adaptive systems*. Mineola, NY: Courier Corporation, 2012.
- [6] E. Lavretsky and K. A. Wise, *Robust Adaptive Control*. London: Springer-Verlag, 2013.
- [7] P. A. Ioannou and J. Sun, *Robust adaptive control*. Mineola, NY: Courier Corporation, 2012.
- [8] C. Rohrs, L. Valavani, M. Athans, and G. Stein, "Robustness of continuous-time adaptive control algorithms in the presence of unmodeled dynamics," *IEEE Transactions on Automatic Control*, vol. 30, no. 9, pp. 881–889, 1985.
- [9] B. Riedle and P. Kokotovic, "A stability-instability boundary for disturbance-free slow adaptation with unmodeled dynamics," *IEEE Transactions on Automatic Control*, vol. 30, no. 10, pp. 1027–1030, 1985.
- [10] M. Matsutani, A. Annaswamy, and E. Lavretsky, "Guaranteed delay margins for adaptive control of scalar plants," in *IEEE Conference on Decision and Control*, pp. 7297–7302, 2012.
- [11] S. M. Naik, P. Kumar, and B. E. Ydstie, "Robust continuous-time adaptive control by parameter projection," *IEEE Transactions on Automatic Control*, vol. 37, no. 2, pp. 182–197, 1992.

- [12] K. M. Dogan, B. C. Gruenwald, T. Yucelen, and J. A. Muse, “Relaxing the stability limit of adaptive control systems in the presence of unmodelled dynamics,” *International Journal of Control*, pp. 1–11, 2017.
- [13] A. J. Koshkouei and A. S. Zinober, “Adaptive output tracking backstepping sliding mode control of nonlinear systems,” *IFAC Proceedings Volumes*, vol. 33, no. 14, pp. 167–172, 2000.
- [14] M. Krstic, I. Kanellakopoulos, and P. V. Kokotovic, *Nonlinear and Adaptive Control Design*. New York, NY: Wiley, 1995.
- [15] T. Yucelen and W. M. Haddad, “Output feedback adaptive stabilization and command following for minimum phase dynamical systems with unmatched uncertainties and disturbances,” *International Journal of Control*, vol. 85, no. 6, pp. 706–721, 2012.
- [16] B.-J. Yang, T. Yucelen, J.-Y. Shin, and A. Calise, “LMI-based analysis of an adaptive flight control system with unmatched uncertainty,” in *AIAA Infotech@ Aerospace*, p. 3436, 2010.
- [17] N. T. Nguyen, “Multi-objective optimal control modification adaptive control method for systems with input and unmatched uncertainties,” in *AIAA Guidance, Navigation, and Control Conference*, pp. 1–15, 2014.
- [18] C. D. Heise and F. Holzapfel, “Uniform ultimate boundedness of a model reference adaptive controller in the presence of unmatched parametric uncertainties,” in *IEEE International Conference on Automation, Robotics, and Applications*, pp. 149–154, 2015.
- [19] E. Arabi, T. Yucelen, and B. C. Gruenwald, “Model reference adaptive control for uncertain dynamical systems with unmatched disturbances: A command governor-based approach,” in *Robotics and Mechatronics for Agriculture*, pp. 193–202, CRC Press, 2017.
- [20] D. P. Wiese, A. M. Annaswamy, J. A. Muse, M. A. Bolender, and E. Lavretsky, “Adaptive output feedback based on closed-loop reference models for hypersonic vehicles,” *Journal of Guidance, Control, and Dynamics*, vol. 38, no. 12, pp. 2429–2440, 2015.
- [21] H. K. Khalil, “Adaptive output feedback control of nonlinear systems represented by input-output models,” *IEEE Transactions on Automatic Control*, vol. 41, no. 2, pp. 177–188, 1996.
- [22] A. Albattat, B. Gruenwald, and T. Yucelen, “Design and analysis of adaptive control systems over wireless networks,” *Journal of Dynamic Systems, Measurement, and Control*, vol. 139, no. 7, p. 074501, 2017.

- [23] E. Lavretsky and N. Hovakimyan, “Stable adaptation in the presence of input constraints,” *Systems & Control Letters*, vol. 56, no. 11-12, pp. 722–729, 2007.
- [24] M. Thiel, D. Schwarzmann, A. M. Annaswamy, M. Schultalbers, and T. Jeansch, “Improved performance for adaptive control of systems with input saturation,” in *American Control Conference*, pp. 6012–6017, 2016.
- [25] M. Schwager and A. M. Annaswamy, “Direct adaptive control of multi-input plants with magnitude saturation constraints,” in *IEEE Conference on Decision and Control*, pp. 783–788, 2005.
- [26] M. Schwager, A. M. Annaswamy, and E. Lavretsky, “Adaptation-based reconfiguration in the presence of actuator failures and saturation,” in *American Control Conference*, pp. 2640–2645, 2005.
- [27] A. Annaswamy and J.-E. Wong, “Adaptive control in the presence of saturation non-linearity,” *International Journal of Adaptive Control and Signal Processing*, vol. 11, no. 1, pp. 3–19, 1997.
- [28] S. P. Karason and A. M. Annaswamy, “Adaptive control in the presence of input constraints,” in *American Control Conference*, pp. 1370–1374, 1993.
- [29] D. Li, N. Hovakimyan, and C. Cao, “Positive invariant set estimation of 11 adaptive controller in the presence of input saturation,” *International Journal of Adaptive Control and Signal Processing*, vol. 27, no. 11, pp. 1012–1030, 2013.
- [30] E. N. Johnson, *Limited authority adaptive flight control*. School of Aerospace Engineering, Georgia Institute of Technology, 2000.
- [31] E. N. Johnson and A. J. Calise, “Limited authority adaptive flight control for reusable launch vehicles,” *Journal of Guidance, Control, and Dynamics*, vol. 26, no. 6, pp. 906–913, 2003.
- [32] E. N. Johnson and A. J. Calise, “Pseudo-control hedging: A new method for adaptive control,” in *Advances in Navigation Guidance and Control Technology Workshop*, pp. 1–2, 2000.
- [33] E. Johnson, A. J. Calise, H. A. El-Shirbiny, and R. T. Rysdyk, “Feedback linearization with neural network augmentation applied to X-33 attitude control,” in *AIAA Guidance, Navigation, and Control Conference*, 2000.
- [34] E. N. Johnson and A. J. Calise, “Neural network adaptive control of systems with input saturation,” in *American Control Conference*, vol. 5, pp. 3527–3532, 2001.

- [35] T. Yucelen and W. M. Haddad, “Low-frequency learning and fast adaptation in model reference adaptive control,” *IEEE Transactions on Automatic Control*, vol. 58, no. 4, pp. 1080–1085, 2013.
- [36] T. Yucelen and E. Johnson, “On achieving predictable adaptive control response for uncertain dynamical systems with large domains of operation,” in *AIAA Guidance, Navigation, and Control Conference*, p. 4774, 2012.
- [37] Z. T. Dydek, A. M. Annaswamy, and E. Lavretsky, “Adaptive control and the NASA X-15-3 flight revisited,” *IEEE Control Systems*, vol. 30, no. 3, pp. 32–48, 2010.
- [38] N. Nguyen, K. Krishnakumar, and J. Boskovic, “An optimal control modification to model-reference adaptive control for fast adaptation,” in *AIAA Guidance, Navigation and Control Conference and Exhibit*, p. 7283, 2008.
- [39] T. T. Georgiou and M. C. Smith, “Robustness analysis of nonlinear feedback systems: An input-output approach,” *IEEE Transactions on Automatic Control*, vol. 42, no. 9, pp. 1200–1221, 1997.
- [40] B. D. O. Anderson, “Failures of adaptive control theory and their resolution,” *Communications in Information & Systems*, vol. 5, no. 1, pp. 1–20, 2005.
- [41] M. A. Duarte and K. S. Narendra, “Combined direct and indirect approach to adaptive control,” *IEEE Transactions on Automatic Control*, vol. 34, no. 10, pp. 1071–1075, 1989.
- [42] J.-J. E. Slotine and W. Li, “Composite adaptive control of robot manipulators,” *Automatica*, vol. 25, no. 4, pp. 509–519, 1989.
- [43] E. Lavretsky, “Combined/composite model reference adaptive control,” *IEEE Transactions on Automatic Control*, vol. 54, no. 11, p. 2692, 2009.
- [44] K. Y. Volyanskyy, A. J. Calise, and B.-J. Yang, “A novel Q -modification term for adaptive control,” in *American Control Conference*, 2006.
- [45] K. Y. Volyanskyy, A. J. Calise, B. J. Yang, and E. Lavretsky, “An error minimization method in adaptive control,” in *AIAA Guidance, Navigation, and Control Conference*, 2006.
- [46] K. Y. Volyanskyy, W. M. Haddad, and A. J. Calise, “A new neuroadaptive control architecture for nonlinear uncertain dynamical systems: Beyond σ - and e -modifications,” *IEEE Transactions on Neural Networks*, vol. 20, no. 11, pp. 1707–1723, 2009.

- [47] G. Chowdhary and E. N. Johnson, "Theory and flight-test validation of a concurrent-learning adaptive controller," *Journal of Guidance, Control, and Dynamics*, vol. 34, no. 2, pp. 592–607, 2011.
- [48] G. Chowdhary, T. Yucelen, M. Mühlegg, and E. N. Johnson, "Concurrent learning adaptive control of linear systems with exponentially convergent bounds," *International Journal of Adaptive Control and Signal Processing*, vol. 27, no. 4, pp. 280–301, 2013.
- [49] T. Yucelen, B. Gruenwald, J. Muse, and G. De La Torre, "Adaptive control with nonlinear reference systems," in *American Control Conference*, 2015.
- [50] *Quanser AERO User Manual*, 2016. Available at <https://www.quanser.com/products/quanser-aero/>.
- [51] X. Wang and N. Hovakimyan, " \mathcal{L}_1 adaptive controller for nonlinear time-varying reference systems," *Systems & Control Letters*, vol. 61, no. 4, pp. 455–463, 2012.
- [52] Y. Kawaguchi, H. Eguchi, T. Fukao, and K. Osuka, "Passivity-based adaptive nonlinear control for active steering," *IEEE International Conference on Control Applications*, pp. 214–219, 2007.
- [53] S. K. Scarritt, "Nonlinear model reference adaptive control for satellite attitude tracking," *AIAA Guidance, Navigation, and Control Conference*, 2008.
- [54] F. Peter, M. Leitao, and F. Holzapfel, "Adaptive augmentation of a new baseline control architecture for tail-controlled missiles using a nonlinear reference model," *AIAA Guidance, Navigation, and Control Conference*, 2012.
- [55] C. Cao and N. Hovakimyan, " \mathcal{L}_1 adaptive controller for systems in the presence of unmodelled actuator dynamics," in *IEEE Conference on Decision and Control*, pp. 891–896, 2007.
- [56] C.-Y. SU and Y. Stepanenko, "Backstepping-based hybrid adaptive control of robot manipulators incorporating actuator dynamics," *International journal of adaptive control and signal processing*, vol. 11, no. 2, pp. 141–153, 1997.
- [57] G. De La Torre, T. Yucelen, and E. Johnson, "Reference control architecture in the presence of measurement noise and actuator dynamics," in *American Control Conference*, pp. 4961–4966, 2014.
- [58] J. Boskovic, J. A. Jackson, and R. Mehra, "Robust adaptive control in the presence of unmodeled actuator dynamics," in *AIAA Guidance, Navigation, and Control Conference*, p. 5194, 2013.
- [59] D. D. Siljak, *Decentralized control of complex systems*. Mineola, NY: Courier Corporation, 2011.

- [60] E. J. Davison and A. G. Aghdam, *Decentralized control of large-scale systems*. New York, NY: Springer Publishing Company, Incorporated, 2014.
- [61] P. A. Ioannou, "Decentralized adaptive control of interconnected systems," *IEEE Transactions on Automatic Control*, vol. 31, no. 4, pp. 291–298, 1986.
- [62] D. T. Gavel and D. D. Siljak, "Decentralized adaptive control: structural conditions for stability," *IEEE Transactions on Automatic Control*, vol. 34, no. 4, pp. 413–426, 1989.
- [63] L. Shi and S. K. Singh, "Decentralized adaptive controller design for large-scale systems with higher order interconnections," *IEEE Transactions on Automatic Control*, vol. 37, no. 8, pp. 1106–1118, 1992.
- [64] C. Wen, "Indirect robust totally decentralized adaptive control of continuous-time interconnected systems," *IEEE Transactions on Automatic Control*, vol. 40, no. 6, pp. 1122–1126, 1995.
- [65] J. T. Spooner and K. M. Passino, "Decentralized adaptive control of nonlinear systems using radial basis neural networks," *IEEE Transactions on Automatic Control*, vol. 44, no. 11, pp. 2050–2057, 1999.
- [66] T. Yucelen, B.-J. Yang, and A. J. Calise, "Derivative-free decentralized adaptive control of large-scale interconnected uncertain systems," in *IEEE Conference on Decision and Control*, pp. 1104–1109, 2011.
- [67] B. M. Mirkin, "Decentralized adaptive controller with zero residual tracking errors," in *Mediterranean Conference on Control and Automation*, pp. 28–30, 1999.
- [68] K. S. Narendra and N. O. Olgac, "Exact output tracking in decentralized adaptive control systems," *IEEE Transactions on Automatic Control*, vol. 47, no. 2, pp. 390–395, 2002.
- [69] B. M. Mirkin, "Comments on "Exact output tracking in decentralized adaptive control"," *IEEE Transactions on Automatic Control*, vol. 48, no. 2, pp. 348–350, 2003.
- [70] K. Narendra, N. Olgac, and S. Mukhopadhyay, "Decentralised adaptive control with partial communication," *IEE Proceedings-Control Theory and Applications*, vol. 153, no. 5, pp. 546–555, 2006.
- [71] P. Panagi and M. M. Polycarpou, "Distributed fault accommodation for a class of interconnected nonlinear systems with partial communication," *IEEE Transactions on Automatic Control*, vol. 56, no. 12, pp. 2962–2967, 2011.

- [72] T. Yucelen and J. S. Shamma, “Adaptive architectures for distributed control of modular systems,” in *American Control Conference*, pp. 1328–1333, 2014.
- [73] T. Guo, “Decentralized control for large-scale interconnected nonlinear systems based on barrier lyapunov function,” *Mathematical Problems in Engineering*, 2015.
- [74] E. Arabi, B. C. Gruenwald, T. Yucelen, and N. T. Nguyen, “A set-theoretic model reference adaptive control architecture for disturbance rejection and uncertainty suppression with strict performance guarantees,” *International Journal of Control*, vol. 91, no. 5, pp. 1195–1208, 2018.
- [75] B. Gruenwald and T. Yucelen, “On transient performance improvement of adaptive control architectures,” *International Journal of Control*, vol. 88, no. 11, pp. 2305–2315, 2015.
- [76] N. Hovakimyan and C. Cao, *\mathcal{L}_1 adaptive control theory: Guaranteed robustness with fast adaptation*, vol. 21. Philadelphia, PA: SIAM, 2010.
- [77] T. Yucelen and W. M. Haddad, “A robust adaptive control architecture for disturbance rejection and uncertainty suppression with \mathcal{L}_∞ transient and steady-state performance guarantees,” *International Journal of Adaptive Control and Signal Processing*, vol. 26, no. 11, pp. 1024–1055, 2012.
- [78] T. Yucelen and A. J. Calise, “Derivative-free model reference adaptive control,” *Journal of Guidance, Control, and Dynamics*, vol. 34, no. 4, pp. 933–950, 2011.
- [79] T. Yucelen and E. N. Johnson, “Artificial basis functions in adaptive control for transient performance improvement,” in *AIAA Guidance, Navigation, and Control Conference*, 2013.
- [80] W. M. Haddad and V. Chellaboina, *Nonlinear dynamical systems and control: A Lyapunov-based approach*. Princeton, NJ: Princeton University Press, 2008.
- [81] T. Yucelen and E. Johnson, “A new command governor architecture for transient response shaping,” *International Journal of Adaptive Control and Signal Processing*, vol. 27, no. 12, pp. 1065–1085, 2013.
- [82] J.-B. Pomet and L. Praly, “Adaptive nonlinear regulation: Estimation from the lyapunov equation,” *IEEE Transactions on Automatic Control*, vol. 37, no. 6, pp. 729–740, 1992.
- [83] T. Yucelen, *Advances in adaptive control theory: Gradient-and derivative-free approaches*. Georgia Institute of Technology, 2012.

- [84] A. J. Calise and T. Yucelen, “Adaptive loop transfer recovery,” *Journal of Guidance, Control, and Dynamics*, vol. 35, no. 3, pp. 807–815, 2012.
- [85] P. Patre, W. MacKunis, C. Makkar, and W. Dixon, “Asymptotic tracking for systems with structured and unstructured uncertainties,” in *IEEE Conference on Decision and Control*, pp. 441–446, 2006.
- [86] B. C. Gruenwald, T. Yucelen, and J. A. Muse, “Direct uncertainty minimization framework for system performance improvement in model reference adaptive control,” *Machines*, vol. 5, no. 1, p. 9, 2017.
- [87] B. Gruenwald, T. Yucelen, and M. Fravolini, “Performance oriented adaptive architectures with guaranteed bounds,” in *AIAA Infotech@Aerospace Conference*, 2014.
- [88] H. K. Khalil, *Nonlinear Systems*. Upper Saddle River, NJ: Prentice Hall, 2002.
- [89] F. L. Lewis, K. Liu, and A. Yesildirek, “Neural net robot controller with guaranteed tracking performance,” *IEEE Transactions on Neural Networks*, vol. 6, no. 3, pp. 703–715, 1995.
- [90] F. L. Lewis, A. Yesildirek, and K. Liu, “Multilayer neural-net robot controller with guaranteed tracking performance,” *IEEE Transactions on Neural Networks*, vol. 7, no. 2, pp. 388–399, 1996.
- [91] F. L. Lewis and V. L. Syrmos, *Optimal control*. New York, NY: Wiley, 1995.
- [92] E. Arabi and T. Yucelen, “Experimental results of set-theoretic model reference adaptive control architecture on an aerospace testbed,” in *AIAA Guidance, Navigation, and Control Conference*, 2019 (submitted).
- [93] K. J. Åström and B. Wittenmark, *Adaptive control*. Mineola, NY: Courier Corporation, 2013.
- [94] C. Cao and N. Hovakimyan, “ \mathcal{L}_1 adaptive controller for systems in the presence of unmodelled actuator dynamics,” in *IEEE Conference on Decision and Control*, pp. 891–896, 2007.
- [95] B. C. Gruenwald, D. Wagner, T. Yucelen, and J. A. Muse, “Computing actuator bandwidth limits for model reference adaptive control,” *International Journal of Control*, vol. 89, no. 12, pp. 2434–2452, 2016.
- [96] J. A. Muse, “Frequency limited adaptive control using a quadratic stability framework: Guaranteed stability limits,” in *AIAA Guidance, Navigation, and Control Conference*, 2014.

- [97] S. Boyd, L. E. Ghaoui, E. Feron, and V. Balakrishnan, *Linear Matrix Inequalities in System and Control Theory*. Philadelphia, PA: SIAM, 1994.
- [98] C. Scherer and S. Weiland, “Linear matrix inequalities in control,” *Lecture Notes, Dutch Institute for Systems and Control, Delft, The Netherlands*, vol. 3, 2000.
- [99] P. Gahinet, P. Apkarian, and M. Chilali, “Affine parameter-dependent Lyapunov functions and real parametric uncertainty,” *IEEE Transactions on Automatic Control*, vol. 41, no. 3, pp. 436–442, 1996.
- [100] J. A. Muse, “Frequency limited adaptive control using a quadratic stability framework: Stability and convergence,” in *AIAA Guidance, Navigation, and Control Conference*, 2014.
- [101] B. C. Gruenwald, J. A. Muse, and T. Yucelen, “Adaptive control for a class of uncertain nonlinear dynamical systems in the presence of high-order actuator dynamics,” in *American Control Conference*, pp. 4430–4435, 2017.
- [102] B. C. Gruenwald, D. Wagner, T. Yucelen, and J. A. Muse, “An LMI-based hedging approach to model reference adaptive control with actuator dynamics,” in *ASME Dynamic Systems and Control Conference*, 2015.
- [103] B. C. Gruenwald, D. Wagner, T. Yucelen, and J. A. Muse, “Computing actuator bandwidth limits for adaptive control,” in *AIAA Guidance, Navigation, and Control Conference*, 2016.
- [104] B. C. Gruenwald, T. Yucelen, J. A. Muse, and D. Wagner, “Computing stability limits of adaptive controllers in the presence of high-order actuator dynamics,” *IEEE Conference on Decision and Control*, 2016.
- [105] B. C. Gruenwald, K. M. Dogan, T. Yucelen, and J. A. Muse, “A model reference adaptive control framework for uncertain dynamical systems with high-order actuator dynamics and unknown actuator outputs,” in *ASME 2017 Dynamic Systems and Control Conference*, 2017.
- [106] T. Yucelen, G. De La Torre, and E. N. Johnson, “Improving transient performance of adaptive control architectures using frequency-limited system error dynamics,” *International Journal of Control*, vol. 87, no. 11, pp. 2383–2397, 2014.
- [107] T. Yucelen, B. Gruenwald, and J. A. Muse, “A direct uncertainty minimization framework in model reference adaptive control,” in *AIAA Guidance, Navigation, and Control Conference*, 2015.
- [108] T. E. Gibson, A. M. Annaswamy, and E. Lavretsky, “On adaptive control with closed-loop reference models: transients, oscillations, and peaking,” *IEEE Access*, vol. 1, pp. 703–717, 2013.

- [109] T. E. Gibson, A. M. Annaswamy, and E. Lavretsky, "Improved transient response in adaptive control using projection algorithms and closed loop reference models," in *AIAA Guidance Navigation and Control Conference*, 2012.
- [110] E. Lavretsky, R. Gadiant, and I. M. Gregory, "Predictor-based model reference adaptive control," *Journal of Guidance, Control, and Dynamics*, vol. 33, no. 4, pp. 1195–1201, 2010.
- [111] Q. Sang and G. Tao, "Performance robustness of MRAC under reduction in actuator effectiveness," in *American Control Conference*, pp. 4506–4511, 2009.
- [112] S. Gayaka and B. Yao, "Accommodation of unknown actuator faults using output feedback-based adaptive robust control," *International Journal of Adaptive Control and Signal Processing*, vol. 25, no. 11, pp. 965–982, 2011.
- [113] S. Gayaka and B. Yao, "Output feedback based adaptive robust fault-tolerant control for a class of uncertain nonlinear systems," *Journal of Systems Engineering and Electronics*, vol. 22, no. 1, pp. 38–51, 2011.
- [114] B. C. Gruenwald, T. Yucelen, and J. A. Muse, "Model reference adaptive control in the presence of actuator dynamics with applications to the input time-delay problem," in *AIAA Guidance, Navigation, and Control Conference*, p. 1491, 2017.
- [115] M. Matsutani, *Robust adaptive flight control systems in the presence of time delay*. Massachusetts Institute of Technology, 2013.
- [116] B. D. Anderson and A. Dehghani, "Challenges of adaptive control—past, permanent and future," *Annual Reviews in Control*, vol. 32, no. 2, pp. 123–135, 2008.
- [117] B. C. Gruenwald, T. Yucelen, K. M. Dogan, J. A. Muse, and D. Wagner, "Computing the stability limits of pole-zero actuator dynamics on adaptive control laws for aerospace applications," in *AIAA Guidance, Navigation, and Control Conference*, 2018.
- [118] B. C. Gruenwald, J. A. Muse, D. Wagner, and T. Yucelen, "Adaptive architectures for control of uncertain dynamical systems with actuator dynamics," in *Advances in Computational Intelligence and Autonomy for Aerospace Systems (Editor: J. Valasek)*, AIAA Progress in Aeronautics and Astronautics Series, American Institute of Aeronautics and Astronautics, (to appear).
- [119] J. Lofberg, "Yalmip: A toolbox for modeling and optimization in matlab," in *IEEE International Symposium on Computer Aided Control Systems Design*, 2004.

- [120] P. Gahinet, A. Nemirovskii, A. J. Laub, and M. Chilali, “The LMI control toolbox,” in *IEEE Conference on Decision and Control*, 1994.
- [121] T. Lombaerts, G. Looye, P. Chu, and J. A. Mulder, “Pseudo control hedging and its application for safe flight envelope protection,” in *AIAA Guidance, Navigation, and Control Conference*, p. 8280, 2010.
- [122] M. D. Tandale and J. Valasek, “Adaptive dynamic inversion control with actuator saturation constraints applied to tracking spacecraft maneuvers,” *Journal of the Astronautical Sciences*, vol. 52, no. 4, pp. 517–530, 2004.
- [123] E. N. Johnson and S. K. Kannan, “Adaptive trajectory control for autonomous helicopters,” *Journal of Guidance, Control, and Dynamics*, vol. 28, no. 3, pp. 524–538, 2005.
- [124] Q. Lam, R. Hindman, W. Shell, and B. Ridgely, “Investigation and preliminary development of a modified pseudo control hedging for missile performance enhancement,” in *AIAA Guidance, Navigation, and Control Conference and Exhibit*, p. 6458, 2005.
- [125] B. C. Gruenwald, T. Yucelen, K. M. Dogan, and J. A. Muse, “A new adaptive control architecture for uncertain dynamical systems with actuator dynamics: Beyond pseudo-control hedging,” *AIAA Guidance, Navigation, and Control Conference*, 2018.
- [126] B. C. Gruenwald, T. Yucelen, K. M. Dogan, and J. A. Muse, “An adaptive architecture for control of uncertain dynamical systems with unknown actuator bandwidths,” in *IFAC Workshop on Networked & Autonomous Air & Space Systems*, 2018 (to appear).
- [127] J. Muse, “A method for enforcing state constraints in adaptive control,” in *AIAA Guidance, Navigation, and Control Conference*, p. 6205, 2011.
- [128] N. Nguyen, “Asymptotic linearity of optimal control modification adaptive law with analytical stability margins,” in *AIAA Infotech@ Aerospace 2010*, p. 3301, 2010.
- [129] B. Sinafar, A. R. Ghiasi, and A. K. Fazli, “A new model reference adaptive control structure for uncertain switched systems with unmodeled input dynamics,” *Transactions of the Institute of Measurement and Control*, vol. 37, no. 10, pp. 1171–1180, 2015.
- [130] T. Bierling, L. Höcht, F. Holzapfel, R. Maier, and A. Wildschek, “Comparative analysis of mrac architectures in a unified framework,” in *AIAA Guidance, Navigation, and Control Conference*, p. 7536, 2010.

- [131] C. D. Heise, S. P. Schatz, and F. Holzapfel, “Modified extended state observer control of linear systems,” in *AIAA Guidance, Navigation, and Control Conference*, p. 0364, 2016.
- [132] M. Pakmehr and T. Yucelen, “Adaptive control of uncertain systems with gain scheduled reference models and constrained control inputs,” *American Control Conference*, pp. 691–696, 2014.
- [133] E. Garone, S. Di Cairano, and I. Kolmanovsky, “Reference and command governors for systems with constraints: A survey on theory and applications,” *Automatica*, vol. 75, pp. 306–328, 2017.
- [134] B. C. Gruenwald, E. Arabi, T. Yucelen, A. Chakravarthy, and D. McNeely, “Decentralized adaptive architectures for control of large-scale active-passive modular systems with stability and performance guarantees,” *International Journal of Control*, 2018 (accepted manuscript).
- [135] G. E. Dullerud and F. Paganini, *A course in robust control theory: A convex approach*, vol. 36. New York, NY: Springer Science & Business Media, 2013.
- [136] Y. Liu and X.-Y. Li, “Decentralized robust adaptive control of nonlinear systems with unmodeled dynamics,” *IEEE Transactions on Automatic Control*, vol. 47, no. 5, pp. 848–856, 2002.
- [137] N. Hovakimyan, E. Lavretsky, B.-J. Yang, and A. J. Calise, “Coordinated decentralized adaptive output feedback control of interconnected systems,” *IEEE Transactions on Neural Networks*, vol. 16, no. 1, pp. 185–194, 2005.
- [138] Y.-J. Liu, S. Tong, and C. P. Chen, “Adaptive fuzzy control via observer design for uncertain nonlinear systems with unmodeled dynamics,” *IEEE Transactions on Fuzzy Systems*, vol. 21, no. 2, pp. 275–288, 2013.
- [139] X. Xia, T. Zhang, and Q. Wang, “Decentralized adaptive output feedback dynamic surface control of interconnected nonlinear systems with unmodeled dynamics,” *Journal of the Franklin Institute*, vol. 352, no. 3, pp. 1031–1055, 2015.
- [140] B. C. Gruenwald, E. Arabi, T. Yucelen, A. Chakravarthy, and D. McNeely, “A decentralized adaptive control architecture for large-scale active-passive modular systems,” in *American Control Conference*, pp. 3347–3352, 2017.
- [141] T. Yucelen and J. D. Peterson, “Active-passive networked multiagent systems,” in *IEEE Conference on Decision and Control*, pp. 6939–6944, 2014.
- [142] J. D. Peterson and T. Yucelen, “An active–passive networked multiagent systems approach to environment surveillance,” in *AIAA Guidance, Navigation, and Control Conference*, 2015.

- [143] J. D. Peterson, T. Yucelen, G. Chowdhary, and S. Kannan, “Exploitation of heterogeneity in distributed sensing: An active-passive networked multiagent systems approach,” in *American Control Conference*, pp. 4112–4117, 2015.
- [144] D. W. Casbeer, Y. Cao, E. Garcia, and D. Milutinovi, “Average bridge consensus: Dealing with active-passive sensors,” in *ASME Dynamic Systems and Control Conference*, 2015.
- [145] J. D. Peterson and T. Yucelen, “Application of active-passive dynamic consensus filter approach to multitarget tracking problem for situational awareness in unknown environments,” in *AIAA Guidance, Navigation, and Control Conference*, 2016.
- [146] T. Yucelen and J. D. Peterson, “Distributed control of active-passive networked multiagent systems,” *IEEE Transactions on Control of Network Systems*, 2016.
- [147] A. Van der Schaft, *\mathcal{L}_2 -gain and passivity techniques in nonlinear control*. New York, NY: Springer Science & Business Media, 2012.
- [148] N. Nguyen, “Elastically shaped future air vehicle concept,” *NASA Innovation Fund Award*, 2010.
- [149] N. Nguyen and J. Urnes, “Aeroelastic modeling of elastically shaped aircraft concept via wing shaping control for drag reduction,” in *AIAA Atmospheric Flight Mechanics Conference*, pp. 13–16, 2012.
- [150] N. Nguyen, K. Trinh, D. Nguyen, and I. Tuzcu, “Nonlinear aeroelasticity of a flexible wing structure coupled with aircraft flight dynamics,” in *AIAA/ASME/ASCE/AHS/ASC Structures, Structural Dynamics, and Materials Conference*, 2012.
- [151] W. Nobleheart, A. Chakravarthy, and N. T. Nguyen, “Optimal and decentralized controller designs for an elastically shaped aircraft,” in *AIAA/ASMe/ASCE/AHS/SC Structures, Structural Dynamics, and Materials Conference*, p. 1042, 2014.
- [152] W. Nobleheart, A. Chakravarthy, and N. Nguyen, “Active wing shaping control of an elastic aircraft,” in *American Control Conference*, pp. 3059–3064, 2014.
- [153] K. B. Ngo, R. Mahony, and Z.-P. Jiang, “Integrator backstepping using barrier functions for systems with multiple state constraints,” in *IEEE Conference on Decision and Control*, pp. 8306–8312, 2005.
- [154] K. P. Tee, S. S. Ge, and F. E. H. Tay, “Adaptive control of electrostatic microactuators with bidirectional drive,” *IEEE Transactions on Control Systems Technology*, vol. 17, no. 2, pp. 340–352, 2009.

- [155] K. P. Tee, S. S. Ge, and E. H. Tay, “Barrier lyapunov functions for the control of output-constrained nonlinear systems,” *Automatica*, vol. 45, no. 4, pp. 918–927, 2009.
- [156] A. K. Kostarigka and G. A. Rovithakis, “Adaptive dynamic output feedback neural network control of uncertain mimo nonlinear systems with prescribed performance,” *IEEE Transactions on Neural Networks and Learning Systems*, vol. 23, no. 1, pp. 138–149, 2012.
- [157] B. Ren, S. S. Ge, K. P. Tee, and T. H. Lee, “Adaptive neural control for output feedback nonlinear systems using a barrier lyapunov function,” *IEEE Transactions on Neural Networks*, vol. 21, no. 8, pp. 1339–1345, 2010.
- [158] M. M. Polycarpou and P. A. Ioannou, “A robust adaptive nonlinear control design,” in *American Control Conference*, pp. 1365–1369, 1993.
- [159] M. L. Fravolini, E. Arabi, and T. Yucelen, “A model reference adaptive control approach for uncertain dynamical systems with strict component-wise performance guarantees,” in *AIAA Guidance, Navigation, and Control Conference*, p. 1572, 2018.
- [160] E. Arabi and T. Yucelen, “A generalization to set-theoretic model reference adaptive control architecture for enforcing user-defined time-varying performance bounds,” in *American Control Conference*, pp. 5077–5082, 2017.
- [161] M. Bisgaard, A. la Cour-Harbo, E. N. Johnson, and J. D. Bendtsen, “Vision aided state estimator for helicopter slung load system,” *IFAC Proceedings Volumes*, vol. 40, no. 7, pp. 425–430, 2007.
- [162] M. Bisgaard, A. la Cour-Harbo, and J. Bendtsen, “Full state estimation for helicopter slung load system,” in *AIAA Guidance, Navigation, and Control Conference and Exhibit*, p. 6762, 2007.
- [163] M. Bisgaard, J. D. Bendtsen, and A. la Cour-Harbo, “Modeling of generic slung load system,” *Journal of Guidance, Control, and Dynamics*, vol. 32, no. 2, pp. 573–585, 2009.
- [164] M. Bisgaard, A. la Cour-Harbo, and J. D. Bendtsen, “Adaptive control system for autonomous helicopter slung load operations,” *Control Engineering Practice*, vol. 18, no. 7, pp. 800–811, 2010.
- [165] M. Bernard and K. Kondak, “Generic slung load transportation system using small size helicopters,” in *IEEE International Conference on Robotics and Automation*, pp. 3258–3264, 2009.
- [166] C. M. Ivler, M. B. Tischler, and J. D. Powell, “Cable angle feedback control systems to improve handling qualities for helicopters with slung loads,” in *AIAA Guidance, Navigation and Control Conference*, 2011.

- [167] L. S. Cicolani and G. E. Ehlers, "Modeling and simulation of a helicopter slung load stabilization device," 2002.
- [168] S. El-Ferik, A. H. Syed, H. M. Omar, and M. A. Deriche, "Anti-swing nonlinear path tracking controller for helicopter slung load system," *IFAC Proceedings Volumes*, vol. 46, no. 30, pp. 134–141, 2013.
- [169] J.-P. Laumond, "Controllability of a multibody mobile robot," *IEEE Transactions on Robotics and Automation*, vol. 9, no. 6, pp. 755–763, 1993.
- [170] K. Kobayashi and T. Yoshikawa, "Controllability of under-actuated planar manipulators with one unactuated joint," *The International Journal of Robotics Research*, vol. 21, no. 5-6, pp. 555–561, 2002.
- [171] N. H. McClamroch, C. Rui, I. Kolmanovsky, S. Cho, and M. Reyhanoglu, "Control problems for planar motion of a rigid body with an unactuated internal degree of freedom," in *American Control Conference*, vol. 1, pp. 229–233, 1998.
- [172] M. Reyhanoglu, A. van der Schaft, N. H. McClamroch, and I. Kolmanovsky, "Dynamics and control of a class of underactuated mechanical systems," *IEEE Transactions on Automatic Control*, vol. 44, no. 9, pp. 1663–1671, 1999.
- [173] R. Olfati-Saber, "Nonlinear control and reduction of underactuated systems with symmetry. ii. unactuated shape variables case," in *IEEE Conference on Decision and Control*, vol. 5, pp. 4164–4169, 2001.
- [174] J. Grizzle, C. H. Moog, and C. Chevallereau, "Nonlinear control of mechanical systems with an unactuated cyclic variable," *IEEE Transactions on Automatic Control*, vol. 50, no. 5, pp. 559–576, 2005.
- [175] S. Cho, M. McClamroch, and M. Reyhanoglu, "Feedback control of a space vehicle with unactuated fuel slosh dynamics," in *AIAA Guidance, Navigation, and Control Conference and Exhibit*, p. 4046, 2000.
- [176] M. Reyhanoglu, "Maneuvering control problems for a spacecraft with unactuated fuel slosh dynamics," in *IEEE Conference on Control Applications*, vol. 1, pp. 695–699, 2003.
- [177] K.-S. Hong, "An open-loop control for underactuated manipulators using oscillatory inputs: Steering capability of an unactuated joint," *IEEE Transactions on Control Systems Technology*, vol. 10, no. 3, pp. 469–480, 2002.

- [178] R. Ortega and M. W. Spong, “Stabilization of underactuated mechanical systems via interconnection and damping assignment,” *IFAC Proceedings Volumes*, vol. 33, no. 2, pp. 69–74, 2000.
- [179] M. W. Spong, “The swing up control problem for the acrobot,” *IEEE Control Systems*, vol. 15, no. 1, pp. 49–55, 1995.
- [180] R. D. Gregg and L. Righetti, “Controlled reduction with unactuated cyclic variables: Application to 3d bipedal walking with passive yaw rotation,” *IEEE Transactions on Automatic Control*, vol. 58, no. 10, pp. 2679–2685, 2013.
- [181] D. J. Braun and M. Goldfarb, “A control approach for actuated dynamic walking in biped robots,” *IEEE Transactions on Robotics*, vol. 25, no. 6, pp. 1292–1303, 2009.
- [182] D. Seto and J. Baillieul, “Control problems in super-articulated mechanical systems,” *IEEE Transactions on Automatic Control*, vol. 39, no. 12, pp. 2442–2453, 1994.
- [183] J. Baillieul, “The behavior of single-input super-articulated mechanisms,” in *American Control Conference*, pp. 1622–1626, 1991.
- [184] J. Baillieul, “Stable average motions of mechanical systems subject to periodic forcing,” *Dynamics and Control of Mechanical Systems: The Falling Cat and Related Problems*, vol. 1, pp. 1–23, 1993.
- [185] Z.-P. Jiang and H. Nijmeijer, “Tracking control of mobile robots: A case study in backstepping,” *Automatica*, vol. 33, no. 7, pp. 1393–1399, 1997.
- [186] Z.-P. Jiang and H. Nijmeijer, “A recursive technique for tracking control of nonholonomic systems in chained form,” *IEEE Transactions on Automatic Control*, vol. 44, no. 2, pp. 265–279, 1999.
- [187] M. I. El-Hawwary, A.-L. Elshafei, H. M. Emara, and H. A. A. Fattah, “Adaptive fuzzy control of the inverted pendulum problem,” *IEEE Transactions on Control Systems Technology*, vol. 14, no. 6, pp. 1135–1144, 2006.
- [188] H.-H. Lee, “Motion planning for three-dimensional overhead cranes with high-speed load hoisting,” *International Journal of Control*, vol. 78, no. 12, pp. 875–886, 2005.
- [189] Y. Fang, B. Ma, P. Wang, and X. Zhang, “A motion planning-based adaptive control method for an underactuated crane system,” *IEEE Transactions on Control Systems Technology*, vol. 20, no. 1, pp. 241–248, 2012.

- [190] Y.-L. Gu, “A direct adaptive control scheme for under-actuated dynamic systems,” in *IEEE Conference on Decision and Control*, pp. 1625–1627, 1993.
- [191] C.-Y. Su and Y. Stepanenko, “Adaptive variable structure set-point control of underactuated robots,” *IEEE Transactions on Automatic Control*, vol. 44, no. 11, pp. 2090–2093, 1999.
- [192] K.-D. Nguyen and H. Dankowicz, “Adaptive control of underactuated robots with unmodeled dynamics,” *Robotics and Autonomous Systems*, vol. 64, pp. 84–99, 2015.
- [193] C.-L. Hwang, C.-C. Chiang, and Y.-W. Yeh, “Adaptive fuzzy hierarchical sliding-mode control for the trajectory tracking of uncertain underactuated nonlinear dynamic systems,” *IEEE Transactions on Fuzzy Systems*, vol. 22, no. 2, pp. 286–299, 2014.
- [194] A. P. Aguiar and J. P. Hespanha, “Trajectory-tracking and path-following of underactuated autonomous vehicles with parametric modeling uncertainty,” *IEEE Transactions on Automatic Control*, vol. 52, no. 8, pp. 1362–1379, 2007.
- [195] B. C. Gruenwald, E. Arabi, T. Yucelen, A. Chakravarthy, D. McNeely, and S. N. Balakrishnan, “Decentralized adaptive stabilization of large-scale active-passive modular systems,” in *AIAA Guidance, Navigation, and Control Conference*, p. 1895, 2017.
- [196] K. Narendra and A. Annaswamy, “A new adaptive law for robust adaptation without persistent excitation,” *IEEE Transactions on Automatic Control*, vol. 32, no. 2, pp. 134–145, 1987.
- [197] T. Yucelen, S. N. Balakrishnan, and E. Arabi, “Adaptive set-theoretic emulator reference architecture (ASTERA): Control of uncertain dynamical systems with performance guarantees and smooth transients,” in *AIAA Guidance, Navigation, and Control Conference*, p. 0874, 2018.
- [198] B. C. Gruenwald, T. Yucelen, K. M. Dogan, and J. A. Muse, “On adaptive control of uncertain dynamical systems in the presence of actuator dynamics and amplitude saturation limits,” in *IEEE Conference on Decision and Control*, 2018 (submitted).

APPENDIX A: PROJECTION OPERATOR

Definition A.1 Consider a convex hypercube in the form $\Omega = \{\theta \in \mathbb{R}^n : (\theta_i^{\min} \leq \theta_i \leq \theta_i^{\max})_{i=1,2, \dots, n}\}$, where $\Omega \in \mathbb{R}^n$, and θ_i^{\min} and θ_i^{\max} respectively represent the minimum and maximum bounds for the i^{th} component of the n -dimensional parameter vector θ . Furthermore, for a sufficiently small positive constant ε_0 , consider another hypercube in the form $\Omega_\varepsilon = \{\theta \in \mathbb{R}^n : (\theta_i^{\min} + \varepsilon_0 \leq \theta_i \leq \theta_i^{\max} - \varepsilon_0)_{i=1,2, \dots, n}\}$, where $\Omega_\varepsilon \subset \Omega$. The projection operator $\text{Proj} : \mathbb{R}^n \times \mathbb{R}^n \rightarrow \mathbb{R}^n$ is then defined component-wise by

$$\text{Proj}(\theta, y) \triangleq \begin{cases} \left(\frac{\theta_i^{\max} - \theta_i}{\varepsilon_0}\right) y_i, & \text{if } \theta_i > \theta_i^{\max} - \varepsilon_0 \text{ and } y_i > 0, \\ \left(\frac{\theta_i - \theta_i^{\min}}{\varepsilon_0}\right) y_i, & \text{if } \theta_i < \theta_i^{\min} + \varepsilon_0 \text{ and } y_i < 0, \\ y_i, & \text{otherwise,} \end{cases} \quad (\text{A.1})$$

where $y \in \mathbb{R}^n$.

Based on Definition A.1 and $\theta^* \in \Omega_\varepsilon$, one can show the inequality $(\theta - \theta^*)^T (\text{Proj}(\theta, y) - y) \leq 0$, holds for $\theta \in \Omega$ and $y \in \mathbb{R}^n$ [6]. In addition, we use a generalization of this definition to matrices as $\text{Proj}_m(\Theta, Y) = (\text{Proj}(\text{col}_1(\Theta), \text{col}_1(Y)) \dots, \text{Proj}(\text{col}_m(\Theta), \text{col}_m(Y)))$, where $\Theta \in \mathbb{R}^{n \times m}$, $Y \in \mathbb{R}^{n \times m}$, and $\text{col}_i(\cdot)$ denotes the i -th column operator. In this case, for a given matrix Θ^* , it follows that $\text{tr} \left[(\Theta - \Theta^*)^T (\text{Proj}_m(\Theta, Y) - Y) \right] = \sum_{i=1}^m \left[\text{col}_i(\Theta - \Theta^*)^T (\text{Proj}(\text{col}_i(\Theta), \text{col}_i(Y)) - \text{col}_i(Y)) \right] \leq 0$, holds.

APPENDIX B: COPYRIGHT PERMISSIONS

The permission below is for the use of material in Chapter 2.



Our Ref: KA/TCON/P18/0868

23 May 2018

Dear Benjamin Gruenwald ,

Material requested: Benjamin Gruenwald & Tansel Yucelen (2015) On transient performance improvement of adaptive control architectures, International Journal of Control, 88:11, 2305-2315,

Thank you for your correspondence requesting permission to reproduce the above mentioned material from our Journal in your printed thesis entitled "Toward Verifiable Adaptive Control Systems: High-Performance and Robust Architectures" and to be posted in the university's repository – University of South Florida

We will be pleased to grant permission on the sole condition that you acknowledge the original source of publication and insert a reference to the article on the Journals website: <http://www.tandfonline.com>

This is the authors accepted manuscript of an article published as the version of record in International Journal of Control © 12 May 2015 - <https://www.tandfonline.com/10.1080/00207179.2015.1041001>

This permission does not cover any third party copyrighted work which may appear in the material requested.

Please note that this license does not allow you to post our content on any third party websites or repositories.

Thank you for your interest in our Journal.

Yours sincerely

Kendyl

Kendyl Anderson – Permissions Administrator, Journals
Taylor & Francis Group
3 Park Square, Milton Park, Abingdon, Oxon, OX14 4RN, UK.
Tel: +44 (0)20 7017 7617
Fax: +44 (0)20 7017 6336
Web: www.tandfonline.com
e-mail: kendyl.anderson@tandf.co.uk



Taylor & Francis is a trading name of Informa UK Limited, registered in England under no. 1072954

The license below is for the material in Chapter 3.



Creative Commons Legal Code

Attribution 4.0 International

Official translations of this license are available [in other languages](#).



Creative Commons Corporation ("Creative Commons") is not a law firm and does not provide legal services or legal advice. Distribution of Creative Commons public licenses does not create a lawyer-client or other relationship. Creative Commons makes its licenses and related information available on an "as-is" basis. Creative Commons gives no warranties regarding its licenses, any material licensed under their terms and conditions, or any related information. Creative Commons disclaims all liability for damages resulting from their use to the fullest extent possible.

Using Creative Commons Public Licenses

Creative Commons public licenses provide a standard set of terms and conditions that creators and other rights holders may use to share original works of authorship and other material subject to copyright and certain other rights specified in the public license below. The following considerations are for informational purposes only, are not exhaustive, and do not form part of our licenses.

Considerations for licensors: *Our public licenses are intended for use by those authorized to give the public permission to use material in ways otherwise restricted by copyright and certain other rights. Our licenses are irrevocable. Licensors should read and understand the terms and conditions of the license they choose before applying it. Licensors should also secure all rights necessary before applying our licenses so that the public can reuse the material as expected. Licensors should clearly mark any material not subject to the license. This includes other CC-licensed material, or material used under an exception or limitation to copyright. [More considerations for licensors](#).*

Considerations for the public: *By using one of our public licenses, a licensor grants the public permission to use the licensed material under specified terms and conditions. If the licensor's permission is not necessary for any reason—for example, because of any applicable exception or limitation to copyright—then that use is not regulated by the license. Our licenses grant only permissions under copyright and certain other rights that a licensor has authority to grant. Use of the licensed material may still be restricted for other reasons, including because others have copyright or other rights in the material. A licensor may make special requests, such as asking that all changes be marked or described. Although not required by our licenses, you are encouraged to respect those requests where reasonable. [More considerations for the public](#).*

Creative Commons Attribution 4.0 International Public License

By exercising the Licensed Rights (defined below), You accept and agree to be bound by the terms and conditions of this Creative Commons Attribution 4.0 International Public License ("Public License"). To the extent this Public License may be interpreted as a contract, You are granted the Licensed Rights in consideration of Your acceptance of these terms and conditions, and the Licensor grants You such rights in consideration of benefits the Licensor receives from making the Licensed Material available under these terms and conditions.

Section 1 – Definitions.

- a. **Adapted Material** means material subject to Copyright and Similar Rights that is derived from or based upon the Licensed Material and in which the Licensed Material is translated, altered, arranged, transformed, or otherwise modified in a manner requiring permission under the Copyright and Similar Rights held by the Licensor. For purposes of this Public License, where the Licensed Material is a musical work, performance, or sound recording, Adapted Material is always produced where the Licensed Material is synched in timed relation with a moving image.
- b. **Adapter's License** means the license You apply to Your Copyright and Similar Rights in Your contributions to Adapted Material in accordance with the terms and conditions of this Public License.
- c. **Copyright and Similar Rights** means copyright and/or similar rights closely related to copyright including, without limitation, performance, broadcast, sound recording, and Sui Generis Database Rights, without regard to how the rights are labeled or categorized. For purposes of this Public License, the rights specified in Section 2(b)(1)-(2) are not Copyright and Similar Rights.
- d. **Effective Technological Measures** means those measures that, in the absence of proper authority, may not be circumvented under laws fulfilling obligations under Article 11 of the WIPO Copyright Treaty adopted on December 20, 1996, and/or similar international agreements.
- e. **Exceptions and Limitations** means fair use, fair dealing, and/or any other exception or limitation to Copyright and Similar Rights that applies to Your use of the Licensed Material.
- f. **Licensed Material** means the artistic or literary work, database, or other material to which the Licensor applied this Public License.
- g. **Licensed Rights** means the rights granted to You subject to the terms and conditions of this Public License, which are limited to all Copyright and Similar Rights that apply to Your use of the Licensed Material and that the Licensor has authority to license.
- h. **Licensor** means the individual(s) or entity(ies) granting rights under this Public License.
- i. **Share** means to provide material to the public by any means or process that requires permission under the Licensed Rights, such as reproduction, public display, public performance, distribution, dissemination, communication, or importation, and to make material available to the public including in ways that members of the public may access the material from a place and at a time individually chosen by them.
- j. **Sui Generis Database Rights** means rights other than copyright resulting from Directive 96/9/EC of the European Parliament and of the Council of 11 March 1996 on the legal protection of databases, as amended and/or succeeded, as well as other essentially equivalent rights anywhere in the world.
- k. **You** means the individual or entity exercising the Licensed Rights under this Public License. **Your** has a corresponding meaning.

Section 2 – Scope.

- a. **License grant.**
 1. Subject to the terms and conditions of this Public License, the Licensor hereby grants You a worldwide, royalty-free, non-sublicensable, non-exclusive, irrevocable license to exercise the Licensed Rights in the Licensed Material to:

- A. reproduce and Share the Licensed Material, in whole or in part; and
 - B. produce, reproduce, and Share Adapted Material.
2. **Exceptions and Limitations.** For the avoidance of doubt, where Exceptions and Limitations apply to Your use, this Public License does not apply, and You do not need to comply with its terms and conditions.
 3. **Term.** The term of this Public License is specified in Section 6(a).
 4. **Media and formats; technical modifications allowed.** The Licensor authorizes You to exercise the Licensed Rights in all media and formats whether now known or hereafter created, and to make technical modifications necessary to do so. The Licensor waives and/or agrees not to assert any right or authority to forbid You from making technical modifications necessary to exercise the Licensed Rights, including technical modifications necessary to circumvent Effective Technological Measures. For purposes of this Public License, simply making modifications authorized by this Section 2(a)(4) never produces Adapted Material.
 5. **Downstream recipients.**
 - A. **Offer from the Licensor – Licensed Material.** Every recipient of the Licensed Material automatically receives an offer from the Licensor to exercise the Licensed Rights under the terms and conditions of this Public License.
 - B. **No downstream restrictions.** You may not offer or impose any additional or different terms or conditions on, or apply any Effective Technological Measures to, the Licensed Material if doing so restricts exercise of the Licensed Rights by any recipient of the Licensed Material.
 6. **No endorsement.** Nothing in this Public License constitutes or may be construed as permission to assert or imply that You are, or that Your use of the Licensed Material is, connected with, or sponsored, endorsed, or granted official status by, the Licensor or others designated to receive attribution as provided in Section 3(a)(1)(A)(i).

b. Other rights.

1. Moral rights, such as the right of integrity, are not licensed under this Public License, nor are publicity, privacy, and/or other similar personality rights; however, to the extent possible, the Licensor waives and/or agrees not to assert any such rights held by the Licensor to the limited extent necessary to allow You to exercise the Licensed Rights, but not otherwise.
2. Patent and trademark rights are not licensed under this Public License.
3. To the extent possible, the Licensor waives any right to collect royalties from You for the exercise of the Licensed Rights, whether directly or through a collecting society under any voluntary or waivable statutory or compulsory licensing scheme. In all other cases the Licensor expressly reserves any right to collect such royalties.

Section 3 – License Conditions.

Your exercise of the Licensed Rights is expressly made subject to the following conditions.

a. Attribution.

1. If You Share the Licensed Material (including in modified form), You must:
 - A. retain the following if it is supplied by the Licensor with the Licensed Material:
 - i. identification of the creator(s) of the Licensed Material and any others designated to receive attribution, in any reasonable manner requested by the Licensor (including by pseudonym if designated);
 - ii. a copyright notice;
 - iii. a notice that refers to this Public License;

- iv. a notice that refers to the disclaimer of warranties;
 - v. a URI or hyperlink to the Licensed Material to the extent reasonably practicable;
- B. indicate if You modified the Licensed Material and retain an indication of any previous modifications; and
- C. indicate the Licensed Material is licensed under this Public License, and include the text of, or the URI or hyperlink to, this Public License.
2. You may satisfy the conditions in Section [3\(a\)\(1\)](#) in any reasonable manner based on the medium, means, and context in which You Share the Licensed Material. For example, it may be reasonable to satisfy the conditions by providing a URI or hyperlink to a resource that includes the required information.
 3. If requested by the Licensor, You must remove any of the information required by Section [3\(a\)\(1\)\(A\)](#) to the extent reasonably practicable.
 4. If You Share Adapted Material You produce, the Adapter's License You apply must not prevent recipients of the Adapted Material from complying with this Public License.

Section 4 – Sui Generis Database Rights.

Where the Licensed Rights include Sui Generis Database Rights that apply to Your use of the Licensed Material:

- a. for the avoidance of doubt, Section [2\(a\)\(1\)](#) grants You the right to extract, reuse, reproduce, and Share all or a substantial portion of the contents of the database;
- b. if You include all or a substantial portion of the database contents in a database in which You have Sui Generis Database Rights, then the database in which You have Sui Generis Database Rights (but not its individual contents) is Adapted Material; and
- c. You must comply with the conditions in Section [3\(a\)](#) if You Share all or a substantial portion of the contents of the database.

For the avoidance of doubt, this Section [4](#) supplements and does not replace Your obligations under this Public License where the Licensed Rights include other Copyright and Similar Rights.

Section 5 – Disclaimer of Warranties and Limitation of Liability.

- a. **Unless otherwise separately undertaken by the Licensor, to the extent possible, the Licensor offers the Licensed Material as-is and as-available, and makes no representations or warranties of any kind concerning the Licensed Material, whether express, implied, statutory, or other. This includes, without limitation, warranties of title, merchantability, fitness for a particular purpose, non-infringement, absence of latent or other defects, accuracy, or the presence or absence of errors, whether or not known or discoverable. Where disclaimers of warranties are not allowed in full or in part, this disclaimer may not apply to You.**
- b. **To the extent possible, in no event will the Licensor be liable to You on any legal theory (including, without limitation, negligence) or otherwise for any direct, special, indirect, incidental, consequential, punitive, exemplary, or other losses, costs, expenses, or damages arising out of this Public License or use of the Licensed Material, even if the Licensor has been advised of the possibility of such losses, costs, expenses, or damages. Where a limitation of liability is not allowed in full or in part, this limitation may not apply to You.**
- c. The disclaimer of warranties and limitation of liability provided above shall be interpreted in a manner that, to the extent possible, most closely approximates an absolute disclaimer and waiver of all liability.

Section 6 – Term and Termination.

- a. This Public License applies for the term of the Copyright and Similar Rights licensed here. However, if You fail to comply with this Public License, then Your rights under this Public License terminate automatically.
- b. Where Your right to use the Licensed Material has terminated under Section [6\(a\)](#), it reinstates:
 1. automatically as of the date the violation is cured, provided it is cured within 30 days of Your discovery of the violation; or
 2. upon express reinstatement by the Licensor.
 For the avoidance of doubt, this Section [6\(b\)](#) does not affect any right the Licensor may have to seek remedies for Your violations of this Public License.
- c. For the avoidance of doubt, the Licensor may also offer the Licensed Material under separate terms or conditions or stop distributing the Licensed Material at any time; however, doing so will not terminate this Public License.
- d. Sections [1](#), [5](#), [6](#), [7](#), and [8](#) survive termination of this Public License.

Section 7 – Other Terms and Conditions.

- a. The Licensor shall not be bound by any additional or different terms or conditions communicated by You unless expressly agreed.
- b. Any arrangements, understandings, or agreements regarding the Licensed Material not stated herein are separate from and independent of the terms and conditions of this Public License.

Section 8 – Interpretation.

- a. For the avoidance of doubt, this Public License does not, and shall not be interpreted to, reduce, limit, restrict, or impose conditions on any use of the Licensed Material that could lawfully be made without permission under this Public License.
- b. To the extent possible, if any provision of this Public License is deemed unenforceable, it shall be automatically reformed to the minimum extent necessary to make it enforceable. If the provision cannot be reformed, it shall be severed from this Public License without affecting the enforceability of the remaining terms and conditions.
- c. No term or condition of this Public License will be waived and no failure to comply consented to unless expressly agreed to by the Licensor.
- d. Nothing in this Public License constitutes or may be interpreted as a limitation upon, or waiver of, any privileges and immunities that apply to the Licensor or You, including from the legal processes of any jurisdiction or authority.

Creative Commons is not a party to its public licenses. Notwithstanding, Creative Commons may elect to apply one of its public licenses to material it publishes and in those instances will be considered the "Licensor." The text of the Creative Commons public licenses is dedicated to the public domain under the [CC0 Public Domain Dedication](#). Except for the limited purpose of indicating that material is shared under a Creative Commons public license or as otherwise permitted by the Creative Commons policies published at creativecommons.org/policies, Creative Commons does not authorize the use of the trademark "Creative Commons" or any other trademark or logo of Creative Commons without its prior written consent including, without limitation, in connection with any unauthorized modifications to any of its public licenses or any other arrangements, understandings, or agreements concerning use of licensed material. For the avoidance of doubt, this paragraph does not form part of the public licenses.

Creative Commons may be contacted at creativecommons.org.

Additional languages available: [Bahasa Indonesia](#), [Deutsch](#), [français](#), [hrvatski](#), [italiano](#), [Nederlands](#), [norsk](#), [polski](#), [suomeksi](#), [svenska](#), [te reo Māori](#), [Türkçe](#), [русский](#), [українська](#), [العربية](#), [日本語](#). Please read the [FAQ](#) for more information about official translations.

The permission below is for the use of material in Chapter 5.

4/23/2018

Rightslink® by Copyright Clearance Center



RightsLink®

Home

Create Account

Help



Title: Adaptive control for a class of uncertain nonlinear dynamical systems in the presence of high-order actuator dynamics
Conference Proceedings: American Control Conference (ACC), 2017
Author: Benjamin C. Gruenwald
Publisher: IEEE
Date: May 2017
Copyright © 2017, IEEE

LOGIN
If you're a [copyright.com user](#), you can login to RightsLink using your copyright.com credentials. Already a [RightsLink user](#) or want to [learn more?](#)

Thesis / Dissertation Reuse

The IEEE does not require individuals working on a thesis to obtain a formal reuse license, however, you may print out this statement to be used as a permission grant:

Requirements to be followed when using any portion (e.g., figure, graph, table, or textual material) of an IEEE copyrighted paper in a thesis:

- 1) In the case of textual material (e.g., using short quotes or referring to the work within these papers) users must give full credit to the original source (author, paper, publication) followed by the IEEE copyright line © 2011 IEEE.
- 2) In the case of illustrations or tabular material, we require that the copyright line © [Year of original publication] IEEE appear prominently with each reprinted figure and/or table.
- 3) If a substantial portion of the original paper is to be used, and if you are not the senior author, also obtain the senior author's approval.

Requirements to be followed when using an entire IEEE copyrighted paper in a thesis:

- 1) The following IEEE copyright/ credit notice should be placed prominently in the references: © [year of original publication] IEEE. Reprinted, with permission, from [author names, paper title, IEEE publication title, and month/year of publication]
- 2) Only the accepted version of an IEEE copyrighted paper can be used when posting the paper or your thesis on-line.
- 3) In placing the thesis on the author's university website, please display the following message in a prominent place on the website: In reference to IEEE copyrighted material which is used with permission in this thesis, the IEEE does not endorse any of [university/educational entity's name goes here]'s products or services. Internal or personal use of this material is permitted. If interested in reprinting/republishing IEEE copyrighted material for advertising or promotional purposes or for creating new collective works for resale or redistribution, please go to http://www.ieee.org/publications_standards/publications/rights/rights_link.html to learn how to obtain a License from RightsLink.

If applicable, University Microfilms and/or ProQuest Library, or the Archives of Canada may supply single copies of the dissertation.

BACK

CLOSE WINDOW

Copyright © 2018 [Copyright Clearance Center, Inc.](#) All Rights Reserved. [Privacy statement.](#) [Terms and Conditions.](#) Comments? We would like to hear from you. E-mail us at customercare@copyright.com

The permission below is for the use of material in Chapter 5.



Benjamin Gruenwald <bcgruenwald@mail.usf.edu>

Permission Request

2 messages

Benjamin Gruenwald <bcgruenwald@mail.usf.edu>
To: permissions@asme.org

Thu, May 3, 2018 at 9:23 AM

Hello,

I am emailing to request permission to use one of my ASME conference papers in my dissertation. I have the completed permission request form attached.

Thank you.
Benjamin

 **Gruenwald_PermissionForm.pdf**
271K

Beth Darchi <DarchiB@asme.org>
To: Benjamin Gruenwald <bcgruenwald@mail.usf.edu>

Thu, May 3, 2018 at 3:29 PM

Dear Prof. Gruenwald,

It is our pleasure to grant you permission to use **all or any part of** the ASME paper "A Model Reference Adaptive Control Framework for Uncertain Dynamical Systems With High-Order Actuator Dynamics and Unknown Actuator Outputs," by Benjamin C. Gruenwald; K. Merve Dogan; Tansel Yucelen; Jonathan A. Muse, Paper Number DSCC2017-5062, cited in your letter for inclusion in a dissertation entitled Toward Verifiable Adaptive Control Systems: High-Performance and Robust Architectures to be published by University of South Florida.

Permission is granted for the specific use as stated herein and does not permit further use of the materials without proper authorization. Proper attribution must be made to the author(s) of the materials. **Please note:** if any or all of the figures and/or Tables are of another source, permission should be granted from that outside source or include the reference of the original source. ASME does not grant permission for outside source material that may be referenced in the ASME works.

As is customary, we request that you ensure full acknowledgment of this material, the author(s), source and ASME as original publisher. Acknowledgment must be retained on all pages where figure is printed and distributed.

Many thanks for your interest in ASME publications.

Sincerely,

Beth Darchi

Publishing Administrator

ASME

2 Park Avenue

New York, NY 10016-5990

darchib@asme.org

The permission below is for the use of material in Chapter 5.



Account Info

Help



Title: AIAA Guidance, Navigation, and Control Conference
Article ID: 9781624104503
Publication: Publication1
Publisher: CCC Reproduction
Date: Jan 1, 2017
 Copyright © 2017, CCC Reproduction

Logged in as:
 Benjamin Gruenwald
 Account #:
 3001278584

LOGOUT

Order Completed

Thank you for your order.

This Agreement between Benjamin Gruenwald ("You") and American Inst of Aeronautics and Astronautics (AIAA) ("American Inst of Aeronautics and Astronautics (AIAA)") consists of your order details and the terms and conditions provided by American Inst of Aeronautics and Astronautics (AIAA) and Copyright Clearance Center.

License number	Reference confirmation email for license number
License date	May, 09 2018
Licensed content publisher	American Inst of Aeronautics and Astronautics (AIAA)
Licensed content title	AIAA Guidance, Navigation, and Control Conference
Licensed content date	Jan 1, 2017
Type of use	Thesis/Dissertation
Requestor type	Author of requested content
Format	Electronic
Portion	chapter/article
Number of pages in chapter/article	10
The requesting person/organization	Benjamin Gruenwald
Title or numeric reference of the portion(s)	AIAA 2017-1491
Title of the article or chapter the portion is from	Model Reference Adaptive Control in the Presence of Actuator Dynamics with Applications to the Input Time-Delay Problem
Editor of portion(s)	N/A
Author of portion(s)	Benjamin Gruenwald
Volume of serial or monograph	N/A
Page range of portion	1-10
Publication date of portion	Jan 1, 2017
Rights for	Main product
Duration of use	Life of current edition
Creation of copies for the disabled	no
With minor editing privileges	yes
For distribution to	Worldwide
In the following language(s)	Original language of publication
With incidental promotional use	no
Lifetime unit quantity of new product	Up to 999
Title	Toward Verifiable Adaptive Control Systems: High-Performance and Robust Architectures
Instructor name	Benjamin Gruenwald
Institution name	University of South Florida
Expected presentation date	Jun 2018
Requestor Location	Benjamin Gruenwald 2949 Lakeside Commons Dr. Apt 202B

Billing Type	Tampa, FL 33616
Billing address	United States
	Attn:
	Invoice
	Benjamin Gruenwald
	
	Attn: Benjamin Gruenwald
Total (may include CCC user fee)	0.00 USD
Total	0.00 USD

[CLOSE WINDOW](#)

Copyright © 2018 [Copyright Clearance Center, Inc.](#) All Rights Reserved. [Privacy statement](#) - [Terms and Conditions](#).
Comments? We would like to hear from you. E-mail us at customercare@copyright.com

The paper below shows the copyright for the use of material in Chapter 5 is owned by the author.



Computing the Stability Limits of Pole-Zero Actuator Dynamics on Adaptive Control Laws for Aerospace Applications*

Benjamin C. Gruenwald*, Tansel Yucelen[†], and K. Merve Dogan[‡]

University of South Florida

Jonathan A. Muse[§]

Air Force Research Laboratory

Daniel Wagner[¶]

Czech Technical University

This paper illustrates an application of a linear matrix inequality-based hedging approach for model reference adaptive control in the presence of pole-zero actuator dynamics. Specifically, this approach uses a hedging signal to alter a given reference model trajectory such that adaptation is not effected by the presence of actuator dynamics, then it uses linear matrix inequalities (LMIs) to compute the stability limits of the adaptive control law as a result of the hedged reference model. In order to demonstrate the capability of the proposed approach in providing safe and predictable limits, multiple cases of pole-zero actuator dynamics are considered on the short-period dynamics of a hypersonic vehicle model, where a feasible region of safe actuation is computed for each pole-zero configuration.

I Introduction

Stability limits of adaptive controllers in the presence of actuator dynamics is a well-known problem. In recent papers by the authors [1–8], a new approach has been proposed using a hedged reference model and linear matrix inequalities (LMIs) to compute stability limits of adaptive controllers. In particular, we have considered a wide range of generalizations of the proposed framework, including the cases known and unknown control input, known and unknown actuator output, linear and nonlinear uncertainties, and first-order and high-order actuator dynamics. In our most recent work [8], an application to a hypersonic vehicle model is also included for first-order actuator models.

*B. C. Gruenwald is a Graduate Research Assistant of the Department of Mechanical Engineering and a Member of the Laboratory for Autonomy, Control, Information, and Systems (LACIS, <http://www.lacis.team/>) at the University of South Florida, Tampa, FL 33620, USA (email: bcgruenwald@mail.usf.edu).

[†]T. Yucelen is an Assistant Professor of the Department of Mechanical Engineering and the Director of the Laboratory for Autonomy, Control, Information, and Systems (LACIS, <http://www.lacis.team/>) at the University of South Florida, Tampa, FL 33620, USA (email: yucelen@usf.edu). T. Yucelen is also a Senior Member of the American Institute of Aeronautics and Astronautics and a Member of the National Academy of Inventors.

[‡]K. M. Dogan is a Graduate Research Assistant of the Department of Mechanical Engineering and a Member of the Laboratory for Autonomy, Control, Information, and Systems (LACIS, <http://www.lacis.team/>) at the University of South Florida, Tampa, FL 33620, USA (email: dogan@mail.usf.edu).

[§]J. A. Muse is a Research Aerospace Engineer of the Autonomous Control Branch at the Air Force Research Laboratory Aerospace Systems Directorate, WPAFB, OH 45433, USA (email: jonathan.muse.2@us.af.mil).

[¶]D. Wagner is with the Advanced Algorithms for Control and Communications Laboratory of the Department of Electrical Engineering at the Czech Technical University, Prague, Czech Republic (email: wagneda1@fel.cvut.cz).

*This research was supported by the Air Force Research Laboratory Aerospace Systems Directorate under the Universal Technology Corporation Grant 17-S8401-02-C1.

The permission below is for the use of material in Chapter 7.



Our Ref: KA/TCON/P18/1172

21 June 2018

Dear Benjamin C. Gruenwald,

Material requested: Benjamin C. Gruenwald, Ehsan Arabi, Tansel Yucelen, Animesh Chakravarthy & Drew McNeely (2018): Decentralized Adaptive Architectures for Control of Large-Scale ActivePassive Modular Systems with Stability and Performance Guarantees, International Journal of Control,

Thank you for your correspondence requesting permission to reproduce the above mentioned material from our Journal in your printed thesis entitled "Toward Verifiable Adaptive Control Systems: High-Performance and Robust Architectures" and to be posted in the university's repository – University of South Florida

We will be pleased to grant permission on the sole condition that you acknowledge the original source of publication and insert a reference to the article on the Journals website: <http://www.tandfonline.com>

This is the authors accepted manuscript of an article published as the version of record in International Journal of Control © 14 Jun 2018

This permission does not cover any third party copyrighted work which may appear in the material requested.

Please note that this license does not allow you to post our content on any third party websites or repositories.

Thank you for your interest in our Journal.

Yours sincerely

Kendyl

Kendyl Anderson – Permissions Administrator, Journals

Taylor & Francis Group
3 Park Square, Milton Park, Abingdon, Oxon, OX14 4RN, UK.
Tel: +44 (0)20 7017 7617
Fax: +44 (0)20 7017 6336
Web: www.tandfonline.com
e-mail: kendyl.anderson@tandf.co.uk



Taylor & Francis is a trading name of Informa UK Limited, registered in England under no. 1072954

The permissions below are for the use of material in Chapters 7 and 8 which are a part of the authors consulting work.



Benjamin Gruenwald <gruenwbc1@gmail.com>

Permission Request

4 messages

Benjamin Gruenwald <gruenwbc1@gmail.com> Thu, May 24, 2018 at 1:54 PM
To: "Chakravarthy, Animesh" <animesh.chakravarthy@wichita.edu>

Dear Dr. Chakravarthy,

I am emailing to request permission to use our paper entitled "Decentralized Adaptive Architectures for Control of Large-Scale Active-Passive Modular Systems with Stability and Performance Guarantees" in my dissertation. This paper is a by-product of my consulting work with you and Wichita State University.

Thank you,
Benjamin

Benjamin Gruenwald <gruenwbc1@gmail.com> Thu, May 24, 2018 at 1:54 PM
To: "Chakravarthy, Animesh" <animesh.chakravarthy@wichita.edu>

Dear Dr. Chakravarthy,

I am emailing to request permission to use our paper entitled "On Adaptive Control of Unactuated Dynamical Systems through Interconnections with Stability and Performance Guarantees" in my dissertation. This paper is a by-product of my consulting work with you and Wichita State University.

Thank you,
Benjamin

Chakravarthy, Animesh <Animesh.Chakravarthy@wichita.edu> Thu, May 24, 2018 at 1:57 PM
To: Benjamin Gruenwald <gruenwbc1@gmail.com>

Benjamin,

I am absolutely fine with your including this paper in your dissertation.

Thanks,
Animesh

From: Benjamin Gruenwald <gruenwbc1@gmail.com>
Sent: Thursday, May 24, 2018 12:55 PM
To: Chakravarthy, Animesh <Animesh.Chakravarthy@wichita.edu>
Subject: Permission Request

[Quoted text hidden]

Chakravarthy, Animesh <Animesh.Chakravarthy@wichita.edu> Thu, May 24, 2018 at 1:57 PM
To: Benjamin Gruenwald <gruenwbc1@gmail.com>

Benjamin,

I am absolutely fine with your including this paper in your dissertation.

Thanks,
Animesh

From: Benjamin Gruenwald <gruenwbc1@gmail.com>
Sent: Thursday, May 24, 2018 12:55 PM
To: Chakravarthy, Animesh <Animesh.Chakravarthy@wichita.edu>
Subject: Permission Request